

Long-chain fatty acid oxidation disorders
biochemical, pathophysiological and clinical aspects

Eugène F. Diekman

Long-chain fatty acid oxidation disorders - Biochemical, pathophysiological and clinical aspects

Eugène Diekman

Thesis with a summary in Dutch, Utrecht University

ISBN: 978-94-6169-644-1

© Copyright 2015 E.F. Diekman, Utrecht, The Netherlands

All rights reserved. No part of this thesis may be reproduced in any form or by any means, electronic, mechanical, by photocopying, recording or otherwise without prior written permission of the author. The copyrights of the publications remain with the publisher.

Cover: Flux -noun- *The rate of flow of a fluid, radiant energy, or particles across a given area.*

(photo: istockphoto.com)

Layout and printing: Optima Grafische Communicatie, Rotterdam, the Netherlands

Printing of this thesis was financially supported by: Sigma-Tau, Vitaflo, ABN Amro, Genzyme, Actelion

Long-chain fatty acid oxidation disorders
biochemical, pathophysiological and clinical aspects

Lange-keten vetzuuroxidatie ziekten
biochemische, pathofysiologische en klinische aspecten

(met een samenvatting in het Nederlands)

PROEFSCHRIFT

ter verkrijging van de graad van doctor aan de Universiteit Utrecht
op gezag van de rector magnificus, prof. dr. G.J. van der Zwaan,
ingevolge het besluit van het college voor promoties in het openbaar
te verdedigen op dinsdag 24 maart 2015 des middags te 2.30 uur

door

Eugène Franciscus Diekman

geboren op 24 oktober 1984
te Deventer

Promotoren: Prof.dr. E.E.S. Nieuwenhuis
Prof.dr. R.J.A. Wanders

Copromotoren: Dr. G. Visser
Dr. S.M. Houten

TABLE OF CONTENTS

Chapter 1	General Introduction and Outline of thesis	7
Chapter 2	Differences between acylcarnitine profiles in plasma and bloodspots	29
Chapter 3	Newborn screening paradox: sensitivity vs overdiagnosis	47
Chapter 4	Fatty acid oxidation flux predicts clinical severity of VLCAD deficient patients	59
Chapter 5	Normal cardiac function with minimal decrease of myocardial contractility in very long-chain acyl-CoA dehydrogenase deficient patients	77
Chapter 6	Muscle MRI in very long-chain acyl-CoA dehydrogenase deficient patients	99
Chapter 7	Abnormal energetics of endurance exercise in very long-chain acyl-CoA dehydrogenase deficiency	119
Chapter 8	Food withdrawal lowers energy expenditure and induces inactivity in long-chain fatty acid oxidation-deficient mouse models	141
Chapter 9	Perioperative measures in very long-chain acyl-CoA dehydrogenase deficiency	165
Chapter 10	Necrotizing enterocolitis and respiratory distress syndrome as first clinical presentation of mitochondrial trifunctional protein deficiency	173
Chapter 11	General discussion & future perspectives	187
Appendix	Nederlandse Samenvatting	203
	Dankwoord	209
	List of publications	215
	Curriculum Vitae	217

CHAPTER 1

General Introduction and Outline
of thesis



INTRODUCTION

Historical perspective of fatty acid oxidation

'Recherches chimiques sur les corps gras d'origine animale' ('Chemical research on animal fats') by Michel Eugène Chevreul (1823). This work is considered to be the first book in lipochemistry. It contains 10 years of dr. Chevreul's lipid research in which the concept of 'fatty acids' arose^{1,2}.

'Der Abbau aromatischer Fettsäuren im Tierkörper' by Franz Knoop (Beitr Chem Physiol Pathol 1904). In this paper dr. Knoop discovered that dogs, fed with labeled fatty acids of odd and even chain lengths, metabolized those by splitting of two carbon atoms, hence the name β -oxidation^{3,4}.

'Effects of carnitine on fatty-acid oxidation by muscle' by Fritz and McEwen (Science, 1959). This landmark paper described the stimulating effect of carnitine on fatty acid oxidation^{3,4}.

Every day, an average human consumes 35% of his total energy intake as fat⁵. Most of this fat consists of long-chain fatty acids. These long-chain fatty acids enter the intestine via enterocytes, where they are incorporated in chylomicrons which consist of triglycerides and long-chain fatty acids⁶. Chylomicrons are secreted into the lymphatic system and then processed by liver, heart, muscle or any other organ. There, long-chain fatty acids from chylomicrons enter the cell via fatty acid transport proteins (CD36-FATP/FABPpm). Intracellular, fatty acids are activated with coenzyme A (CoA) by acyl-CoA synthetases. In contrast to medium- and short-chain fatty acids, long-chain acyl-CoAs (C12-C18) can not enter mitochondria directly. For entrance into the mitochondria, long-chain acyl-CoAs have to be converted to acylcarnitines by carnitine palmitoyltransferase 1 (CPT1). CPT1 substitutes -CoA with -carnitine (Figure 1). CPT1 is an important rate-limiting step in fatty acid oxidation. Acetyl-CoA, a product of fatty acid oxidation, can be converted into malonyl-CoA (by acetyl-CoA carboxylase), which is an inhibitor of CPT1. Next, long-chain acylcarnitines are translocated into the mitochondria by carnitine acylcarnitine translocase (CACT) and then reconverted into long-chain acyl-CoAs by carnitine palmitoyltransferase 2 (CPT2). The long-chain acyl-CoA are then processed by enzymes involved in β -oxidation such as very long-chain acyl-CoA dehydrogenase (VLCAD) and mitochondrial trifunctional protein (MTP). All these enzymes are necessary to produce acetyl-CoA, a crucial component in the production of energy.

For each of these enzymes involved in the carnitine cycle and the β -oxidation cycle, human disorders have been described. OCTN2 is a carnitine transporter that transports carnitine into the cell. OCTN2 deficiency (OMIM 212140) is rare and causes primary car-

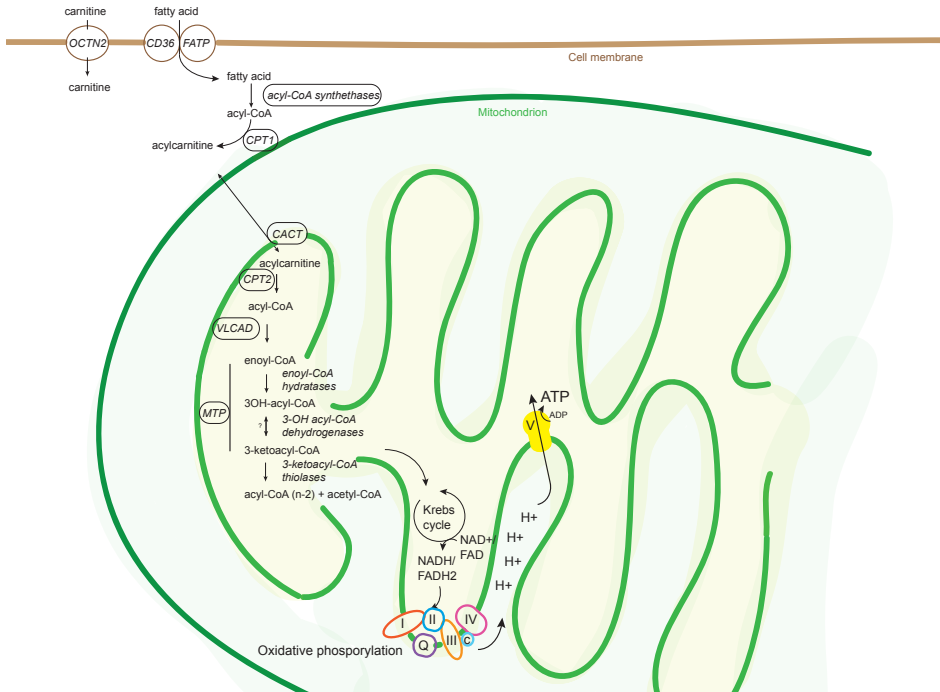


Figure 1. The long-chain fatty acid oxidation pathway. CD36-FATP/FABPpm = fatty acid transport proteins; OCTN2 = carnitine transporter; CPT1 = carnitine palmitoyltransferase 1; CPT2 = carnitine palmitoyl transferase 2; CACT = carnitine acylcarnitine translocase; VLCAD = very long-chain acyl-CoA dehydrogenase; MTP = mitochondrial trifunctional protein complex. I, II, III, IV, V (ATP-ase) and c (cytochrome c) = mitochondrial complex enzymes.

nitine deficiency, which was first described in 1975⁷. Intracellular carnitine is then used by CPT1 to convert acyl-CoA into acyl-carnitine. There are three isoforms of CPT1, including CPT1A (liver)⁴, CPT1B (muscle)⁴ and CPT1C (brain)⁸, but only patients with CPT1A deficiency (OMIM 255120) have been described. After acylcarnitine formation, CACT transports these acylcarnitines across the inner mitochondrial membrane⁹. Patients with CACT deficiency (OMIM 613698) were first described in 1992¹⁰. CACT deficiency is very rare and there is no common mutation that causes the disorder⁹ (Figure 1). The acylcarnitines have to be converted back to acyl-CoAs by CPT2. CPT2 deficiency (OMIM 600650) was the first FAO disorder described¹¹. It has an estimated incidence of 1:750.000¹²⁻¹⁵. The most common mutation (60%) causing CPT2 deficiency is the p.Ser113Leu amino acid substitution¹⁶. A deficiency of CPT2 results in accumulation of acylcarnitines within the mitochondria that can be transported to blood plasma via CACT and an unknown transporter in the cell membrane¹⁷.

VLCAD and VLCAD deficiency (OMIM 201475) were first described in 1992¹⁸. VLCAD deficiency is the most common long-chain fatty acid oxidation (lcFAO) disorder with an

incidence of 1:71.000-1:94.000¹³. No single common mutation has been described, but in the Netherlands p.Val283Ala is the most prevalent mutation. VLCAD is necessary for the first step in the mitochondrial β -oxidation cycle. VLCAD converts acyl-CoAs + FAD into trans-2-enoyl-CoA + FADH₂^{18,19}. Without VLCAD, saturated and unsaturated long-chain fatty acids (C12-CoA up to C18-CoA) accumulate in the mitochondria. These accumulating CoA esters will be converted into carnitine esters (C12-carnitine up to C18-carnitine) by CPT2, and subsequently transported out of the mitochondria via CACT and out of the cell via an unknown transporter (Figure 1)¹⁷. It has recently been discovered that C12-carnitine and C14:1-carnitine specifically accumulate, because of an alternative degradation route involving acyl-CoA dehydrogenase 9 (ACAD9)²⁰. VLCAD is, however, necessary for the further metabolism of C12-CoA and C14:1-CoA^{19,20}. The β -oxidation cycle of long-chain enoyl-CoAs is completed by MTP, a protein complex that harbours three enzyme activities including: an enoyl-CoA hydratase, 3-hydroxyacyl-CoA dehydrogenase (LCHAD) and 3-keto acyl-CoA thiolase activity. These three enzyme activities are encoded by 2 genes: HADHA and HADHB gene. MTP deficiency (OMIM 600890 and 143450) was first described in 1992²¹ with an estimated incidence of 1:250.000¹³. MTP deficiency results in an accumulation of enoyl-CoAs and depending on residual activity of the MTP complex also hydroxyacyl- and ketoacyl-CoAs (Figure 1). Isolated LCHAD deficiency (OMIM 600890) was first described in 1989²² with an incidence of >1:75.000-1:750.000¹³. The most frequent mutation that causes isolated LCHAD deficiency is p.Glu510Gln (c.1528G>C, allele frequency 86%²³). LCHAD converts 3-hydroxyacyl-CoA + NAD⁺ into 3-ketoacyl-CoA + NADH^{19,24-27}. Hydratase and thiolase activity are only mildly affected in isolated LCHAD deficiency.

DIAGNOSIS

Currently, a positive newborn screening result for an lcfAO disorder is the first step towards an lcfAO diagnosis in many countries around the world^{13,28}. Newborn screening is based on bloodspot measurement of acylcarnitines by tandem mass spectrometry. When a marker acylcarnitine level is above a certain threshold, neonates are referred to a consultant with metabolic expertise. To confirm diagnosis, plasma acylcarnitines and enzymatic activity (in lymphocytes or fibroblasts) can be measured. In addition, mutation analysis will often be performed. Subjects with a homozygous mutation or compound heterozygous mutations will be considered patients. To predict whether a patient is mildly or severely affected is difficult and subject of debate. Symptomatic carriers of heterozygote mutations have not been described so far, and are therefore not considered as patients. In VLCAD deficient patients, a genotype phenotype correlation has been established. Nonsense mutations result in a severe and early presentation²⁹⁻³¹,

the more frequent missense mutations are however associated with both severe or attenuated presentations³². A genotype phenotype correlation study in CPT2, LCHAD and MTP deficiency has not been performed. Based on literature it seems that not all LCHAD deficient patients with the same mutation experience the same symptoms²³.

SYMPTOMS

Without proper carnitine import into the cell/mitochondria (OCTN2/CACT deficiency), or conversion of acyl-CoA or acylcarnitines (CPT1A, CPT2 deficiency), or proper degradation of acyl-CoAs (VLCAD/MTP deficiency), long-chain fatty acids cannot be used for the production of acetyl-CoA. To compensate, a patient has to rely on glucose for the production of acetyl-CoA via glycolysis and pyruvate dehydrogenation. Glucose stores in the form of glycogen are limited. In resting conditions, a human has a glucose concentration of 5mmol/L, or 4500mg per 5 Liter blood. The body uses >120grams per 24h⁶ or 83mg/minute solely for the brain. This means that after 50 minutes, almost all circulating glucose molecule has been used by glycolysis. Therefore, amino acids derived from protein will also be converted into glucose via a process called gluconeogenesis. The breakdown of proteins is however a last resort, because it impairs normal cellular function. This is why fatty acid oxidation is so important.

Hypoglycemia

To prevent hypoglycemia and excessive erosion of protein stores, fatty acids have to be oxidized to produce acetyl-CoA. Acetyl-CoA is necessary 1) for the production of ATP (via Krebs cycle and oxidative phosphorylation) (Figure 1 and 2) for the production of ketones via ketogenesis. Patients that are not able to oxidize fatty acids are therefore at high risk of developing hypoketotic hypoglycemia and present with convulsions or develop coma, especially in catabolic situations, such as illness, fever, fasting and exercise. Hypoglycemia has been frequently reported in all IcFAO disorders³³.

Cardiomyopathy and arrhythmia

Besides hypoglycemia, patients can develop cardiomyopathy. A healthy heart relies on fatty acids for 60-90% of its energetic needs^{34,35}. The occurrence of cardiac problems such as hypertrophic or dilated cardiomyopathy and arrhythmias is therefore not surprising. Cardiomyopathy as a presenting symptom has been demonstrated in a few studies. According to literature 36 to 47 percent^{33,36} of VLCAD deficient patients had cardiomyopathy at the time of diagnosis. Thirty to 38 percent of MTP deficient patients^{37,38}; forty-six percent of LCHAD deficient²³ and an unknown percentage of patients with CACT⁹ and CPT2³⁹ deficiency had cardiomyopathy at time of diagnosis. Patients with CPT1A defi-

ciency have no cardiomyopathy⁴⁰. In OCTN2 deficient patients, dilated cardiomyopathy has been described⁴¹.

Another cardiac problem described as presenting symptom in patients with IcFAO disorders (except OCTN2 and CPT1A), is arrhythmia. In a retrospective study, twenty-three to thirty-one percent of IcFAO deficient patients presented with rhythm disturbances, primarily ventricular tachycardia^{42,43}. The primary focus of these studies was on presenting symptoms^{33,42,44}. Follow-up or cross-sectional studies of patients with IcFAO deficiencies with or without arrhythmias and/or cardiomyopathy have not yet been undertaken.

Myopathy

Patients with IcFAO disorders can develop skeletal myopathy. Muscle relies on fatty acid oxidation for much of its energetic needs, especially during exercise, despite the availability of glycogen. Skeletal myopathy most often involves the breakdown of muscle (rhabdomyolysis). The pathophysiology of myopathy and rhabdomyolysis in VLCAD deficient patients is not completely understood. The likely mechanisms behind the exercise-induced rhabdomyolysis and myopathy in VLCAD deficient are 1) a failing compensatory mechanism during requirement of extra energy (e.g. during exercise, illness, fever, fasting) or 2) toxicity caused by the accumulation of FAO intermediates. Reported muscle biopsies have remained inconclusive with normal muscle fibre structure, diffuse lipid accumulation in some biopsies and aspecific abnormalities⁴⁵.

Hepatomegaly

Hepatomegaly arises as a consequence of accumulating fatty acids in the liver with fatty liver disease. It is a frequently reported albeit subjective symptom (>92%)³³.

Peripheral neuropathy

In contrast to patients with OCTN2, CPT1A, CPT2 and VLCAD deficiency, patients with LCHAD and MTP deficiency can develop polyneuropathy (peripheral neuropathy)^{23,38,46}. The cause of polyneuropathy is unknown.

Retinopathy

LCHAD deficient patients (and MTP deficient patients but to a lesser extent) also develop retinopathy, in contrast to VLCAD and CPT2 deficiency⁴⁷⁻⁴⁹. What is causing the degeneration of the retina is unknown.

Other symptoms

Other symptoms such as feeding difficulties (LCHAD and MTP deficiency), lethargy (LCHAD and MTP deficiency) and psychomotor retardation have been described^{23,38}. For an overview of all symptoms per disorder and their frequency, see Table 1.

Table 1. Overview of all symptoms per disorder and their known frequency.

Symptoms	CPT1A	OCTN2	CACT	CPT2	VLCAD	MTP	LCHAD
mortality			high	+	37%-43%	76%	38%
hypoglycemia/lethargy	+	+	+	+	30%-43%	57%	30%
cardiomyopathy/ respiratory problems	-	+	+	+	52%-36%	73%	49%
arrhythmia	-	-	+		18%	10%	18%
myopathy/cramps/ rhabdomyolysis	-	+		96%	20%-4%	83%	
hypotonia	-	+	-	-	-	100%- 80%	61%
hepatomegaly/ hepatopathy	+	+	+	+	61%-96%	60%	78%
polyneuropathy	-	-	-	-	-	70%-70%	3%
Retinopathy	-	-	-	-	-	11%	29%
References	40	41	9	39	33,36,84	37,38,49,85	23,47

CURRENT THERAPIES

Most patients are advised to avoid prolonged fasting as this will result in a catabolic state and thus a need for fatty acid oxidation. Generally patients get frequent feedings and some have continuous nocturnal gastric drip-feeding as well. As patients grow older, fasting times can generally be prolonged. To get more insight into the maximal fasting time, a fasting test can be performed⁵⁰.

Long-chain fatty acid restriction

Dietary long-chain fatty acid restriction can be a component of dietary intervention. The rationale is to reduce the long-chain fatty acid load and hereby lowering possible toxic effects of long-chain acyl-CoA/acylcarnitine accumulation. The consequent loss in energy intake should be compensated by increasing the amount of carbohydrates and/or proteins in the diet and by medium-chain fatty acids supplementation⁵¹. No trials have been performed that tested the efficacy of LCT restriction. As for all different treatment options today, evidence is based on expert opinions in combination with consensus meetings (Table 2)⁵¹.

Table 2. Recommended dietary treatment of lcFAO deficient patients. Studies that describe dietary treatment of various lcFAO disorders based on expert opinions in combination with data from consensus meetings. These strict guidelines are currently subject of debate. MCT=medium-chain triglyceride; symp.= symptomatic; asymp.= asymptomatic.

	Age	Symptom	Dietary intervention
Arnold 2009	<12m	max. fasting time	1h per kg body wt up to 8h
		cardiomyopathy	symp. continuation bottled + max. MCT diet asymp. continuation breastfeeding + MCT supplementation
	<12m	hypoglycemia or myopathy	asymp. or continuation bottled + max. MCT supplementation
			symp. continuation breastfeeding/bottled + MCT supplementation
	>12m	cardiomyopathy	asymp. continuation breastfeeding or bottled feeding symp. LCT restriction + MCT supplementation
>12m	hypoglycemia or myopathy	asymp. continuation bottled + MCT supplementation symp. fasting prevention, LCT restriction, continuation breastfeeding/bottled + MCT supplementation	
Solis 2002	VLCAD deficiency		asymp. fasting prevention continuation breastfeeding/bottled + MCT supplementation increased frequency of meals supplementation with cornstarch (at night) fat restriction
		MTP/LCHAD deficiency	increased frequency of meals supplementation with cornstarch (at night) fat restriction supplementation with carnitine

Medium-chain triglyceride supplementation

Fat is an important energy source. In case of long-chain fatty acid restriction, patients need additional supply of calories, which is generally supplied in the form of extra carbohydrates. In patients with lcFAO deficiency, enzymes that degrade short and medium chain fatty acids are unaffected. Therefore theoretically, medium-chain fatty acids (C6-C12) can be broken down by medium-chain acyl-CoA dehydrogenase (MCAD). In addition, the liver will convert MCT into ketone bodies, which will also serve as an alternative energy source. No trials have been performed that tested the efficacy of MCT supplementation and MCT supplementation, as well as LCT restriction are therefore currently subject of debate (see also chapter 11, General Discussion).

Carnitine

In patients with lcFAO disorders, acylcarnitines accumulate and secondary carnitine deficiency can develop. Carnitine supplementation can replenish the carnitine level. Use of carnitine is however controversial since accumulation of long-chain acylcarnitines have been observed in hearts of VLCAD^{-/-} mice⁵² supplemented with carnitine. This is considered harmful since long-chain acylcarnitine accumulation has been associated with ventricular fibrillation⁵³. A recent study in which the LCAD^{-/-} mouse model was treated with carnitine contradicts these considerations⁵⁴. This mouse model has a more severe phenotype and resembles human VLCAD deficiency better than the VLCAD^{-/-} mouse model. This study revealed that carnitine supplementation is actually beneficial for the heart, alleviating toxicity by exporting acylcarnitines out of the myocardium, rather than promoting lipotoxicity⁵⁴.

Carbohydrates

To increase the amount of calories that are lost due to long-chain fatty acid restriction, carbohydrate intake is increased. Despite supplementation of carbohydrates and/or glucose IV, not all metabolic derailments with rhabdomyolysis or cardiomyopathy can be prevented⁵⁵⁻⁶⁰.

Protein

Protein content can be increased to counterbalance the loss of calories due to long-chain fatty acid restriction (max 1.5g/kg/day, or 10-35En%). In literature no significant side effects of a high protein diet are described in lcFAO deficient⁶¹ and healthy people^{62,63}.

Triheptanoic

Depletion of catalytic units from the Krebs cycle may further decrease energy levels in lcFAO deficient patients. This depletion could occur because of leakage of intermediates from the Krebs out of the cells, called cataplerosis. The mechanisms that should

refill the pools of these intermediates, anaplerosis, cannot compensate for the excessive leakage^{64,65}. Supplementation of these Krebs cycle intermediates by triheptanoin is therefore proposed. Triheptanoin, a medium-odd-chain fatty acid (C7), is degraded to form acetyl-CoA and propionyl-CoA. Propionyl-CoA is an efficient anaplerotic substrate, because carboxylation of propionyl-CoA leads to formation of succinyl-CoA, which is a Krebs cycle intermediate. A pilot study in three patients demonstrated beneficial effects in patients with severe IcFAO disorders⁶⁴. Several clinical trials are currently in progress to evaluate the potential beneficial effect in a larger cohort.

Small molecules: Bezafibrate/Resveratrol

Mitochondrial FAO enzymes are transcriptionally regulated^{66,67}. Mitochondrial function can therefore be restored via pharmacological approaches at various levels⁶⁸. This includes mitochondrial quality control, energy production, and dynamics, i.e. fusion and fission of mitochondria.

One way to increase mitochondrial function is to stimulate transcription of FAO enzymes via Peroxisome Proliferator-Activated Receptor (PPAR) agonists. Bezafibrate is such a PPAR-agonist. It has been investigated primarily in fibroblasts of IcFAO deficient patients^{15,69-73}. An overall beneficial effect of bezafibrate on FAO has been demonstrated (see Table 3 for an overview). This beneficial effect is supported by a pilot study in humans with CPT2 deficiency¹⁴. Clinical trials with more patients are necessary to validate these potentially beneficial effects⁷⁴. Another (co-)activator of PPARs is the Peroxisome Proliferator-Activated Receptor γ co-activator-1 α (PGC-1 α). PGC1 α also activates a number of other transcription factors and is one of the main regulators of mitochondrial biogenesis and mitochondrial oxidative metabolism⁷⁵. Several classes of molecules have been identified to be involved in the activation of PGC-1 α ⁷⁶. Resveratrol activates the energy sensor AMPK (AMP-activated protein kinase) and SIRT1 (Sirtuin 1, deacetylase) thereby inducing mitochondrial biogenesis via PGC-1 α ⁷⁶ (Figure 2).

Bezafibrate has been used as a hypolipidemic drug for more than 30 years⁷⁷. Resveratrol is a naturally occurring compound that can be used at relatively high concentrations without obvious side effects. Resveratrol has even been tested as anti-obesity therapy in humans⁷⁸. Hence, both bezafibrate and resveratrol have been used previously for the treatment of other metabolic disorders, and are thus attractive compounds for the treatment of FAO deficiency.

Table 3. The effects of various treatments on IcfAO in fibroblasts. Studies that describe the effects of bezafibrate, resveratrol and AICAR on a biochemical level. EA=enzymatic activity; Flux=FAO-flux; sign.= significant

Reference	Disorder	Tissue	Compound	dosage	Enzyme activity
Djouadi 2003	CPT2	fibroblasts	bezafibrate	800uM 3d	EA: sign. increase +54%-135% in 4 mild patient fibroblasts (40-70% residual activity of controls). No change in 2 severe patient fibroblasts.
Djouadi 2005	CPT2	myoblasts	bezafibrate	200uM 2d	Acylcarnitine measurement after palmitate loading: normalization acylcarnitines
Bonnefont 2010	CPT2	humans	bezafibrate	200mg	Flux: ¹⁴ C trend; Fatima test: sign. increased FAO-flux (palmitoyl-CoA oxidation) +39%-206% in 6 patient muscle (19-50% residual activity of controls).
Djouadi 2005	VLCAD	fibroblasts	bezafibrate	500uM 2d	EA: sign. increase +80%-775% in 3 mild patient fibroblasts (15-20% residual activity of controls). No change in 1 severe patient fibroblasts.
Li 2010	VLCAD	fibroblasts	bezafibrate	400uM 3d	Acylcarnitine measurement after palmitate loading test: sign. decrease AC's
Gobin-Limballe 2007	VLCAD	fibroblasts	bezafibrate	400uM 2d	EA: sign. increases in 2/3 'groups', 50%-230% and full restoration
Yamaguchi 2012	IcfAO	fibroblasts	bezafibrate	400uM 3d	
Bastin 2011	VLCAD	fibroblasts	resveratrol	75uM 2d	Acylcarnitine measurement after palmitate loading: sign. increase FAO-flux (palm. Ox) +50%→360% in 11/13 patients (mild)
	CPT2	fibroblasts	resveratrol	75uM 2d	Acylcarnitine measurement after palmitate loading: sign. increase FAO-flux (palm. Ox) 40%→80% in 5/6 patients (mild)
Bastin 2011	CPT2 and VLCAD	fibroblasts	aicar	500uM	EA: no change in activity

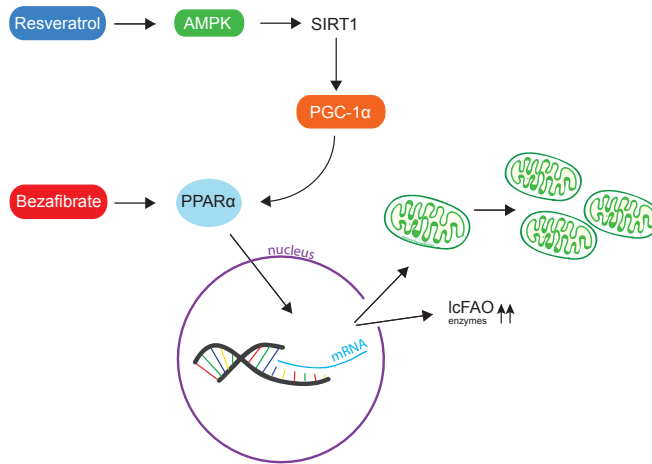


Figure 2. Compounds that induce mitochondrial biogenesis and function. AMPK = AMP activated protein kinase; PGC-1 α = Peroxisome Proliferator-Activated Receptor γ co-activator-1 α ; PPAR α = Peroxisome Proliferator-Activated Receptor

MOUSE MODELS

Mouse models are vital to study the pathogenesis of human inherited metabolic disorders. Several knock-out FAO mouse models have been developed. The VLCAD^{-/-} mouse has a mild phenotype with slight hepatic steatosis, microvesicular lipid accumulation in the heart, and facilitated induction of polymorphic ventricular tachycardia in response to fasting and cold challenge²⁴⁻²⁷. The LCAD^{-/-} mouse model displays a severe phenotype with fasting-induced hypoglycemia and hepatomegaly, hypertrophic cardiomyopathy, and an acylcarnitine profile comparable to VLCAD deficiency in humans^{24,34,65,66,79,80}. However, clinically relevant and important symptoms such as fatigability, exercise intolerance, and myopathy cannot be investigated in the current mouse models.

MTP^{-/-} and CPT1a/b^{-/-} mouse models have been characterized, but these mice all die in the neonatal or embryonic stage⁸¹⁻⁸³ and can consequently not be used for experimental studies.

OUTLINE OF THESIS

While newborn screening in IcfAO deficient patients is performed using bloodspot acylcarnitine analysis, the follow-up of patients with a IcfAO disorder is usually done by

plasma acylcarnitine analysis. In **chapter 2**, the differences between acylcarnitine profiles in plasma and bloodspots are described. Although bloodspot acylcarnitine analysis is a good way to determine very long-chain acyl-CoA dehydrogenase (VLCAD) deficiency, patients were missed. In **chapter 3** a new marker that enhanced the sensitivity to detect VLCAD deficiency are described. A major challenge in VLCAD deficiency is however to predict disease severity based on biochemical and molecular testing. In **chapter 4**, the best predictor for clinical outcome of VLCAD deficient patients was investigated. Fatty acid oxidation flux in cultured fibroblasts appeared to be the best predictor.

Many clinical studies in the past have focused on disease presentations. In **chapter 5**, cardiac function of lcFAO deficient children that have been diagnosed years before is described. Normal cardiac function with only a minimal decrease in myocardial contractility was observed. In **chapter 6**, the consequences of rhabdomyolysis on muscle of patients with lcFAO disorders have been visualized. Specific abnormalities are observed on MRI, which may reflect lipid accumulation secondary to lcFAO deficiency or due to accumulating muscle damage.

To investigate the cause of rhabdomyolysis of which the pathogenic basis has been poorly understood, MRS during prolonged exercise of the vastus lateralis muscle was performed. In **chapter 7**, impaired ATP homeostasis during prolonged exercise in VLCADD patients was described. Mouse models are crucial to gain mechanistic insight in disease symptoms. In **chapter 8**, a new mouse model for lcFAO deficiency was studied. Fasting lowers energy expenditure and induces inactivity in these mice.

Surgical procedures in patients with lcFAO disorders require specific measures to improve energy homeostasis and reduce long-chain fatty acid load to prevent symptoms such as rhabdomyolysis. Hence, a specific perioperative regimen in patients with very long chain acyl-CoA dehydrogenase deficiency (VLCADD) is discussed in **chapter 9**.

Newborn screening does not discriminate between isolated LCHAD deficiency, isolated long-chain keto acyl-CoA (LCKAT) deficiency and general mitochondrial trifunctional protein (MTP) deficiency. In **chapter 10** a classification system to discriminate between these disorders based on enzymatic measurements is described and applied to two new cases. One of whom presented with necrotizing enterocolitis, a symptom previously not associated with MTP deficiency. Finally, in chapter 11, all the findings are discussed and future research directions are provided.

REFERENCES

1. Gidez LI. The lore of lipids. *The Journal of Lipid Research*. 1984;25(13):1430–1436.
2. Leray C. Cyberlipid. www.cyberlipid.org. 2013.
3. Ghisla S. β -Oxidation of fatty acids. *European Journal of Biochemistry*. 2004. doi:10.1046/j.1432-1033.2003.03952.x.
4. Houten SM, Wanders RJA. A general introduction to the biochemistry of mitochondrial fatty acid β -oxidation. *J Inherit Metab Dis*. 2010;33(5):469–477. doi:10.1007/s10545-010-9061-2.
5. Hautvast JGAJ. Gezondheidsraad: energie, eiwitten, vetten en verteerbare koolhydraten. 2002:1–174.
6. Frayn KN. *Metabolic Regulation*. John Wiley & Sons; 2013.
7. Karpati G, Carpenter S, Engel AG, et al. The syndrome of systemic carnitine deficiency. Clinical, morphologic, biochemical, and pathophysiologic features. *Neurology*. 1975;25(1):16–24.
8. Wolfgang MJ, Kurama T, Dai Y, et al. The brain-specific carnitine palmitoyltransferase-1c regulates energy homeostasis. *Proc Natl Acad Sci USA*. 2006;103(19):7282–7287. doi:10.1073/pnas.0602205103.
9. Rubio-Gozalbo ME, Bakker JA, Waterham HR, Wanders RJA. Carnitine-acylcarnitine translocase deficiency, clinical, biochemical and genetic aspects. *Mol Aspects Med*. 2004;25(5-6):521–532. doi:10.1016/j.mam.2004.06.007.
10. Stanley CA, Hale DE, Berry GT, Deleeuw S, Boxer J, Bonnefont JP. Brief report: a deficiency of carnitine-acylcarnitine translocase in the inner mitochondrial membrane. *New England Journal of Medicine*. 1992;327(1):19–23. doi:10.1056/NEJM199207023270104.
11. DiMauro S, DiMauro PM. Muscle carnitine palmitoyltransferase deficiency and myoglobinuria. *Science*. 1973;182(4115):929–931.
12. Bastin J, Lopes-Costa A, Djouadi F. Exposure to resveratrol triggers pharmacological correction of fatty acid utilization in human fatty acid oxidation-deficient fibroblasts. *Hum Mol Genet*. 2011;20(10):2048–2057. doi:10.1093/hmg/ddr089.
13. Lindner M, Hoffmann GF, Matern D. Newborn screening for disorders of fatty-acid oxidation: experience and recommendations from an expert meeting. *J Inherit Metab Dis*. 2010;33(5):521–526. doi:10.1007/s10545-010-9076-8.
14. Bonnefont JP, Bastin J, Laforêt P, et al. Long-term follow-up of bezafibrate treatment in patients with the myopathic form of carnitine palmitoyltransferase 2 deficiency. *Clin Pharmacol Ther*. 2010;88(1):101–108. doi:10.1038/clpt.2010.55.
15. Bonnefont J-P, Bastin J, Behin A, Djouadi F. Bezafibrate for an inborn mitochondrial beta-oxidation defect. *N Engl J Med*. 2009;360(8):838–840. doi:10.1056/NEJMc0806334.
16. Wieser T, Deschauer M, Olek K, Hermann T, Zierz S. Carnitine palmitoyltransferase II deficiency: molecular and biochemical analysis of 32 patients. *Neurology*. 2003;60(8):1351–1353. doi:10.1212/01.WNL.0000055901.58642.48.
17. Violante S, IJLst L, van Lenthe H, de Almeida IT, WANDERS RJ, Ventura FV. Carnitine palmitoyltransferase 2: New insights on the substrate specificity and implications for acylcarnitine profiling. *Biochim Biophys Acta*. 2010;1802(9):728–732. doi:10.1016/j.bbadis.2010.06.002.
18. Iwai K, Uchida Y, Orii T, Yamamoto S, Hashimoto T. Novel fatty acid beta-oxidation enzymes in rat liver mitochondria. I. Purification and properties of very-long-chain acyl-coenzyme A dehydrogenase. *J Biol Chem*. 1992;267(2):1027–1033.

19. Wanders RJA, Ruiten JPN, IJLst L, Waterham HR, Houten SM. The enzymology of mitochondrial fatty acid beta-oxidation and its application to follow-up analysis of positive neonatal screening results. *J Inherit Metab Dis*. 2010;33(5):479–494. doi:10.1007/s10545-010-9104-8.
20. Nouws J, Brinke te H, Nijtmans LG, Houten SM. ACAD9, a complex I assembly factor with a moonlighting function in fatty acid oxidation deficiencies. *Hum Mol Genet*. 2013. doi:10.1093/hmg/ddt521.
21. Wanders RJ, IJlst L, Poggi F, et al. Human trifunctional protein deficiency: a new disorder of mitochondrial fatty acid beta-oxidation. *Biochem Biophys Res Commun*. 1992;188(3):1139–1145.
22. Wanders RJ, Duran M, IJlst L, et al. Sudden infant death and long-chain 3-hydroxyacyl-CoA dehydrogenase. *Lancet*. 1989;2(8653):52–53.
23. Boer den MEJ, Wanders RJA, Morris AAM, IJlst L, Heymans HSA, Wijburg FA. Long-chain 3-hydroxyacyl-CoA dehydrogenase deficiency: clinical presentation and follow-up of 50 patients. *Pediatrics*. 2002;109(1):99–104.
24. Cox KB, Hamm DA, Millington DS, et al. Gestational, pathologic and biochemical differences between very long-chain acyl-CoA dehydrogenase deficiency and long-chain acyl-CoA dehydrogenase deficiency in the mouse. *Hum Mol Genet*. 2001;10(19):2069–2077.
25. Exil VJ, Roberts RL, Sims H, et al. Very-long-chain acyl-coenzyme a dehydrogenase deficiency in mice. *Circ Res*. 2003;93(5):448–455. doi:10.1161/01.RES.0000088786.19197.E4.
26. Exil VJ, Gardner CD, Rottman JN, et al. Abnormal mitochondrial bioenergetics and heart rate dysfunction in mice lacking very-long-chain acyl-CoA dehydrogenase. *Am J Physiol Heart Circ Physiol*. 2006;290(3):H1289–97. doi:10.1152/ajpheart.00811.2005.
27. Veld ter F, Primassin S, Hoffmann L, MAYATEPEK E, Spiekerkoetter U. Corresponding increase in long-chain acyl-CoA and acylcarnitine after exercise in muscle from VLCAD mice. *The Journal of Lipid Research*. 2009;50(8):1556–1562. doi:10.1194/jlr.M800221-JLR200.
28. Loeber JG, Burgard P, Cornel MC, et al. Newborn screening programmes in Europe; arguments and efforts regarding harmonization. Part 1. From blood spot to screening result. *J Inherit Metab Dis*. 2012;35(4):603–611. doi:10.1007/s10545-012-9483-0.
29. Andresen BS, Olpin S, Poorthuis BJ, et al. Clear correlation of genotype with disease phenotype in very-long-chain acyl-CoA dehydrogenase deficiency. *Am J Hum Genet*. 1999;64(2):479–494. doi:10.1086/302261.
30. Mathur A, Sims HF, Gopalakrishnan D, et al. Molecular heterogeneity in very-long-chain acyl-CoA dehydrogenase deficiency causing pediatric cardiomyopathy and sudden death. *Circulation*. 1999;99(10):1337–1343. doi:10.1161/01.CIR.99.10.1337.
31. Gregersen N, Andresen BS, Corydon MJ, et al. Mutation analysis in mitochondrial fatty acid oxidation defects: Exemplified by acyl-CoA dehydrogenase deficiencies, with special focus on genotype–phenotype relationship. *Hum Mutat*. 2001;18(3):169–189. doi:10.1002/humu.1174.
32. Hoffmann L, Haussmann U, Mueller M, Spiekerkoetter U. VLCAD enzyme activity determinations in newborns identified by screening: a valuable tool for risk assessment. *J Inherit Metab Dis*. 2011. doi:10.1007/s10545-011-9391-8.
33. Baruteau J, Sachs P, Broué P, et al. Clinical and biological features at diagnosis in mitochondrial fatty acid beta-oxidation defects: a French pediatric study from 187 patients. Complementary data. *J Inherit Metab Dis*. 2014;37(1):137–139. doi:10.1007/s10545-013-9628-9.
34. Houten SM, Herrema H, Brinke te H, et al. Impaired amino acid metabolism contributes to fasting-induced hypoglycemia in fatty acid oxidation defects. *Hum Mol Genet*. 2013;22(25):5249–5261. doi:10.1093/hmg/ddt382.

35. Hue L, Taegtmeyer H. The Randle cycle revisited: a new head for an old hat. *AJP: Endocrinology and Metabolism*. 2009;297(3):E578–91. doi:10.1152/ajpendo.00093.2009.
36. Vianey-Saban C, Divry P, Brivet M, et al. Mitochondrial very-long-chain acyl-coenzyme A dehydrogenase deficiency: clinical characteristics and diagnostic considerations in 30 patients. *Clin Chim Acta*. 1998;269(1):43–62.
37. Spiekerkoetter U, Sun B, Khuchua Z, Bennett MJ, Strauss AW. Molecular and phenotypic heterogeneity in mitochondrial trifunctional protein deficiency due to beta-subunit mutations. *Hum Mutat*. 2003;21(6):598–607. doi:10.1002/humu.10211.
38. Boer den MEJ, Dionisi-Vici C, Chakrapani A, van Thuijl AOJ, Wanders RJA, Wijburg FA. Mitochondrial trifunctional protein deficiency: a severe fatty acid oxidation disorder with cardiac and neurologic involvement. *J Pediatr*. 2003;142(6):684–689. doi:10.1067/mpd.2003.231.
39. Bonnefont JP, Demaugre F, Prip-Buus C, et al. Carnitine palmitoyltransferase deficiencies. *Molecular Genetics and Metabolism*. 1999;68(4):424–440. doi:10.1006/mgme.1999.2938.
40. Bonnefont J-P, Djouadi F, Prip-Buus C, Gobin S, Munnich A, Bastin J. Carnitine palmitoyltransferases 1 and 2: biochemical, molecular and medical aspects. *Mol Aspects Med*. 2004;25(5-6):495–520. doi:10.1016/j.mam.2004.06.004.
41. Shibbani K, Fahed AC, Al-Shaar L, et al. Primary carnitine deficiency: novel mutations and insights into the cardiac phenotype. *Clin Genet*. 2014;85(2):127–137. doi:10.1111/cge.12112.
42. Bonnet D, Martin D, Pascale de Lonlay, et al. Arrhythmias and conduction defects as presenting symptoms of fatty acid oxidation disorders in children. *Circulation*. 1999;100(22):2248–2253. doi:10.1161/01.CIR.100.22.2248.
43. Baruteau J, Sachs P, Broué P, et al. Clinical and biological features at diagnosis in mitochondrial fatty acid beta-oxidation defects: a French pediatric study of 187 patients. *J Inherit Metab Dis*. 2012. doi:10.1007/s10545-012-9542-6.
44. Saudubray JM, Martin D, de Lonlay P, et al. Recognition and management of fatty acid oxidation defects: a series of 107 patients. *J Inherit Metab Dis*. 1999;22(4):488–502.
45. Laforêt P, Vianey-Saban C. Disorders of muscle lipid metabolism: diagnostic and therapeutic challenges. *Neuromuscul Disord*. 2010;20(11):693–700. doi:10.1016/j.nmd.2010.06.018.
46. Spiekerkoetter U, Khuchua Z, Yue Z, Bennett MJ, Strauss AW. General mitochondrial trifunctional protein (TFP) deficiency as a result of either alpha- or beta-subunit mutations exhibits similar phenotypes because mutations in either subunit alter TFP complex expression and subunit turnover. *Pediatric Research*. 2004;55(2):190–196. doi:10.1203/01.PDR.0000103931.80055.06.
47. Tyni T, Johnson M, Eaton S, Pourfarzam M, Andrews R, Turnbull DM. Mitochondrial fatty acid beta-oxidation in the retinal pigment epithelium. *Pediatric Research*. 2002;52(4):595–600. doi:10.1203/00006450-200210000-00021.
48. Oey NA, Ruiten JPN, Attié-Bitach T, IJLst L, Wanders RJA, Wijburg FA. Fatty acid oxidation in the human fetus: implications for fetal and adult disease. *J Inherit Metab Dis*. 2006;29(1):71–75. doi:10.1007/s10545-006-0199-x.
49. Fletcher AL, Pennesi ME, Harding CO, Weleber RG, Gillingham MB. Observations regarding retinopathy in mitochondrial trifunctional protein deficiencies. *Molecular Genetics and Metabolism*. 2012. doi:10.1016/j.ymgme.2012.02.015.
50. van Veen MR, van Hasselt PM, de Sain-van der Velden MGM, et al. Metabolic profiles in children during fasting. *Pediatrics*. 2011;127(4):e1021–7. doi:10.1542/peds.2010-1706.
51. Arnold GL, VanHove J, Freedenberg D, et al. A Delphi clinical practice protocol for the management of very long chain acyl-CoA dehydrogenase deficiency. *Molecular Genetics and Metabolism*. 2009;96(3):85–90. doi:10.1016/j.ymgme.2008.09.008.

52. Primassin S, Veld ter F, MAYATEPEK E, Spiekerkoetter U. Carnitine supplementation induces acylcarnitine production in tissues of very long-chain acyl-CoA dehydrogenase-deficient mice, without replenishing low free carnitine. *Pediatric Research*. 2008;63(6):632–637. doi:10.1203/PDR.0b013e31816ff6f0.
53. Corr PB, Creer MH, Yamada KA, Saffitz JE, Sobel BE. Prophylaxis of early ventricular fibrillation by inhibition of acylcarnitine accumulation. *J Clin Invest*. 1989;83(3):927–936. doi:10.1172/JCI113978.
54. Bakermans AJ, van Weeghel M, Denis S, Nicolay K, Prompers JJ, Houten SM. Carnitine supplementation attenuates myocardial lipid accumulation in long-chain acyl-CoA dehydrogenase knockout mice. *J Inherit Metab Dis*. 2013. doi:10.1007/s10545-013-9604-4.
55. Brown-Harrison MC, Nada MA, Sprecher H, et al. Very long chain acyl-CoA dehydrogenase deficiency: successful treatment of acute cardiomyopathy. *Biochem Mol Med*. 1996;58(1):59–65.
56. Souri M, Aoyama T, Orii K, Yamaguchi S, Hashimoto T. Mutation analysis of very-long-chain acyl-coenzyme A dehydrogenase (VLCAD) deficiency: identification and characterization of mutant VLCAD cDNAs from four patients. *Am J Hum Genet*. 1996;58(1):97–106.
57. Andresen BS, Bross P, Vianey-Saban C, et al. Cloning and characterization of human very-long-chain acyl-CoA dehydrogenase cDNA, chromosomal assignment of the gene and identification in four patients of nine different mutations within the VLCAD gene. *Hum Mol Genet*. 1996;5(4):461–472.
58. Sluysmans T, Tuerlinckx D, Hubinont C, Verellen-Dumoulin C, Brivet M, Vianey-Saban C. Very long chain acyl-coenzyme A dehydrogenase deficiency in two siblings: evolution after prenatal diagnosis and prompt management. *J Pediatr*. 1997;131(3):444–446.
59. Touma EH, Rashed MS, Vianey-Saban C, et al. A severe genotype with favourable outcome in very long chain acyl-CoA dehydrogenase deficiency. *Arch Dis Child*. 2001;84(1):58–60. doi:10.1136/adc.84.1.58.
60. Spiekerkoetter U, Tenenbaum T, Heusch A, Wendel U. Cardiomyopathy and pericardial effusion in infancy point to a fatty acid b-oxidation defect after exclusion of an underlying infection. *Pediatr Cardiol*. 2003;24(3):295–297. doi:10.1007/s00246-002-0277-2.
61. Gillingham MB, Purnell JQ, Jordan J, Stadler D, Haqq AM, Harding CO. Effects of higher dietary protein intake on energy balance and metabolic control in children with long-chain 3-hydroxy acyl-CoA dehydrogenase (LCHAD) or trifunctional protein (TFP) deficiency. *Molecular Genetics and Metabolism*. 2007;90(1):64–69. doi:10.1016/j.ymgme.2006.08.002.
62. Virtue S, Even P, Vidal-Puig A. Below thermoneutrality, changes in activity do not drive changes in total daily energy expenditure between groups of mice. *Cell Metabolism*. 2012;16(5):665–671. doi:10.1016/j.cmet.2012.10.008.
63. Martin WF, Armstrong LE, Rodriguez NR. Dietary protein intake and renal function. *Nutr Metab (Lond)*. 2005;2:25. doi:10.1186/1743-7075-2-25.
64. Roe CR, Sweetman L, Roe DS, David F, Brunengraber H. Treatment of cardiomyopathy and rhabdomyolysis in long-chain fat oxidation disorders using an anaplerotic odd-chain triglyceride. *J Clin Invest*. 2002;110(2):259–269. doi:10.1172/JCI15311.
65. Bakermans AJ, Dodd MS, Nicolay K, Prompers JJ, Tyler DJ, Houten SM. Myocardial energy shortage and unmet anaplerotic needs in the fasted long-chain acyl-CoA dehydrogenase knockout mouse. *Cardiovasc Res*. 2013. doi:10.1093/cvr/cvt212.
66. Kurtz DM, Rinaldo P, Rhead WJ, et al. Targeted disruption of mouse long-chain acyl-CoA dehydrogenase gene reveals crucial roles for fatty acid oxidation. *Proc Natl Acad Sci USA*. 1998;95(26):15592–15597.

67. Lee C-H, Olson P, Evans RM. Minireview: lipid metabolism, metabolic diseases, and peroxisome proliferator-activated receptors. *Endocrinology*. 2003;144(6):2201–2207. doi:10.1210/en.2003-0288.
68. Andreux PA, Houtkooper RH, Auwerx J. Pharmacological approaches to restore mitochondrial function. *Nat Rev Drug Discov*. 2013;12(6):465–483. doi:10.1038/nrd4023.
69. Gobin-Limballe S, Djouadi F, Aubey F, et al. Genetic basis for correction of very-long-chain acyl-coenzyme A dehydrogenase deficiency by bezafibrate in patient fibroblasts: toward a genotype-based therapy. *Am J Hum Genet*. 2007;81(6):1133–1143. doi:10.1086/522375.
70. Djouadi F, Bonnefont J-P, Munnich A, Bastin J. Characterization of fatty acid oxidation in human muscle mitochondria and myoblasts. *Molecular Genetics and Metabolism*. 2003;78(2):112–118. doi:10.1016/S1096-7192(03)00017-9.
71. Djouadi F. Bezafibrate increases very-long-chain acyl-CoA dehydrogenase protein and mRNA expression in deficient fibroblasts and is a potential therapy for fatty acid oxidation disorders. *Hum Mol Genet*. 2005;14(18):2695–2703. doi:10.1093/hmg/ddi303.
72. Li H, Fukuda S, Hasegawa Y, et al. Effect of heat stress and bezafibrate on mitochondrial beta-oxidation: comparison between cultured cells from normal and mitochondrial fatty acid oxidation disorder children using in vitro probe acylcarnitine profiling assay. *Brain Dev*. 2010;32(5):362–370. doi:10.1016/j.braindev.2009.06.001.
73. Yamaguchi S, Li H, Purevsuren J, et al. Bezafibrate can be a new treatment option for mitochondrial fatty acid oxidation disorders: Evaluation by in vitro probe acylcarnitine assay. *Molecular Genetics and Metabolism*. 2012. doi:10.1016/j.ymgme.2012.07.004.
74. Orngreen MC, Madsen KL, Preisler N, Andersen G, Vissing J, Laforêt P. Bezafibrate in skeletal muscle fatty acid oxidation disorders: A randomized clinical trial. *Neurology*. 2014. doi:10.1212/WNL.0000000000000118.
75. Finck BN, Kelly DP. PGC-1 coactivators: inducible regulators of energy metabolism in health and disease. *J Clin Invest*. 2006;116(3):615–622. doi:10.1172/JCI27794.
76. Cantó C, Auwerx J. PGC-1 α , SIRT1 and AMPK, an energy sensing network that controls energy expenditure. *Curr Opin Lipidol*. 2009;20(2):98–105. doi:10.1097/MOL.0b013e328328d0a4.
77. Tenenbaum A, Motro M, Fisman EZ. Dual and pan-peroxisome proliferator-activated receptors (PPAR) co-agonism: the bezafibrate lessons. *Cardiovasc Diabetol*. 2005;4:14. doi:10.1186/1475-2840-4-14.
78. Timmers S, Auwerx J, Schrauwen P. The journey of resveratrol from yeast to human. *Aging (Albany NY)*. 2012;4(3):146–158.
79. Chegary M, Brinke HT, Ruiten JPN, et al. Mitochondrial long chain fatty acid beta-oxidation in man and mouse. *Biochim Biophys Acta*. 2009;1791(8):806–815. doi:10.1016/j.bbali.2009.05.006.
80. Bakermans AJ, Geraedts TR, van Weeghel M, et al. Fasting-Induced Myocardial Lipid Accumulation in Long-Chain Acyl-CoA Dehydrogenase Knockout Mice Is Accompanied by Impaired Left Ventricular Function. *Circulation: Cardiovascular Imaging*. 2011;4(5):558–565. doi:10.1161/CIRCIMAGING.111.963751.
81. Ibdah JA, Paul H, Zhao Y, et al. Lack of mitochondrial trifunctional protein in mice causes neonatal hypoglycemia and sudden death. *J Clin Invest*. 2001;107(11):1403–1409. doi:10.1172/JCI12590.
82. Nyman LR, Cox KB, Hoppel CL, et al. Homozygous carnitine palmitoyltransferase 1a (liver isoform) deficiency is lethal in the mouse. *Molecular Genetics and Metabolism*. 2005;86(1-2):179–187. doi:10.1016/j.ymgme.2005.07.021.

83. Ji S, You Y, Kerner J, et al. Homozygous carnitine palmitoyltransferase 1b (muscle isoform) deficiency is lethal in the mouse. *Molecular Genetics and Metabolism*. 2008;93(3):314–322. doi:10.1016/j.ymgme.2007.10.006.
84. Laforêt P, Acquaviva-Bourdain C, Rigal O, et al. Diagnostic assessment and long-term follow-up of 13 patients with Very Long-Chain Acyl-Coenzyme A dehydrogenase (VLCAD) deficiency. *Neuromuscul Disord*. 2009;19(5):324–329. doi:10.1016/j.nmd.2009.02.007.
85. Spiekerkoetter U, Bennett MJ, Ben-Zeev B, Strauss AW, Tein I. Peripheral neuropathy, episodic myoglobinuria, and respiratory failure in deficiency of the mitochondrial trifunctional protein. *Muscle Nerve*. 2004;29(1):66–72. doi:10.1002/mus.10500.

CHAPTER 2

Differences between acylcarnitine profiles in plasma and bloodspots

Monique G.M. de Sain-van der Velden¹, Eugene F. Diekman²,
Judith J. Jans¹, Maria van der Ham¹, Berthil H.C.M.T. Prinsen¹, Gepke Visser²,
Nanda M. Verhoeven-Duif²

¹ Department of Medical Genetics, UMC Utrecht, The Netherlands Wilhelmina Children's Hospital, University Medical Centre (UMC) Utrecht, Utrecht, The Netherlands

² Department of Metabolic Diseases, UMC Utrecht, The Netherlands Wilhelmina Children's Hospital, University Medical Centre (UMC) Utrecht, Utrecht, The Netherlands

Molecular Genetics and Metabolism, 2013, doi:10.1016/j.ymgme.2013.04.008

ABSTRACT

Quantification of acylcarnitines is used for screening and diagnosis of inborn error of metabolism (IEM). While newborn screening is performed in dried blood spots (DBSs), general metabolic investigation is often performed in plasma. Information on the correlation between plasma and DBS acylcarnitine profiles is scarce. In this study, we directly compared acylcarnitine concentrations measured in DBS with those in the corresponding plasma sample. Additionally, we tested whether ratios of acylcarnitines in both matrices are helpful for diagnostic purpose when primary markers fail.

Study design: DBS and plasma were obtained from controls and patients with a known IEM. (Acyl)carnitines were converted to their corresponding butyl esters and analyzed using HPLC/MS/MS.

Results: Free carnitine concentrations were 36% higher in plasma compared to DBS. In contrast, in patients with carnitine palmitoyltransferase 1 (CPT1) deficiency free carnitine concentration in DBS was 4 times the concentration measured in plasma. In carnitine palmitoyltransferase 2 (CPT2) deficiency, primary diagnostic markers were abnormal in plasma but could also be normal in DBS. The calculated ratios for CPT1 ($C0/(C16 + C18)$) and CPT2 ($(C16 + C18:1)/C2$) revealed abnormal values in plasma. However, normal ratios were found in DBS of two (out of five) samples obtained from patients diagnosed with CPT2.

Conclusions: Relying on primary acylcarnitine markers, CPT1 deficiency can be missed when analysis is performed in plasma, whereas CPT2 deficiency can be missed when analysis is performed in DBS. Ratios of the primary markers to other acylcarnitines restore diagnostic recognition completely for CPT1 and CPT2 in plasma, while CPT2 can still be missed in DBS.

INTRODUCTION

As the mitochondrial membrane is impermeable to long chain fatty acids, the carnitine shuttle is used to import acyl-CoA's. Acyl-CoA's can cross the mitochondrial membrane via carnitine acylcarnitine translocase (CACT) after conversion to acylcarnitines by carnitine-palmitoyl CoA transferase 1 (CPT1). Reconversion of acylcarnitines to acyl-CoA's by carnitine-palmitoyl CoA transferase 2 (CPT2) provides very-long chain acyl-CoA dehydrogenase (VLCAD) with the degradable acyl-CoA's to ensure energy supply. In addition, potentially toxic acyl-CoA's can be removed via the same route. Accumulation of specific acyl-CoA's due to a metabolic block leaves the cell as acylcarnitines^{1,2}.

In body fluids, the acylcarnitine profile is not only a diagnostic test for inherited disorders of fatty acid metabolism, but also for defects in branched-chain amino acid catabolism². Patients with these types of metabolic disorders accumulate disease-specific acylcarnitines, since degradation of amino acids produces, in many cases, odd-chain acyl-compounds that are esterified with carnitine.

While in biochemical genetic laboratories plasma is routinely used for acylcarnitine analysis, newborn screening programs use whole blood dried on filter paper (DBS) as the standard specimen. Newborns who show abnormal screening results are referred to the clinical unit for diagnosis and treatment. The workflow in our department primarily involves confirmation by biochemical testing (by measurement of plasma acylcarnitine profile) followed by additional tests (e.g. enzymatic assays or DNA mutation analysis). While cut-off points for free carnitine and acylcarnitine esters have been published for both DBS^{3,4} and plasma^{5,6} only limited information is available on the correlation between plasma and DBS.

Comparison between free carnitine in plasma and DBS from patients with organic acidurias and fatty acid oxidation disorders were reported by Primassin and Spiekerkoetter⁷. Data on comparison between acylcarnitine concentrations in the different matrices is scarce.

The use of absolute concentrations may lead to be potential interpretative problems. In newborn screening programs several ratios between different acylcarnitines have been reported that could help as a discriminate factor⁴. Such information is widely available for DBS but only limited for plasma.

This study examines acylcarnitines profiles in plasma and DBS simultaneously in samples from patients with well-defined inborn errors of metabolism (IEM). Subsequently, we evaluated whether ratios of acylcarnitines in plasma are just as helpful as these ratios are in DBS when primary markers fail to be conclusive.

MATERIALS AND METHODS

Study population

Blood was collected (for therapeutic control) from patients with confirmed (enzymatic or molecular) inherited metabolic diseases. These included plasma and DBS from patients diagnosed with different enzyme or transporter deficiencies: CPT1 deficiency (n = 6 samples, 2 patients), CPT2 deficiency (n = 5 samples, 4 patients), VLCAD deficiency (n = 12 samples, 11 patients), long-chain 3-hydroxyacyl-CoA dehydrogenase (LCHAD) deficiency (n = 2), and medium-chain

acyl-CoA dehydrogenase (MCAD) deficiency (n = 27 samples, 21 patients).

Patients with organic acidemias such as propionic acidemia (PA) (n = 12 samples, 5 patients), methylmalonic acidemia (MMA) (n = 9 samples, 6 patients), glutaric acidemia I (GA-I) (n = 4 samples, 2 patients) and β -ketothiolase (β KT) (n = 3 samples, 2 patients) deficiency were also included. All values were compared with age related (<1 month, >1 month and <18 years and >18 years) reference values. Reference values for plasma were determined using 281, 2835 and 393 samples respectively. Reference values for DBS were determined using 39, 24 and 63 samples respectively.

Additionally, 54 patients without metabolic defect were investigated for acylcarnitine profiles in plasma and DBS simultaneously.

Sampling

Blood samples were collected by venous puncture in heparin containing tubes. Aliquots of whole heparinized blood were aspirated and spotted onto Guthrie card filter papers (Whatman no. 903 Pro-tein Saver TM cards, formerly Schleicher & Schuell, Keene, USA). The blood tubes were then centrifuged and the resulting plasma was stored at -20°C until further analysis. The Guthrie card filter papers were left to dry for at least 4h at room temperature and were stored at -20°C in a foil bag with a desiccant package pending further analysis. All blood spots were inspected visually to make sure that the blood spot circle was completely filled.

Analysis

To prepare the DBS sample for analysis, a disc (6 mm \varnothing) was punched out from one blood spot circle using a hole puncher. To extract the acylcarnitines and free carnitine from the Guthrie card filter paper, the DBS was placed in 500 μL methanol which contained the stable isotope internal standards (D3-carnitine, D3-C4-carnitine, D3-C8-carnitine, D3-C16 carnitine) and the sample was sonicated for 20 min. The methanol eluate was evaporated under heated (40°C) nitrogen to dryness and butylated for 15 min at 60°C . After incubation, excess reagent was evaporated to dryness and residue was reconstituted in 100 μL acetonitrile.

100 μ L plasma was added to 500 μ L acetonitrile containing the stable isotope internal standards. After centrifugation, to remove the precipitated proteins, the supernatant was evaporated at 40 °C using nitrogen. After butylation (15 min at 40 °C) and evaporation (40 °C using nitrogen) the sample was reconstituted in 100 μ L acetonitrile. A calibration curve of eight standards containing C0-, C3-, C4-, C5-, C6-, C8-, C10-, C12-, C14-, C16-, and C18-carnitine was used for quantification. Concentrations of free carnitine and 37 acylcarnitines from paired samples of DBS and plasma were analyzed by flow injection using liquid chromatography (Alliance 2790, Waters) coupled to a Micromass Quattro Ultima mass spectrometer (HPLC/MS/MS).

MRM transitions of butyl ester derivatives of acylcarnitines and internal standards were analyzed in positive electrospray ionization (ESI+). Acylcarnitines were quantified by calculating the concentrations of metabolites relative to the deuterated internal standard closest in mass. The concentrations (or ratios) found in the patient sample were compared with the upper reference limit, defined as the 95th percentile. In addition, a precursor ion scan was made to search for presence of interfering compounds and poor derivatization. Internal control samples for both plasma and DBS were analyzed within every batch tested. In addition, we participated in a qualitative blood spot acylcarnitine quality assurance program. Both internal and external quality samples showed excellent results.

Statistical analysis

For statistical analysis, Prism 4.0 (GraphPad Software) was used. Significance was defined as $p < 0.05$.

RESULTS

Figure 1 shows representative acylcarnitine profiles in DBS and plasma from a neonatal control subject. When focusing on individual acylcarnitines, significant differences between plasma and DBS were observed (Table 1). In general, free carnitine concentrations were 36% higher in plasma compared to free carnitine concentrations in DBS (Table 1; Fig. 2; $P < 0.0001$). Plasma C8 carnitine concentration was twice the concentration measured in DBS (for controls as well as patients diagnosed with MCAD deficiency ($y = 0.52x - 0.02$, $r^2 = 0.95$, $n = 81$)).

Table 2 shows a list of disorders, their primary marker(s) and the range found in plasma as well as in DBS in our patient group. Elevation of the primary metabolite above the 95th percentile identified patient(s) with VLCAD-, LCHAD-, MCAD-, β KT deficiencies and with PA, MMA and GA-I in both plasma as well as in DBS. In all 6 samples obtained from patients with CPT1 deficiency, the concentration of free carnitine, the primary metabo-

Table 1. Comparison of total carnitine, free carnitine and acylcarnitines in plasma and corresponding DBS from controls. Mean values \pm standard deviation of the concentrations (in $\mu\text{mol/L}$); AC sum of the measured individual acylcarnitines; total carnitine: sum of free carnitine plus AC. DC; dicarbonic acid.

	Plasma (n=54)	DBS (n=54)	P (paired t-test)
Total carnitine	33.3 \pm 16.0	31.4 \pm 12.3	0.11
Free carnitine	26.8 \pm 14.0	19.2 \pm 8.5	<0.0001
Acyl carnitine (AC)	6.5 \pm 3.7	12.1 \pm 5.1	<0.0001
C2-carnitine	4.4 \pm 3.1	7.2 \pm 3.3	<0.0001
C3-carnitine	0.31 \pm 0.21	0.86 \pm 0.53	<0.0001
C4-carnitine	0.16 \pm 0.09	0.16 \pm 0.11	0.34
C5:1-carnitine	0.01 \pm 0.01	0.02 \pm 0.02	0.002
C5-carnitine	0.14 \pm 0.10	0.12 \pm 0.07	0.04
C4:3-OH-carnitine	0.03 \pm 0.04	0.07 \pm 0.06	<0.0001
C6-carnitine	0.04 \pm 0.02	0.03 \pm 0.02	0.0001
C5-OH-carnitine	0.03 \pm 0.03	0.16 \pm 0.19	<0.0001
C8:1-carnitine	0.17 \pm 0.11	0.07 \pm 0.05	<0.0001
C8 carnitine	0.07 \pm 0.04	0.04 \pm 0.03	<0.0001
C3-DC-carnitine	0.02 \pm 0.01	0.01 \pm 0.01	<0.0001
C10:2-carnitine	0.06 \pm 0.04	0.01 \pm 0.01	<0.0001
C10:1-carnitine	0.10 \pm 0.06	0.04 \pm 0.03	<0.0001
C10-carnitine	0.06 \pm 0.08	0.06 \pm 0.04	0.37
C4-DC-carnitine	0.04 \pm 0.02	0.28 \pm 0.17	<0.0001
C5-DC-carnitine	0.03 \pm 0.01	0.02 \pm 0.02	<0.0001
12:1-carnitine	0.04 \pm 0.03	0.02 \pm 0.02	<0.0001
12-carnitine	0.06 \pm 0.03	0.04 \pm 0.02	<0.0001
C6-DC-carnitine	0.05 \pm 0.03	0.02 \pm 0.02	<0.0001
C14:2-carnitine	0.03 \pm 0.02	0.03 \pm 0.01	0.13
C14:1-carnitine	0.04 \pm 0.03	0.03 \pm 0.02	0.002
C14-carnitine	0.04 \pm 0.02	0.08 \pm 0.04	<0.0001
C8-DC-carnitine	0.01 \pm 0.01	0.01 \pm 0.01	0.38
C14-OH-carnitine	0.01 \pm 0.01	0.02 \pm 0.01	<0.0001
C16:1-carnitine	0.03 \pm 0.02	0.06 \pm 0.04	<0.0001
C16-carnitine	0.11 \pm 0.06	0.93 \pm 0.58	<0.0001
C10-DC-carnitine	0.01 \pm 0.01	0.05 \pm 0.02	<0.0001
C16:1-OH-carnitine	0.01 \pm 0.01	0.03 \pm 0.02	<0.0001
C16-OH-carnitine	0.01 \pm 0.01	0.02 \pm 0.02	0.008
C18:2-carnitine	0.06 \pm 0.05	0.25 \pm 0.21	<0.0001
C18:1-carnitine	0.15 \pm 0.09	0.83 \pm 0.49	<0.0001
C18-carnitine	0.04 \pm 0.02	0.46 \pm 0.24	<0.0001
C18:2-OH-carnitine	0.0 \pm 0.01	0.01 \pm 0.01	0.001
C18:1-OH-carnitine	0.01 \pm 0.01	0.02 \pm 0.01	0.007
C18-OH-carnitine	0.01 \pm 0.01	0.02 \pm 0.01	0.36
C16-DC-carnitine	0.01 \pm 0.01	0.02 \pm 0.01	0.27
C18:1-DC-carnitine	0.01 \pm 0.01	0.02 \pm 0.01	0.27

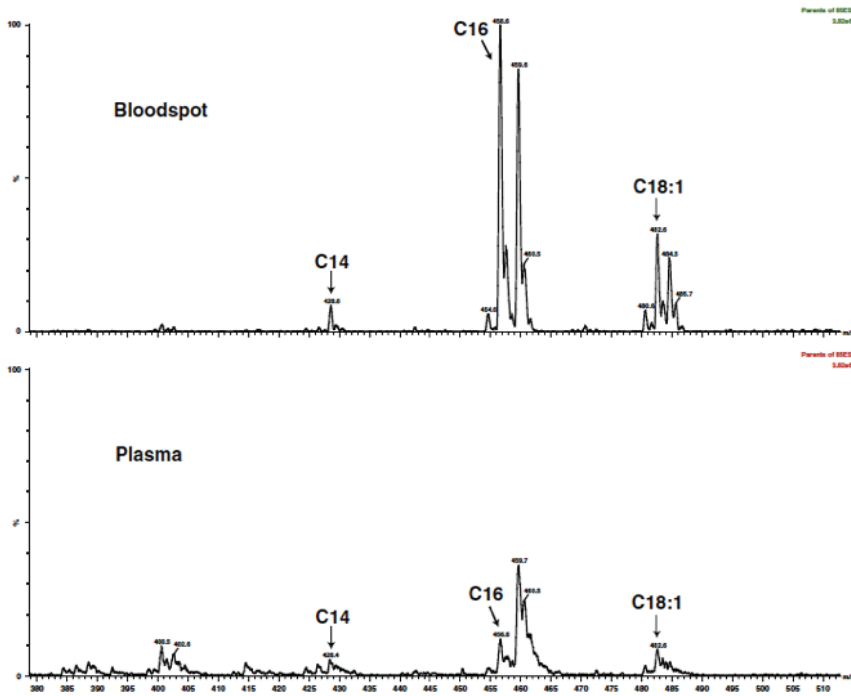


Figure 1. Acylcarnitine profile in plasma and its corresponding DBS in a neonatal control subject.

lite for CPT1 deficiency was below the 95th percentile of controls in plasma (Table 2). In contrast, the C0 carnitine was significantly increased in corresponding DBS samples (Table 2, Fig. 2). The concentration of the primary metabolite for CPT2 deficiency, C18, was in one sample above 95th percentile of age related controls in DBS and the concentration of the primary metabolite C18:1 was abnormal in the same sample (Table 2, Fig. 3). Since the primary markers for CPT1 deficiency in plasma and for CPT2 deficiency in DBS lack sensitivity, additional diagnostic criteria were evaluated. For CPT1 deficiency the $C0/(C16 + C18)$ ratio was calculated in all plasma and DBS specimens (Table 3). We found an increased ratio in plasma as well as in DBS in all patients compared to controls. The ratio in patients was between 2063 and 13,927 for plasma and between 3369 and 7944 for DBS. All values are at least 4 and 78 times above the highest value found in control subjects for plasma and DBS respectively. To facilitate the diagnostic recognition of CPT2 deficiency, $(C16 + C18:1)/C2$ was evaluated. Table 3 shows that the calculated ratios (0.21, 0.36, 0.27, 0.27, and 0.39) in all cases were above the 95th percentile of controls in plasma. In DBS, the ratio (0.36, 0.51, 0.34, 0.42 and 0.60) was indicative for CPT2 deficiency in three out of five samples.

Table 2. Acylcarnitine concentration in plasma and DBS of patients and controls.

Primary Marker	IEM	n	Age	Patient (range) in plasma ($\mu\text{mol/L}$)	Control 95 th percentile in plasma	Patient (range) in DBS ($\mu\text{mol/L}$)	Control 95 th percentile in DBS
C0	CPT-1	3	1 month- 18 year	41.8-49.0	49.0	147-183	46.5
C16	CPT-2	3	>18 year	24.8-36.2	51.4	109-168	34.0
C18		5	>18 year	0.40-1.0	0.20	0.66-1.5	1.1
C18:1				0.15-0.41	0.08	0.51-1.1	0.81
C18:2				0.38-1.1	0.35	0.77-1.8	1.4
C14:1	VLCAD	1	< 1 month	0.15-0.49	0.20	0.22-0.56	0.55
		7	1 month-18 year	5.0	0.12	4.9	0.06
		4	>18 year	0.29-2.9	0.18	0.16-1.6	0.13
C16OH	LCHAD	2	1 month-18 year	1.0-8.9	0.13	0.61-4.5	0.06
C8	MCAD	10	< 1 month	0.09-0.50	0.04	0.09-0.44	0.07
		11	1 month-18 year	0.27-7.6	0.14	0.22-3.7	0.07
		6	>18 year	0.85-10.0	0.18	0.41-5.3	0.13
C3	PA	12	1 month-18 year	1.7-6.8	0.26	0.61-4.6	0.12
C3	MMA	9	1 month-18 year	31.6-75.3	0.80	17.3-50.4	2.0
				3.6-96.6	0.80	2.1-54.5	2.0
C4DC				0.10-3.7	0.05	0.28-2.2	0.58
C5DC	GA-I	4	1 month-18 year	0.47-0.78	0.05	0.17-0.42	0.06
C5OH	β KT	3	1 month-18 year	0.21-0.25	0.03	1.3-2.8	0.25

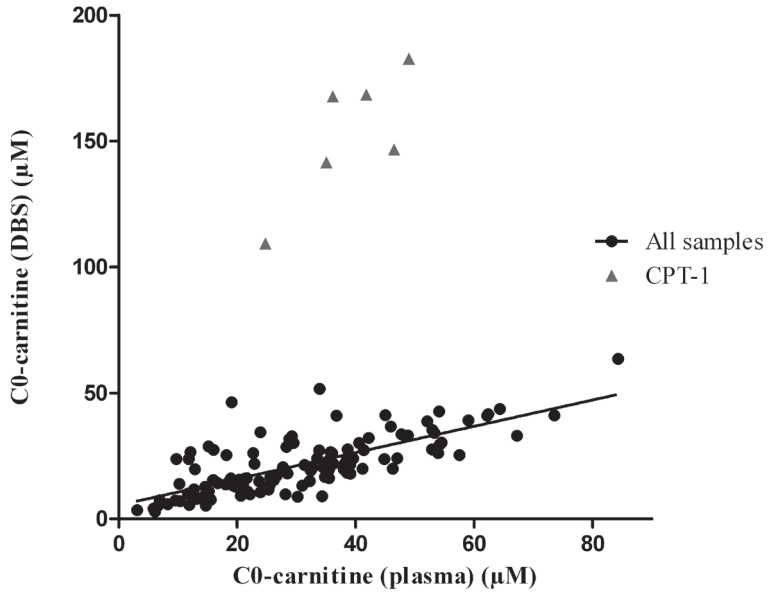


Figure 2. Correlation between free carnitine in DBS specimen and their corresponding plasma sample (n = 125). ▲ represents free carnitine concentration in patients with proven CPT-1 deficiency. ● represents free carnitine concentration in all samples.

Table 3. Ratios for acylcarnitines in plasma and DBS from CPT-1 and CPT-2 patients.

Ratio	IEM	n	Age	Range in plasma	Control 95 th centile in plasma	Range in DBS	Control 95 th centile in DBS
C0/(C16+C18)	CPT-1	3	1 month -18 year	2323-13927	510	3369-7944	43
			> 18 year	2063-12050	441	2831-4756	33
(C16+C18:1)/C2	CPT-2	5	> 18 year	0.21-0.39	0.15	0.34-0.60	0.37

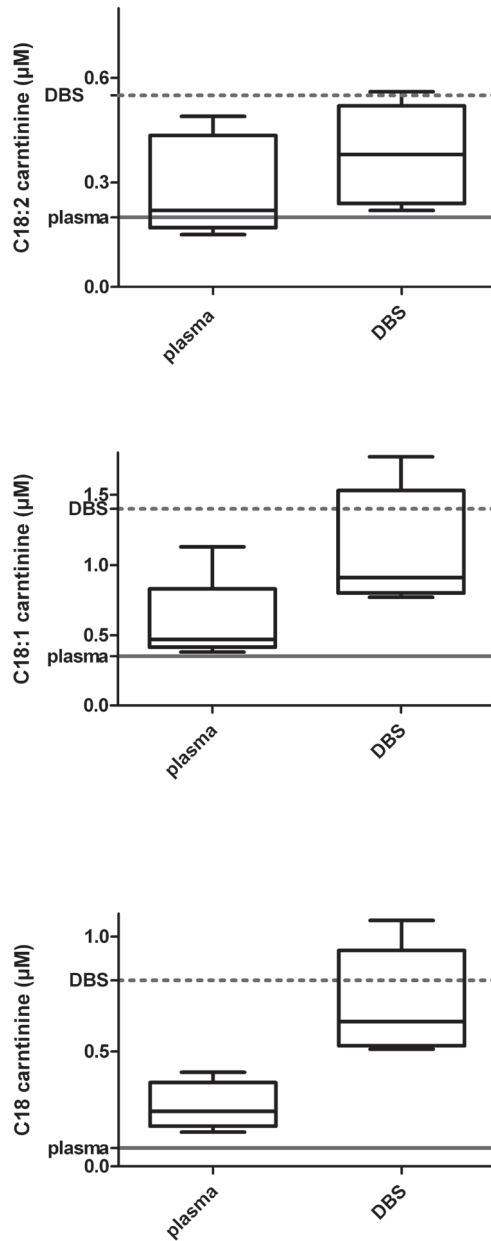


Figure 3. Box-plots for C18:2-carnitine, C18:1-carnitine and C18-carnitine in plasma and DBS in four patients diagnosed with CPT-2 deficiency. Straight line represents 95th percentile of (age related) controls in plasma. Dotted line represents 95th percentile of (age related) controls in DBS.

DISCUSSION

HPLC/MS/MS is the method of choice for the quantification of (acyl)carnitines in body fluids. While it is known that carnitine concentrations in tissues are normally 20- to 50-fold higher than in serum⁸, there is no consensus concerning the clinical specimen (plasma or DBS) that would best reflect the carnitine status of various body compartments. DBS offers a number of advantages over conventional plasma collection. DBS is preferred since it requires a less invasive sampling method (finger or heel prick, rather than conventional venous cannula). DBS can be conveniently collected by patients themselves (or guardians) with minimum training. Less blood is required and DBSs offer a simpler storage and easier transfer. In addition, metabolites are reasonably stable and DBSs reduce the infection risk of HIV/AIDS and other infectious pathogens to a minimum⁹. Because of these advantages and the fact that DBSs allow screening for additional metabolic disorders (e.g. lysosomal disorders by measuring enzyme activities), the use of DBS in clinical metabolic settings has expanded. There is a high level of very long chain acylcarnitines in DBS compared to plasma (Fig. 1). This underscores the need for matrix-based reference values for correct interpretation. Table 1 shows the significant difference between plasma and DBS concentrations of acylcarnitine and free carnitine in controls. This observation could be explained by differences between acylcarnitine concentrations in plasma and in the cellular compartment of a blood spot. It can be argued that the preferred sample type for an acylcarnitines profile is a DBS because long-chain acylcarnitines are absorbed on the surface of red blood cells². Therefore, elevations of these long-chain acylcarnitines may not be as reliably detected in plasma as they are in DBS. On the other hand it has been stated that high endogenous levels of long-chain acylcarnitines in normal erythrocytes reduced the diagnostic specificity in blood spots compared with plasma samples¹⁰.

To assess the usefulness of plasma and DBS acylcarnitine analysis for diagnostic purposes, primary markers (expected to be consistently expressed with their associated disorders) in both matrices of 80 samples from patients with confirmed IEM were reviewed. Twenty-eight samples were obtained from patients who were previously diagnosed with organic acid disorders and fifty-two samples were obtained from patients with fatty acid oxidation disorders.

CPT1 deficiency

In CPT1 deficiency elevated free carnitine concentrations and low acylcarnitine concentrations are diagnostic. We observed that free carnitine in DBS from patients with CPT1 deficiency was 4.0 ± 0.5 times higher than free carnitine in plasma (Table 2, Fig. 2). Since free carnitine concentrations in control subjects were significantly higher in plasma, the increase of free carnitine concentration in DBS from CPT1 patients reflects a disease-

dependent carnitine accumulation in red blood cells. The present study (Fig. 2) shows that CPT1 deficiency may be missed when analysis is performed in plasma which is in accordance with Primassin and Spiekerkoetter⁷. In line with this observation is the report of a CPT1 patient with a positive newborn screening in whom acylcarnitines in a follow-up plasma sample were normal¹¹. On the other hand, it has been reported that free carnitine concentrations even in DBS of CPT1 deficient patients can be within the reference interval in the newborn period¹².

An elevation of the C0/(C16 + C18) ratio has been described in CPT1 deficiency^{4,12}. This ratio is highly specific to diagnose CPT1 deficiency in DBS. The present study shows that the application of this ratio in plasma is also very helpful (Table 3). Hence, when increased concentrations of C0 carnitine are used as a single marker, CPT1 deficiency may be missed in plasma while introduction of the C0/(C16 + C18) ratio is highly specific.

CPT2 deficiency

CPT2 deficiency leads to a pronounced elevation of C16 and C18 acylcarnitines in plasma (Table 2)¹³. This elevation was not seen in all DBS samples obtained from patients diagnosed with CPT2 deficiency (Table 2). Therefore, in contrast to CPT1, plasma is a better choice to diagnose CPT2 deficiency.

Newborn screening for CPT2 deficiency is included in 7 of the 37 European newborn screening programs¹⁴ and CPT2 deficiency has been described in only 22 affected families¹⁵. There is a case report of one patient with CPT2 deficiency that was not detected in the newborn period. In DBS, the most sensitive indicator to diagnose CPT2 deficiency is an elevated (C16 + C18:1)/C2 ratio^{4,13}. In the present study we tested whether this ratio is also indicative for CPT2 deficiency in plasma by comparing this ratio calculated from the five CPT2 samples with age related control samples. Table 3 shows that the calculated ratio in plasma may help in diagnosing CPT2 deficiency. In contrast, in DBS, this ratio was not informative in two samples obtained from patients diagnosed with CPT2 deficiency. We therefore conclude that CPT2 deficiency cannot be excluded upon acylcarnitine quantification in DBS.

VLCAD deficiency

For VLCAD deficiency, C14:1 is used as primary marker (Table 2). It has been suggested that VLCAD deficiency can be reliably diagnosed by examination of an early DBS but may be missed if the child is asymptomatic and older than four days¹⁶. The present study uses DBS and plasma from the same sampling time. In our data set, C14:1 carnitine seems to be appropriate to diagnose VLCAD deficiency in DBS and plasma, also in older children.

LCHAD deficiency

In LCHAD deficiency, elevations of the long chain acylcarnitines (particular C16OH) are evident [10]. It has been recently reported that hydroxyacylcarnitines can be identified and separated in DBS, whereas in plasma the peaks are near the limit of detection¹⁷. Van Hove et al.¹⁰ recommend analysis of acylcarnitines in plasma since there is a reduced number of elevated metabolites in blood spots compared to plasma in patients with proven LCHAD deficiency. We support this recommendation since six hydroxyacylcarnitines were elevated in plasma in contrast to two hydroxyacylcarnitines in DBS in one patient with LCHAD deficiency (data not shown).

MCAD deficiency

For screening on MCAD deficiency, C8 carnitine is routinely measured. In this study, all twenty-one patients diagnosed with MCAD deficiency showed the classic acylcarnitine profile in both plasma and DBS with significantly increased C8 carnitine (Table 2), C6 carnitine, C8 > C6 and increased C8/C10 ratio in plasma as well as in DBS.

Organic acidurias

In our data set, elevation of the most characteristic metabolites (above the 95th percentile) identified all patients with an organic aciduria (PA, MMA, GA-I, and β KT) using plasma or DBS (Table 2). Absolute values of the specific acylcarnitines differ however. False negative neonatal screening results for β KT^{18,19}, GA-1^{19,20} and MMA^{19,21} have been reported. This could be due to sampling time and chosen cut-off values which influence detection rates of milder variants, rather than choice of matrix. Further comparison between plasma and DBS is necessary especially for those organic acidurias in which a small number of patients were included.

CONCLUSION

The present study shows that, when only absolute concentrations of acylcarnitines are considered, the choice of matrix for diagnostic acylcarnitine profiling is critical. Whereas the majority of fatty acid oxidation defects can be diagnosed by plasma investigation, CPT1 deficiency can be missed in plasma when relying on free carnitine. It is however not clear whether the clinical condition (symptomatic/asymptomatic) influences this observation.

However, diagnostic sensitivity for CPT1 deficiency in plasma is improved to 100% when taking a ratio between free carnitine and acylcarnitines into account. To detect CPT2 deficiency, plasma is the matrix of choice, as this diagnosis may be missed in DBS.

For all other metabolic disorders tested in the present study, both plasma and DBS can be diagnostically used.

ACKNOWLEDGMENTS

We would like to thank Karen van Baal for performing HPLC/MS/MS experiments.

REFERENCES

1. Houten SM, Wanders RJA. A general introduction to the biochemistry of mitochondrial fatty acid β -oxidation. *J Inherit Metab Dis*. 2010;33(5):469–477. doi:10.1007/s10545-010-9061-2.
2. Reuter SE, Evans AM. Carnitine and acylcarnitines: pharmacokinetic, pharmacological and clinical aspects. *Clin Pharmacokinet*. 2012;51(9):553–572. doi:10.2165/11633940-000000000-00000.
3. Schulze A, Lindner M, Kohlmüller D, Olgemöller K, MAYATEPEK E, Hoffmann GF. Expanded newborn screening for inborn errors of metabolism by electrospray ionization-tandem mass spectrometry: results, outcome, and implications. *Pediatrics*. 2003;111(6 Pt 1):1399–1406.
4. McHugh DMS, Cameron CA, Abdenur JE, et al. Clinical validation of cutoff target ranges in newborn screening of metabolic disorders by tandem mass spectrometry: a worldwide collaborative project. *Genet Med*. 2011;13(3):230–254. doi:10.1097/GIM.0b013e31820d5e67.
5. Vreken P, van Lint AE, Bootsma AH, Overmars H, Wanders RJ, van Gennip AH. Quantitative plasma acylcarnitine analysis using electrospray tandem mass spectrometry for the diagnosis of organic acidaemias and fatty acid oxidation defects. *J Inherit Metab Dis*. 1999;22(3):302–306.
6. Silva MF, Selhorst J, Overmars H, et al. Characterization of plasma acylcarnitines in patients under valproate monotherapy using ESI-MS/MS. *Clin Biochem*. 2001;34(8):635–638. doi:10.1016/S0009-9120(01)00272-7.
7. Primassin S, Spiekerkoetter U. ESI-MS/MS measurement of free carnitine and its precursor γ -butyrobetaine in plasma and dried blood spots from patients with organic acidurias and fatty acid oxidation disorders. *Molecular Genetics and Metabolism*. 2010;101(2-3):141–145. doi:10.1016/j.ymgme.2010.06.012.
8. Stanley CA. New genetic defects in mitochondrial fatty acid oxidation and carnitine deficiency. *Adv Pediatr*. 1987;34:59–88.
9. Parker SP, Cubitt WD. The use of the dried blood spot sample in epidemiological studies. *J Clin Pathol*. 1999;52(9):633–639.
10. van Hove JL, Kahler SG, Feezor MD, et al. Acylcarnitines in plasma and blood spots of patients with long-chain 3-hydroxyacyl-coenzyme A dehydrogenase deficiency. *J Inherit Metab Dis*. 2000;23(6):571–582.
11. Borch L, Lund AM, Wibrand F, et al. Normal Levels of Plasma Free Carnitine and Acylcarnitines in Follow-Up Samples from a Presymptomatic Case of Carnitine Palmitoyl Transferase 1 (CPT1) Deficiency Detected Through Newborn Screening in Denmark. *JIMD Rep*. 2012;3:11–15. doi:10.1007/8904_2011_35.
12. Fingerhut R, Röschinger W, Muntau AC, et al. Hepatic carnitine palmitoyltransferase I deficiency: acylcarnitine profiles in blood spots are highly specific. *Clinical Chemistry*. 2001;47(10):1763–1768.
13. Gempel K, Kiechl S, Hofmann S, et al. Screening for carnitine palmitoyltransferase II deficiency by tandem mass spectrometry. *J Inherit Metab Dis*. 2002;25(1):17–27.
14. Loeber JG, Burgard P, Cornel MC, et al. Newborn screening programmes in Europe; arguments and efforts regarding harmonization. Part 1. From blood spot to screening result. *J Inherit Metab Dis*. 2012;35(4):603–611. doi:10.1007/s10545-012-9483-0.
15. Yahyaoui R, Espinosa MG, Gómez C, et al. Neonatal carnitine palmitoyltransferase II deficiency associated with Dandy-Walker syndrome and sudden death. *Molecular Genetics and Metabolism*. 2011;104(3):414–416. doi:10.1016/j.ymgme.2011.05.003.
16. Boneh A, Andresen BS, Gregersen N, et al. VLCAD deficiency: pitfalls in newborn screening and confirmation of diagnosis by mutation analysis. *Molecular Genetics and Metabolism*. 2006;88(2):166–170. doi:10.1016/j.ymgme.2005.12.012.

17. Kobayashi H, Hasegawa Y, Endo M, Purevsuren J, Yamaguchi S. A retrospective ESI-MS/MS analysis of newborn blood spots from 18 symptomatic patients with organic acid and fatty acid oxidation disorders diagnosed either in infancy or in childhood. *J Inherit Metab Dis.* 2007;30(4):606. doi:10.1007/s10545-007-0642-7.
18. Sarafoglou K, Matern D, Redlinger-Grosse K, et al. Siblings with mitochondrial acetoacetyl-CoA thiolase deficiency not identified by newborn screening. *Pediatrics.* 2011;128(1):e246–50. doi:10.1542/peds.2010-3918.
19. Frazier DM, Millington DS, McCandless SE, et al. The tandem mass spectrometry newborn screening experience in North Carolina: 1997–2005. *J Inherit Metab Dis.* 2006;29(1):76–85. doi:10.1007/s10545-006-0228-9.
20. Couce ML, Castiñeiras DE, Bóveda MD, et al. Evaluation and long-term follow-up of infants with inborn errors of metabolism identified in an expanded screening programme. *Molecular Genetics and Metabolism.* 2011;104(4):470–475. doi:10.1016/j.ymgme.2011.09.021.
21. Juan-Fita MJ, Egea-Mellado JM, González-Gallego I, Moya-Quiles MR, Fernández-Sánchez A. [Expanded newborn screening in the Region of Murcia, Spain. Three-years experience]. *Med Clin (Barc).* 2012;139(13):566–571. doi:10.1016/j.medcli.2011.10.007..

CHAPTER 3

Newborn screening paradox: sensitivity vs overdiagnosis

Eugene Diekman^{1,2}, Monique de Sain-van der Velden³, Hans Waterham¹,
A.J. Kluijtmans⁴ PhD, Peter Schielen⁵, Evert Ben van Veen⁵ LL.M,
Sacha Ferdinandusse¹, F.A. Wijburg¹, Gepke Visser²

1 Laboratory Genetic Metabolic Diseases, Department of Clinical Chemistry and Pediatrics, Emma Children's Hospital, Academic Medical Centre, University of Amsterdam, The Netherlands

2 Department of Paediatric Gastroenterology and Metabolic Diseases, Wilhelmina Children's Hospital, UMC Utrecht, The Netherlands

3 Department of Medical Genetics, Wilhelmina Children's Hospital, UMC Utrecht, The Netherlands

4 Department of Laboratory Medicine, Translational Metabolic Laboratory, Radboud University Medical Center Nijmegen, The Netherlands

5 National Institute for Public Health and the Environment (RIVM), Reference laboratory for pre- and neonatal screening, Bilthoven, The Netherlands

Under revision Journal of Inherited Metabolic Disease

ABSTRACT

Objective: To improve the efficacy of newborn screening (NBS) for Very Long-chain acyl-CoA Dehydrogenase Deficiency (VLCADD).

Patients and Methods: Data on all dried bloodspots collected by the Dutch NBS from 2007–October 2010 (742,728) were included. Based solely on the C14:1 levels (cut off $\geq 0.8 \mu\text{mol/l}$), 6 newborns with VLCADD had been identified through NBS during this period. The ratio of C14:1 over C2 was calculated. DNA of all bloodspots with a C14:1/C2 ratio of ≥ 0.020 was isolated and sequenced. Children homozygous or compound heterozygous for mutations in the ACADVL gene were traced back and invited for detailed clinical, biochemical and genetic evaluation.

Results: Rescreening based on the C14:1/C2 ratio with a cut off of >0.020 identified an additional 5 children with known ACADVL mutations and low enzymatic activity. All were still asymptomatic at the time of diagnosis (age 2–5 yrs). Increasing the cut off to >0.023 resulted in a sensitivity of 93% and a positive predictive value of 37%. The sensitivity of the previously used screening approach (C14:1 ≥ 0.8) was 50%.

Conclusion: This study shows that the ratio C14:1/C2 is a more sensitive marker than C14:1 for identifying VLCADD patients in NBS. However, as these patients were all asymptomatic at the time of diagnosis, this suggests that a more sensitive screening approach may also identify individuals who may never develop clinical disease. Long-term follow up studies are needed to establish the risk of these VLCADD deficient individuals for developing clinical signs and symptoms.

INTRODUCTION

Many newborn screening (NBS) programs in the world, including the Dutch NBS program, have Very Long-chain acyl-CoA Dehydrogenase Deficiency (VLCADD) in their disease panel^{1,2}. VLCADD is a disorder of long chain fatty acid beta-oxidation (OMIM 609575) that compromises energy homeostasis and leads to accumulation of long-chain fatty acids and derivatives. Patients may present with hypoglycemia, hepatomegaly and cardiomyopathy in the neonatal period and rhabdomyolysis in early childhood. These features can be induced by fasting, exercise, illness and fever³⁻⁶. VLCADD is included in NBS programs mainly because life-threatening symptoms as hypoglycemia and cardiomyopathy can be prevented by dietary measures.

NBS for VLCADD is performed by measuring the concentration of accumulating long-chain acylcarnitines in bloodspots, especially tetradecenoyl carnitine (C14:1). In the Netherlands, the cut-off level of C14:1 for referral of newborns was initially ≥ 0.80 $\mu\text{mol/L}$. However, because patients were missed the cut-off level for referral was reduced to ≥ 0.60 $\mu\text{mol/L}$. Results of the Region4 database⁷, which contains collaborative data on the outcome of NBS programs worldwide⁸, indicated that the ratio of C14:1 over acetylcarnitine (C2), might further improve the sensitivity of the screening procedure⁹. C2 concentrations are often measured in NBS screening programs as secondary marker for screening of isovaleric acidemia. In order to improve the NBS on VLCADD we retrospectively investigated whether the ratio C14:1/C2 is a better marker for VLCADD than the original marker C14:1.

PATIENTS AND METHODS

We calculated the C14:1/C2 ratios and C14:1 levels of all 742.728 NBS bloodspots from the Dutch NBS program taken in the period 2007-2010. The levels were measured within 7 days after birth. All bloodspots with a C14:1/C2 cut-off value of ≥ 0.020 and/or C14:1 ≥ 0.60 $\mu\text{mol/l}$ were selected for further analysis. DNA of the selected bloodspots was isolated using the NucleoSpin Tissue genomic DNA purification kit (Macherey-Nagel, Düren, Germany). All exons plus flanking intronic regions of the ACADVL gene were subsequently sequenced. Three proven VLCADD patients were included in a blinded manner as positive controls.

VLCAD enzymatic activity was measured in lymphocytes by using ferricinium hexafluorophosphate as the electron acceptor, followed by UPLC, to separate the different acyl-CoA species¹⁰. Acylcarnitines were measured as described previously¹¹.

Based on the duty of care principle¹², the patients who were originally classified as non-affected but who turned out positive upon evaluation of the C14:1/C2-ratio, were

traced back and contacted for care. All were alive and all accepted the invitation for neurological, cardiological, biochemical and genetic evaluation.

RESULTS

Acylcarnitine measurement and mutation analysis in bloodspots

We found a C14:1/C2 ratio of ≥ 0.020 in 67 bloodspots. Sequence analysis of the ACADVL gene in this group revealed five patients who were either homozygous for a single mutation or compound heterozygous for two different mutations. These mutations were confirmed in independent samples (bloodspot and blood). In addition, we identified 18 children who were carriers of one mutation in the ACADVL gene (Table 1).

The enzymatic activity of VLCAD in lymphocytes was severely deficient in two of the five detected patients (PID 1 and 2), and mildly reduced in the other three patients (PID 3-5). VLCADD was subsequently also confirmed in two siblings (Table 1).

In the period 2007-2010, six VLCADD patients had been identified by the Dutch NBS program based on the original screening selection criteria: C14:1 ≥ 0.80 $\mu\text{mol/L}$. The five additional patients detected in this study were not referred at the time. However, based on the current cut-off value of C14:1 ≥ 0.6 $\mu\text{mol/L}$ (adopted 2013), patient 1 would have been referred.

Two of the three plasma acylcarnitine levels were below the age adjusted reference value (95th percentile) of < 0.26 $\mu\text{mol/L}$ (patient 3 and 5).

Clinical phenotype

All newly identified patients were evaluated for clinical symptoms (Table 1). None of these patients reported muscle-related symptoms and none had neurological or cardiological abnormalities. All were normoglycemic upon evaluation and none had suffered metabolic decompensation. Growth varied with a length range < -1.5 SD below the target height to appropriate to target height and a weight-length range of -2.18 to $+1.94$. The median creatine kinase level at the first evaluation was 120 U/L (range 91-200 U/L).

Sensitivity and positive predictive value

Our results indicate that the sensitivity of C14:1 (≥ 0.8) is 50% and the sensitivity of C14:1 (≥ 0.6) is 58%, while the sensitivity of C14:1/C2 (≥ 0.020) is 93%. In addition, the positive predictive values of C14:1 (≥ 0.8 and ≥ 0.6) and C14:1/C2 (≥ 0.020) are 66%, 47% and 16%, respectively (Figure 1). With a C14:1/C2 cut-off value of ≥ 0.023 , the sensitivity remains 93%, while the positive predictive value increases to 37% (Figure 1).

Table 1. Patient characteristics. Clinical, biochemical and genetic details of each patient.

Patient ID	Age (yr)	Gender	Bloodspot	Plasma	Enzymatic Activity	Genotype	Neurological examination	Cardiological examination	Other symptoms						
1	5	M	[C14:1] (normal) <0.60 $\mu\text{mol/l}$	C14:1/C2 [C14:1] (normal) <0.26 $\mu\text{mol/l}$	C14:1/C2 lymphocytes (% of controls) <7	allele 1 p.G441D missense	allele 2 normal (MRC 5)	normal (no echo/ECG abnormalities)	no hepatomegaly, fatigue, sometimes myalgia	creatine kinase (normal <250)					
2	5	M	0.70	0.058	0.220	0.60	0.780	0.292	0.780	<7	p.P89HfsX28 frameshift	normal	normal	no hepatomegaly, no complaints	198
Sib of 2	11	F	0.36	0.040	11	2.92	0.780	0.292	0.780	11	p.P89HfsX28 frameshift	normal	normal	no hepatomegaly, no complaints	n.a.
3	4	F	0.33	0.024	21	0.15	0.069	0.15	0.069	21	p.V283A missense	normal	normal	no hepatomegaly, no complaints	96
4	5	M	0.25	0.050	14	0.38	0.18	0.38	0.18	14	p.V283A missense	normal	normal	no hepatomegaly, no complaints	200
5	2	M	0.55	0.039	46	0.14	0.094	0.14	0.094	46	p.G441D missense	normal	normal	no hepatomegaly, no complaints	120
Sib of 5	2	F	0.70	0.058	40	0.60	0.220	0.60	0.220	40	p.G441D missense	normal	normal	no hepatomegaly, no complaints	n.a.

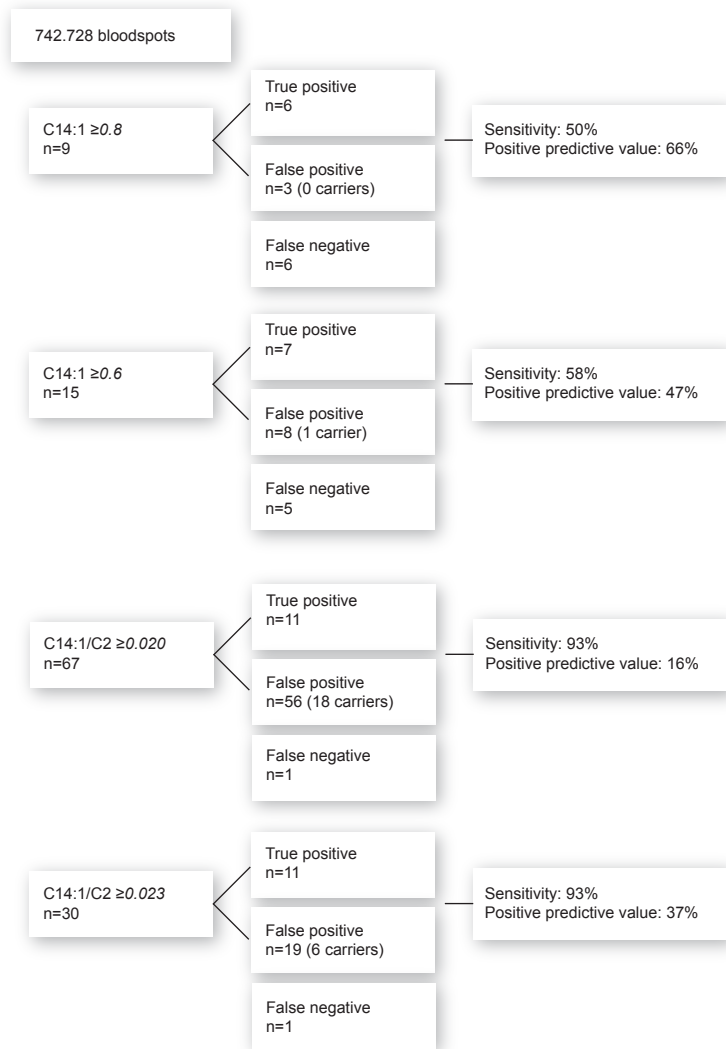


Figure 1. Sensitivity and positive predictive values of C14:1 and C14:1/C2 with the various cut-off-values.

DISCUSSION

This study shows that inclusion of the ratio C14:1/C2 to the NBS increases the sensitivity to detect VLCADD patients. Accordingly, this ratio is now added to the Dutch NBS as primary marker for screening on VLCADD.

Introducing C14:1/C2 into the expanded NBS program has advantages as well as limitations. The inclusion of this ratio will increase the sensitivity from 50% to 93% which leads to less false negative results and thus less missed patients. But, the increase of the sensitivity is at the expense of a lower positive predictive value. A false positive NBS result may have great impact on the parents of newborns and the families involved^{13,14}. Special care and a best practice for communication between health care providers and parents is therefore essential in mitigating the stress involved¹⁵. Compared to other disease in the NBS, a positive predictive value of 37% is high⁹.

Retrospective analyses allowed us to identify five missed patients who, on clinical evaluation were all asymptomatic, but in whom the diagnosis VLCADD was confirmed by mutation analysis in combination with a decreased VLCAD enzymatic activity. These patients may be at high risk of future metabolic crises and/or later-onset disease. However, it is not possible to define which outcomes are clinically relevant^{16,17}, especially in patients with a residual enzymatic activity <20%¹⁸.

With the current development rate of new techniques in genetics and biochemistry, sensitivity will probably increase even more in the coming years^{16,19}. Although the introduction of worldwide NBS programs has offered significant health gain for many patients, it might be argued that too sensitive NBS methods can lead to “over-diagnosing” and as such may be harmful for patients and their families^{20,21}.

CONCLUSION

In summary, we show that the biomarker C14:1/C2 (≥ 0.023) is a better marker (sensitivity 93%) compared to C14:1 (≥ 0.8 , sensitivity 50%) to detect VLCADD patients and thus leads to less missed patients. However, the identified missed patients were all asymptomatic at the time of diagnosis. This suggests that a more sensitive screening approach may also identify individuals who may never develop clinical disease. Long-term follow up studies are needed to establish the risk of these VLCADD deficient individuals for developing clinical signs and symptoms.

ACKNOWLEDGEMENTS

We are most grateful to Dr. B. Elvers, of the National Institute for Public Health and the Environment (RIVM) for providing the selected bloodspots for further analyses, and to Dr. P. Verkerk of TNO (Applied Scientific Research Institute) and Prof. Dr. E.E.S. Nieuwenhuis of the Wilhelmina's Childrens Hospital/University Medical Centre Utrecht (WKZ/UMCU) for their biochemical and ethical advice. They were not compensated for their efforts.

REFERENCES

1. Lindner M, Hoffmann GF, Matern D. Newborn screening for disorders of fatty-acid oxidation: experience and recommendations from an expert meeting. *J Inherit Metab Dis.* 2010;33(5):521–526. doi:10.1007/s10545-010-9076-8.
2. Loeber JG, Burgard P, Cornel MC, et al. Newborn screening programmes in Europe; arguments and efforts regarding harmonization. Part 1. From blood spot to screening result. *J Inherit Metab Dis.* 2012;35(4):603–611. doi:10.1007/s10545-012-9483-0.
3. Baruteau J, Sachs P, Broué P, et al. Clinical and biological features at diagnosis in mitochondrial fatty acid beta-oxidation defects: a French pediatric study from 187 patients. Complementary data. *J Inherit Metab Dis.* 2014;37(1):137–139. doi:10.1007/s10545-013-9628-9.
4. Vianey-Saban C, Divry P, Brivet M, et al. Mitochondrial very-long-chain acyl-coenzyme A dehydrogenase deficiency: clinical characteristics and diagnostic considerations in 30 patients. *Clin Chim Acta.* 1998;269(1):43–62.
5. Andresen BS, Olpin S, Poorthuis BJ, et al. Clear correlation of genotype with disease phenotype in very-long-chain acyl-CoA dehydrogenase deficiency. *Am J Hum Genet.* 1999;64(2):479–494. doi:10.1086/302261.
6. Laforêt P, Acquaviva-Bourdain C, Rigal O, et al. Diagnostic assessment and long-term follow-up of 13 patients with Very Long-Chain Acyl-Coenzyme A dehydrogenase (VLCAD) deficiency. *Neuromuscul Disord.* 2009;19(5):324–329. doi:10.1016/j.nmd.2009.02.007.
7. McHugh DMS, Cameron CA, Abdenur JE, et al. Clinical validation of cutoff target ranges in newborn screening of metabolic disorders by tandem mass spectrometry: a worldwide collaborative project. *Genet Med.* 2011;13(3):230–254. doi:10.1097/GIM.0b013e31820d5e67.
8. Houten SM, Herrema H, Brinke te H, et al. Impaired amino acid metabolism contributes to fasting-induced hypoglycemia in fatty acid oxidation defects. *Hum Mol Genet.* 2013;22(25):5249–5261. doi:10.1093/hmg/ddt382.
9. Hall PL, Marquardt G, McHugh DMS, et al. Postanalytical tools improve performance of newborn screening by tandem mass spectrometry. *Genet Med.* 2014. doi:10.1038/gim.2014.62.
10. Wanders RJA, Ruiters JPN, IJLst L, Waterham HR, Houten SM. The enzymology of mitochondrial fatty acid beta-oxidation and its application to follow-up analysis of positive neonatal screening results. *J Inherit Metab Dis.* 2010;33(5):479–494. doi:10.1007/s10545-010-9104-8.
11. Vreken P, van Lint AE, Bootsma AH, Overmars H, Wanders RJ, van Gennip AH. Quantitative plasma acylcarnitine analysis using electrospray tandem mass spectrometry for the diagnosis of organic acidaemias and fatty acid oxidation defects. *J Inherit Metab Dis.* 1999;22(3):302–306.
12. Sokol DK. Law, ethics, and the duty of care. *BMJ.* 2012;345:e6804. doi:10.1212/WNL.0b013e318228c15f.
13. Waisbren SE, Albers S, Amato S, et al. Effect of Expanded Newborn Screening for Biochemical Genetic Disorders on Child Outcomes and Parental Stress. *JAMA.* 2003;290(19):2564–2572. doi:10.1001/jama.290.19.2564.
14. Gurian EA, Kinnamon DD, Henry JJ, Waisbren SE. Expanded newborn screening for biochemical disorders: the effect of a false-positive result. *Pediatrics.* 2006;117(6):1915–1921. doi:10.1542/peds.2005-2294.
15. Schmidt JL, Castellanos-Brown K, Childress S, et al. The impact of false-positive newborn screening results on families: a qualitative study. *Genet Med.* 2012;14(1):76–80. doi:10.1038/gim.2011.5.
16. Bonham JR. Impact of new screening technologies: should we screen and does phenotype influence this decision? *J Inherit Metab Dis.* 2013;36(4):681–686. doi:10.1007/s10545-013-9598-y.

17. Wilcken B. Fatty acid oxidation disorders: outcome and long-term prognosis. *J Inherit Metab Dis.* 2010;33(5):501–506. doi:10.1007/s10545-009-9001-1.
18. Hoffmann L, Haussmann U, Mueller M, Spiekerkoetter U. VLCAD enzyme activity determinations in newborns identified by screening: a valuable tool for risk assessment. *J Inherit Metab Dis.* 2011. doi:10.1007/s10545-011-9391-8.
19. Dixon S, Shackley P, Bonham J, Ibbotson R. Putting a value on the avoidance of false positive results when screening for inherited metabolic disease in the newborn. *J Inherit Metab Dis.* 2012;35(1):169–176. doi:10.1007/s10545-011-9354-0.
20. Timmermans S, Buchbinder M. Patients-in-waiting: Living between sickness and health in the genomics era. *J Health Soc Behav.* 2010;51(4):408–423. doi:10.1177/0022146510386794.
21. Kwon JM, Steiner RD. “I’m fine; I’m just waiting for my disease”: the new and growing class of presymptomatic patients. *Neurology.* 2011;77(6):522–523. doi:10.1212/WNL.0b013e318228c15f.

CHAPTER 4

Fatty acid oxidation flux predicts clinical severity of VLCAD deficient patients

Eugene F. Diekman^{1,2}, Sacha Ferdinandusse¹, Ludo van der Pol²,
Hans R. Waterham¹, Jos P.N. Ruiten¹, Lodewijk Ijlst¹, Ronald J. Wanders¹,
Sander M. Houten PhD^{1,3}, Frits A. Wijburg¹, A. Christiaan Blank⁴,
Folkert W. Asselbergs MD PhD⁵, Riekelt H. Houtkooper PhD^{1*}, Gepke Visser^{6*}

¹ Laboratory Genetic Metabolic Diseases, Department of Clinical Chemistry, and Pediatrics, Emma Children's Hospital, Academic Medical Center, University of Amsterdam, The Netherlands

² Rudolf Magnus Institute of Neuroscience, Spieren voor Spieren Kindercentrum, Department of Neurology and Neurosurgery, University Medical Center, the Netherlands

³ Department of Genetics and Genomic Sciences, Icahn Institute for Genomics and Multiscale Biology, Icahn School of Medicine at Mount Sinai, New York, New York, USA

⁴ Department of Paediatric Cardiology, Wilhelmina Children's Hospital, UMC Utrecht, The Netherlands

⁵ Department of Cardiology, UMC Utrecht, The Netherlands

⁶ Department of Paediatric Gastroenterology and Metabolic Diseases, Wilhelmina Children's Hospital, UMC Utrecht, The Netherlands

* co-corresponding author

Accepted by Genetics in Medicine

ABSTRACT

Purpose: Very long-chain acyl-CoA dehydrogenase deficiency (VLCADD) is an inherited disorder of mitochondrial long-chain fatty acid β -oxidation (LC-FAO), which is included in many newborn screening programs worldwide. Patients may present with hypoketotic hypoglycemia, cardiomyopathy and/or myopathy, but clinical severity varies widely and the clinical outcome is unpredictable. We investigated predictive markers that may determine clinical severity.

Methods: We developed a clinical severity score (CSS). This CSS was determined for 13 Dutch VLCADD patients all diagnosed before the introduction of VLCADD in NBS to prevent bias from early diagnosis. In cultured skin fibroblasts from these patients, we measured LC-FAO flux (the rate of oleate oxidation), VLCAD activity, and acylcarnitine profiles following palmitate loading.

Results: The strongest correlation, $r=0.93$ ($p<0.0001$), was observed between LC-FAO flux and the CSS. VLCAD activity measurement and the C14/C16-acylcarnitine ratio correlated much less. A median LC-FAO flux of 6% of control values (range 5.6-6.8%) was associated with cardiomyopathy ($p<0.01$) and 32.4% (range 5.6-50.5%) was associated with myopathy ($p<0.05$).

Conclusion: Our results demonstrate a very strong correlation between LC-FAO flux in fibroblasts and the clinical severity of VLCADD patients. LC-FAO flux measurements may thus predict whether patients are likely to develop symptoms.

INTRODUCTION

Very long-chain acyl-CoA dehydrogenase deficiency (VLCADD), an autosomal recessive inherited disorder of mitochondrial long-chain fatty acid β -oxidation (LC-FAO), is caused by mutations in the ACADVL gene. Patients may present with a variety of clinical signs and symptoms, including hypoketotic hypoglycemia, hepatomegaly, cardiomyopathy and myopathy. These symptoms can be triggered by illness, fever, exercise, and fasting¹⁻⁴. Currently, VLCADD is included in many newborn screening (NBS) programs all over the world^{5,6}. Most newborns with VLCADD identified by NBS are asymptomatic at the time of referral⁷. As these patients are considered to be at risk of potentially life threatening symptoms, parents often get dietary advice including strict avoidance of fasting⁸. However, since the introduction of VLCADD in NBS panels, it has become clear that a significant number of newborns with VLCADD actually have a very low risk for metabolic decompensation and may even remain fully asymptomatic if left untreated⁹⁻¹¹. Unfortunately, there is currently no reliable method to assess the expected phenotypic severity at the time of diagnosis through NBS. The available literature is biased by reports of symptomatic patients and, consequently, genotype-phenotype correlation studies concern more severe presentations. These studies show that nonsense mutations in the encoding gene (ACADVL) result in a severe and early presentation with cardiomyopathy¹²⁻¹⁴, but that the more frequent missense mutations are associated with both severe or attenuated presentations¹⁰.

Functional tests, including determination of the residual activity of the VLCAD enzyme^{10,15}, have been used to test the effects of various mutations on LC-FAO activity. VLCAD enzyme activity measurement as sole functional readout has the disadvantage that it is not well suited to estimate the influence of genetic variations in potential compensatory enzymes (e.g. MCAD¹⁵ or ACAD9¹⁶). For this reason, we also performed flux studies and determined the rate of oleate oxidation (C18:1) in whole cells (LC-FAO flux). In addition we performed acylcarnitine profiling after loading cultured skin fibroblasts with labeled palmitate (in vitro probe assay)^{15,17-21}.

To identify potential predictors for disease severity in VLCADD, we studied clinical severity in 13 patients by applying a new VLCADD clinical severity score. Patients identified by NBS were excluded because early start of treatment will affect the natural history and mask the clinical severity prediction. In our pre-NBS patients we found a strong correlation between the clinical severity score with LC-FAO flux, while VLCAD enzyme activity and acylcarnitine measurements after palmitate loading was less predictive.

MATERIALS AND METHODS

The study was approved by the medical ethics committee of the University Medical Centre Utrecht (METC 10-430/C). All patients gave written informed consent for participation in this study.

Clinical severity score algorithm

We used the most frequently reported objectively verifiable signs and symptoms in the literature^{12,22,23} (Supplementary table 1), to develop a clinical severity score (CSS). The CSS encompasses the following criteria: (1) hypoglycemia, i.e. documented glucose < 2.5 mmol/L; (2) cardiomyopathy and/or arrhythmia, i.e. documented abnormal results on echocardiography (with left or right ventricular wall thickness of at least one segment >2SD, corrected for age) and/or ECG abnormalities, and (3) myopathy, i.e. documented CK levels >250U/L (ref values 70-170U/L), and in addition at least two of the following clinically relevant symptoms: myoglobulinuria, myalgia, exercise intolerance, muscle weakness (medical research council (MRC) grade 4 or less) and/or frequent fatigue.

For each criterion present, a score of one point was given resulting in a CSS of 0, 1, 2 or 3.

Hepatomegaly was not included in the CSS because in most patients no standardized measurement of liver size had been performed either by ultrasound or MRI.

Assays in fibroblasts

Fibroblasts of all patients and controls were cultured in HAM F-10 in parallel and all tests were performed in all cell lines on the same day, in order to prevent inter-assay variability. In addition, fibroblasts were cultured for 2 weeks at 30, 37 and 40°C before the biochemical assays were performed.

LC-FAO flux analysis

LC-FAO flux was determined by measuring the production of radiolabeled H₂O from [9,10-³H(N)]-oleic acid as described previously^{18,21,24}. Measurements were done at 37°C, in quadruplicate and oxidation rates were expressed as nmol of fatty acid oxidized per hour per milligram of cellular protein (nmol/h. mg protein).

VLCAD activity measurements

Very long-chain acyl-CoA dehydrogenase activity was determined in fibroblasts using C16:0-CoA as substrate and ferrocenium hexafluorophosphate as electron acceptor followed by UPLC to separate the different acyl-CoA species as described previously^{15,25}. Measurements were done at 37°C and in duplicate.

Acylcarnitine profiling

Fibroblasts were cultured in 12-well plates and incubated for 96 hours at 37°C, 5% CO₂ in MEM medium with a 1% mixture of penicillin, streptomycin and fungizone (Gibco). Furthermore, 0.4 mM L-carnitine, 0.4% BSA and 100 μM of [U-13C]palmitate were added to the medium. After 96 hours, the medium was removed from the cells followed by deproteinization using acetonitrile with subsequent analysis of the acylcarnitines by tandem mass spectrometry^{17,26}. These measurements were done in duplicate.

Statistical analysis

Statistical analysis was performed using Graphpad Prism 5. We used the Pearson correlation coefficient to test correlation between CSS and functional tests. An unpaired t-test was used to test differences between the two groups with and without myopathy, cardiomyopathy and hypoglycemia. Statistical significance is indicated as follows: *P < 0.05, **P < 0.01.

RESULTS

Patients characteristics and clinical severity score

Thirteen patients diagnosed with VLCADD in the Netherlands between January 1972 and January 2007, before the introduction of VLCADD in the NBS program, were included in this study. Patient characteristics are summarized in Table 1. Two patients had a clinical severity score (CSS) of 0, four patients had a score of 1, three had a score of 2 and four had a clinical severity score of 3 points. (Table 1)

Genotype

The genotypes of all patients are presented in Table 2. In total, 16 different mutations were detected, including five mutations that were not reported before. The most common mutations were c.104delC, p.Pro35LeufsX26 (n=3, 5 alleles) and c.848T>C, p.Val283Ala (n=4, 4 alleles).

Functional assays

Fibroblasts were available of all 13 VLCADD patients. Patient ID's (PID) were assigned based on the results of LC-FAO flux analysis at 37°C, with PID1 having the lowest LC-FAO flux and PID13 the highest LC-FAO flux. To evaluate the effect of temperature on the activity of VLCAD and on LC-FAO flux, we cultured fibroblasts for a period of 2 weeks at 30, 37 and 40°C. Culturing at 30°C allows more efficient protein folding, and may stimulate LC-FAO flux, while 40°C decreases stability and mimics a situation in which cells and thus FAO enzymes have to deal with the stress imposed by increased temperatures in vitro.

Table 1. Patient characteristics and clinical severity score. Lifetime occurrence of clinical symptoms in patients with VLCADD. CK=creatine kinase, exe intol. = exercise intolerance, myoglobin.=myoglobinuria, max walk <peers = maximum walking distance is less than peers.

Patient ID	gender	current age	start of symptoms	Cardiac problems			Myopathy >2 of the 5 criteria (lifetime)					Hypoglycemia			Clinical severity score
				abnormalities echocardiography	arrhythmia	CK	myalgia	exe intol.	myoglob.	fatigue	loss of muscle force	Hypoglycemia (recorded value)	epilepsy	Total	
1	female	10	0	yes	no	2031	yes	yes	yes	yes	yes	yes	yes (0,7)	yes	3
2	male	5	0,3	yes	no	2030	no	no	no	no	yes	yes	yes (1,3)	no	3
3	male	11	0	yes	yes	3058	yes	yes	no	no	yes	no	no	no	3
4	female	14	0,1	yes	yes	28900	yes	yes	yes	yes	yes	no	yes (1,7)	yes	3
5	female	15	1,25	no	no	400	yes	yes	yes	yes	no	no	yes (0,2)	no	2
6	male	31	12	no	no	3279	yes	yes	no	no	no	no	no	no	1
7	male	30	1	no	no	208971	yes	no	yes	yes	yes	no	Yes (0,9)	no	2
8	female	15	0,75	no	no	999	no	yes	no	no	no	no	yes (0,5)	yes	1
9	female	20	1,5	no	no	571	no	yes	no	yes	yes	yes	yes (1,0)	yes	2
10	male	18	15	no	no	1853	yes	no	yes	no	no	no	no	no	1
11	male	8	0	no	no	2324	no	no	no	no	no	no	yes (1,9)	no	1
12	male	36	2	no	no	544	no	no	no	no	no	no	no	no	0
13	female	18	-	no	no	90	no	no	no	no	yes	no	no	no	0
(14)	male	39	6	no	no	100000	yes	yes	yes	yes	yes	no	no	no	1
		16,5 (median)	1	4 yes	2 yes	2031 (median)	8 yes	8 yes	6 yes	8 yes	8 yes	3 yes	8 yes	4 yes	

Table 2. Genotype of included VLCADD patients. PID= patient identification number.

Patient ID	Allele 1		Allele 2	
1	c.643T>C	p.Cys215Arg	c.643T>C	p.Cys215Arg
2	IVS12+1G>A; c.1269+1G>A	-	IVS12+1G>A; c.1269+1G>A	-
3	c.104delC	p.Pro35LeufsX26	c.104delC	p.Pro35LeufsX26
4	c.104delC	p.Pro35LeufsX26	c.104delC	p.Pro35LeufsX26
5	c.848T>C	p.Val283Ala	c.1141-43delGAG	p.Glu381del
6	c.877C>T	p.His293Tyr	c.1322G>A	p.Gly441Asp
7	c.1406G>A	p.Arg469Gln	c.1406G>A	p.Arg469Gln
8	c.848T>C	p.Val283Ala	c.1322G>A	p.Gly441Asp
9	c.104delC	p.Pro35LeufsX26	c.848T>C	p.Val283Ala
10	c.541dupC	p.His181ProfsX72	c.1072A>G	p.Lys358Glu
11	c.272C>A	p.Pro91Gln	c.577G>C	p.Gly193Arg
12	c.848T>C	p.Val283Ala	c.1444_1448delAAGGA and 1511_1516delAGAGG	p.Lys482AlafsX78 and p.Glu504_Ala505del
13	c.1411T>C	p.Phe471Leu	c.1411T>C	p.Phe471Leu
(14)	c.520G>A	p.Val174Met	c.833_835delAAG	p.Lys278del

LC-FAO flux was very low in patients PID 1-4 (range 5.6-6.6% of controls) regardless of temperature, and higher in PID 5-13 (range 32.4-93.0% of controls) (Figure 1A). Interestingly, LC-FAO flux improved in virtually all patients at 30°C. In some, activity increased more than 50% as compared to LC-FAO flux in control fibroblasts cultured at 37°C (PID 5,6,8,9). At 40°C, LC-FAO flux was considerably lower in both control and patient fibroblasts. In some patients, LC-FAO flux decreased by as much as 40% compared to cells cultured at 37°C (PID 6,7, 9-13) (Figure 1A).

VLCAD enzyme activity was markedly reduced in all patients at 37°C (<16% of control fibroblasts) and not detectable at 40°C. At 30°C, VLCAD activity increased up to 18% to 27% in patients PID 5, 6, 8-13 (Figure 1B), whereas VLCAD activity remained undetectable in PID1-4.

Strikingly, LC-FAO flux was relatively high even with low residual VLCAD enzymatic activity. It is noteworthy that a VLCAD residual activity of 20% appears sufficient to allow normal rates of whole cell oleate oxidation (Supplementary figure 1).

Acylcarnitine profiling shows that several patients displayed a 4-5 fold accumulation of C14 and a 2-3 fold increase in C16 level (PID 1-4) (Figure 1C). The level of C14 was lower in patients PID 5-13 compared to PID1-4. In patients 1, 2 and 4, a >2-fold decrease in C2 levels was found compared to other patients (Figure 1D). The ratio of C14/C2 was particularly high in PID 1-4, in line with their almost full block in LC-FAO flux. In contrast, C12/C16 was decreased up to 3-fold in PID 1-4 compared to other patients (Figure 1E). (Supplementary table 2).

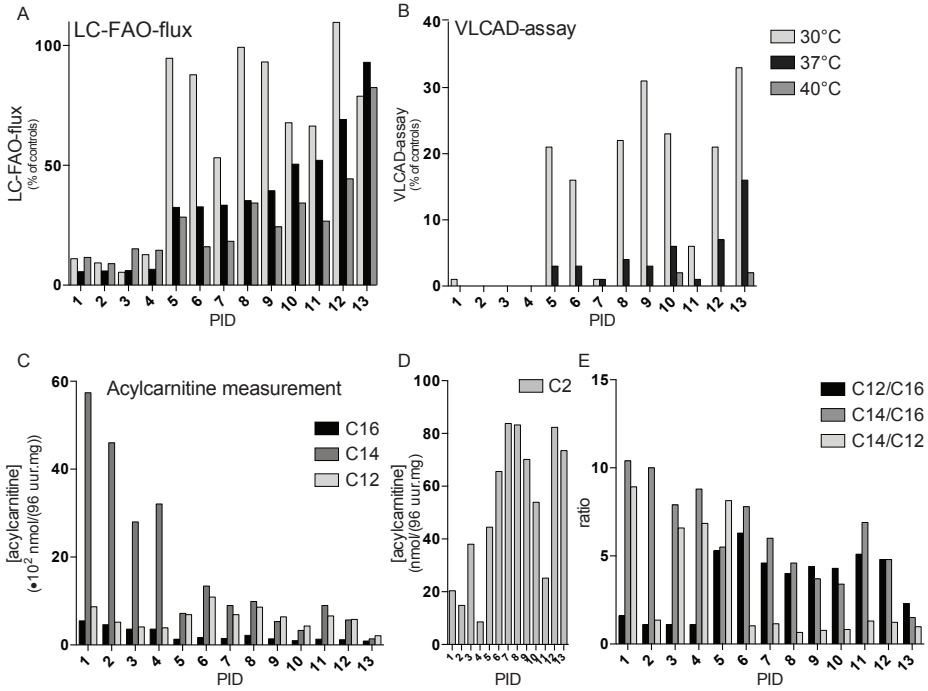


Figure 1. LC-FAO flux, VLCAD activity and acylcarnitine assay. LC-FAO flux ([9,10-3H(N)]-oleic acid oxidation rate) (A) and VLCAD-activity (with palmitoyl-CoA as substrate) (B) were measured in 13 patients after being cultured for 2 weeks at 30, 37 and 40°C. Concentrations of various (long-chain) acylcarnitines after 96 hours of incubation with [U-13C]palmitate at 37°C were plotted including C12/C14/C16 (C), C2 (D), and their corresponding ratio's C12/C16; C14/C16; C14/C2 (E). Patient ID's (PID) were assigned based on the results of LC-FAO flux analysis at 37°C, with PID1 having the lowest LC-FAO flux and PID13 the highest LC-FAO flux. PID= patient identification number.

Correlation of CSS with functional studies

We investigated the correlation between the various fibroblast tests and the CSS. As shown in Figure 2, a strong and highly significant (Pearson correlation coefficient of -0.93, $p < 0.0001$) correlation was found between LC-FAO flux and CSS (Figure 2A). Residual VLCAD enzymatic activity measurement and the C14/C16-acylcarnitine ratio also correlated significantly with the CSS, but to a lesser extent (VLCAD: Pearson $r = -0.78$, $p = 0.0014$; Figure 2B; Acylcarnitines: $r = 0.75$, $p = 0.003$, Supplementary Figure 2). In particular, LC-FAO flux has more distinctive power and accuracy in the lower activity range.

We then determined what level of LC-FAO flux is associated with the presentation of the three main symptoms. We observed that patients with cardiomyopathy have a median LC-FAO flux of 6.0% of control values (range 5.6-6.6) compared to 39.4% (range

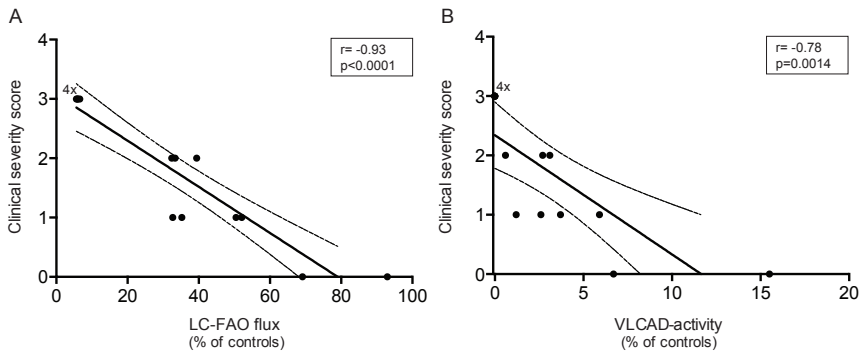


Figure 2. LC-FAO flux vs clinical severity score (A) and VLCAD activity vs clinical severity score (B). $r =$ pearson correlation coefficient.

32.4-93.0) in patients without cardiomyopathy ($p < 0.01$) (Figure 3A). Patients with myopathy had a median LC-FAO flux of 32.4% (range 5.6-50.5) compared to 60.6% (range 35.3-93.0) in patients without myopathy ($p < 0.05$) (Figure 3B). Patients with hypoglycemia had a median LC-FAO flux of 32.9% (range 5.6-52.0), compared to a median flux of 50.4% (range 6.0-93.0) in patients that did not experience hypoglycemia ($p = 0.22$) (Figure 3C).

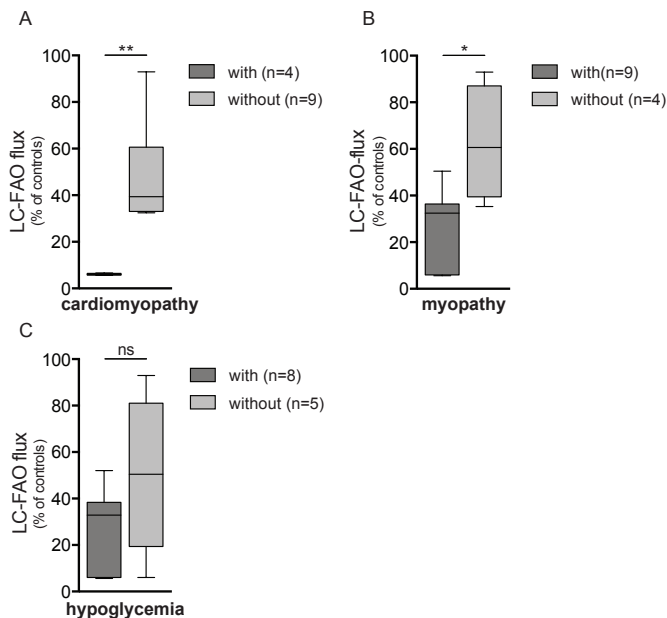


Figure 3 LC-FAO flux per symptom. Cardiomyopathy (A), myopathy (B), hypoglycemia (C). Box and whiskers (2,5-97,5 percentile).

DISCUSSION

Since the introduction of VLCADD in NBS programs, an increasing number of asymptomatic individuals has been identified^{10,11,27}. Our study aimed to develop a tool that predicts the clinical phenotype in individuals with VLCADD detected by NBS. In this paper, we show a strong correlation between LC-FAO flux in cultured skin fibroblasts and the clinical severity of the phenotype in patients with VLCADD diagnosed before introduction of VLCADD in the Dutch NBS program. We performed all tests in all cell lines on the same day to prevent inter-assay variability. We show that compared to the other assays, LC-FAO flux is a particularly accurate measure in the lower range of residual activity. In addition, LC-FAO flux measurement in fibroblasts cultured at 37°C has the most distinctive power since it ranges between 6 and 93% of control value, compared to 0-16% for the VLCAD assay. Hence we suggest that LC-FAO flux analysis in cultured fibroblasts is a useful tool for predicting the risk of developing symptoms.

We demonstrate that LC-FAO flux in fibroblasts at 37°C is the most distinctive way to map a VLCADD patient's capacity to break down long-chain fatty acids. We used a protocol that has been described before¹⁸ and widely used, and proven reproducible.

Remarkably, LC-FAO flux was much higher than expected on the basis of VLCAD-activity alone. For instance, even at a residual VLCAD activity of 20%, the flux through the LC-FAO system is equal to controls. This is also observed in fibroblasts of patients with carnitine palmitoyl transferase 2 (CPT2) deficiency²⁸. Which is fully in line with our clinical findings, since the patients with the highest residual VLCAD activity, 6 and 18% for PID12 and 13 respectively, do not display symptoms.

Interestingly, despite a residual VLCAD-activity of less than 1%, patients are still able to maintain a LC-FAO flux of approximately 6%. This strongly suggests that the residual activity is VLCAD-independent. It is likely that MCAD, ACAD9 and/or peroxisomal fatty acid oxidation may be responsible for this activity^{15,16,29,30}.

In addition to measuring LC-FAO flux at 37°C, we also studied flux in cultured fibroblasts at different temperatures which revealed that cell lines from some patients show a significant decrease in LC-FAO flux when cultured at 40°C. Indeed, in patients with a LC-FAO flux of more than 6%, a 40% decrease in LC-FAO flux was observed at 40°C (PID 6, 7, 11). Hence, some patients with a relatively high residual enzyme activity and no or only very mild symptoms under normal conditions, may develop severe symptoms during a situation in which FAO enzymes have to deal with the stress imposed by increased temperatures because of the drop in LC-FAO flux.

Fibroblasts of some patients (PID 5-12) show a marked increase in LC-FAO flux when cultured at 30°C. This indicates that VLCAD in these cell lines is more stable at 30°C, suggesting that protein misfolding and subsequent rapid degradation plays a role in the loss of activity at higher temperatures. The use of chemical chaperones for VLCAD

might therefore have a beneficial effect by stabilizing the mutant protein and enhance protein folding at 37°C³¹.

Our data suggest that functional assays in fibroblasts are better predictors of clinical severity than specific genotypes. Missense mutation often cause variable clinical phenotypes. For example, clinical phenotypes of patients with c.643T>C (p.Cys215Arg) resulted in a very severe phenotype. Patients with one c.848T>C (p.Val283Ala) allele, ranged from expected mild^{10,12}, to quite severe phenotypes (PID5 and 9, Table 1 and 2).

A potential limitation of our study is its relative small sample size. This could have resulted in inclusion bias, in particular overrepresentation of certain clinical phenotypes. We think this is unlikely, since we included Dutch patients that were identified pre-NBS, and which represent the full range of clinical phenotypes, from mild to severe. Although additional studies are needed to corroborate our findings, it is very important to only include treatment-naïve patients, because therapy interferes with the natural history.

In summary, our biochemical and clinical data demonstrate that LC-FAO flux has a strong correlation with clinical severity in patients with VLCADD. In addition, LC-FAO flux of some patients decreased with 40% when cells were cultured at 40°C. Measurement of LC-FAO flux in asymptomatic individuals with VLCADD might therefore be a useful tool to predict whether patients are likely to develop symptoms in situation of metabolic stress. Treatment could thereafter be adjusted accordingly.

REFERENCES

1. Bonnet D, Martin D, Pascale de Lonlay, et al. Arrhythmias and conduction defects as presenting symptoms of fatty acid oxidation disorders in children. *Circulation*. 1999;100(22):2248–2253. doi:10.1161/01.CIR.100.22.2248.
2. Rinaldo P, Matern D, Bennett MJ. Fatty acid oxidation disorders. *Annu Rev Physiol*. 2002;64:477–502. doi:10.1146/annurev.physiol.64.082201.154705.
3. Spiekerkoetter U, Bastin J, Gillingham M, Morris A, Wijburg F, Wilcken B. Current issues regarding treatment of mitochondrial fatty acid oxidation disorders. *J Inherit Metab Dis*. 2010;33(5):555–561. doi:10.1007/s10545-010-9188-1.
4. Wanders RJ, Vreken P, Boer den ME, Wijburg FA, van Gennip AH, IJlst L. Disorders of mitochondrial fatty acyl-CoA beta-oxidation. *J Inherit Metab Dis*. 1999;22(4):442–487.
5. Lindner M, Hoffmann GF, Matern D. Newborn screening for disorders of fatty-acid oxidation: experience and recommendations from an expert meeting. *J Inherit Metab Dis*. 2010;33(5):521–526. doi:10.1007/s10545-010-9076-8.
6. Loeber JG, Burgard P, Cornel MC, et al. Newborn screening programmes in Europe; arguments and efforts regarding harmonization. Part 1. From blood spot to screening result. *J Inherit Metab Dis*. 2012;35(4):603–611. doi:10.1007/s10545-012-9483-0.
7. Spiekerkoetter U, Sun B, Zytovicz T, Wanders R, Strauss AW, Wendel U. MS/MS-based newborn and family screening detects asymptomatic patients with very-long-chain acyl-CoA dehydrogenase deficiency. *J Pediatr*. 2003;143(3):335–342. doi:10.1067/S0022-3476(03)00292-0.
8. Arnold GL, VanHove J, Freedenberg D, et al. A Delphi clinical practice protocol for the management of very long chain acyl-CoA dehydrogenase deficiency. *Molecular Genetics and Metabolism*. 2009;96(3):85–90. doi:10.1016/j.ymgme.2008.09.008.
9. Wilcken B. Newborn Screening: Gaps in the Evidence. *Science*. 2013;342(6155):197–198. doi:10.1126/science.1243944.
10. Hoffmann L, Haussmann U, Mueller M, Spiekerkoetter U. VLCAD enzyme activity determinations in newborns identified by screening: a valuable tool for risk assessment. *J Inherit Metab Dis*. 2011. doi:10.1007/s10545-011-9391-8.
11. Schiff M, Mohsen A-W, Karunanidhi A, McCracken E, Yeasted R, Vockley J. Molecular and cellular pathology of very-long-chain acyl-CoA dehydrogenase deficiency. *Molecular Genetics and Metabolism*. 2013. doi:10.1016/j.ymgme.2013.02.002.
12. Andresen BS, Olpin S, Poorthuis BJ, et al. Clear correlation of genotype with disease phenotype in very-long-chain acyl-CoA dehydrogenase deficiency. *Am J Hum Genet*. 1999;64(2):479–494. doi:10.1086/302261.
13. Mathur A, Sims HF, Gopalakrishnan D, et al. Molecular heterogeneity in very-long-chain acyl-CoA dehydrogenase deficiency causing pediatric cardiomyopathy and sudden death. *Circulation*. 1999;99(10):1337–1343. doi:10.1161/01.CIR.99.10.1337.
14. Gregersen N, Andresen BS, Corydon MJ, et al. Mutation analysis in mitochondrial fatty acid oxidation defects: Exemplified by acyl-CoA dehydrogenase deficiencies, with special focus on genotype–phenotype relationship. *Hum Mutat*. 2001;18(3):169–189. doi:10.1002/humu.1174.
15. Wanders RJA, Ruiten JPN, IJlst L, Waterham HR, Houten SM. The enzymology of mitochondrial fatty acid beta-oxidation and its application to follow-up analysis of positive neonatal screening results. *J Inherit Metab Dis*. 2010;33(5):479–494. doi:10.1007/s10545-010-9104-8.

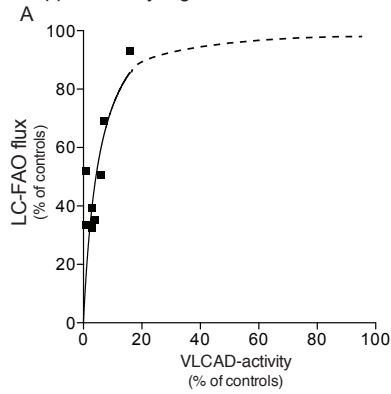
16. Nouws J, Brinke te H, Nijtmans LG, Houten SM. ACAD9, a complex I assembly factor with a moonlighting function in fatty acid oxidation deficiencies. *Hum Mol Genet.* 2013. doi:10.1093/hmg/ddt521.
17. Ventura FV, Costa CG, Struys EA, et al. Quantitative acylcarnitine profiling in fibroblasts using [U-13C] palmitic acid: an improved tool for the diagnosis of fatty acid oxidation defects. *Clin Chim Acta.* 1999;281(1-2):1–17.
18. Manning NJ, Olpin SE, Pollitt RJ, Webley J. A comparison of [9,10-3H]palmitic and [9,10-3H]myristic acids for the detection of defects of fatty acid oxidation in intact cultured fibroblasts. *J Inherit Metab Dis.* 1990;13(1):58–68.
19. Bastin J, Lopes-Costa A, Djouadi F. Exposure to resveratrol triggers pharmacological correction of fatty acid utilization in human fatty acid oxidation-deficient fibroblasts. *Hum Mol Genet.* 2011;20(10):2048–2057. doi:10.1093/hmg/ddr089.
20. Yamaguchi S, Li H, Purevsuren J, et al. Bezafibrate can be a new treatment option for mitochondrial fatty acid oxidation disorders: Evaluation by in vitro probe acylcarnitine assay. *Molecular Genetics and Metabolism.* 2012. doi:10.1016/j.ymgme.2012.07.004.
21. Olpin SE, Manning NJ, Pollitt RJ, Clarke S. Improved detection of long-chain fatty acid oxidation defects in intact cells using [9,10-3H]oleic acid. *J Inherit Metab Dis.* 1997;20(3):415–419.
22. Vianey-Saban C, Divry P, Brivet M, et al. Mitochondrial very-long-chain acyl-coenzyme A dehydrogenase deficiency: clinical characteristics and diagnostic considerations in 30 patients. *Clin Chim Acta.* 1998;269(1):43–62.
23. Baruteau J, Sachs P, Broué P, et al. Clinical and biological features at diagnosis in mitochondrial fatty acid beta-oxidation defects: a French pediatric study from 187 patients. Complementary data. *J Inherit Metab Dis.* 2014;37(1):137–139. doi:10.1007/s10545-013-9628-9.
24. Olpin SE, Manning NJ, Pollitt RJ, Bonham JR, Downing M, Clark S. The use of [9,10-3H]myristate, [9,10-3H]palmitate and [9,10-3H]oleate for the detection and diagnosis of medium and long-chain fatty acid oxidation disorders in intact cultured fibroblasts. *Adv Exp Med Biol.* 1999;466:321–325.
25. Wanders RJ, IJlst L, Poggi F, et al. Human trifunctional protein deficiency: a new disorder of mitochondrial fatty acid beta-oxidation. *Biochem Biophys Res Commun.* 1992;188(3):1139–1145.
26. Chegary M, Brinke HT, Ruiters JPN, et al. Mitochondrial long chain fatty acid beta-oxidation in man and mouse. *Biochim Biophys Acta.* 2009;1791(8):806–815. doi:10.1016/j.bbali.2009.05.006.
27. Merritt JL, Vedal S, Abdenuer JE, et al. Infants suspected to have very-long chain acyl-CoA dehydrogenase deficiency from newborn screening. *Molecular Genetics and Metabolism.* 2014;111(4):484–492. doi:10.1016/j.ymgme.2014.01.009.
28. Bonnefont JP, Taroni F, Cavadini P, et al. Molecular analysis of carnitine palmitoyltransferase II deficiency with hepatocardiomyocardial expression. *Am J Hum Genet.* 1996;58(5):971–978.
29. Chegary M, Brinke te H, Doolaard M, et al. Characterization of L-aminocarnitine, an inhibitor of fatty acid oxidation. *Molecular Genetics and Metabolism.* 2008;93(4):403–410. doi:10.1016/j.ymgme.2007.11.001.
30. Violante S, IJlst L, van Lenthe H, de Almeida IT, WANDERS RJ, Ventura FV. Carnitine palmitoyltransferase 2: New insights on the substrate specificity and implications for acylcarnitine profiling. *Biochim Biophys Acta.* 2010;1802(9):728–732. doi:10.1016/j.bbadi.2010.06.002.
31. Berendse K, Ebberink MS, IJlst L, Poll-The BT, Wanders RJA, Waterham HR. Arginine improves peroxisome functioning in cells from patients with a mild peroxisome biogenesis disorder. *Orphanet J Rare Dis.* 2013;8(1):138. doi:10.1186/1750-1172-8-138.

Supplementary Table 1. Clinical symptoms described in literature.

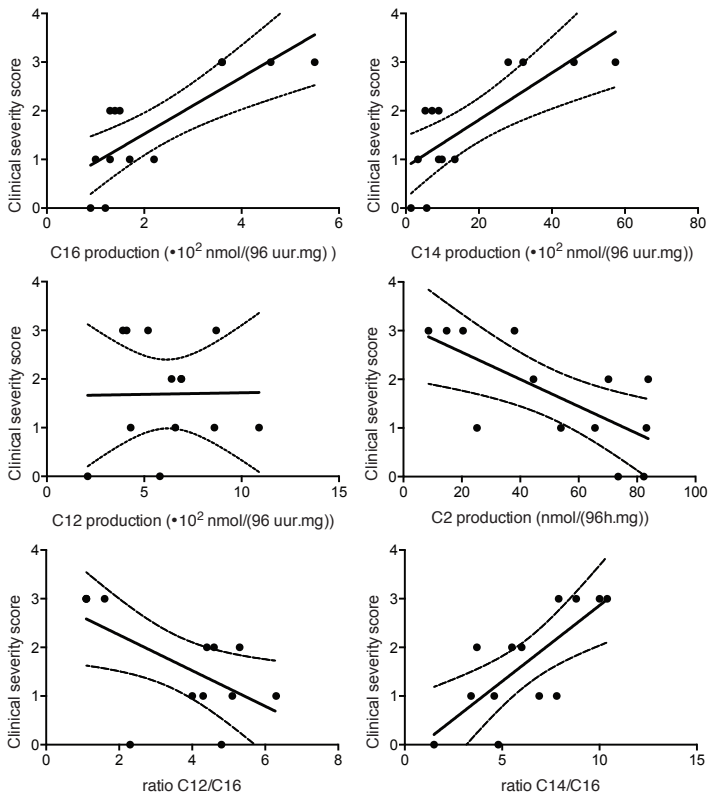
Symptoms	<i>Vianey 1998</i>	<i>Andresen 1999</i>	<i>Baruteau 2014</i>
hepatomegaly		61%	96%
increased transaminases			95%
hypoglycemia/lethargy	43%	30%	73%
cardiomyopathy/	36%	52%	61%
arrhythmia	18%		52%
myopathy/cramps/rhabdomyolysis	4%	20%	85%
hypotonia		50%	
neurological symptoms			56%

Supplementary Table 2. LC-FAO flux, VLCAD activity and acylcarnitine assay measurements of all patients. LC-FAO flux ([9,10-³H(N)]-oleic acid oxidation rate) and VLCAD-activity (with palmitoyl-CoA as substrate) were measured after being cultured for 2 weeks at 30, 37 and 40°C. Various (long-chain) acylcarnitine concentrations were measured after 96 hours of incubation with [U-13C]palmitate at 37°C. Measurements were performed in 13 patients. Patient ID's (PID) were assigned based on the results of LC-FAO flux analysis at 37°C, with PID1 having the lowest LC-FAO flux and PID13 the highest LC-FAO flux. PID= patient identification number. % = percentage of controls.

	LC-FAO flux			VLCAD-activity			Acylcarnitine measurements																
	30°C			37°C			40°C			30°C			40°C			37°C							
	nmol/(h.mg)	% of controls	SD	nmol/(h.mg)	% of controls	SD	nmol/(h.mg)	% of controls	SD	% of controls	% of controls	C16 nmol/(96µr.mg)	% of controls (Y10 ³)	C14 nmol/(96µr.mg)	% of controls (Y10 ³)	C12 nmol/(96µr.mg)	% of controls (Y10 ³)	C2 nmol/(96µr.mg)	% of controls (Y10 ³)	% of controls	C12/C16	C14/C16	C14/C2
1	0,6	11,1	0,5	0,1	5,6	0,8	11,6	0,6	0,00	0,03	0,0	0,0	2,8	5,5	12,4	57,4	15,2	8,7	4,9	20,4	1,6	10,4	281
2	0,5	9,3	0,5	0,1	5,9	0,6	9,0	0,0	0,00	0,02	0,0	0,0	1,7	4,6	9,9	46,0	12,6	5,2	3,5	14,8	1,1	10,0	310
3	0,3	5,4	0,5	0,1	6,1	1,1	15,1	0,0	0,00	0,03	0,0	0,0	1,3	3,6	6,1	28,0	9,8	4,1	9,1	38,0	1,1	7,9	74
4	0,7	12,7	0,6	0,1	6,6	1,1	14,5	0,0	0,00	0,03	0,0	0,0	1,3	3,6	6,9	32,1	10,0	3,9	2,1	8,6	1,1	8,8	371
5	5,6	94,7	2,9	0,3	32,4	2,1	28,4	21,3	0,10	0,01	2,7	0,0	2,2	1,3	1,6	7,2	3,6	6,9	10,6	44,5	5,3	5,5	16
6	5,2	87,8	2,9	0,1	32,7	1,2	16,0	15,8	0,10	0,01	2,6	0,0	3,5	1,7	2,9	13,4	4,7	10,9	15,7	65,6	6,3	7,8	20
7	3,1	53,2	3,0	0,2	33,4	1,3	18,3	1,2	0,02	0,01	0,6	0,0	2,2	1,5	1,9	9,0	4,1	6,9	20,0	83,8	4,6	6,0	11
8	5,8	99,2	3,2	0,1	35,3	2,5	34,3	22,2	0,14	0,03	3,7	0,0	2,8	2,2	2,2	9,9	5,9	8,6	19,9	83,2	4,0	4,6	12
9	5,5	93,1	3,6	0,3	39,4	1,8	24,4	30,7	0,12	0,02	3,1	0,0	2,1	1,4	1,1	5,3	3,9	6,4	16,8	70,2	4,4	3,7	8
10	4,0	67,8	4,6	0,2	50,5	2,5	34,3	23,1	0,22	0,03	5,9	1,6	1,4	1,0	0,7	3,3	2,7	4,3	12,9	53,9	4,3	3,4	6
11	3,9	66,4	4,7	0,6	52,1	1,9	26,7	6,4	0,04	0,02	1,2	0,0	2,1	1,3	1,9	9,0	3,6	6,6	6,0	25,2	5,1	6,9	36
12	6,4	109,7	6,2	1,2	69,1	3,2	44,3	20,9	0,25	0,03	6,7	0,2	1,9	1,2	1,2	5,7	3,3	5,8	19,7	82,3	4,8	4,8	7
13	4,6	78,8	8,4	1,0	93,0	6,0	82,4	32,9	0,58	0,08	15,5	2,4	0,7	0,9	0,3	1,4	2,4	2,1	17,6	73,5	2,3	1,5	2



Supplementary Figure 1. Relationship between VLCAD activity and total LC-FAO flux. VLCAD activity in fibroblasts is plotted against the corresponding LC-FAO flux measured in fibroblasts after being cultured for 2 weeks at 37°C.



Supplementary Figure 2. Acylcarnitine assay vs clinical severity score.

CHAPTER 5

Normal cardiac function with minimal decrease of myocardial contractility in very long-chain acyl-CoA dehydrogenase deficient patients

E.F. Diekman^{1,2}, A.C. Blank³, F. Asselbergs⁴, M. de Vries⁵, M.E. Rubio Gozalbo⁶, T. Derks⁷, M. Williams⁸, M.F. Mulder⁹, S.M. Houten¹⁰, W.L. van der Pol¹¹, F.A. Wijburg², G. Visser¹

¹ Department of Metabolic and Endocrine diseases, Wilhelmina Children's Hospital, UMC Utrecht, The Netherlands

² Laboratory Genetic Metabolic Diseases, Departments of Clinical Chemistry and Pediatrics, Emma Children's Hospital, Academic Medical Center, University of Amsterdam, The Netherlands

³ Department of Pediatric Cardiology, University Medical Center Utrecht, The Netherlands

⁴ Department of Cardiology, University Medical Center Utrecht, The Netherlands

⁵ Department of Pediatrics, Metabolic and Endocrine Disorders, Radboud University Nijmegen Medical Center (RUN-MC), The Netherlands

⁶ Department of Pediatrics, Metabolic diseases, Maastricht University, The Netherlands

⁷ Department of Pediatrics, Metabolic diseases, Beatrix Children's hospital, University Medical Center Groningen, The Netherlands

⁸ Department of Pediatrics, Metabolic diseases, Sophia Children's hospital, University Medical Center Rotterdam, The Netherlands

⁹ Department of Pediatrics, Metabolic diseases, VU Medical Center Amsterdam, The Netherlands

¹⁰ Department of Genetics and Genomic Sciences, Icahn Institute for Genomics and Multiscale Biology, Icahn School of Medicine at Mount Sinai, New York, New York, USA

¹¹ Department of Neurology, University Medical Center Utrecht, The Netherlands

Manuscript in preparation

ABSTRACT

Background: Mitochondrial long-chain fatty acid β -oxidation (lcFAO) disorders are included in newborn screening programs (NBS) worldwide. Patients with lcFAO deficiencies can present with cardiomyopathy and loss of cardiac function. Myocardial strain echocardiography is able to detect subclinical myocardial dysfunction at an early stage.

Aim: To investigate myocardial function in lcFAO deficient children.

Methods: Transthoracic echocardiograms were acquired in 20 lcFAO deficient children and 16 age-matched healthy controls. Fractional shortening (%), LVEDs/d (Z-score), IVSs/d (Z-score), LVPWs/d (Z-score) and circumferential (%), radial (%), and longitudinal peak systolic (%) strain values were determined.

Results: Fractional shortening was $>30\%$ in 18 of the 20 patients (90%). Z-scores of LVEDd, LVPWd, IVSs and/or LVPWs were within normal range ($<2SD$) in 17 of 20 patients. Circumferential anterior and posterior peak systolic strain was reduced by 42% ($p<0.01$) and 68% ($p<0.05$) in patients compared to age matched healthy controls. Radial posterior peak systolic strain and inferior peak systolic strain were reduced by 49% ($p<0.05$) and 36% ($p<0.05$). ECG and Holter-ECG analysis revealed rhythm disturbances in 25% (5 out of 20) of patients.

Conclusion: Despite a disturbed mitochondrial fatty-acid β -oxidation, we observed normal cardiac function with only a minimal decrease in myocardial contractility and no arrhythmia, in the majority of pediatric lcFAO deficient patients.

INTRODUCTION

Long chain fatty acid oxidation (lcFAO) disorders are caused by inherited enzyme deficiencies which all lead to a disturbed mitochondrial β -oxidation. lcFAO disorders include very long-chain acyl-CoA dehydrogenase deficiency (VLCADD); mitochondrial trifunctional protein deficiency (MTPD) and long-chain hydroxyl acyl-CoA dehydrogenase deficiency (LCHADD). A healthy heart relies on mitochondrial β -oxidation for 60-90% of its energetic needs¹⁻³. It is therefore not surprising that patients with lcFAO disorders may present with cardiac problems. The combination of severe and potentially life threatening complications and a favourable response to treatment, has led to the inclusion of lcFAO disorders in newborn screening (NBS) programs worldwide in the last decades. The prevalence of lcFAO disorders has increased ever since.

Before the inclusion of lcFAO disorders in NBS programs, a frequently reported presenting symptom in lcFAO disorders was cardiomyopathy. Hypertrophic as well as dilated cardiomyopathy have been described⁴⁻¹⁴. According to literature 36 to 47 percent^{4,15} of VLCADD patients had cardiomyopathy at the time of diagnosis. The numbers for MTPD¹⁶, and LCHADD¹⁷ patients are 30 and 46%, respectively. Another cardiac problem, which has been described as presenting symptom in patients with lcFAO deficiency, is arrhythmia. In a retrospective study, thirty-one percent of lcFAO deficient patients presented with rhythm disturbances, primarily ventricular tachycardia⁴. These studies are primarily focused on presenting symptoms and do not describe follow-up of patients with lcFAO deficiency with or without arrhythmias and/or cardiomyopathy. In addition, due to newborn screening now also "presymptomatic" patients are identified and potentially subclinical cardiac problems in this patients group have not yet been investigated. We therefore evaluated cardiac function in lcFAO deficient patients identified by symptoms or by newborn screening and made use of transthoracic echocardiography with myocardial¹⁸ strain to be able to detect clinical and subclinical myocardial dysfunction.

METHODS

Patients & controls

20 Dutch patients (age range 0-18yrs, median 10.5yrs, 11 male, 9 female) with genetically confirmed lcFAO disorders were studied. Detailed information is given in Table 1 and 2. All patients were examined in our centre. Fifteen patients with very long-chain acyl-CoA dehydrogenase deficiency (VLCADD), 4 with mitochondrial protein deficiency (MTPD) and one with long-chain hydroxyl acyl-CoA deficiency (LCHADD) patients were included in the study. Four patients have or have had hypertrophic or dilated cardiomyopathy (HCM, DCM). Mutation analysis revealed c.848T>C as most frequent mutation

Table 1. Patient characteristics. PID= patient identification number, m= male, f= female.

PID	Gender	Age	Disease	Allele 1	Allele 2	Cardiac history	Walking distance	Medication	LCT restriction	MCT-enrichment			
1	m	2.0	VLcADD	c.1322G>A	p.Gly441Asp	p.Gly441Asp	c.1322G>A	p.Gly441Asp	no abnormalities (1st check 0yrs)	< peers	no	no	
2	f	3.0	VLcADD	c.1044delC	p.Pro35LeufsX26	p.Pro35LeufsX26	c.848T>C	p.Val283Ala	no abnormalities (1st check 0yrs)	normal	yes	yes	
3	m	3.1	VLcADD	c.1322G>A	p.Gly441Asp	p.Gly441Asp	c.1844G>A	p.Arg615Gln	normal	normal	no	no	
4	f	4.4	VLcADD	c.848T>C	p.Val283Ala	p.Val283Ala	c.848T>C	p.Val283Ala	normal	normal	yes	no	
5	m	5.0	VLcADD	c.1322G>A	p.Gly441Asp	p.Gly441Asp	c.1468G>C	p.Ala490Pro	normal	normal	no	no	
6	m	5.1	VLcADD	c.848T>C	p.Val283Ala	p.Val283Ala	c.848T>C	p.Val283Ala	normal	normal	yes	no	
7	m	5.4	VLcADD	IVS12+1G>A; c.1269+1G>A	p.?	p.?	IVS12+1G>A; c.1269+1G>A	p.?	HCM and mild pericard-effusie (1st check 0 yrs)	normal	anti-hypertensive drugs	yes	yes
8	m	6.2	VLcADD	c.848T>C	p.Val283Ala	p.Val283Ala	c.266DelC	p.Pro89HisfsX28	normal	normal	yes	no	
9	f	10.4	VLcADD	c.643T>C	p.Cys215Arg	p.Cys215Arg	c.643T>C	p.Cys215Arg	no abnormalities (1st check 0yrs)	< peers	yes	yes	
10	m	11.0	VLcADD	c.272C>A	p.Pro91Gln	p.Pro91Gln	c.577G>C	p.Gly193Arg	no abnormalities (1st check 0yrs)	normal	no	no	
11	m	11.6	VLcADD	c.1044delC	p.Pro35LeufsX26	p.Pro35LeufsX26	c.1044delC	p.Pro35LeufsX26	no abnormalities (1st check 0yrs)	normal	yes	yes	
12	f	14.8	VLcADD	c.1044delC	p.Pro35LeufsX26	p.Pro35LeufsX26	c.1044delC	p.Pro35LeufsX26	HCM (1st check 0 yrs)	< peers	yes	yes	
13	f	15.4	VLcADD	c.848T>C	p.Val283Ala	p.Val283Ala	c.1141-43delGAG	p.Glu381del	no abnormalities (1st check 1yr)	normal	no	no	
14	f	15.4	VLcADD	c.848T>C	p.Val283Ala	p.Val283Ala	c.1322G>A	p.Gly441Asp	no abnormalities (1st check 1yr)	normal	no	no	
15	f	18.7	VLcADD	c.1411T>C	p.Phe471Leu	p.Phe471Leu	c.1411T>C	p.Phe471Leu	deceased, DCM (1st check 0yrs)	normal	n.a.	n.a.	
16	f	0.0	MTPD	c.212+1G>C			c.212+1G>C		DCM (1st check 0 yrs)	< peers	yes	yes	
17	f	10.7	MTPD	c.2027G>T	p.R676L	p.R676L	c.2027G>T	p.R676L	DCM (1st check 0 yrs)	< peers	yes	yes	

Table 1. Patient characteristics. PID= patient identification number, m= male, f= female. (continued)

PID	Gender	Age	Disease	Allele 1	Allele 2	Cardiac history	Walking distance	Medication	LCT restriction	MCT- enrichment
18	m	12.9	MTPD	c.556C>G	p.Q186E c.1336Del57nt ivs13+1G>A	p.?	< peers		yes	yes
19	m	14.8	MTPD	c.556C>G	p.Q186E c.1336Del57nt ivs13+1G>A	p.?	< peers	no abnormalities (1st check 9yrs)	yes	yes
20	m	13.3	LCHADD	c.1528G>C	p.Glu510Gln c.1712T>C	p.Leu571Pro	normal	no abnormalities (1st check 1yr)	yes	yes

Table 2. Echocardiographic measurements patients and controls. LVEDs/d= systolic and diastolic left ventricular end-diastolic wall thickness, IVSs/d= systolic and diastolic interventricular septum thickness, LVPWs/d= systolic and diastolic end-diastolic posterior wall thickness, FS= left ventricular (LV) fractional shortening. Stdev = standard deviation, *Krukis-Wallis + Dunn's multiple comparison's test.

	Controls		Patients		p-value*	effect pairing
	mean	stdev	mean	stdev		
Age	9,2	4,7	9,2	5,5	0.999	r=0.999, p=0.0001
Gender	6f/10m		9f/11m			
Height (cm)	136,7	28,5	132,1	33,8	0.999	
Weight (kg)	36,2	16,6	38,0	21,6	0.999	
LVEDd (Z)	0,4	0,6	-0,1	1,1	0.556	
IVSd (Z)	-0,3	0,4	0,1	0,6	0.8310	
LVPWd (Z)	0,3	0,8	0,6	1,3	0.999	
LVEDs (Z)	0,5	0,5	0,4	1,2	0.999	
IVSs (Z)	-0,2	0,7	-0,3	0,9	0.999	
LVPWs (Z)	-0,3	0,6	0,6	1,1	0.188	
FS(%)	36,0	3,9	34,4	5,5	0.999	

(25% of 20x2 alleles). Eight of the 20 patients were diagnosed before inclusion of IcFAO disorders in NBS. Six patients were not able to walk as far as their peers, or needed a wheelchair and 7 patients were not able to practice sports, and 1 patient was too young to do both. One patient used antihypertensive medication. Twelve patients were on a long-chain triglyceride restricted (LCT) diet. Nine of which were enriched with medium-chain triglycerides.

Age-matched controls were selected randomly from our database. We only included healthy people that received echocardiography to rule out disease.

Echocardiography

Transthoracic echocardiograms were performed using a standardized protocol as described by the American association of echocardiography¹. All echos were reviewed for any abnormalities by 2 technicians and supervised by a cardiologist (ACB). In all children, left ventricular systolic and end-diastolic wall thickness (LVEDs/d), systolic and diastolic interventricular septum thickness (IVSs/d) and systolic and end-diastolic posterior wall thickness (LVPWs/d) were measured. Left ventricular (LV) fractional shortening was measured as index for LV systolic function. All parameters were adjusted for body-size, expressed as a Z-score. In addition, circumferential (%), radial (%) and longitudinal peak systolic (%) strain values were determined.

Electrocardiogram

A six lead-electrocardiogram was performed in all patients. All traces were reviewed by a cardiologist (ACB) and any abnormalities in HF, SR, QRS-axis, QRS time, PR time, QTc time, conduction, repolarisation/voltage abnormalities were reported.

Holter-electrocardiogram

Holter-electrocardiogram was recorded in 14 patients. The existence of premature atrial contractions (PACs) and premature ventricular contractions (PVCs) was reported.

Laboratory measurements

(NT-Pro)BNP, troponin, CK, CK-MB as well as triglyceride and cholesterol were measured in all patients on the day that echocardiography was performed.

Diet

An extensive dietary analysis was performed in 17 out of 20 patients. Dietary analysis was based on a 3-day diary and subsequent questionnaire by a nutritionist and included information about protein, carbohydrate, and fat intake. LCT and MCT intake was subsequently calculated (calculated as energy% (En%)). LCT restriction was defined as <25En% derived from fat.

RESULTS

Transthoracic echocardiography was done in all patients. Cardiac function was abnormal in 2 out of 20 patients, with a fractional shortening of 18% and 26%. The first patient died shortly after birth due to cardiopulmonary distress. Median fractional shortening was 34.1%. Left ventricular wall thickness was abnormal in three patients. Patient 5 had an LVEDd Z-score of 2 and LVEDs of 3.7, patient 7 had IVSs of -2.1 and patient 16 had LVEDs of -2.5, a LVPWd of 4.7 and LVPWs of 3.8 (Supplementary Table 1). Two of which have been diagnosed with HCM with normal function. Median Z-score LVEDd of -0.3, IVSd 0.1, LVPWd 0.2, LVEDs 0.2, IVSs -0.4, LVPWs 0.6.

Strain echocardiography was performed to reveal any subclinical myocardial dysfunction. Strain echocardiography was abnormal in many patients (Figure 1, Table 3 and supplementary tables 2, 3, and 4). Mean circumferential anterior peak systolic strain was decreased to -9.8% in patients compared to -20.5% in healthy controls (=53% decrease, $p < 0.004$). Mean radial anterior, lateral and septal peak systolic strain were all significantly decreased to 32.2%, 31.9% and 44.7% in patients compared to 53.7%, 56.1, and 65.3% in healthy controls, (=41%, 44% and 32% decrease, $p < 0.05$). Median radial posterior and inferior peak systolic strain was decreased to 36.6 and 41.1% in patients compared to

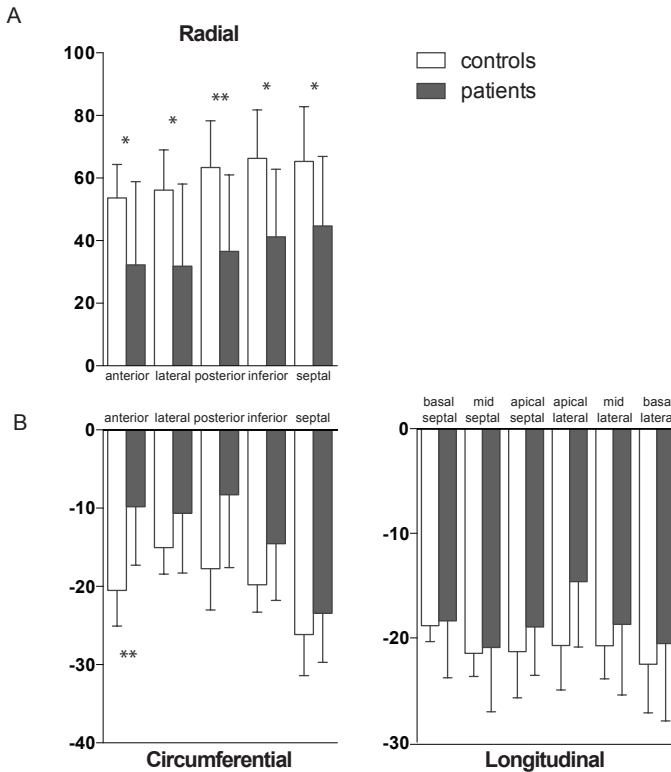


Figure 1. Strain echocardiography in pediatric LcFAO patients. Mean circumferential/radial anterior/lateral/posterior/inferior/septal peak systolic strain and longitudinal basal/mid/apical septal and apical/mid/basal lateral peak systolic strain are displayed in LcFAO deficient patients compared to controls. Error bars indicate +SD, * = $p < 0.05$; ** = $p < 0.01$.

63.4% and 66.3% in healthy controls (=42 and 38% decrease, $p < 0.01$) (Figure 1, Table 3, suppl. Table 2,3,4). Longitudinal strain could not be obtained in many patients. Based on the available data median longitudinal strain values were not different from controls (Figure 1, Table 3, suppl. Table 2,3,4).

ECG analysis was performed in 20 of the 20 patients and revealed rhythm disturbances (1st degree AV-block) in 1 patient. Holter ECG was performed in 12 of the 20 patients and revealed 5 patients with rhythm disturbances. Two patients with Premature Atrial Contractions (PACs) $> 1/h$ (with a max of 10/hour); 2 patients revealed Premature Ventricular Contractions (PVCs) $> 2/h$ (with a max of 46/hour); 2 patients showed a second degree AV block (Mobitz 1) and 1 patient showed an AVJ escape beat (Table 4).

Table 3. Circumferential (%), radial (%) and longitudinal peak systolic (%) strain values in patients and controls. Stdev = standard deviation, *Krukis-Wallis + Dunn's multiple comparison's test.

		Controls		Patients		p-value*
		mean	stdev	mean	stdev	
Circumferential	anterior	-20,5	4,5	-9,8	7,5	0.004
	lateral	-15,1	3,4	-10,6	7,6	0.999
	posterior	-17,7	5,3	-8,3	9,3	0.209
	inferior	-19,8	3,5	-14,5	7,3	0.232
	septal	-26,1	5,3	-23,4	6,3	0.999
Radial	anterior	53,7	10,7	32,2	26,7	0.036
	lateral	56,1	12,9	31,9	26,2	0.015
	posterior	63,4	14,9	36,6	24,4	0.002
	inferior	66,3	15,5	41,1	21,6	0.006
	septal	65,3	17,5	44,7	22,2	0.039
Longitudinal	basal septal	-18,8	1,5	-18,4	5,4	0.999
	mid septal	-21,5	2,2	-20,9	6,2	0.999
	ap septal	-21,3	4,4	-18,9	4,6	0.913
	ap lateral	-20,7	4,3	-14,6	6,2	0.930
	mid lateral	-20,7	3,2	-18,7	6,8	0.999
	bas lateral	-22,5	4,6	-20,5	7,4	0.999

Median CK level was 198 U/L (range 91-30267), CK-MB 4.1 (range 1.3-69.5), ASAT 31.5 (range 12-577), ALAT 24 (range 7-892), cholesterol 3.6 (range 2.3-4.8) and triglycerides of 0.9 (range 0.3-4.6), BNP 5 (range 2-16), troponin 0.01 (range 0.01-0.06) (Table 5).

Twelve patients were on an LCT restricted diet, of which 9 patients received MCT enrichment. No association could be observed between fractional shortening and wall-thickness (data not shown). We did observe a correlation between LCT En% and radial strain, in particular septal radial strain (Supplementary Figure 1, $r=0.71$, $p=0.004$).

Table 4. Electrocardiography (ECG) measurements. Bpm = beats per minute, ms= milliseconds, s= seconds, PAC= premature atrial contraction, PVC= premature ventricular contraction, AV= atrioventricular, AVJ= atrioventricular junction.

PID	Sinus rhythm	HF (bpm)	QRS-axis (°)	PR (ms)	QRS (s)	QTc (s)	Remarks	Repolarisation/ voltage	Holter-ECG	Valve
1	no atrial rhythm with positive P in I and II and negative P in aVF	153	-18	100	106	434		normal		
2	yes	105	60	108	66	409		normal		
3	yes	107	80	110	62	432		normal		
4	yes	111	122	112	84	419		normal		
5	yes	82	67	130	76	429		normal		
6	yes	110	38	120	64	407		normal	1x 2 nd degree AV-block Mobitz I	
7	yes	78	60	136	82	456		normal		
8	yes	89		104	70	403		normal		
9	yes	65		154	74	407		not normal		
10	yes	64	50	160	98	375		normal		
11	yes	69	65	162	88	394		normal	PACs max 10/h, total 24/24h. PVCs max 46/h, total 169/24h.	
12	yes	65	67	160	104	411	1 st degree AV-block	not normal	PACs max 2/h, total 10/24h. 1x AVJ escape beat. 1x atrial escape beat.	
13	yes	81	64	140	100	415		normal	No PACs, PVCs max 10/h, total 42/24h	
14	yes	71		158	90	402				
15	yes	85		166	80	418		normal		
16										
17	yes	98	47	134	70	449		normal		
18	yes	73	54	106	88	403		normal		
19	yes	71	79	128	96	415		normal		
20	yes	77	57	170	92	427		normal	1x 2 nd degree AV-block Mobitz I	

Table 5. Various laboratory measurements on the day of echocardiography.

PID	CK max (U/L)	CK (U/L)	CK MB (U/L)	ASAT	ALAT	Cholesterol	Triglycerides	BNP	Troponin
1	163610	1822							
2	170	170	4,1	29	28	3,6	1	10	0,01
3	120	120	2,7	49	15	4,8	2,1	7	0,01
4	96	96	1,8	27	10	3,6	0,8	3	0,01
5	91	91	3,8	31	14	3,6	1,2	7	0,01
6	200	200	6,1	38	15	4	0,5	3	0,01
7	2030	209	14,7	61	76	4,2	0,9	16	0,04
8	198	198	5,1	30	13	3,6	0,6	13	0,01
9	2031	251	11,5	40	80	4,3	4,6	4	0,01
10	2324	212	4,5	32	19	3,8	1	5	0,01
11	3058	708	17,5	41	72	3,8	0,3	3	0,01
12	28900	11180	69,5	577	892	3,2	0,4	16	0,06
13	174	35			11			3	
14	999	140	3	14	29			8	0,01
15	90	90	1,3	12	7	4,4	1,1	4	0,01
16				54	24				
17	114552	30267		491	153				
18	9642	160	3,8	20	28	2,8	1,6	2	0,01
19	12721	549		23	28	2,3	0,6	5	0,01
20	197	197	2,7	30	24	3,3	0,4	6	0,01
	999	198	4,1	31,5	24	3,6	0,9	5	0,01

DISCUSSION

We observed normal cardiac function with only a minimal decrease in myocardial contractility in patients with IcFAO disorders. Our study shows that peak circumferential and radial systolic strain are reduced in many patients (42-68%), suggesting subclinical myocardial dysfunction. Myocardial strain echocardiography, is able to detect regional myocardial muscle shortening and lengthening (contractility) throughout the cardiac cycle^{18,19}. It has been observed that despite preserved ejection fraction, abnormal shortening en lengthening can precede development of hypertrophic cardiomyopathy²⁰⁻²². Interestingly, reduced peak systolic strain was not only present in the patient with HCM at the start of this study, but also in patients detected via newborn screening. Whether this means that these patients are prone to develop cardiomyopathy remains to be elucidated and should be investigated in future follow-up studies.

Furthermore, myocardial strain echocardiography is able to assess the relative contribution of scar versus other myocardial derangements to regional functional impairment²³ and it relates to local differences in myocardial metabolism²⁴. The observed decrease in peak circumferential and radial systolic strain could indicate myocardial disarray or alterations in myocardial metabolism. Two explanations have been described that might cause altered myocardial metabolism in VLCADD patients. The first explanation involves lipotoxicity. Studies performed in obese and diabetic patients suggest that myocardial lipid accumulation may decrease heart function^{25,26}. In *IcFAO* deficient knock-out mouse, increased myocardial lipid levels and cardiac hypertrophy have been reported²⁷⁻³⁰. More specific, fasting-induced lipid accumulation is accompanied by impaired left ventricular function³¹ and autopsy of a patient with VLCADD showed mild to moderate lipid accumulation¹³. In our patient population, LCT restriction (a decrease in lipid load) or MCT supplementation, did not influence cardiac function. At most we observed the opposite, because normal dietary En% LCT is associated with better radial myocardial contractility (Supplementary Figure 1). However, this observation is in line with the fact that patients with less symptoms generally do not use an LCT-restricted diet.

An alternative, or additional explanation could be an impaired myocardial energy status. *IcFAO* deficient knock-out mice have an elevated reliance on glucose oxidation, disturbed protein homeostasis and an impaired myocardial energy status after fasting^{32,33}. The observed altered myocardial metabolism, may also be true for *IcFAO* deficient patients and lead to abnormal contractility. Impaired myocardial energy status and/or lipotoxicity may also cause rhythm disturbances³⁴. However, we observed only 1 patient (5%) who had mild rhythm disturbances and 4 patients who had above average PACs and/or PVCs or a second degree AV block (Mobitz 1) or AVJ escape beat on their Holter ECG.

In summary, a healthy heart relies on mitochondrial *IcFAO* for a great part of its energetic needs. However, in the majority of pediatric *IcFAO* deficient patients, we observed normal cardiac function with only a minimal decrease in myocardial contractility and no arrhythmia.

REFERENCES

1. Gottdiener JS, Bednarz J, Devereux R, Gardin J, Klein A, Manning WJ, Morehead A, Kitzman D, Oh J, Quinones M, Schiller NB, Stein JH, Weissman NJ, American Society of Echocardiography. American Society of Echocardiography recommendations for use of echocardiography in clinical trials. *J Am Soc Echocardiogr*. 2004;17:1086–1119.
2. Hue L, Taegtmeyer H. The Randle cycle revisited: a new head for an old hat. *AJP: Endocrinology and Metabolism*. 2009;297:E578–91.
3. Randle PJ, Garland PB, Hales CN, Newsholme EA. The glucose fatty-acid cycle. Its role in insulin sensitivity and the metabolic disturbances of diabetes mellitus. *Lancet*. 1963;1:785–789.
4. Baruteau J, Sachs P, Broué P, Brivet M, Abdoul H, Vianey-Saban C, Ogier De Baulny H. Clinical and biological features at diagnosis in mitochondrial fatty acid beta-oxidation defects: a French pediatric study of 187 patients. *J Inherit Metab Dis*. 2012;
5. Treem WR, Stanley CA, Hale DE, Leopold HB, Hyams JS. Hypoglycemia, hypotonia, and cardiomyopathy: the evolving clinical picture of long-chain acyl-CoA dehydrogenase deficiency. *Pediatrics*. 1991;87:328–333.
6. Brown-Harrison MC, Nada MA, Sprecher H, Vianey-Saban C, Farquhar J, Gilladoga AC, Roe CR. Very long chain acyl-CoA dehydrogenase deficiency: successful treatment of acute cardiomyopathy. *Biochem Mol Med*. 1996;58:59–65.
7. Sourì M, Aoyama T, Orii K, Yamaguchi S, Hashimoto T. Mutation analysis of very-long-chain acyl-coenzyme A dehydrogenase (VLCAD) deficiency: identification and characterization of mutant VLCAD cDNAs from four patients. *Am J Hum Genet*. 1996;58:97–106.
8. Mathur A, Sims HF, Gopalakrishnan D, Gibson B, Rinaldo P, Vockley J, Hug G, Strauss AW. Molecular heterogeneity in very-long-chain acyl-CoA dehydrogenase deficiency causing pediatric cardiomyopathy and sudden death. *Circulation*. 1999;99:1337–1343.
9. Sluysmans T, Tuerlinckx D, Hubinont C, Verellen-Dumoulin C, Brivet M, Vianey-Saban C. Very long chain acyl-coenzyme A dehydrogenase deficiency in two siblings: evolution after prenatal diagnosis and prompt management. *J Pediatr*. 1997;131:444–446.
10. Cox GF, Sourì M, Aoyama T, Rockenmacher S, Varvogli L, Rohr F, Hashimoto T, Korson MS. Reversal of severe hypertrophic cardiomyopathy and excellent neuropsychologic outcome in very-long-chain acyl-coenzyme A dehydrogenase deficiency. *J Pediatr*. 1998;133:247–253.
11. Roe CR, Sweetman L, Roe DS, David F, Brunengraber H. Treatment of cardiomyopathy and rhabdomyolysis in long-chain fat oxidation disorders using an anaplerotic odd-chain triglyceride. *J Clin Invest*. 2002;110:259–269.
12. Spiekerkoetter U, Tenenbaum T, Heusch A, Wendel U. Cardiomyopathy and pericardial effusion in infancy point to a fatty acid b-oxidation defect after exclusion of an underlying infection. *Pediatr Cardiol*. 2003;24:295–297.
13. Aliefendiođlu D, Dursun A, Coşkun T, Akçören Z, Wanders RJA, Waterham HR. A newborn with VLCAD deficiency. Clinical, biochemical, and histopathological findings. *Eur J Pediatr*. 2007;166:1077–1080.
14. Pervaiz MA, Kendal F, Hegde M, Singh RH. MCT oil-based diet reverses hypertrophic cardiomyopathy in a patient with very long chain acyl-coA dehydrogenase deficiency. *Indian J Hum Genet*. 2011;17:29–32.
15. Vianey-Saban C, Divry P, Brivet M, Nada M, Zabot MT, Mathieu M, Roe C. Mitochondrial very-long-chain acyl-coenzyme A dehydrogenase deficiency: clinical characteristics and diagnostic considerations in 30 patients. *Clin Chim Acta*. 1998;269:43–62.

16. Spiekerkoetter U, Sun B, Khuchua Z, Bennett MJ, Strauss AW. Molecular and phenotypic heterogeneity in mitochondrial trifunctional protein deficiency due to beta-subunit mutations. *Hum Mutat.* 2003;21:598–607.
17. Boer den MEJ, Wanders RJA, Morris AAM, IJLst L, Heymans HSA, Wijburg FA. Long-chain 3-hydroxyacyl-CoA dehydrogenase deficiency: clinical presentation and follow-up of 50 patients. *Pediatrics.* 2002;109:99–104.
18. Marcus KA, Mavinkurve-Groothuis AMC, Barends M, van Dijk A, Feuth T, de Korte C, Kapusta L. Reference values for myocardial two-dimensional strain echocardiography in a healthy pediatric and young adult cohort. *J Am Soc Echocardiogr.* 2011;24:625–636.
19. Shah AM, Solomon SD. Myocardial deformation imaging: current status and future directions. *Circulation.* 2012;125:e244–8.
20. Vinereanu D, Ionescu AA, Fraser AG. Assessment of left ventricular long axis contraction can detect early myocardial dysfunction in asymptomatic patients with severe aortic regurgitation. *Heart.* 2001;85:30–36.
21. El-Menyar AA, Galzerano D, Asaad N, Al-Mulla A, Arafa SEO, Suwaidi Al J. Detection of myocardial dysfunction in the presence of normal ejection fraction. *J Cardiovasc Med (Hagerstown).* 2007;8:923–933.
22. Aurigemma GP, Silver KH, Priest MA, Gaasch WH. Geometric changes allow normal ejection fraction despite depressed myocardial shortening in hypertensive left ventricular hypertrophy. *J Am Coll Cardiol.* 1995;26:195–202.
23. Aletras AH, Tilak GS, Hsu L-Y, Arai AE. Heterogeneity of intramural function in hypertrophic cardiomyopathy: mechanistic insights from MRI late gadolinium enhancement and high-resolution displacement encoding with stimulated echoes strain maps. *Circulation: Cardiovascular Imaging.* 2011;4:425–434.
24. Masci PG, Marinelli M, Piacenti M, Lorenzoni V, Positano V, Lombardi M, L'Abbate A, Neglia D. Myocardial structural, perfusion, and metabolic correlates of left bundle branch block mechanical derangement in patients with dilated cardiomyopathy: a tagged cardiac magnetic resonance and positron emission tomography study. *Circulation: Cardiovascular Imaging.* 2010;3:482–490.
25. Szczepaniak LS, Dobbins RL, Metzger GJ, Sartoni-D'Ambrosia G, Arbique D, Vongpatanasin W, Unger R, Victor RG. Myocardial triglycerides and systolic function in humans: in vivo evaluation by localized proton spectroscopy and cardiac imaging. *Magn Reson Med.* 2003;49:417–423.
26. Rijzewijk LJ, van der Meer RW, Smit JWA, Diamant M, Bax JJ, Hammer S, Romijn JA, de Roos A, Lamb HJ. Myocardial steatosis is an independent predictor of diastolic dysfunction in type 2 diabetes mellitus. *J Am Coll Cardiol.* 2008;52:1793–1799.
27. Kurtz DM, Rinaldo P, Rhead WJ, Tian L, Millington DS, Vockley J, Hamm DA, Brix AE, Lindsey JR, Pinkert CA, O'Brien WE, Wood PA. Targeted disruption of mouse long-chain acyl-CoA dehydrogenase gene reveals crucial roles for fatty acid oxidation. *Proc Natl Acad Sci USA.* 1998;95:15592–15597.
28. Cox KB, Hamm DA, Millington DS, Matern D, Vockley J, Rinaldo P, Pinkert CA, Rhead WJ, Lindsey JR, Wood PA. Gestational, pathologic and biochemical differences between very long-chain acyl-CoA dehydrogenase deficiency and long-chain acyl-CoA dehydrogenase deficiency in the mouse. *Hum Mol Genet.* 2001;10:2069–2077.
29. Exil VJ, Roberts RL, Sims H, McLaughlin JE, Malkin RA, Gardner CD, Ni G, Rottman JN, Strauss AW. Very-long-chain acyl-coenzyme a dehydrogenase deficiency in mice. *Circ Res.* 2003;93:448–455.

30. Cox KB, Liu J, Tian L, Barnes S, Yang Q, Wood PA. Cardiac hypertrophy in mice with long-chain acyl-CoA dehydrogenase or very long-chain acyl-CoA dehydrogenase deficiency. *Lab Invest.* 2009;89:1348–1354.
31. Bakermans AJ, Geraedts TR, van Weeghel M, Denis S, Ferraz MJ, Aerts JMFG, Aten J, Nicolay K, Houten SM, Prompers JJ. Fasting-Induced Myocardial Lipid Accumulation in Long-Chain Acyl-CoA Dehydrogenase Knockout Mice Is Accompanied by Impaired Left Ventricular Function. *Circulation: Cardiovascular Imaging.* 2011;4:558–565.
32. Bakermans AJ, Dodd MS, Nicolay K, Prompers JJ, Tyler DJ, Houten SM. Myocardial energy shortage and unmet anaplerotic needs in the fasted long-chain acyl-CoA dehydrogenase knockout mouse. *Cardiovasc Res.* 2013;
33. Houten SM, Herrema H, Brinke te H, Denis S, Ruiter JPN, van Dijk TH, Argmann CA, Ottenhoff R, Müller M, Groen AK, Kuipers F, Reijngoud D-J, Wanders RJA. Impaired amino acid metabolism contributes to fasting-induced hypoglycemia in fatty acid oxidation defects. *Hum Mol Genet.* 2013;22:5249–5261.
34. Corr PB, Creer MH, Yamada KA, Saffitz JE, Sobel BE. Prophylaxis of early ventricular fibrillation by inhibition of acylcarnitine accumulation. *J Clin Invest.* 1989;83:927–936.

Supplementary table 1. Echocardiographic measurements per patient. LVEDs/d= systolic and diastolic left ventricular end-diastolic wall thickness, IVSs/d= systolic and diastolic interventricular septum thickness, LVPWs/d= systolic and diastolic end-diastolic posterior wall thickness, FS= left ventricular (LV) fractional shortening. M= male, f= female, stdev = standard deviation.

Patients	Age	Gender	Height (cm)	Weight (kg)	LVEDd (Z)	IVSd	LVPWd	LVEDs	IVSs	LVPWs	FS(%)
1	2,2	m	96	14	-0,7	0,2	0,3	-0,6	0,6	1,8	38,7
2	3,0	f	100	16,6	0,1	-0,5	-1	-0,2	0,2	0,5	41,9
3	3,1	m	90	12,1	0,1	0	0	0,1	0,9	0,5	38,2
4	4,4	f	119	23,3	-0,7	0,8	0,3	0,2	-1,1	-0,7	31,5
5	5,0	m	112	17,7	0,9	-1,1	0,9	1,5	-2,1	-0,8	32
6	5,1	m	116	20,5	-0,2	-0,4	-0,3	-0,4	-1,2	0,7	39,9
7	5,4	m	117	23,5	-2,5	0,1	4,7	-1,5	-1,3	3,8	34
8	6,2	m	127	28,7	-0,4	-0,1	-0,3	0,4	0	0,3	32,4
9	10,4	f	147	53,8	0,1	1,1	1,2	0,3	1,8	1,2	36,8
10	11,0	m	165	53	1,4	1	0,1	2	-0,4	-0,9	30,5
11	11,6	m	154	41	0,5	0,1	2	0,5	0,8	0,8	37,3
12	14,8	f	167	60,2	-0,6	0,9	0,3	0,9	-0,4	1,3	26,5
13	15,4	f	158	71,3	-1	0,1	1,5	-0,3	-1,1	0,7	33,8
14	15,4	f	163	71	-0,5	0,5	-0,3	0,1	-0,7	-0,6	34,2
15	18,7	f	153	69	0	-0,3	0,1	0,6	-0,5	0	32,7
16	0,0	f	40	2,1	2	0,2	-0,1	3,7	-0,2	-0,8	18,9
17	10,7	f	134	32,7	-0,3	-0,8	-1	0,2	-1,1	0,9	33,9
18	12,9	m	146	43	-1,1	1	1,4	-1,8	-0,2	1,1	44,8
19	14,8	m	170,8	53,3	-0,6	0,2	0,1	-0,1	0,5	0,4	34,7
20	13,3	m	167	52,7	1,9	-0,4	1,1	2	-0,8	0,8	34,5
mean	9,2		132,1	38,0	-0,1	0,1	0,6	0,4	-0,3	0,6	34,4
stdev	5,5		33,8	21,6	1,1	0,6	1,3	1,2	0,9	1,1	5,5

Supplementary table 2. Circumferential strain per patient and per control (%), stdev= standard deviation.

<i>Patients</i>	<i>SC Peak S ant 1</i>	<i>SC Peak S lat 1</i>	<i>SC Peak S post 1</i>	<i>SC Peak S inf 1</i>	<i>SC Peak S sept 1</i>
1					-34,48
2					
3	-7,95	-16,35	-23,15	-16,08	-21,8
4					
5	-14,59	-1,23	-6,57	-8,78	-19,71
6		-14,79	-16,63	0,07	-21,57
7	-14,32	0,01	-0,74	-13,21	-25,78
8	-0,03	-1,94	-0,37	-13,22	-29,18
9	0,02	-13,68	-32,72	-16,69	-21,59
10	-10,76	-19,04	-13,37	-11,63	-18,91
11	-5,72	-14,01	-17,44	-28,66	-25,33
12	0	-7,06	-5,27	-21,35	-23,77
13	-17,97	-18,78	-3,63	-11,39	-23,38
14	-24,87	-15,94	-0,69	-8,43	-22,97
15	-17,52	-1,98	-4,35	-16,82	-19,23
16	-6,04	-5,8	-0,1	-3,18	-4,7
17	-11,79	-24,14	-6,03	-22,4	-27,52
18	-12,1	0	-0,86	-13,47	-27,73
19	0,01	-11,77	-3,37	-21,99	-30,82
20	-13,45	-14,4	-5,69	-20,04	-23,37
mean	-9,8	-10,6	-8,3	-14,5	-23,4
stdev	7,5	7,6	9,3	7,3	6,3
Controls	SC Peak S ant 1	SC Peak S lat 1	SC Peak S post 1	SC Peak S inf 1	SC Peak S sept 1
	-27,35	-13,71		-19,88	-27,92
	-18,38			-15,71	-18,48
	-17,73			-23,22	-27,75
			-23,91	-23,59	-27,04
	-15,97	-11,62	-25,52	-19,85	-18,28
	-17,13	-22,01	-14,97	-23,12	-32,34
			-16,06		-16,83
	-22,33				-24,97
	-21,44	-13,36	-12,66	-19,35	-21,76
	-22,53	-13,79		-21,46	-31,13
	-21,58			-17,4	-27,03

Supplementary table 2. Circumferential strain per patient and per control (%), stdev= standard deviation. (continued)

Controls	SC Peak S ant 1	SC Peak S lat 1	SC Peak S post 1	SC Peak S inf 1	SC Peak S sept 1
	-30,81	-14,49		-16,09	-21,75
	-19,26	-15,96	-12,13	-23,65	-27,69
	-16,77	-11,29		-17,3	-31,88
		-19,68	-18,85	-23,59	-31,39
	-15,53	-14,6		-13,02	-32,03
mean	-20,5	-15,1	-17,7	-19,8	-26,1
stdev	4,5	3,4	5,3	3,5	5,3

Supplementary table 3. Radial strain per patient and per control (%), stdev= standard deviation.

Patients	SR Peak G ant 1	SR Peak G lat 1	SR Peak G post 1	SR Peak G inf 1	SR Peak G sept 1
1					79,9
2					
3	106	101	99,09	93,31	85,55
4					
5	16,77	21,26	33,4	47,62	66,98
6		11,38	18,75	29,92	41,46
7	31,14	25,31	30,54	45,21	52,33
8	8,96	10,27	17,11	22,66	20,94
9	54,62	63,17	56,46	58,93	61,7
10	21,27	26,58	32,45	28,78	20,3
11	64,53	63,57	62,71	61,93	63,08
12	43,88	52,23	61,45	62,08	51,92
13	44,23	49,68	58,46	59,26	49,14
14	21,01	12,74	14,62	21,88	31,85
15	16,68	20,2	24,99	27,77	20,3
16	0,84	0,79	1,43	4,82	8,3
17	23,86	24,61	22,16	23,47	18,02
18	3,13	4,58	13,14	24,61	35,14
19	19,13	18,7	31,57	36,48	39,52
20	39,52	35,72	43,44	50,61	57,61
mean	32,2	31,9	36,6	41,1	44,7
stdev	26,7	26,2	24,4	21,6	22,2

Supplementary table 3. Radial strain per patient and per control (%), stdev= standard deviation. (continued)

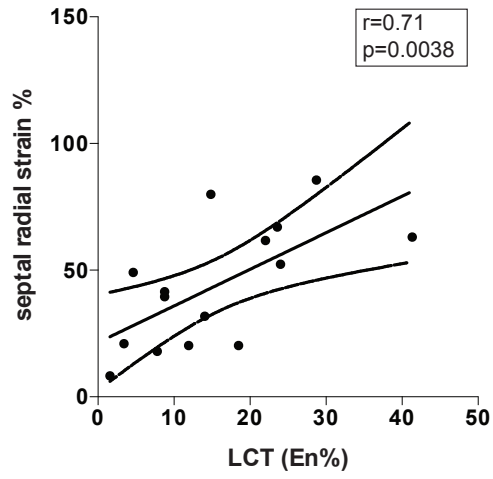
Controls	SR Peak G ant 1	SR Peak G lat 1	SR Peak G post 1	SR Peak G inf 1	SR Peak G sept 1
	50,03	54,06	76,22	65,21	59,29
	60,33	60,84	59,92	58,78	57,94
	67,43	73,14	83,46	80,94	75,52
	63,09	62,25	66,78	68,1	65,75
	53,17	60,79	81,06	91,35	101
	67,83	68,94	72,03	74,39	65,5
	55,6	58,38	59,7	62,29	62,02
	42,24	46,03	53,49	57,77	47,6
	35,62	38,41	47,2	49,13	44,9
	51,23	50,28	54,40	59,3	60,29
	47,04	44,11	47,59	54,09	56,71
	45,37	43,69	48,86	57,17	65,78
	55,66	55,63	62,52	66,24	68,66
	70,21	81,79	91,24	99,03	98,44
	36,33	34,98	38,73	39,11	34,94
	57,55	64,95	70,7	78,01	81,13
mean	53,7	56,1	63,4	66,3	65,3
stdev	10,7	12,9	14,9	15,5	17,5

Supplementary table 4. Longitudinal strain per patient and per control (%), stdev= standard deviation.

Patients	SL Peak bas sept 1	SL Peak mid sept 1	SL Peak ap sept 1	SL Peak ap lat 1	SL Peak mid lat 1	SL Peak bas lat 1
1						
2						
3	-20,15	-22,21	-20,76			-21,88
4						
5	-21,96	-24,73	-19,14			
6	-22,67	-28,02	-28,08			
7	-16,07	-18,29				-16,97
8						
9	-22,98	-25,54	-10,96	-13,48	-21,25	-18,47
10	-22,43	-22,95	-15,66			-19,88
11	-17,25	-20,56	-25,71			

Supplementary table 4. Longitudinal strain per patient and per control (%), stdev= standard deviation. (continued)

<i>Patients</i>	SL Peak bas sept 1	SL Peak mid sept 1	SL Peak ap sept 1	SL Peak ap lat 1	SL Peak mid lat 1	SL Peak bas lat 1
12	-13,69	-18,32	-17,79		-19,58	-33,08
13	-19,27	-19,9	-13,86			-18,36
14	-19,65	-23,63	-17,9	-9,02	-20,89	-28,29
15						
16	-1,88	-2,02			-7,1	-3,73
17			-16,72		-24,69	-21,78
18	-21,3	-25,2	-18,34			
19	-19,26	-21,64	-23	-21,36		-18,41
20	-18,57	-19,65	-18,36			-24,88
mean	-18,4	-20,9	-18,9	-14,6	-18,7	-20,5
stdev	5,4	6,2	4,6	6,2	6,8	7,4
<i>Controls</i>	SL Peak bas sept 1	SL Peak mid sept 1	SL Peak ap sept 1	SL Peak ap lat 1	SL Peak mid lat 1	SL Peak bas lat 1
	-16,15	-20,61	-20,78	-17,86	-21,29	-24,11
		-18,1	-21,85	-20,78	-16,87	
	-20,48	-22,69	-24,33	-22,81	-22,74	-20,64
	-17,33	-23,75	-24,37	-15,75	-13,22	-25,8
	-18,64	-22,67	-28,51	-29,38	-26,31	-19,26
	-21,16	-24,83	-27,23	-24,34	-24,66	-23,34
	-16,81	-19,38	-17,89	-15,72	-21,97	
		-16,86	-14,58		-18,21	-20,21
	-19,75	-22,12	-17,59		-16,93	-34,07
	-17,79	-20,59	-24,2	-23,69	-20,68	-18,08
	-20,58	-22,76	-16,56		-21	-22,87
	-18,88	-24,52	-28,33	-21,68	-22,93	-23,53
	-18,19	-19,93	-18,32		-20,59	-24,07
	-18,66	-22,13	-18,29	-16,24	-21,61	-13,08
	-20,5	-21,93	-17,18		-21,88	-23,67
	-18,66	-20,76	-20,7	-19,63	-20,88	-22,42
mean	-18,8	-21,5	-21,3	-20,7	-20,7	-22,5
stdev	1,5	2,2	4,4	4,3	3,2	4,6



Supplementary Figure 1. Correlation of septal radial peak systolic strain vs long-chain triglyceride(LCT) intake (En%).

CHAPTER 6

Muscle MRI in very long-chain acyl-CoA dehydrogenase deficient patients

E.F. Diekman^{1,2}, W.L. van der Pol³, R.A.J. Nivelstein⁴, S.M. Houten^{2,5},
F.A. Wijburg⁵, G. Visser¹

¹ Department of Paediatric Gastroenterology and Metabolic Diseases, Wilhelmina Children's Hospital, UMC Utrecht, the Netherlands

² Laboratory Genetic Metabolic Diseases, Department of Clinical Chemistry, Academic Medical Center, University of Amsterdam, the Netherlands

³ Brain Center Rudolf Magnus, Spieren voor Spieren Kindercentrum, Department of Neurology and Neurosurgery, University Medical Center, the Netherlands

⁴ Department of Radiology, University Medical Center, the Netherlands

⁵ Department of Paediatrics, Academic Medical Center, University of Amsterdam, the Netherlands

Journal of Inherited Metabolic Disease, 2013, doi:10.1007/s10545-013-9666-3

ABSTRACT

Introduction: Muscle Magnetic Resonance Imaging (MRI) is a useful tool for visualizing abnormalities in neuromuscular disorders. The value of muscle MRI has not been studied in long-chain fatty acid oxidation (lcFAO) disorders. lcFAO disorders may present with metabolic myopathy including episodic rhabdomyolysis.

Objective: To investigate whether lcFAO disorders are associated with muscle MRI abnormalities.

Methods: Lower body MRI was performed in 20 patients with lcFAO disorders, i.e. 3 carnitine palmitoyltransferase 2 deficiency (CPT2D), 12 very long-chain acyl-CoA dehydrogenase deficiency (VLCADD), 3 mitochondrial trifunctional protein deficiency (MTPD) and 2 isolated long-chain hydroxyacyl-CoA dehydrogenase deficiency (LCHADD).

Results: At the time of MRI, 4 patients had muscle weakness, 14 had muscle pain and 13 were exercise intolerant. Median creatine kinase (CK) level of patients at the day of MRI was 398 U/L (range 35-12,483). T1W and STIR signal intensity (SI) were markedly increased in MTPD patients from girdle to lower leg. VLCADD patients showed predominantly proximal T1W SI changes, whereas LCHADD patients mostly showed distal T1W SI changes. Prominent STIR weighted signal intensity increases of almost all muscle groups were observed in patients with VLCADD and LCHADD with very high CK (>11.000) levels.

Conclusions and relevance: lcFAO disorders are associated with specific patterns of increased T1W and STIR signal intensity. These patterns may reflect lipid accumulation and inflammation secondary to lcFAO defects and progressive muscle damage. Future studies are needed to investigate whether muscle MRI might be a useful tool to monitor disease course and to study pathogenesis of lcFAO related myopathy.

INTRODUCTION

Muscle magnetic resonance imaging (MRI) is a useful technique for diagnostic workup and follow-up of a range of myopathies. In muscular dystrophies and congenital myopathies characteristic patterns of T1 weighted (T1W) changes in signal intensity are found¹⁻⁷. Inflammatory myopathies are often associated with Short Tau Inversion Recovery (STIR) signal intensity changes⁸⁻¹¹. High T1W and STIR signal intensity are caused by increased fat or water content, respectively, and may reflect underlying pathogenic mechanisms. Muscle MRI is also a promising non-invasive tool to monitor disease progression and biomarker for efficacy of treatment strategies^{7,12}.

Few studies addressed the potential of muscle MRI for diagnosis, and follow-up of metabolic myopathies¹³⁻¹⁵. Especially inborn errors of long-chain fatty acid oxidation (lcFAO) have not been studied in detail. Mitochondrial lcFAO plays a pivotal role in energy homeostasis and enzyme deficiencies, specifically carnitine palmitoyltransferase 2 deficiency (CPT2D), very long-chain acyl-CoA dehydrogenase deficiency (VLCADD), mitochondrial trifunctional protein deficiency (MTPD) and isolated long-chain hydroxyacyl-CoA dehydrogenase deficiency (LCHADD), can cause myopathy¹⁶⁻¹⁸. The combination of severe and potentially life threatening complications and a favourable response to treatment, has led to the inclusion of lcFAO disorders in newborn screening (NBS) programs worldwide¹⁹. This led to an increased number of diagnosed patients over the last decade. The individual risk of these patients to develop disease symptoms is difficult to predict. Novel approaches to monitor disease course and effect of treatment are needed.

In infancy patients with lcFAO disorders may present with hypoglycaemia and cardiomyopathy, but thereafter myopathy with recurrent episodes of rhabdomyolysis and exercise intolerance are the most common symptoms. In addition, patients with MTPD/LCHADD may suffer from polyneuropathy and retinopathy. Conditions leading to an increased energy demand, such as fasting, exercise, febrile illness or certain medications, may induce rhabdomyolysis²⁰⁻²⁵. The precise mechanisms causing rhabdomyolysis and long-term consequences on muscle function are, however, unknown. We assessed whether muscle MRI is a useful tool in patients with lcFAO disorders.

METHODS

Patients and controls

Twenty patients with a genetically confirmed lcFAO disorder were included. Table 1 summarizes patient characteristics. Muscle strength was examined using the Medical Research Council (MRC) scale. Fourteen patients (70%) reported muscle pain at rest or

Table 1. Patient characteristics. Pt. nr.= patient number; PNP= polyneuropathy; EA= enzymatic activity in lymphocytes; CK= Creatine Kinase. Exercise intolerance was defined as: wheelchair bound, able to walk less than 500m or able to perform exercise less than expected for age. Patients are classified as LCHADD or MTPD based on enzymatic activity of LCHAD and LCKAT (Diekman et al. 2013). All three MTPD patients have very low/absent LCHAD and LCKAT(thiolase) enzymatic activity, whereas LCHAD patients still have LCKAT (thiolase) activity.

Pt. nr.	Disease	gender	current age (years)	current related symptoms	muscle power during neurological exam	mutation	Max CK (U/L)	T1 (Sum of affected muscle)	STIR (Sum of affected muscle)
1	CPT2D	m	43	muscle pain (after exercise)	normal	homozyg. c.338C>T	1,344	1	0.5
2	CPT2D	m	48	exercise intolerance, muscle pain (after exercise)	normal	homozyg. c.338C>T	110	1	1.5
3	CPT2D	m	51	exercise intolerance, muscle pain	normal	c.338C>T; c.371C>T	96	6	0
4	VLCADD	m	3	exercise intolerance, muscle pain	not normal, pos. Gowers sign	homozyg. c.1322G>A	163,610	0	2.5
5	VLCADD	m	10	no symptoms	normal	homozyg. c.577G>C	212	0	0
6	VLCADD	f	11	exercise intolerance, muscle pain	not normal, limb-girdle weakness MRC grade 4	homozyg. c.643T>C	2,031	5.5	6.5
7	VLCADD	f	12	exercise intolerance, muscle pain	normal	homozyg. c.104delC	3,058	0	1
8	VLCADD	f	15	exercise intolerance, muscle pain	normal	homozyg. c.104delC	28,900	1.5	21.5
9	VLCADD	f	16	exercise intolerance, muscle pain	normal	homozyg. c.1141-43delGAG	1,740	2	0

Table 1. Patient characteristics. Pt. nr.= patient number; PNP= polyneuropathy; EA= enzymatic activity in lymphocytes; CK= Creatine Kinase. Exercise intolerance was defined as: wheelchair bound, able to walk less than 500m or able to perform exercise less than expected for age. Patients are classified as LCHADD or MTPD based on enzymatic activity of LCHAD and LCKAT (Diekman et al. 2013). All three MTPD patients have very low/absent LCHAD and LCKAT(thiolase) enzymatic activity, whereas LCHAD patients still have LCKAT (thiolase) activity. (continued)

Pt. nr.	Disease	gender	current age (years)	current muscle related symptoms	muscle power during neurological exam	mutation	Max CK (U/L)	CK (U/L)	T1 (Sum of affected muscle)	STIR (Sum of affected muscle)
10	VLCADD	f	19	no symptoms	normal	homozyg. c.1411T>C	90	90	2.5	0
11	VLCADD	m	32	muscle pain	normal	homozyg. c.1406G>A	3,279	3,279	7	2
12	VLCADD	m	31	exercise intolerance, muscle pain	normal	homozyg. c.1322G>A	208,971	1,275	1	2.5
13	VLCADD	m	36	no symptoms	normal	c.1444_1448delAAGGA; 1511_1516delAAGG	544	544	5	1.5
14	VLCADD	m	40	exercise intolerance, muscle pain	normal	homozyg. c.833_835delAAG	6,363	90	2	2
15	VLCADD	m	41	no symptoms	normal	c.848T>C; c.1444_1448delAAGGA; c.1509_1514delAAGGC	382	382	0.5	2
16	LCHADD	m	13	no symptoms	normal	c.1528G>C; c.1712T>C	197	197	0	0
17	LCHADD	f	32	muscle weakness, exercise intolerance, muscle pain	not normal, distal muscle weakness (legs) and areflexia, PNP (legs)	homozyg. c.1528G>C	12,483	12,483	6	8.5

Table 1. Patient characteristics. Pt. nr.= patient number; PNP= polyneuropathy; EA= enzymatic activity in lymphocytes; CK= Creatine Kinase. Exercise intolerance was defined as: wheelchair bound, able to walk less than 500m or able to perform exercise less than expected for age. Patients are classified as LCHAD or MTPD based on enzymatic activity of LCHAD and LCKAT (Diekman et al. 2013). All three MTPD patients have very low/absent LCHAD and LCKAT(thiolase) enzymatic activity, whereas LCHAD patients still have LCKAT (thiolase) activity. (continued)

Pt. nr.	Disease	gender	current age (years)	current muscle related symptoms	muscle power during neurological exam	mutation	Max CK (U/L)	CK (U/L)	T1 (Sum of affected muscle)	STIR (Sum of affected muscle)
18	MTPD	f	10	muscle weakness, exercise intolerance, muscle pain, wheelchair bound	not normal, severe muscle weakness proximal and distal limbs.MRC 2-3 with atrophy and areflexia, severe PNP	homozyg. c.2027G>T	>100,000	30,264	18	11.5
19	MTPD	m	13	muscle weakness, exercise intolerance, muscle pain, wheelchair bound	not normal, severe muscle weakness proximal (MRC3/4) and distal limbs MRC 0, severe distal atrophy and areflexia, severe PNP	c.546C>G; c.1336-1393del57nt	9,642	160	23.5	9
20	MTPD	m	15	muscle weakness, exercise intolerance, wheelchair bound	not normal, severe muscle weakness proximal (MRC3/4) and distal limbs MRC 1, severe distal atrophy and areflexia, severe PNP	c.546C>G; c.1336-1393del57nt	12,721	549	17.5	15.5

after mild exercise, 13 patients (65%) had exercise intolerance and 6 patients (30%) had signs of muscle weakness at neurological examination. Two patients with VLCADD had predominant proximal weakness, whereas all patients with MTPD and 1 with LCHADD had distal weakness. Median creatine kinase (CK) level at the day of MRI was 463 U/L (range 35-12,483 U/L). Median highest previously documented CK level was 9,642U/L (range 544-208,971U/L) (Table 1) Six healthy individuals or individuals that underwent lower body MRI for other reasons than myopathies, such as bone disorders or vascular abnormalities were included in this study. Three males and three females with a median age of 17yrs and an age range of 8-25yrs.

The study was approved by the medical ethics committee of the University Medical Centre Utrecht (METC 10-430/C). All patients provided written informed consent for participation in this study.

Laboratory measurements

CK measurements were performed at the time of MRI. CK was measured using standard enzymatic methods. Normal values in our laboratory range from 0-170 U/L.

Muscle MRI

MRI of the pelvic and leg muscles was performed using a 1.5 Tesla MRI scanner (Ingenia, Philips Healthcare, Best, The Netherlands) and a protocol optimized for lower body MRI scanning. T1W Turbo spin echo (TSE) and STIR sequences were acquired in the transverse plane. Sequence parameters were as follows: T1W TSE [TR 664ms, TE 12ms, TSE factor 10, NSA 1, slice thickness 7 mm, slice gap 33 mm, FOV 550 mm]. STIR [TR 3087 ms, IR 160 ms, TE 60 ms, TSE factor 23, NSA 1, slice thickness 7 mm, slice gap 33 mm, FOV 550 mm] Total scanning time was 30 minutes.

Two independent observers (RJN and WLP) assessed the MRI images. Each of the following muscle groups were evaluated for the presence or absence of signal intensity changes on T1W or STIR images: m. erector spinae; m. iliopsoas; m. tensor fascia latae; m. gluteus maximus; m. gluteus medius (limb girdle); m. adductor longus; m. adductor magnus; m. rectus femoris; m. vastus medialis; m. vastus lateralis; m. vastus intermedius; m. sartorius; m. gracilis; m. biceps femoris; m. semitendinosus; m. semimembranosus (upper leg); m. tibialis anterior; m. peroneus; m. soleus; m. gastrocnemius lateralis; m. gastrocnemius medialis (lower leg). In addition, the signal intensity of each muscle group was subjectively graded as follows: 0= no increase in signal intensity (no muscle involvement); 1= mildly increased signal intensity (mild to moderate involvement); 2= high increase of signal intensity (severe muscle involvement). The muscle sum score (Σ) was calculated based on the score of both observers and averaged per muscle (supplemental Fig e-1). Each muscle was assigned to one of three groups: hip girdle, upper leg or lower leg. A total amount of muscle with increased signal intensity per group of >1

was considered abnormal. Inter-observer variability was assessed using Cohen's kappa. κ of abnormal vs normal was 0.710 (good) for T1W and 0.462 (moderate) for STIR.

RESULTS

T1-weighted signal intensities

MRI of control subjects showed normal and homogeneous T1W signal intensity. Patients with VLCADD predominantly showed proximal T1W signal intensity changes and patients with LCHADD predominantly distal T1W signal intensity changes. MTPD patients showed T1W signal intensity changes of upper and lower legs. The MRI of one patient (33%) with CPTD2 showed a mild increase in signal intensity of the m. gluteus medius and maximus on T1W images. Mildly increased T1W signal intensity of the m. gluteus maximus and m. tensor fascia latae (girdle) (supplemental Fig e-1A) was found in 7 out of 12 patients (58%) with VLCADD, and 3 had additional mildly increased T1W signal intensity of the biceps femoris and hamstrings (supplemental Fig e-1B). There were no

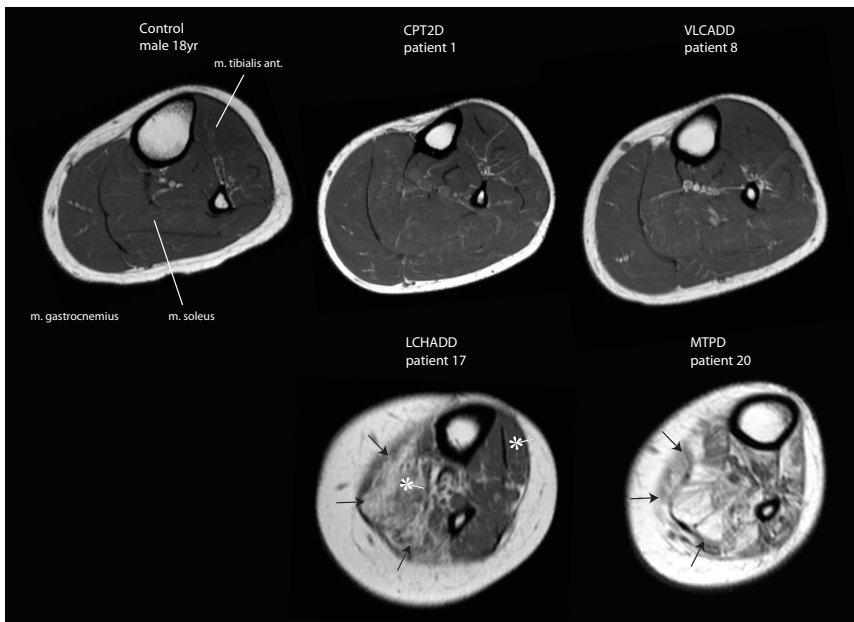


Figure 1. T1-weighted images of lower left leg. T1-weighted transversal images of the lower left leg in control and CPT2D, VLCADD, LCHADD and MTPD patients. Black arrows indicate high signal intensity in the muscles (LCHADD and MTPD). The asterisk emphasizes the difference in signal intensity between m. gastrocnemius and m. tibialis.

T1W signal intensity changes in distal muscles of patients with CPT2D and VLCADD (Fig 1). Virtually every muscle in the upper leg of all 3 MTPD patients showed moderate to highly increased T1W signal intensity (high: vastus intermedius, lateralis and medialis) and marked muscle atrophy (Fig 3 and supplemental 1B-C). The lower leg (m. tibialis anterior; m. peroneus and m. soleus) showed highly increased T1W signal intensity as well (Fig 1, supplemental Fig e-1B-C). Finally, one patient with LCHADD had high T1W signal intensity in the lower legs, primarily in the m. gastrocnemius lateralis and medialis (Fig 1, supplemental Fig e-1C).

Short Tau Inversion Recovery (STIR) signal intensities

MRI of control subjects showed normal and homogeneous STIR signal intensity. Increased signal intensity was found in patients with VLCADD, LCHAD and MTPD but not in CPT2D. (Table 1, supplemental Fig e-1A-C). Four of the 12 (33%) patients with VLCADD had mildly increased signal intensity in the upper leg muscles (m. biceps femoris and/or hamstrings) and 5 (42%) had mildly increased signal intensity in the lower leg muscles (m. soleus) (Fig 2, 4, supplemental Fig e-1B-C). A generalized increase of STIR signal intensity was detected in one patient with VLCADD (Fig 2, 4, supplemental Fig e-1A-C)

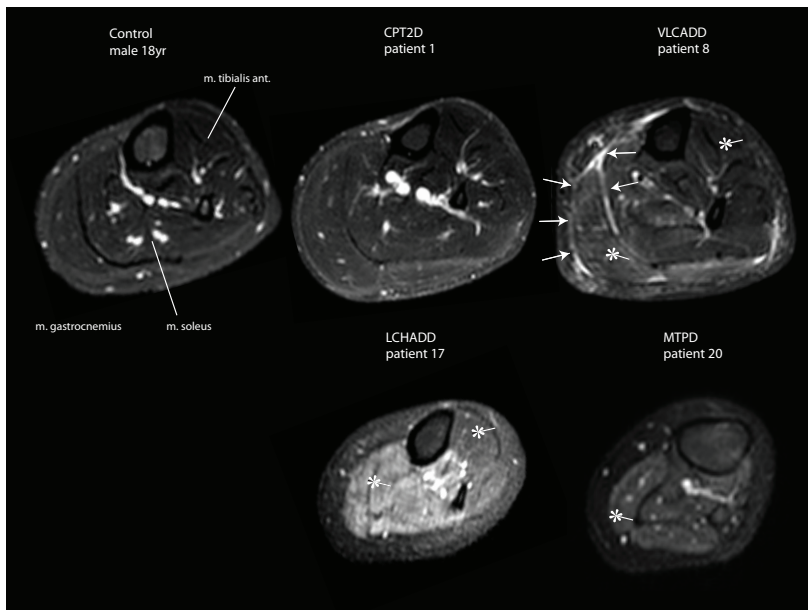


Figure 2. STIR-weighted images of lower left leg. STIR-weighted transversal images of the lower left leg in healthy control and patients with CPT2D, VLCADD, LCHADD and MTPD. White arrows indicate increased muscle signal intensity. Asterixes emphasize the difference in signal intensity between m. gastrocnemius and m. tibialis (VLCADD and LCHADD) or higher signal intensity in comparison to the intensity of the subcutis (MTPD).

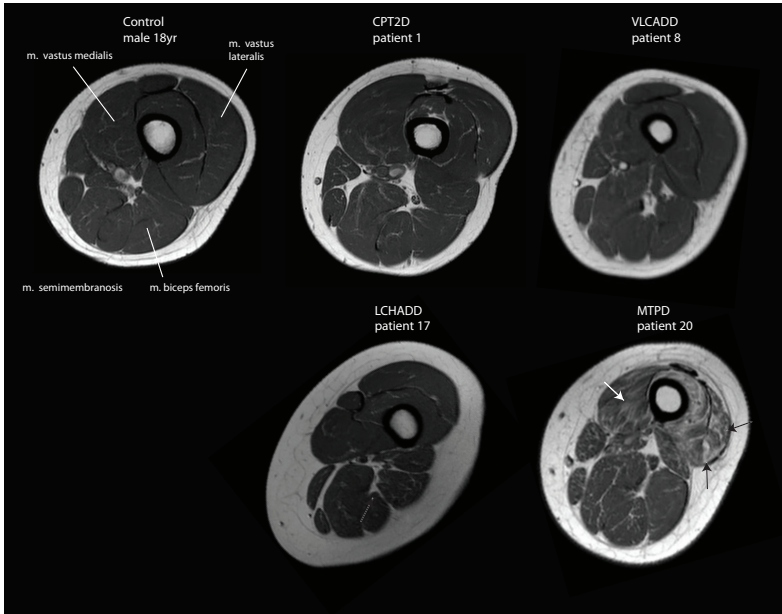


Figure 3. T1-weighted images of upper left leg. T1-weighted transversal images of the upper left leg in healthy control and patients with CPT2D, VLCADD, LCHADD and MTPD. Black and white arrows indicate increased signal intensity (LCHADD and MTPD).

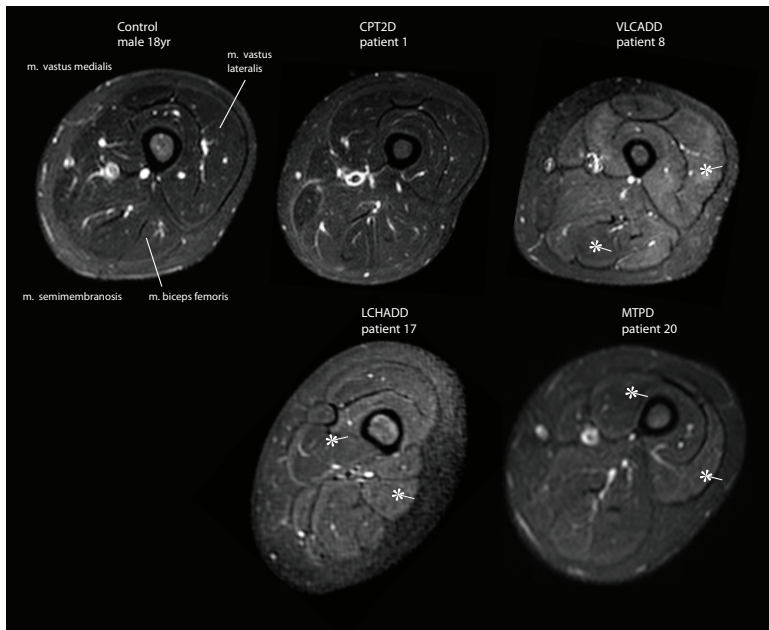


Figure 4. STIR-weighted images of upper left leg. STIR-weighted transversal images of the upper left leg in healthy control and patients with CPT2D, VLCADD, LCHADD and MTPD. Asterisks emphasize the difference in signal intensity between m. vastus lateralis and an unaffected muscle (VLCADD, LCHADD and MTPD).

(high in: m. adductor longus; m. adductor magnus; m. sartorius; m. vastus intermedius, lateralis and medialis; m. biceps femoris; m. soleus; m. gastrocnemius) in combination with a high CK level of 11,180 U/L. A pattern of increased signal intensity of the lateral vastus muscle and all lower leg muscles (m. tibialis anterior; m. peroneus; m. soleus; m. gastrocnemius lateralis and medialis) was observed in all 3 MTPD patients (Fig 4, supplemental Fig e-1B-C). One of the two patients with LCHADD had high STIR signal intensity of m. gastrocnemius medialis and lateralis (Fig 2, supplemental Fig e-1B-C) and moderate increased STIR signal intensity in other muscles (i.e. generalized pattern). CK level of this patient at the time of MRI was 12,483 U/L (Fig 2, 4).

There was correlation between the muscle sum score of affected muscles with STIR signal intensity changes and CK level (Spearman correlation coefficient $\rho=0.58$, $p<0.01$) (Supplemental Fig e-2).

DISCUSSION

Muscle MRI in patients with IcFAO disorders show specific patterns of T1W and STIR signal intensity changes. Both T1W and STIR changes were most prominent in MTPD patients from girdle to lower leg. VLCADD patients predominantly showed proximal T1W signal intensity changes, whereas predominantly distal T1W signal intensity changes were observed in LCHADD patients. STIR signal intensity changes were very prominent in patients with very high CK levels, suggesting that STIR changes reflect rhabdomyolysis.

The differences in muscle MRI abnormalities between IcFAO disorders are striking, since all IcFAO disorders are characterized by the accumulation of acylcarnitines. The type of accumulating acylcarnitines differs however. CPT2D and VLCADD patients accumulate saturated and unsaturated acyl-CoAs; MTPD patients only accumulate trans-2-enoyl-CoAs whereas LCHADD patients accumulate trans-2-enoyl-CoA and 3-hydroxy-acyl-CoAs (both metabolites are in equilibrium). It is known that acyl-CoAs inhibit certain process that can harm mitochondria and cells²⁶⁻²⁸. Furthermore, trans-2-enoyl-CoA is a competitive inhibitor of CPT2, thereby affecting the primary way for cells to detoxify accumulating acyl-CoAs²⁹⁻³². Muscle and nerve cells might be sensitive to the accumulation of one of these harmful substrates and certain substrates could even be more harmful for nerve cells than to muscle cells. The difference in sensitivity might explain the specific patterns of muscle involvement in IcFAO.

Increased T1W signal intensity reflects fatty infiltration of muscle tissue. In muscular dystrophies, T1W changes may reflect histopathological abnormalities that reflect accumulating muscle damage. In IcFAO disorders, increased T1W signal intensity may also reflect myocellular increases of lipid content. Previous studies have shown increased intracellular lipid storage in primarily type 1 muscle fibres in muscle biopsies from only

a few patients with MTPD and VLCADD^{20,24,33,34}. Lipid storage in muscle from patients with IcFAO disorders may be caused by the intracellular accumulation of triglycerides as observed in hearts of IcFAO deficient knock-out mice³⁵. Alternatively, the differentiation of bipotent progenitor cells (Fibro-Adipogenic-Progenitor cells (FAPs)) into adipocytes, a process that we hypothesize to be triggered by frequent rhabdomyolysis, could lead to intercellular lipid accumulation³⁶⁻³⁸. Future studies with magnetic resonance spectroscopy (MRS) could possibly determine whether there is intra- or intercellular lipid accumulation.

It should be noted that all MTPD patients also had an (atactic) polyneuropathy (PNP), distal atrophy, areflexia and are wheelchair bound. Neuropathy could explain the signal intensity changes on both STIR and T1W images^{39,40}. However, predicting whether the observed muscular abnormalities are due to a neuropathic or myopathic cause is difficult⁴¹. Three observations were less compatible with neuropathy. First, the muscle groups of the posterior and anterior muscle groups of the lower leg were similarly affected, where relative sparing of the posterior compartment might be expected. Second, the extensive involvement of muscle groups in the upper leg is more compatible with a myopathic etiology. Third, an increased CK level in 2 of the 3 MTPD patients at time of MRI also more compatible with a myopathic etiology⁴². Future studies linking EMG with MRI and clinical data might address this issue.

High STIR signal intensity suggests increased water content, due to cellular lysis (cytotoxic edema), or fluid accumulation secondary to inflammation. The increased STIR signal intensity in specific muscles may reflect differences in susceptibility to specific IcFAO disorders. The possible value of STIR abnormalities as a biomarker of IcFAO disease activity is further shown by the extensive STIR abnormalities in 2 patients who experienced a period of rhabdomyolysis and very high CK levels (Fig 2, 3, 4 and supplemental Fig e-1A-C). In clinical practice, plasma CK levels are used to assess the activity of metabolic myopathy in patients with IcFAO disorders. Since CK levels may rise and fall within hours or days, MRI may be more sensitive to study the subacute and long-term effects of IcFAO disease on muscle. The moderate correlation between CK levels and the number of affected muscle on STIR delineates this, as several patients show a number of affected muscles, without a severely increased CK level. Sequential muscle MRI studies may reveal the value of MRI to study disease course over longer periods of time.

Both observers were able to distinguish patients with and without muscle abnormalities. Grading however appeared more difficult. Quantitative grey-scale analysis of STIR images would possibly differentiate more accurately between normal, mild and severely affected patients.

In conclusion, IcFAO disorders are associated each with a specific pattern of increased T1W and STIR signal intensity, which may reflect lipid accumulation secondary to IcFAO deficiency or due to accumulating muscle damage. Future studies are needed to investi-

gate whether muscle MRI might be a useful tool to monitor disease course and to study pathogenesis of lCFAO related myopathy.

ACKNOWLEDGEMENTS

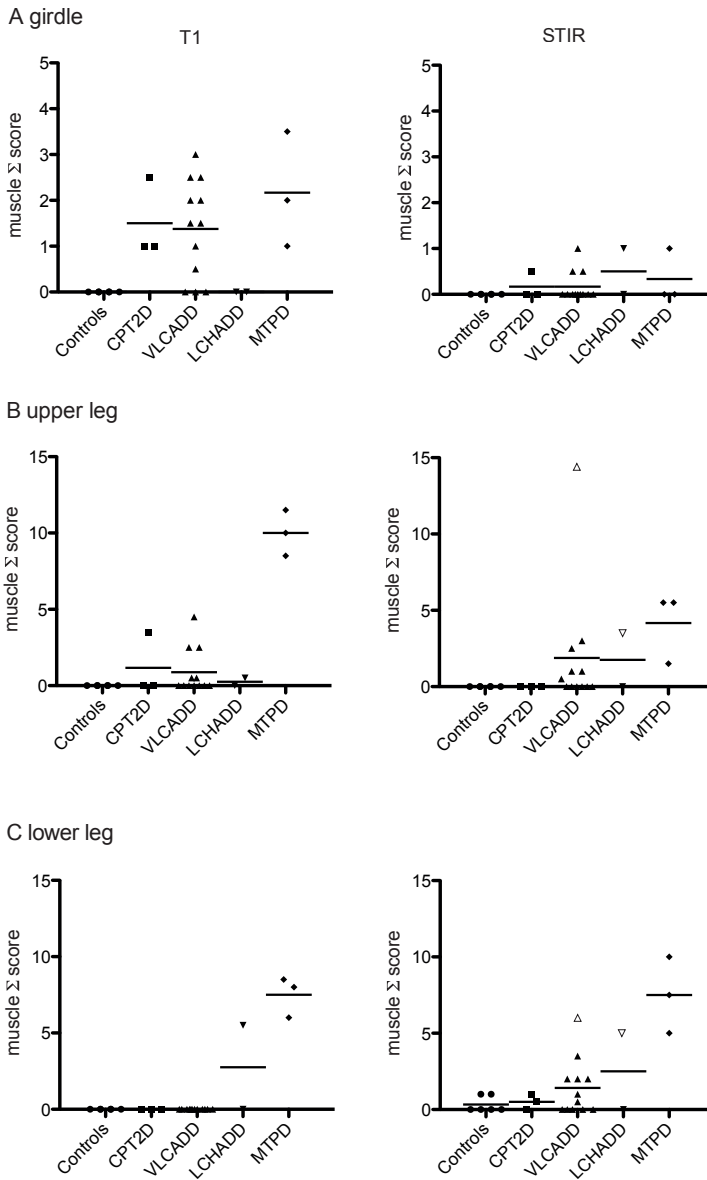
Study funding: Eugene Diekman is paid by a grant of ZonMW (The Netherlands Organisation for Health Research and Development, dossier 200320006) and Metakids.

REFERENCES

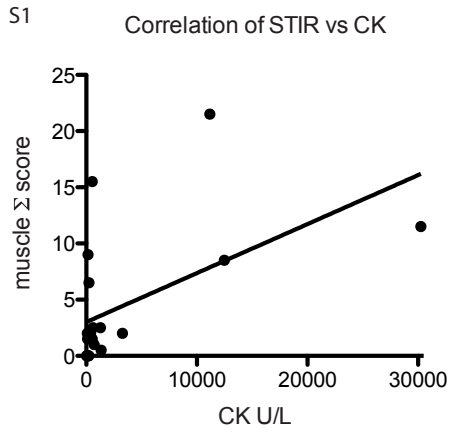
1. Mercuri E, Pichiecchio A, Allsop J, Messina S, Pane M, Muntoni F. Muscle MRI in inherited neuromuscular disorders: past, present, and future. *J Magn Reson Imaging*. 2007;25(2):433–440. doi:10.1002/jmri.20804.
2. Degardin A, Morillon D, Lacour A, Cotten A, Vermersch P, Stojkovic T. Morphologic imaging in muscular dystrophies and inflammatory myopathies. *Skeletal Radiol*. 2010;39(12):1219–1227. doi:10.1007/s00256-010-0930-4.
3. Wattjes MP, Kley RA, Fischer D. Neuromuscular imaging in inherited muscle diseases. *Eur Radiol*. 2010;20(10):2447–2460. doi:10.1007/s00330-010-1799-2.
4. Schulze M, Kötter I, Ernemann U, et al. MRI findings in inflammatory muscle diseases and their noninflammatory mimics. *AJR Am J Roentgenol*. 2009;192(6):1708–1716. doi:10.2214/AJR.08.1764.
5. Murphy WA, Totty WG, Carroll JE. MRI of normal and pathologic skeletal muscle. *AJR Am J Roentgenol*. 1986;146(3):565–574.
6. Mercuri E, Jungbluth H, Muntoni F. Muscle imaging in clinical practice: diagnostic value of muscle magnetic resonance imaging in inherited neuromuscular disorders. *Curr Opin Neurol*. 2005;18(5):526–537.
7. Kinali M, Arechavala-Gomez V, Cirak S, et al. Muscle histology vs MRI in Duchenne muscular dystrophy. *Neurology*. 2011;76(4):346–353. doi:10.1212/WNL.0b013e318208811f.
8. Tzaribachev N, Well C, Schedel J, Horger M. Whole-body MRI: a helpful diagnostic tool for juvenile dermatomyositis case report and review of the literature. *Rheumatol Int*. 2009;29(12):1511–1514. doi:10.1007/s00296-009-0890-y.
9. Adams EM, Chow CK, Premkumar A, Plotz PH. The idiopathic inflammatory myopathies: spectrum of MR imaging findings. *Radiographics*. 1995;15(3):563–574.
10. Gardner-Medwin JMM, Irwin G, Johnson K. MRI in Juvenile Idiopathic Arthritis and Juvenile Dermatomyositis. *Annals of the New York Academy of Sciences*. 2009;1154(1):52–83. doi:10.1111/j.1749-6632.2009.04498.x.
11. Cox FM, Reijnierse M, van Rijswijk CSP, Wintzen AR, Verschuuren JJ, Badrising UA. Magnetic resonance imaging of skeletal muscles in sporadic inclusion body myositis. *Rheumatology (Oxford)*. 2011;50(6):1153–1161. doi:10.1093/rheumatology/ker001.
12. Kim HK, Laor T, Horn PS, Wong B. Quantitative assessment of the T2 relaxation time of the gluteus muscles in children with Duchenne muscular dystrophy: a comparative study before and after steroid treatment. *Korean J Radiol*. 2010;11(3):304–311. doi:10.3348/kjr.2010.11.3.304.
13. Pichiecchio A, Uggetti C, Ravaglia S, et al. Muscle MRI in adult-onset acid maltase deficiency. *Neuromuscul Disord*. 2004;14(1):51–55.
14. Carlier R-Y, Laforêt P, Wary C, et al. Whole-body muscle MRI in 20 patients suffering from late onset Pompe disease: Involvement patterns. *Neuromuscul Disord*. 2011. doi:10.1016/j.nmd.2011.06.748.
15. Dlamini N, Jan W, Norwood F, et al. Muscle MRI findings in siblings with juvenile-onset acid maltase deficiency (Pompe disease). *Neuromuscul Disord*. 2008;18(5):408–409. doi:10.1016/j.nmd.2008.02.006.
16. Wanders RJA, Ruiten JPN, IJLst L, Waterham HR, Houten SM. The enzymology of mitochondrial fatty acid beta-oxidation and its application to follow-up analysis of positive neonatal screening results. *J Inherit Metab Dis*. 2010;33(5):479–494. doi:10.1007/s10545-010-9104-8.
17. Boneh A, Andresen BS, Gregersen N, et al. VLCAD deficiency: pitfalls in newborn screening and confirmation of diagnosis by mutation analysis. *Molecular Genetics and Metabolism*. 2006;88(2):166–170. doi:10.1016/j.ymgme.2005.12.012.

18. Lindner M, Hoffmann GF, Matern D. Newborn screening for disorders of fatty-acid oxidation: experience and recommendations from an expert meeting. *J Inherit Metab Dis.* 2010;33(5):521–526. doi:10.1007/s10545-010-9076-8.
19. McHugh DMS, Cameron CA, Abdenur JE, et al. Clinical validation of cutoff target ranges in newborn screening of metabolic disorders by tandem mass spectrometry: a worldwide collaborative project. *Genet Med.* 2011;13(3):230–254. doi:10.1097/GIM.0b013e31820d5e67.
20. Laforêt P, Vianey-Saban C. Disorders of muscle lipid metabolism: diagnostic and therapeutic challenges. *Neuromuscul Disord.* 2010;20(11):693–700. doi:10.1016/j.nmd.2010.06.018.
21. Houten SM, Wanders RJA. A general introduction to the biochemistry of mitochondrial fatty acid β -oxidation. *J Inherit Metab Dis.* 2010;33(5):469–477. doi:10.1007/s10545-010-9061-2.
22. Vianey-Saban C, Divry P, Brivet M, et al. Mitochondrial very-long-chain acyl-coenzyme A dehydrogenase deficiency: clinical characteristics and diagnostic considerations in 30 patients. *Clin Chim Acta.* 1998;269(1):43–62.
23. Andresen BS, Olpin S, Poorthuis BJ, et al. Clear correlation of genotype with disease phenotype in very-long-chain acyl-CoA dehydrogenase deficiency. *Am J Hum Genet.* 1999;64(2):479–494. doi:10.1086/302261.
24. Laforêt P, Acquaviva-Bourdain C, Rigal O, et al. Diagnostic assessment and long-term follow-up of 13 patients with Very Long-Chain Acyl-Coenzyme A dehydrogenase (VLCAD) deficiency. *Neuromuscul Disord.* 2009;19(5):324–329. doi:10.1016/j.nmd.2009.02.007.
25. Spiekerkoetter U. Mitochondrial fatty acid oxidation disorders: clinical presentation of long-chain fatty acid oxidation defects before and after newborn screening. *J Inherit Metab Dis.* 2010;33(5):527–532. doi:10.1007/s10545-010-9090-x.
26. Ventura FV, Ruiter J, Ijlst L, de Almeida IT, Wanders RJA. Differential inhibitory effect of long-chain acyl-CoA esters on succinate and glutamate transport into rat liver mitochondria and its possible implications for long-chain fatty acid oxidation defects. *Molecular Genetics and Metabolism.* 2005;86(3):344–352. doi:10.1016/j.ymgme.2005.07.030.
27. Ventura FV, Ruiter JP, Ijlst L, Almeida IT, Wanders RJ. Inhibition of oxidative phosphorylation by palmitoyl-CoA in digitonin permeabilized fibroblasts: implications for long-chain fatty acid β -oxidation disorders. *Biochim Biophys Acta.* 1995;1272(1):14–20.
28. Ciapaite J, Van Eikenhorst G, Bakker SJL, et al. Modular kinetic analysis of the adenine nucleotide translocator-mediated effects of palmitoyl-CoA on the oxidative phosphorylation in isolated rat liver mitochondria. *Diabetes.* 2005;54(4):944–951.
29. Violante S, IJLst L, van Lenthe H, de Almeida IT, WANDERS RJ, Ventura FV. Carnitine palmitoyltransferase 2: New insights on the substrate specificity and implications for acylcarnitine profiling. *Biochim Biophys Acta.* 2010;1802(9):728–732. doi:10.1016/j.bbadis.2010.06.002.
30. Morel F, Lauquin G, Lunardi J, Duszynski J, Vignais PV. An appraisal of the functional significance of the inhibitory effect of long chain acyl-CoAs on mitochondrial transports. *FEBS Lett.* 1974;39(2):133–138.
31. Halperin ML, Robinson BH, Fritz IB. Effects of palmitoyl CoA on citrate and malate transport by rat liver mitochondria. *Proc Natl Acad Sci USA.* 1972;69(4):1003–1007.
32. Vaartjes WJ, Kemp A, Souverijn JHM, van den Bergh SG. Inhibition by fatty acyl esters of adenine nucleotide translocation in rat-liver mitochondria. *FEBS Lett.* 1972;23(3):303–308.
33. Purevsuren J, Fukao T, Hasegawa Y, et al. Clinical and molecular aspects of Japanese patients with mitochondrial trifunctional protein deficiency. *Molecular Genetics and Metabolism.* 2009;98(4):372–377. doi:10.1016/j.ymgme.2009.07.011.

34. Shchelochkov O, Wong L-J, Shaibani A, Shinawi M. Atypical presentation of VLCAD deficiency associated with a novel ACADVL splicing mutation. *Muscle Nerve*. 2009;39(3):374–382. doi:10.1002/mus.21157.
35. Bakermans AJ, Geraedts TR, van Weeghel M, et al. Fasting-Induced Myocardial Lipid Accumulation in Long-Chain Acyl-CoA Dehydrogenase Knockout Mice Is Accompanied by Impaired Left Ventricular Function. *Circulation: Cardiovascular Imaging*. 2011;4(5):558–565. doi:10.1161/CIRCIMAGING.111.963751.
36. Rodeheffer MS. Tipping the scale: muscle versus fat. *Nat Cell Biol*. 2010;12(2):102–104. doi:10.1038/ncb0210-102.
37. Uezumi A, Fukada S-I, Yamamoto N, Takeda S, Tsuchida K. Mesenchymal progenitors distinct from satellite cells contribute to ectopic fat cell formation in skeletal muscle. *Nat Cell Biol*. 2010;12(2):143–152. doi:10.1038/ncb2014.
38. Joe AWB, Yi L, Natarajan A, et al. Muscle injury activates resident fibro/adipogenic progenitors that facilitate myogenesis. *Nat Cell Biol*. 2010;12(2):153–163. doi:10.1038/ncb2015.
39. Viddeleer AR, Sijens PE, van Ooyen PMA, Kuypers PDL, Hovius SER, Oudkerk M. Sequential MR imaging of denervated and reinnervated skeletal muscle as correlated to functional outcome. *Radiology*. 2012;264(2):522–530. doi:10.1148/radiol.12111915.
40. Chung KW, Suh BC, Shy ME, et al. Different clinical and magnetic resonance imaging features between Charcot-Marie-Tooth disease type 1A and 2A. *Neuromuscul Disord*. 2008;18(8):610–618. doi:10.1016/j.nmd.2008.05.012.
41. Costa AF, Di Primio GA, Schweitzer ME. Magnetic resonance imaging of muscle disease: A pattern-based approach. *Muscle Nerve*. 2012;46(4):465–481. doi:10.1002/mus.23370.
42. Pareyson D, Marchesi C. Diagnosis, natural history, and management of Charcot-Marie-Tooth disease. *Lancet Neurol*. 2009;8(7):654–667. doi:10.1016/S1474-4422(09)70110-3.



Supplemental Figure 1. Muscle sum scores per disease. Each muscle was assigned to one of three groups: hip girdle, upper leg or lower leg. Every muscle with mild or high increased signal intensity of muscle on MRI was added per patient to calculate muscle sum score. T1W = T1-weighted, STIR=Short Tau Inversion Recovery. CPT2D n=3; VLCADD n=12; LCHADD n=2; MTPD n=3. Open triangles represent a VLCADD and a LCHADD patient with CK of 11180 and 12483 at moment of MRI.



Supplemental Figure 2. Moderate correlation between STIR and creatine kinase. Moderate correlation between STIR sum of affected muscle and creatine kinase levels. Spearman's correlation coefficient ρ 0.58 ($p < 0.01$).

CHAPTER 7

Abnormal energetics of endurance exercise in very long-chain acyl-CoA dehydrogenase deficiency

E.F. Diekman¹, G. Visser¹, R.A.J. Nivelstein², M. de Sain¹, J.P.J. Schmitz³,
M. Wardrop⁴, L. Van der Pol⁶, S.M. Houten⁵, T. Takken⁴, J.A.L. Jeneson⁴

¹ Department of Paediatric Gastroenterology and Medical Genetics, Wilhelmina Children's Hospital, University Medical Center Utrecht, the Netherlands

² Department of Radiology, UMCU

³ Systems Bioinformatics, Department of Life and Earth Sciences, Vrije Universiteit, Amsterdam

⁴ Child Development & Exercise Center, Wilhelmina Children's Hospital, University Medical Center Utrecht, the Netherlands

⁵ Department of Clinical Chemistry, Laboratory Genetic Metabolic Diseases, Academic Medical Center, University of Amsterdam, The Netherlands

⁶ Department of Neurology

Manuscript in preparation

ABSTRACT

Exertional rhabdomyolysis is common in very long-chain acyl-CoA dehydrogenase deficiency (VLCADD). Typically, ATP depletion during exercise has been invoked as pathogenic mechanism. Here, four symptomatic and one asymptomatic VLCADD patients and five healthy controls performed 45 min of bicycling exercise at a workload corresponding to their individual maximal rate of fatty acid oxidation. The final five min of bicycling exercise were performed inside an MRI scanner for continuous ^{31}P magnetic resonance spectroscopic recordings from the quadriceps muscle during exercise and subsequent recovery. Blood samples were taken before, five and 180 minutes after the endurance exercise test, respectively. We found a threefold higher rise of quadriceps Pi and concomitant depletion of PCr during exercise in both symptomatic as well as asymptomatic VLCADD patients compared to healthy controls, but normal metabolic recovery kinetics post-exercise. Three hours post- but not immediately after endurance exercise, acetyl-carnitine levels were twofold lower in patients. Computational modeling analysis showed that these results may be explained by a partial slow-to-fast shift in fiber type composition of the quadriceps muscle in VLCADD patients. Such a phenotypic change would aggravate the problem of sole reliance on finite intramuscular carbohydrate stores in VLCADD explaining the elevated risk of exertional energy crisis and rhabdomyolysis in this disease.

INTRODUCTION

The mitochondrial enzyme very-long chain Acyl-CoA dehydrogenase (VLCAD, OMIM 201475) is the first enzyme in the fatty acid oxidation cycle and, as such, a key enzyme in this pathway for mitochondrial energy transduction from fatty acids^{1,2}. Deficiency of VLCAD enzyme activity is a relatively rare cause of human disease³. The clinical presentation is a spectrum with lethal disease in early childhood associated with fasting intolerance and failing glucose homeostasis^{1,4}, to exercise intolerance with episodic rhabdomyolysis and myalgia in (early-)childhood and adult life^{4,6}, to asymptomatic individuals. VLCAD deficiency (VLCADD) has been included in newborn screening programs all over the world. Treatment of VLCADD consists of dietary treatment aimed at prevention of catabolism⁷.

Clinical management of VLCAD deficient patients poses a major challenge. At present, there is no effective therapy to alleviate severe exercise intolerance and myalgia with risk of episodic rhabdomyolysis⁸. Exercise, prolonged fasting and fever/illness can trigger rhabdomyolysis. This symptom forms a grave complication that may lead to kidney damage and even renal failure⁵. Patients are typically advised to engage only in light physical work in combination with timely and ample intake of carbohydrates and/or medium-chain triglyceride. Given the generic health benefits of physical exercise, however, the long-term health outcome of lifelong restricted physical activity is a serious concern. As such, patients with VLCADD would greatly benefit from detailed mechanistic understanding of how VLCAD (dys)function impacts muscle health and function. Such level of understanding, however, is currently unavailable. Typically, ATP depletion and ensuing calcium overload have been invoked as pathogenic mechanism of rhabdomyolysis following heavy and/or prolonged exercise^{9,10}. It was, however, previously noted that, while exertional rhabdomyolysis is common in VLCADD and other long-chain fatty acid oxidation¹¹⁻¹⁴, it is relatively rare in myopathies caused by impaired mitochondrial ATP synthetic function due to respiratory chain enzyme defects^{15,16}. Perhaps even more puzzling, VLCAD dysfunction is associated with episodic rhabdomyolytic events rather than chronic rhabdomyolysis in response to exercise, including a lifelong absence of any such event in some patients^{4,5}.

Here, we further investigated muscle energetics in relation to prolonged exercise in human VLCADD disease was further investigated using *in vivo* ³¹P magnetic resonance spectroscopy (³¹P MRS), metabolic profiling of blood samples and computational modelling. Our findings offer a new clue to understanding the pathogenesis of exertional rhabdomyolysis in VLCADD disease.

METHODS

Design and study selection

Five patients with VLCADD (Table 1A and B) and five age-matched healthy controls were recruited. Patients with myopathic exacerbation at time of experiment, cardiomyopathy/arrhythmia, epilepsy or pregnancy were excluded from the study, as well as the presence of conventional contra-indications for $^{31}\text{P}/^1\text{H}$ MRS (MRI) measurements. The study consisted of two separate exercise test-sessions separated by at least two weeks. First, subjects performed a standard cardio-pulmonary exercise test on an upright bicycle ergometer. From the results of this test, the workload corresponding to maximal bodily fat oxidation (FATMAX) was determined for each subject. Two or more weeks later, subjects performed 45 minutes of bicycling exercise at their individual FATMAX workload, of which the final five minutes were performed supine inside the MR scanner using a MR-compatible bicycle ergometer¹⁷. Blood samples were taken at three timepoints: before, 5 and 180 minutes after the FATMAX exercise test, respectively. The study was approved by the medical ethics committee of the University Medical Centre Utrecht (METC 12-211/K). All patients provided written informed consent for participation in this study.

Dietary standardization

Patients and healthy controls were asked to keep a food record the three days preceding the test day. A light meal was allowed before the test. An extensive dietary analysis based on a three-day diary and subsequent interview by a nutritionist was performed in all patients, prior to the second exercise test (NEVO-table 2011 (Dutch Food Composition Table), RIVM/Voedingscentrum, Den Haag 2011).

Exercise testing

1. Cardio-pulmonary exercise test (CPET)

Maximal exercise capacity was measured during the baseline graded CPET. The participant performed exercise on a standard upright bicycle ergometer under increasing load until exhaustion (duration +/- 10min). By using the respiratory gas exchange parameters, the intensity of maximal fat oxidation (FATMAX) could be determined¹⁸. Subjects sat placed on an upright cycle ergometer and fitted with a 12-lead ECG, a pulse oximeter on the index finger or forehead, an automatic blood pressure cuff, and a small face mask attached to a breath-by-breath gas analysis system. Subjects performed a pulmonary function test at rest to determine the forced expiratory volume in 1 sec (FEV_1) and forced vital capacity (FVC). After this measurement, subjects began the test with 5 minutes of resting measurements while sitting on the cycle ergometer. A modified protocol for determining the maximal fat oxidation (FATMAX) as recommended for testing on a cycle

Table 1A Patient characteristics and plasma concentration of several metabolites in resting conditions. PID=Patient Identification number; y=year; M=male/F=female; BMI=body mass index; EA=enzymatic activity measured in fibroblasts; CK=creatine kinase. Contr. = controls Mean \pm SEM is reported.

PID	Age (y)	Sex	Height (cm)	Weight (kg)	BMI	EA	C14:1-carnitine (μ mol/L)	Basal CK	# of hospital admissions	Symptoms	Activities in daily life
1	13	M	171	53	18,1	<5%	1.2	1553	6	muscle pain	in school; abstains from any voluntary activity
2	17	F	158	79	31,7	5%	1.0	36	11	muscle pain, fatigue	in school; abstains from any voluntary activity
3	32	M	175	74	24,2	<5%	8.9	1253	2	muscle pain, fatigue	heavy manual labor; recreational sports (soccer)
4	41	M	187	87	24,9	12%	1.1	156	2	muscle pain, fatigue	not able to work; abstains from any voluntary activity
5	37	M	186	87	25,2	13%	1.8	83	1	asymptomatic	College graduate office worker; recreational outdoor sports
Contr.	26 \pm 4	1F, 4M	179 \pm 6	71 \pm 7	21.8 \pm 1.3		0.04 \pm 0.1	113 \pm 20			

Table 1B. Mutation analysis of patients. PID= patient identification number.

PID	Mutation
1	homozyg. c.104delC
2	homozyg. c.1141-43delGAG
3	homozyg. c.1406G>A
4	c.520G>A; c.833_835delAAG
5	c.848T>C; c.1444_1448delAAGGA and c.1511_1516delAGAG

p.Pro35LeufsX26

p.Glu381del

p.Arg469Gln

p.Val174Met; p.Lys278del

p.Val283Ala; p.Lys482AlafsX78 and p.Glu504_ Ala505del

ergometer (Lode Corival, Lode BV, Groningen, the Netherlands) was used¹⁹. The subjects were instructed to cycle at an increasing load of 35 watts every 3 minutes, starting with 0 watts and ending at voluntary exhaustion. During this time several measurements were taken: a full electrocardiogram (ECG; Cardioperfect, Accuramed BVBA, Lummen, Belgium), oxygen (O₂) saturation (Masimo, Rad 8, Masimo BV, Tilburg, the Netherlands), heart rate (HR), blood pressure (BP) (Suntech Tango, Suntech Med, Morrisville, NC, USA), minute ventilation (VE), oxygen uptake (VO₂), carbon dioxide output (VCO₂), respiratory exchange ratio (RER), workload (W), using a calibrated metabolic cart (ZAN 600, Accuramed BVBA, Lummen, Belgium). Subjects were asked to keep their cadence per minute between 60-80, and were given verbal encouragement to continue if they fell below that range. Immediately after exhaustion, the load was decreased to 0 watts and subjects were asked to cool down for 5 minutes.

FATMAX workload was calculated according to the formula proposed by Péronnet and Massicotte for calculating fat oxidation, as it is both accurate in estimating fat oxidation and does not require an estimate of protein degradation during exercise (eqn (1));²⁰:

$$\text{Fat oxidation (mg}\cdot\text{min}^{-1}) = 1.695 \times \text{VO}_2 \text{ (mL}\cdot\text{min}^{-1}) - 1.701 \times \text{VCO}_2 \text{ (mL}\cdot\text{min}^{-1}) \quad \text{eqn (1)}$$

Workload, the independent variable for the FATMAX curve, was taken in terms of HR, Watt, and percentage of VO_{2peak}. The final 60 seconds of exercise for each workload interval were averaged to achieve steady-state values. Each set of steady-state FATMAX values were fit along a second order polynomial curve.

II. Endurance exercise test

Subjects were asked to exercise at their individual FATMAX workload for a total of 45 minutes. Of these, 40 minutes were performed on an upright standard bicycle ergometer (Lode, Groningen, the Netherlands) in a room adjacent to the MRI scanner. Next, subjects were moved to the MR scanner and performed the final five minutes of exercise task in supine position inside the MR scanner at a workload equivalent to FATMAX. Hereto, the braking force on the MR-compatible bicycle ergometer was gravimetrically adjusted to the appropriate amount using 30 N as empirical reference for maximal sustainable braking force in healthy subjects (data not shown).

31P-Magnetic Resonance Spectroscopy

Subjects were positioned feet-forward in a supine position in a 1.5T Philips MR Achieva scanner (Philips Healthcare, Best, the Netherlands). The upper body was supported by a wedge-shaped cushion to facilitate supine bicycling. A 6-cm diameter single-turn ³¹P surface coil supplied by the manufacturer was fastened over the m. vastus lateralis of the right leg. Subjects then performed a short bout of bicycling supervised by an on-site coach to familiarize them with the supine exercise task. The desired pedalling frequency (target setting: 75 rpm) was set by a metronome audible over the in-magnet speaker

system. Next, a series of scout MR images was acquired to evaluate correct positioning of the subject and the coil and image-based shimming was performed. ^{31}P NMR spectra were acquired from the m. vastus lateralis at rest, during exercise and recovery using an adiabatic half-passage excitation pulse as described elsewhere¹⁷. First, a resting spectrum was acquired under fully-relaxed conditions (repetition time (TR) 20 s). During exercise and recovery, four and two free induction decays (FIDs), respectively, were acquired with a TR of 3s and averaged, yielding time resolution of 12 and 6 seconds, respectively, in each dynamic phase.

31P-MRS data processing

FIDs were processed and analyzed in the time domain using the AMARES algorithm in the public jMRUI software environment (version 3.0) as described elsewhere¹⁷. Kramer-Rao bounds of the AMARES Lorentzian model fitting were used as statistical information on accuracy of peak area estimation. Absolute PCr and Pi concentrations were calculated after correction for signal saturation assuming total adenylate nucleotide and creatine pool sizes of 8.2 and 42.7 mM, respectively, as previously described²¹. Intramuscular pH was determined from the resonance frequency of Pi using standard methods²¹. Steady-state PCr and Pi concentrations during exercise were determined from summed FIDs acquired 60s after onset of bicycling. Datasets were analysed in a blinded fashion.

Computational Modeling

A multi-fiber kinetic model of oxidative ATP metabolism in human skeletal muscle²² was used to investigate if, and if so, what magnitude of fiber type composition changes in VLCADD skeletal muscle may contribute to any measured average change in stationary states of energy balance at FATMAX exercise in VLCADD versus healthy muscle. Briefly, the multi-fiber model was composed of three fiber-type specific submodels corresponding to type I, IIA and IIX, respectively, individually parameterized to capture known differences in contractile and oxidative ATP metabolic capacity between these fiber types²². The core kinetic model of oxidative ATP metabolism in each submodel has been described in detail elsewhere²³. A summary of fiber-type specific submodel parameterization with regard to oxidative ATP metabolism and default healthy quadriceps composition is given in Supplemental Table 2; other model parameters were assumed to be non-fiber type specific. The relation between measured average Pi and PCr concentrations in the sampled quadriceps muscle mass during FATMAX exercise and fiber-type-specific concentrations was described by (eqn (2))

$$M_{average} = X_{typeI} \cdot M_{typeI} + X_{typeIIA} \cdot M_{typeIIA} + X_{typeIIX} \cdot M_{typeIIX} \quad \text{eqn (2)}$$

where M_{typeI} , $M_{typeIIA}$, $M_{typeIIX}$ denote the fiber-type specific concentration of metabolite PCr or Pi according to the model, and X_{typeI} , $X_{typeIIA}$, $X_{typeIIX}$ denote the fraction of quadriceps

muscle composed of type I (slow-oxidative; SO), type IIA (fast-oxidative/glycolytic; FOG) and type IIX (fast-glycolytic; FG) fibers, respectively. The default model parameterization for X_{typeI} , X_{typeIIA} , X_{typeIIX} was 0.5, 0.35 and 0.15, respectively²⁴. In the simulations, it was assumed that the maximal mechanical output that muscle fibers can sustain without any significant fatigue gives rise to a respiratory rate equal to 80% of maximal rate^{25,26}. The model was implemented in Matlab 7.5.0 (The Mathworks, Natick, MA, USA). Ordinary differential equations were solved numerically by using ODE15s with absolute and relative tolerances set to 10^{-8} .

Analysis of blood samples

Plasma of blood samples were profiled for glucose, lactate, acylcarnitines and creatine kinase. Plasma was stored at -20°C . Plasma acylcarnitines were measured as described previously²⁷ using internal standards. Blood for measurement of lactate and pyruvate was treated immediately after withdrawal with an equal volume of 1M perchloric acid and subsequently stored at -20°C . Plasma glucose and creatine kinase (CK) level were measured using standard enzymatic assays²⁸. Blood lactate and pyruvate, were measured using tandem mass spectrometry²⁹. All samples were analysed in a blinded fashion.

Statistics

Two-tailed Mann Whitney U-tests were used to determine significant differences between control and patients at $p < 0.05$. Data are presented as mean \pm standard error of mean (SEM) unless specified otherwise. Time courses of variables were analysed and characterized kinetically using non-linear curve-fitting (Origin 6.0, Caltech Pasadena, US). Whenever possible, statistical information on data accuracy was incorporated in the curve-fitting by means of statistical weighting.

RESULTS

Baseline characteristics of subjects

Five VLCAD deficient patients were included, of which 3 patients had an enzymatic activity of $\leq 5\%$, and 2 patients $\leq 13\%$ (compared to reference control fibroblasts). One patient was asymptomatic, 4 patients report exercise intolerance, myalgia and fatigue. Symptomatic patients have been admitted to the hospital at least twice in their lives (range 2-11) (Table 1). The basal plasma creatine kinase level was increased mildly in 2 of 5 patients. C14:1-carnitine was significantly increased in VLCADD patients compared to controls ($p=0.02$). Age, height, weight and BMI were comparable between controls and VLCADD patients (Table 1). Dietary intake of the last three days before the second

test did not differ significantly between controls and VLCADD patients (Supplementary table 2).

Cardio-pulmonary exercise test

Maximal workload was 46% lower in all four symptomatic VLCAD deficient patients compared to controls (Table 2 and Figure 1A). In contrast, maximal workload of the asymptomatic patient was identical to healthy controls (Table 2). Two patients (PID #2 and #3) had a RER_{peak} comparable to controls, while the other three patients (including

Table 2 Graded CPET exercise test characteristics of controls and patients. PID= patient identification number. HR_{peak} = peak heart rate; RER = respiratory exchange ratio. Mean \pm SEM is reported.

PID	Max workload (W)	HR _{peak} (beats/min)	Resting RER	VO _{2peak} (mL/kg/min)	Peak ventilation (L/min)	Max Fat oxidation (% of VO _{2peak})	Max Fat oxidation (mg/kg/min)	FATMAX intensity (W)
1	142	185	0.90	34.8	58	30.0	0.85	3
2	142	182	0.84	26.6	60	55.0	4.13	50
3	113	149	0.83	19.3	36	54.5	2.09	32
4	130	175	1.04	21.0	79	29.0	0.0	0
5	294	184	0.94	45.6	143	41.7	2.52	81
Contr.	242 \pm 24*	189 \pm 5	0.83 \pm 0.02	45 \pm 4*	114 \pm 11*	38 \pm 4	3.8 \pm 1.0	51 \pm 16

the asymptomatic patient) had an elevated RER_{peak} between 0.90 and 1.04. VO_{2peak} as well as peak ventilation was 49% decreased in symptomatic VLCAD deficient patients (Table 2 and Figure 1B). The peak rate of fat oxidation per kg of bodymass in symptomatic patients was 54% lower compared to controls (Table 2 and Figure 1C). FATMAX workload in symptomatic patients was 58% lower than controls (Table 2).

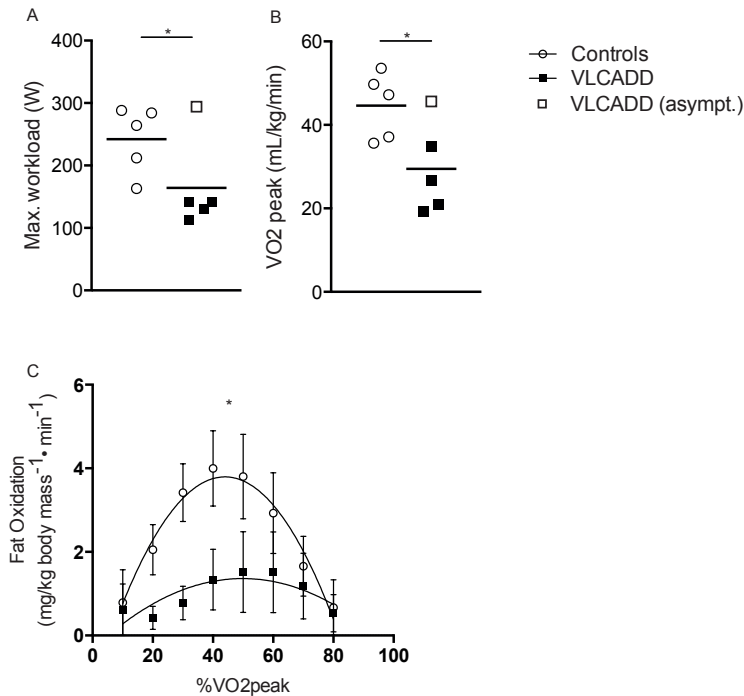


Figure 1. Maximal workload of symptomatic (■) and asymptomatic (□) VLCADD patients and controls (○) (A). Peak VO₂ max. in symptomatic (■) and asymptomatic (□) VLCADD patients and controls (○) (B). Fatty acid oxidation in mg/kg body mass/min in VLCADD patients (■) and controls (○) (C). Error bars indicate \pm SEM. * $P < 0.05$ for polynomial curve.

Endurance exercise test.

All subjects completed the task of 40 min upright bicycling at their individual FATMAX workload outside MR scanner. All subjects except patient #4 completed the task of 5 min supine bicycling against a workload corresponding to their individual FATMAX workload inside scanner. Patient #4 was only able to maintain the workload for three minutes.

Quadriceps muscle energetics

In resting vastus lateralis muscle, ³¹P metabolite concentrations and intramuscular pH were not different between VLCADD patients and healthy controls (Supplementary table 1)

Figure 2A shows a time series of ³¹P NMR spectra recorded sequentially from the vastus lateralis muscle of a healthy control (upper trace) and a VLCADD patient (lower trace) during supine bicycling exercise at FATMAX workload. Figure 2B shows the corresponding ³¹P NMR spectra of the summed FIDs recorded after 60s into the exercise for these subjects. In healthy control subjects, only minor changes in steady-state Pi and

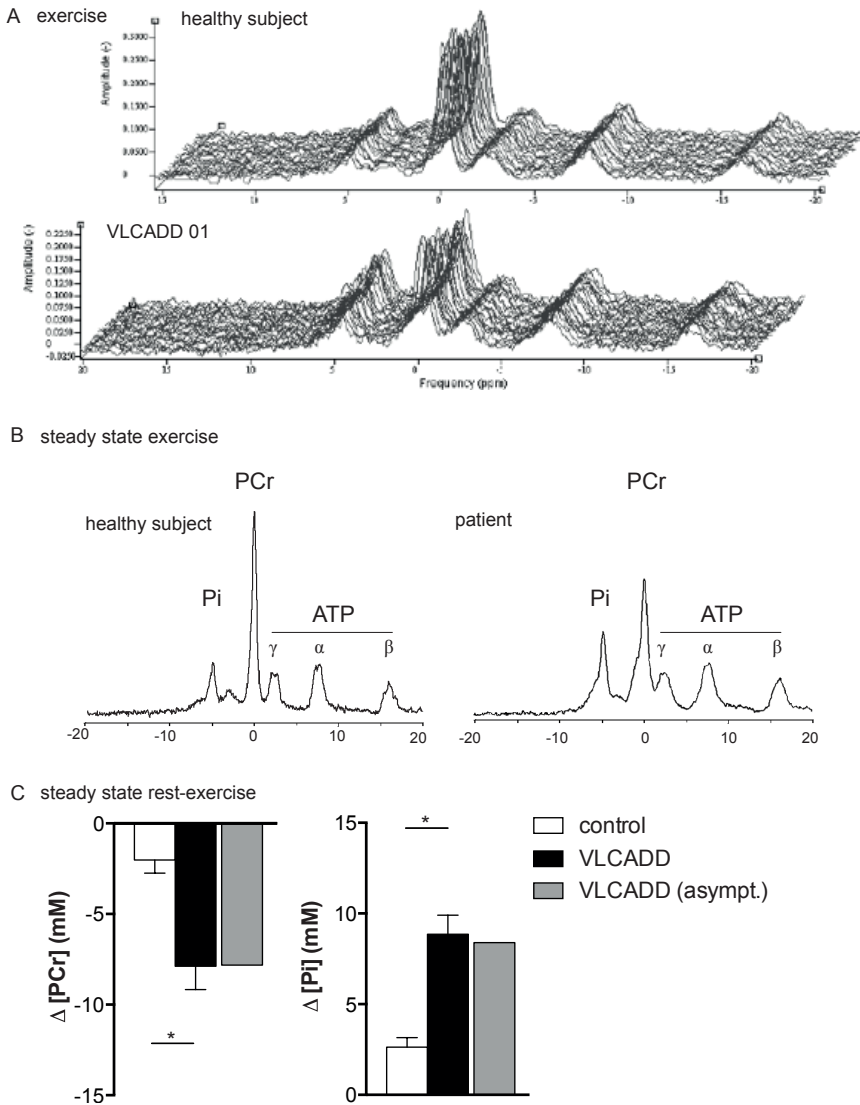


Figure 2. ^{31}P NMR spectra acquired from the lateral head of the quadriceps muscle of the right leg of a VLCAD deficient patient versus a healthy control subject during 5 min of bicycling exercise at a workload equivalent to FATMAX in each subject. Each spectrum represents the sum of the FIDs collected after 60 s of exercise. FIDs were apodized in the time domain using a 10-Hz low-pass filter prior to Fourier transform and phasing. Peak assignments: Pi inorganic phosphate, PCr phosphocreatine, ATP adenosine triphosphate (γ , α and β , resonances, respectively). (A and B) Average change in PCr and Pi during exercise (in mM) in healthy control subjects versus symptomatic and asymptomatic VLCAD deficient patients. Error bars indicate mean \pm SEM, * $P < 0.05$. (C)

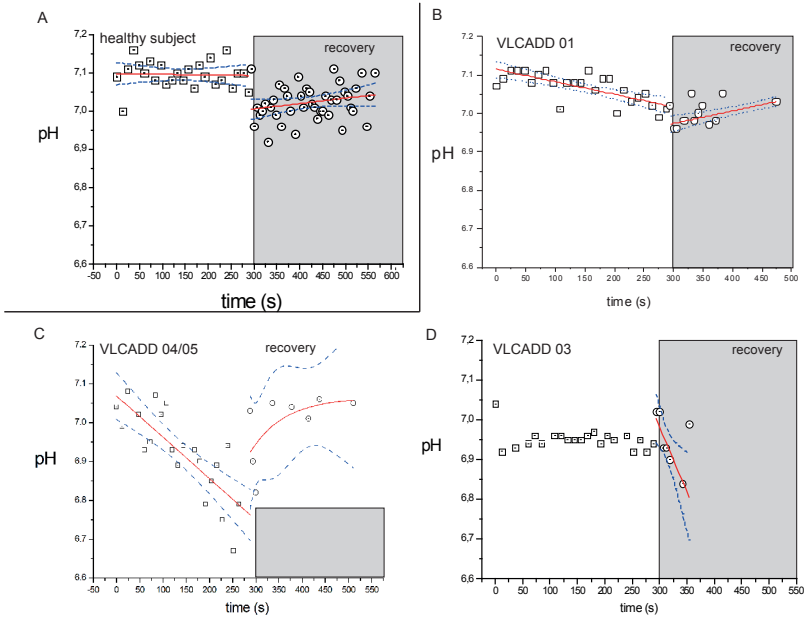


Figure 3. PH dynamics during exercise and first minutes of recovery in healthy controls (A) and VLCADD patients (B-D).

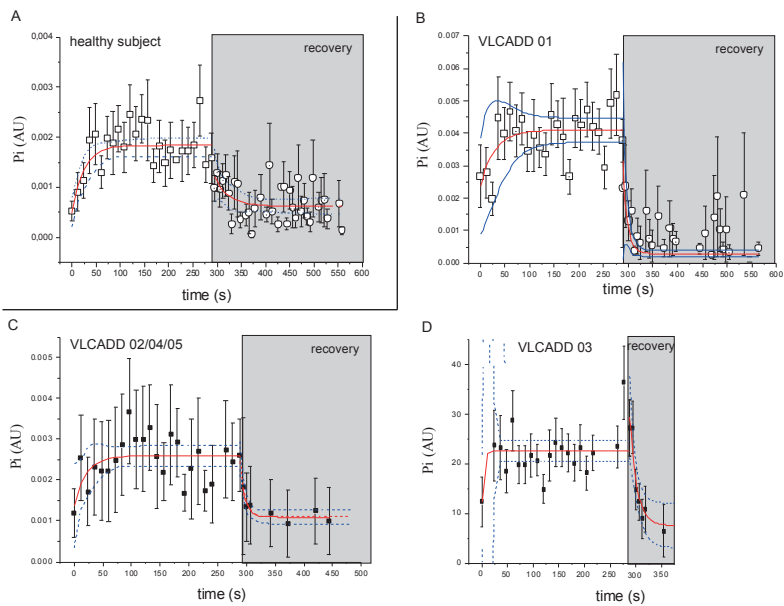


Figure 4. Pi recovery rates of healthy controls (A) and VLCADD patients (B-D).

Table 3 PCr and Pi recovery rates. #value for vastus lateralis muscle of healthy human subjects²², ^Pi recovery kinetics are similar although not quite identical to PCr recovery³⁹.

PID	tau PCr (s)	tau Pi (s)
#1	21 ± 9	12 ± 7
#3	ND	12 ± 5
#2	16 ± 9	21 ± 13
#4	28 ± 13	19 ± 14
#5	ND	9 ± 5
Controls	24 ± 5 [#]	24 ± 5 [^]

PCr concentrations from resting values were observed (Δ PCr: -2.0 ± 0.7 mM; Δ Pi: $+2.6 \pm 1.0$ mM (mean + SEM) (Figure 2A-C). Intramuscular pH during exercise did not fall below 7.0 in any healthy control subject (Figure 3A). In all VLCADD patients almost identical, pronounced changes in quadriceps Pi and PCr concentrations from resting values were observed during steady-state exercise at FATMAX workload (Δ PCr: -7.9 ± 1.0 mM; Δ Pi: $+8.8 \pm 0.8$ mM (mean + SEM) (Figure 2A-C). Quadriceps pH in patient PID#01 did not fall below 7.0 during exercise similar to healthy controls (3B). In patients PID#02 (not shown), #04 and #05 intramuscular pH progressively dropped during exercise to values as low as 6.7 (Figure 3C). In patient #03, intramuscular pH during exercise dropped 0.1 units to 6.95 at onset of exercise and remained stable at this value during the remainder of the exercise (Figure 3D).

In none of the VLCADD patients, any significantly slower recovery of Pi and PCr concentrations was found compared to typical literature values for human quadriceps muscle (Table 3 and Figure 4). Metabolic recovery was even faster in some VLCADD patients compared to healthy controls (Table 3 and Figure 4). In healthy subjects the dynamics of PCr and Pi recovery to basal levels were typically too difficult to quantify due to the minor changes in these concentrations during exercise at FATMAX workload (Figure 2A-C).

The dynamics of intramuscular pH following exercise shown in Figure 3 did not reveal any major abnormalities between VLCADD patients and healthy controls. The typical drop in intramuscular pH at the onset of recovery followed by a slow recovery to resting values typically observed in healthy control subjects (Figure 3A) was likewise observed in patients PID#01 and #03 (Figure 3B and D). In the other patients, intramuscular pH recovered without any ancillary further drop of pH at the onset of recovery (Figure 3C).

Model simulations

Computational modelling analysis was used to investigate whether a shift in fiber type composition of the quadriceps muscle in VLCADD patients could explain the observed muscle energetics. It was found for healthy controls that within the set of assumptions

Table 4. results of numerical analysis of fiber type recruitment (in % of total pool size) during voluntary exercise at FATMAX in healthy control subjects and VLCADD patients. X: fraction of fiber type in quadriceps muscle; three fiber types; sum of all fractions = 1.0. SO= slow oxidative fiber. FOG= Fast oxidative glycolytic. FG= Fast-glycolytic.

Scenario I:	X type I = 0.5	X type IIA = 0.35	X type IIX = 0.15
	SO	FOG	FG
Controls	70%	0%	0%
VLCADD	100%	0%	0%
Scenario II:	X type I = 0.35	X type IIA = 0.5	X type IIX = 0.15
	SO	FOG	FG
Controls	70%	0%	0%
VLCADD	100%	35%	0%

described in the Methods section, recruitment of 70% of all fibers of the quadriceps during steady-state exercise at FATMAX workload would explain the average concentrations of quadriceps PCr and Pi observed by ^{31}P MRS in this group (Table 4). Next, two scenarios were explored numerically to explain the ^{31}P MRS observation of altered energy balance in the VLCADD patients. In the first scenario, no phenotypic change in quadriceps fiber type composition was allowed. Recruitment of the complete fraction of fibers of the quadriceps was then required to give rise to the average concentrations of quadriceps PCr and Pi observed by ^{31}P MRS in exercising patients (Table 4). In the second scenario, it was assumed that the fraction of required fibers was 30% reduced in VLCADD compared to healthy controls and substituted by FOG fibers. We found that the observations by ^{31}P MRS in exercising patients could be explained if all fibers and 35% of the FOG pool were recruited during voluntary exercise at FATMAX (Table 4).

Blood metabolic profile in response to FATMAX exercise test

Glucose levels remained unchanged (Figure 5A). Lactate levels were not different between controls and symptomatic VLCADD patients (Figure 5B). In the asymptomatic patient lactate levels increased from 1.3 to 5 mmol/L during exercise at FATMAX (Figure 5B). Basal CK levels were normal (i.e., <250U/L) in all controls and three VLCADD patients Table 1. After the FATMAX exercise test, CK levels in two patients slightly increased (PID #2 and #4; 400 and 576 U/L, respectively) but still remained low. As expected, plasma C14:1 acyl-carnitine levels were increased significantly at rest in VLCADD patients (Table 1). Resting acetyl-carnitine (C2-carnitine) levels were similar between patients

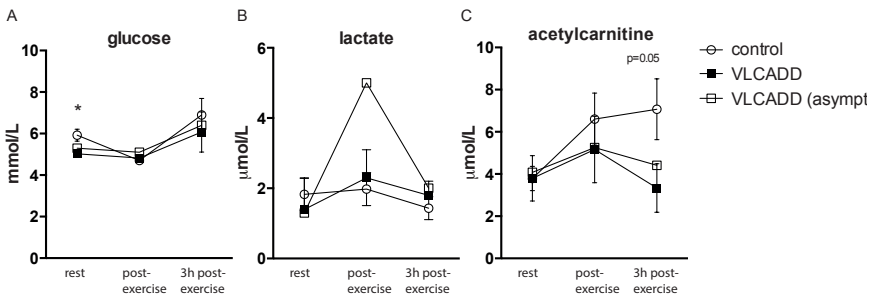


Figure 5. Glucose (A), lactate (B) and acetylcarnitine (C) levels at $t=0$ (rest), $t=1$ (directly after exercise) and $t=2$ (3 hours after exercise) in symptomatic VLCADD patients and controls. Error bars indicate mean \pm SEM, * $P < 0.05$.

and healthy controls (Figure 5C). Three hours post- but not immediately after FATMAX exercise, acetyl-carnitine levels were twofold lower in patients (Figure 5C).

DISCUSSION

We sought to investigate muscle energetics in relation to prolonged exercise in human VLCADD disease using in vivo ^{31}P MRS, metabolic profiling of blood samples and computational modelling. We found a threefold higher rise of Pi and concomitant depletion of PCr during mild exercise in VLCADD patients compared to healthy controls, with normal-to-fast recovery rates following exercise (Figure 2C, 4, Table 3). Numerical analysis showed that these results may be explained by a partial slow-to-fast shift in fiber type composition of the quadriceps muscle in VLCADD patients.

Any altered cellular energy balance in a muscle engaged in a standardized exercise task can be the result of altered cellular capacity for ATP synthesis, altered ATP cost of force production, or a combination of both³⁰. Human examples include observations in mitochondrial myopathies caused by respiratory chain defects^{31,32}. In VLCADD, impaired mitochondrial ATP synthetic capacity was, however, ruled out by the finding of normal if not faster post-exercise recovery kinetics in the patients (Table 3) despite indications for low concentrations of mitochondrial acetyl-CoA's. Specifically, plasma acetyl-carnitine levels barely increased during and 3 hours after exercise in VLCADD patients compared to controls (Figure 5), whereby low concentrations of acetyl-carnitine in blood plasma are typically assumed to reflect low concentrations of mitochondrial acetyl-CoA's³³. Therefore, it was concluded that the ATP cost of cyclic quadriceps muscle contraction and relaxation during voluntary exercise at FATMAX was higher in VLCADD patients compared to healthy controls.

In voluntary exercise, the ATP cost of contraction is determined first and foremost by which fiber type is recruited by the motor cortex of the brain to produce a desired power output³⁴. Human muscles are composed of three fiber types – slow-oxidative (SO), fast oxidative glycolytic (FOG), fast glycolytic (FG) – organized in fibers that vary in properties including size, contractile speed, ATP cost of contraction and relaxation, power-output, oxidative fuel source, mitochondrial density and vascularisation³⁵. Fiber types are recruited in a stepwise order according to the size principle whereby SO fibers are the smallest, followed by FOG and finally FG³⁴. The simplest explanation of the main result of the present study would thus be that in VLCADD patients performing voluntary bicycling exercise at FATMAX more relatively ATP-inefficient (fast-twitch) fibers were recruited than in healthy controls to perform this task.

This conclusion was confirmed by the results of model simulations. Within the set of assumptions made for these computations numerical, solutions for two alternative fiber recruitment scenarios during the exercise test in VLCADD patients were found (Table 4). A first solution was that VLCADD patients in comparison to healthy controls recruited a significantly greater (100% instead of 70%) fraction of SO fibers to execute the same normalized physical task (Table 4, scenario I). This would imply that SO fibers would create less power output of contraction and thus loss of overall force of muscle contraction in VLCADD patients compared to healthy controls. However, no evidence for any loss of force of muscle contraction has been documented in VLCADD patients. Therefore, this solution was deemed unrealistic. The alternative numerical solution required a phenotypical adaptation of the quadriceps muscle in the patients with respect to fiber type composition. Specifically, it involved the assumption of a reduction of slow oxidative fiber fraction in VLCADD to 0.35 (instead of 0.50) of the assumed pool size in healthy controls concomitant with a complementary increase of the total fraction of FOG fibers (0.50 instead of 0.35) (Table 4, scenario II). In this scenario, the observed elevated changes in Pi and PCr concentrations in exercising quadriceps in VLCADD compared to healthy controls could be explained by recruitment of 100% of slow-oxidative fibers and 35% of all FOG fibers during the physical task (Table 4, scenario II). Objectification of this solution of the analysis would require taking a biopsy of the quadriceps muscle of the patients for histological analysis. In the present study, this was deemed inadmissible in view of the myopathy of the majority of the patients and inclusion of paediatric patients. However, a moderate slow-to-fast phenotypic adaptation of quadriceps muscle in VLCADD was indeed found recently in a mouse model of this disease³⁶.

A slow-to-fast phenotypic adaptation of skeletal muscle fiber type composition would aggravate the problem in VLCADD of sole reliance on finite intramuscular carbohydrate stores during exercise, since fast-twitch muscle fibers are energetically much less efficient than slow-twitch fibers³⁶. Indeed, it has been shown that typically type II muscle fibers are lost in rhabdomyolysis³⁷. As such, this explanation of the observations may

offer a possible mechanism for the elevated risk of exertional energy crisis and rhabdomyolysis in this disease.

Finally, these observations in VLCADD patients also offer clues to successful therapeutic approaches in this disease. First of all, any approach resorting in glycogen sparing during exercise including acute nutritional ketosis³⁸ should be considered testing. Secondly, and paradoxically, regular modest physical activity should be encouraged to stimulate formation of type I muscle fibers. Interestingly, patient #3 does lead an active lifestyle including heavy work and playing soccer, albeit a higher basal CK indicating more structural muscle damage. His quality of life has been however better than that experienced by the inactive patients. Moreover, his long-term prospects of cardiovascular health and diabetes are also better. This could suggest that performing a certain amount of physical activity might paradoxically be beneficial.

In summary, we found a threefold higher rise of Pi and concomitant depletion of PCr during mild exercise in VLCADD patients compared to healthy controls, with fast-to-normal recovery rates following exercise (Figure 2C, 4, Table 3). Numerical analysis showed that these results may be explained by a partial slow-to-fast shift in fiber type composition of the quadriceps muscle in VLCADD patients. Such a phenotypic transformation of VLCADD muscle could aggravate dependence on carbohydrate stores rendering the muscle even more susceptible to a glycogen-depletion energy crisis and rhabdomyolysis in response to strenuous exercise in human VLCADD disease.

ACKNOWLEDGEMENTS

Funding/Support: This research was supported by the Roorda foundation, ZonMW (dossier 200320006) and the National Institutes of Health USA through a subcontract to Grant HL-072011 (to JAJ).

REFERENCES

1. Strauss AW, Powell CK, Hale DE, et al. Molecular basis of human mitochondrial very-long-chain acyl-CoA dehydrogenase deficiency causing cardiomyopathy and sudden death in childhood. *Proc Natl Acad Sci USA*. 1995;92(23):10496–10500.
2. Houten SM, Wanders RJA. A general introduction to the biochemistry of mitochondrial fatty acid β -oxidation. *J Inherit Metab Dis*. 2010;33(5):469–477. doi:10.1007/s10545-010-9061-2.
3. Lindner M, Hoffmann GF, Matern D. Newborn screening for disorders of fatty-acid oxidation: experience and recommendations from an expert meeting. *J Inherit Metab Dis*. 2010;33(5):521–526. doi:10.1007/s10545-010-9076-8.
4. Vianey-Saban C, Divry P, Brivet M, et al. Mitochondrial very-long-chain acyl-coenzyme A dehydrogenase deficiency: clinical characteristics and diagnostic considerations in 30 patients. *Clin Chim Acta*. 1998;269(1):43–62.
5. Laforêt P, Acquaviva-Bourdain C, Rigal O, et al. Diagnostic assessment and long-term follow-up of 13 patients with Very Long-Chain Acyl-Coenzyme A dehydrogenase (VLCAD) deficiency. *Neuromuscul Disord*. 2009;19(5):324–329. doi:10.1016/j.nmd.2009.02.007.
6. Baruteau J, Sachs P, Broué P, et al. Clinical and biological features at diagnosis in mitochondrial fatty acid β -oxidation defects: a French pediatric study of 187 patients. *J Inherit Metab Dis*. 2012. doi:10.1007/s10545-012-9542-6.
7. Arnold GL, VanHove J, Freedenberg D, et al. A Delphi clinical practice protocol for the management of very long chain acyl-CoA dehydrogenase deficiency. *Molecular Genetics and Metabolism*. 2009;96(3):85–90. doi:10.1016/j.ymgme.2008.09.008.
8. Orngreen MC, Madsen KL, Preisler N, Andersen G, Vissing J, Laforêt P. Bezafibrate in skeletal muscle fatty acid oxidation disorders: A randomized clinical trial. *Neurology*. 2014. doi:10.1212/WNL.000000000000118.
9. Huerta-Alardín AL, Varon J, Marik PE. Bench-to-bedside review: Rhabdomyolysis -- an overview for clinicians. *Crit Care*. 2005;9(2):158–169. doi:10.1186/cc2978.
10. Visweswaran P, Guntupalli J. Rhabdomyolysis. 1999;15(2):415–28, ix–x.
11. Boer den MEJ, Wanders RJA, Morris AAM, IJLst L, Heymans HSA, Wijburg FA. Long-chain 3-hydroxyacyl-CoA dehydrogenase deficiency: clinical presentation and follow-up of 50 patients. *Pediatrics*. 2002;109(1):99–104.
12. Boer den MEJ, Dionisi-Vici C, Chakrapani A, van Thuijl AOJ, Wanders RJA, Wijburg FA. Mitochondrial trifunctional protein deficiency: a severe fatty acid oxidation disorder with cardiac and neurologic involvement. *J Pediatr*. 2003;142(6):684–689. doi:10.1067/mpd.2003.231.
13. Bonnefont JP, Demaugre F, Prip-Buus C, et al. Carnitine palmitoyltransferase deficiencies. *Molecular Genetics and Metabolism*. 1999;68(4):424–440. doi:10.1006/mgme.1999.2938.
14. Rubio-Gozalbo ME, Bakker JA, Waterham HR, Wanders RJA. Carnitine-acylcarnitine translocase deficiency, clinical, biochemical and genetic aspects. *Mol Aspects Med*. 2004;25(5-6):521–532. doi:10.1016/j.mam.2004.06.007.
15. Milone M, Wong L-J. Diagnosis of mitochondrial myopathies. *Molecular Genetics and Metabolism*. 2013;110(1-2):35–41. doi:10.1016/j.ymgme.2013.07.007.
16. Vissing CR, Dunø M, Olesen JH, et al. Recurrent myoglobinuria and deranged acylcarnitines due to a mutation in the mtDNA MT-CO2 gene. *Neurology*. 2013;80(20):1908–1910. doi:10.1212/WNL.0b013e3182929fb2.

17. Jeneson JAL, Schmitz JPJ, Hilbers PAJ, Nicolay K. An MR-compatible bicycle ergometer for in-magnet whole-body human exercise testing. *Magn Reson Med*. 2010;63(1):257–261. doi:10.1002/mrm.22179.
18. Zakrzewski J, Tolfrey K. Exercise protocols to estimate Fatmax and maximal fat oxidation in children. *Pediatr Exerc Sci*. 2011;23(1):122–135.
19. Achten J, Gleeson M, Jeukendrup AE. Determination of the exercise intensity that elicits maximal fat oxidation. *Med Sci Sports Exerc*. 2002;34(1):92–97.
20. Péronnet F, Massicotte D. Table of nonprotein respiratory quotient: an update. *Can J Sport Science*. 1991;16(1):23–29.
21. Jeneson JA, Wiseman RW, Kushmerick MJ. Non-invasive quantitative 31P MRS assay of mitochondrial function in skeletal muscle in situ. *Mol Cell Biochem*. 1997;174(1-2):17–22.
22. Schmitz JPJ. Systems Biology of Energy Metabolism in Skeletal Muscle. 2012:1–211.
23. van Oorschoot JWM, Schmitz JPJ, Webb A, Nicolay K, Jeneson JAL, Kan HE. 31P MR spectroscopy and computational modeling identify a direct relation between Pi content of an alkaline compartment in resting muscle and phosphocreatine resynthesis kinetics in active muscle in humans. *PLoS ONE*. 2013;8(9):e76628. doi:10.1371/journal.pone.0076628.
24. Staron RS, Hagerman FC, Hikida RS, et al. Fiber type composition of the vastus lateralis muscle of young men and women. *J Histochem Cytochem*. 2000;48(5):623–629. doi:10.1177/002215540004800506.
25. Veld ter F, Nicolay K, Jeneson JAL. Increased resistance to fatigue in creatine kinase deficient muscle is not due to improved contractile economy. *Pflugers Arch*. 2006;452(3):342–348. doi:10.1007/s00424-005-0041-6.
26. Jeneson JAL, Veld ter F, Schmitz JPJ, Meyer RA, Hilbers PAJ, Nicolay K. Similar mitochondrial activation kinetics in wild-type and creatine kinase-deficient fast-twitch muscle indicate significant Pi control of respiration. *Am J Physiol Regul Integr Comp Physiol*. 2011;300(6):R1316–25. doi:10.1152/ajpregu.00204.2010.
27. de Sain-van der Velden MGM, Diekman EF, Jans JJ, et al. Differences between acylcarnitine profiles in plasma and bloodspots. *Molecular Genetics and Metabolism*. 2013. doi:10.1016/j.ymgme.2013.04.008.
28. Bergmeyer HU. *Methods of Enzymatic Analysis*. Wiley-VCH; 1986.
29. Chuang C-K, Wang T-J, Yeung C-Y, et al. A method for lactate and pyruvate determination in filter-paper dried blood spots. *J Chromatogr A*. 2009;1216(51):8947–8952. doi:10.1016/j.chroma.2009.10.074.
30. Dudley GA, Tullson PC, Terjung RL. Influence of mitochondrial content on the sensitivity of respiratory control. *J Biol Chem*. 1987;262(19):9109–9114.
31. Bakker HD, Scholte HR, Jeneson JA, Busch HF, Abeling NG, van Gennip AH. Vitamin-responsive complex I deficiency in a myopathic patient with increased activity of the terminal respiratory chain and lactic acidosis. *J Inherit Metab Dis*. 1994;17(2):196–204. doi:10.1007/BF00711617.
32. Argov Z, Bank WJ. Phosphorus magnetic resonance spectroscopy (31P MRS) in neuromuscular disorders - Argov - 2004 - *Annals of Neurology* - Wiley Online Library. *Ann Neurol*. 1991;30:97. doi:10.1002/ana.410300116.
33. Violante S, IJLst L, van Lenthe H, de Almeida IT, WANDERS RJ, Ventura FV. Carnitine palmitoyltransferase 2: New insights on the substrate specificity and implications for acylcarnitine profiling. *Biochim Biophys Acta*. 2010;1802(9):728–732. doi:10.1016/j.bbadis.2010.06.002.
34. Rowell LB, Shepherd JT. *Handbook of Physiology: Exercise: Regulation and Integration of Multiple Systems*.

35. Bottinelli R, Reggiani C. Human skeletal muscle fibres: molecular and functional diversity. *Prog Biophys Mol Biol.* 2000;73(2-4):195–262.
36. Tucci S, Herebian D, Sturm M, Seibt A, Spiekerkoetter U. Tissue-Specific Strategies of the Very-Long Chain Acyl-CoA Dehydrogenase-Deficient (VLCAD^{-/-}) Mouse to Compensate a Defective Fatty Acid β -Oxidation. Guerrero-Hernandez A, ed. *PLoS ONE.* 2012;7(9):e45429. doi:10.1371/journal.pone.0045429.t002.
37. Kushmerick MJ, Meyer RA. Chemical changes in rat leg muscle by phosphorus nuclear magnetic resonance. *American Journal of Physiology-* 1985.
38. Veech RL, Chance B, Kashiwaya Y, Lardy HA, Cahill GF. Ketone Bodies, Potential Therapeutic Uses. *IUBMB Life.* 2001;51(4):241–247. doi:10.1080/152165401753311780.
39. Westerhoff HV, van Echteld CJ, Jeneson JA. On the expected relationship between Gibbs energy of ATP hydrolysis and muscle performance. *Biophys Chem.* 1995;54(2):137–142.

Supplementary Table 1. Fiber-type-specific submodel parameterization.

Parameter	Type I	Type IIA	Type IIX	References
Mitochondrial volume (%)	6.0	4.5	2.3	S1
[PCr] _{resting state}	0.9 x {Measured average [PCr]}	1.1 x {Measured average [PCr]}	1.1 x {Measured average [PCr]}	S2, S3
Total creatine poolsize (mM)	[PCr] _{resting state} _Type I /0.85	[PCr] _{resting state} _Type IIA /0.85	[PCr] _{resting state} _Type IIX /0.85	S4
[Pi] _{resting state} (mM)	4	2	2	S5

Supplemental references:

S1. Howald H, Hoppeler H, Claassen H, Mathieu O, Straub R. Influences of endurance training on the ultra-structural composition of the different muscle fibers in humans. *Pflügers Archiv* 403: 369-376, 1985. S2. Sahlin K, Soderlund K, Tonkonogi M, Hirakoba K. Phosphocreatine content in single fibers of human muscle after sustained submaximal exercise. *Am J Physiol* 273: C172-178, 1997. S3. Soderlund K, Hultman E. ATP and phosphocreatine changes in single human fibers after intense electrical stimulation. *Am J Physiol* 261: E737-741, 1991. S4. Boska M. ATP production rates as a function of force level in the human gastrocnemius/soleus using ³¹P MRS. *Magn Reson Med* 32: 1-10, 1994. S5. Bottinelli R, Reggiani C. Human skeletal muscle fibers: molecular and functional diversity. *Prog Biophys Mol Biol* 73: 195-262, 2000

Supplementary Table 2. Results of 3-day diary prior to second test. Mean is reported.

CPET test (2nd test)			
t=0	controls	patients	p-value
Energy intake (kcal)	2131	2320	0.55
Protein intake (gram/energy%)	88.6 (16.7)	79.2 (14.0)	0.31 (0.22)
Carbohydrate intake (gram/energy%)	237.0 (44.5)	294.9 (50.0)	0.55 (0.22)
Total fat intake (gram/energy%)	74.6 (32.0)	76.1 (35.2)	0.69 (0.42)
LCT intake (gram/% of total fat intake)	74.6 (100.0)	74.6 (85.2)	0.69 (0.31)
MCT intake (gram/% of total fat intake)	0.0 (0.0)	8.3 (14.8)	0.31 (0.31)

CHAPTER 8

Food withdrawal lowers energy expenditure and induces inactivity in long-chain fatty acid oxidation-deficient mouse models

Eugene F. Diekman^{1,2*}, Michel van Weeghel^{2*}, Ronald J.A. Wanders^{2,3},
Gepke Visser¹, Sander M. Houten^{2,3,4}

¹ Department of Metabolic Diseases, Wilhelmina Children's Hospital, UMC Utrecht, the Netherlands, Lundlaan 6, 3584 EA, Utrecht, The Netherlands

² Department of Clinical Chemistry, Laboratory Genetic Metabolic Diseases Academic Medical Center, University of Amsterdam, Meibergdreef 9, 1105 AZ Amsterdam, The Netherlands

³ Department of Pediatrics, Emma Children's Hospital, Academic Medical Center, University of Amsterdam, Meibergdreef 9, 1105 AZ Amsterdam, The Netherlands

⁴ Department of Genetics and Genomic Sciences, Icahn Institute for Genomics and Multiscale Biology, Icahn School of Medicine at Mount Sinai, 1425 Madison Avenue, Box 1498, New York

*both authors contributed equally

FASEB Journal, 2014, doi: 10.1096/fj.14-250241

ABSTRACT

Very long-chain acyl-CoA dehydrogenase deficiency (VLCAD) deficiency is an inherited disorder of mitochondrial long-chain fatty acid β -oxidation (FAO). Patients with VLCAD deficiency may present with hypoglycemia, hepatomegaly, cardiomyopathy and myopathy. Although several mouse models have been developed to aid the study of the pathogenesis of long-chain FAO defects, the muscular phenotype is however 'underexposed'. To address the muscular phenotype, we used a newly developed mouse model on a mixed genetic background with a more severe defect in FAO (LCAD^{-/-}; VLCAD^{+/-}) in addition to a validated mouse model (LCAD^{-/-}; VLCAD^{+/+}) and compared them with WT mice. We found that upon fasting, both mouse models show a 20% reduction in energy expenditure (EE) and a 3-fold decrease in locomotor activity. In addition we found a 1.7-degree drop in body temperature upon fasting in LCAD^{-/-}; VLCAD^{+/-} compared to WT. We conclude that fasting-induced inactivity, hypothermia and reduction in EE are novel phenotypes associated with FAO deficiency in mice. Unexpectedly, inactivity was not explained by rhabdomyolysis, but rather reflected the overall reduced capacity of these mice to generate heat. We suggest that mice are partly protected against the negative consequence of a FAO defect.

INTRODUCTION

Very long-chain acyl-CoA dehydrogenase (VLCAD) deficiency is a disorder of mitochondrial fatty acid β -oxidation (FAO) that compromises energy homeostasis and leads to the accumulation of long-chain fatty acid derivatives. Patients with VLCAD deficiency may develop hypoketotic hypoglycemia, hepatomegaly, cardiomyopathy and myopathy with rhabdomyolysis. These features can be induced by illness, fever, exercise, and fasting¹⁻⁴. The main reason for the inclusion of FAO defects in the expanded neonatal screening programs is that life-threatening symptoms such as hypoglycemia and cardiomyopathy can be prevented.

Multiple treatment options exist. Many patients are on dietary long-chain triglyceride (LCT) restriction and medium-chain triglyceride (MCT) supplementation. Patients also often receive carnitine supplementation. Interestingly, clinical improvement was observed in patients treated with anaplerotic odd-chain triglycerides⁵. In addition, bezafibrate has been shown to improve myopathy and rhabdomyolysis in patients with long-chain FAO disorders^{6,7}, although a recent randomized clinical trial suggests that bezafibrate is ineffective⁸. Thus, the effectiveness of all treatments needs to be confirmed in a larger cohort of patients preferably in a double blind study.

Several mouse models have been developed to aid the study of the pathogenesis of long-chain FAO defects. Mouse models are usually selected based on similarities in phenotype and genetic defect. For the first step of long-chain FAO, mice have two acyl-CoA dehydrogenase (ACAD) enzymes, very long-chain acyl-CoA dehydrogenase (VLCAD) and long-chain acyl-CoA dehydrogenase (LCAD)⁹. VLCAD KO (VLCAD^{-/-}) and LCAD KO (LCAD^{-/-}) mice have been generated and characterized¹⁰⁻¹³. Using these models, we and others have shown that LCAD and VLCAD have overlapping and distinct roles in FAO^{10,13,14}. Surprisingly, the absence of VLCAD in mice is apparently fully compensated, whereas LCAD deficiency is not. LCAD plays an essential role in the oxidation of unsaturated fatty acids such as oleic acid, but seems redundant in the oxidation of saturated fatty acids¹⁴. In agreement with this, the VLCAD^{-/-} mouse has a phenotype comprising mild hepatic steatosis, mild fatty changes and microvesicular lipid accumulation in the heart, facilitated induction of polymorphic ventricular tachycardia in response to fasting and cold challenge, and reduced exercise capacity^{10-12,15}. The LCAD^{-/-} mouse has a more severe phenotype, resembling human VLCAD deficiency better than the VLCAD^{-/-} mouse. Characteristics include fasting-induced hypoketotic hypoglycemia and marked fatty changes in liver and heart. LCAD^{-/-} hearts display triglyceride and ceramide accumulation, and develop fasting-induced cardiac dysfunction^{10,13,14,16-18}.

Although the LCAD^{-/-} mouse model is closely related to human VLCAD deficiency, the muscular phenotype is 'underexposed', which might be explained by functional redundancy between VLCAD and LCAD. To address the mechanisms underlying myopathy

with rhabdomyolysis during fasting and exercise, we studied the muscular phenotype in an established and in a newly developed more severe FAO-deficient mouse model. We hypothesized that in $LCAD^{-/-}$ mice, VLCAD is rate limiting in the FAO pathway, and reasoned that deletion of VLCAD in the $LCAD^{-/-}$ mouse would make a mouse model that better reflects human VLCAD deficiency. As $LCAD/VLCAD$ double KO mice are not viable¹⁰, we generated a mouse model in which one VLCAD allele was deleted in the $LCAD^{-/-}$ mice.

MATERIALS AND METHODS

Materials

Human serum albumin (HSA) and bicinchoninic acid (BCA) were obtained from Sigma-Aldrich. Complete mini protease inhibitor cocktail tablets were obtained from Roche. Cell culture medium DMEM, nutrient mixture (25 mM HEPES + L-glutamine) and the trypsin-EDTA solution were acquired from Gibco. 1-butanol, 1-propanol, and acetylchloride were obtained from Merck. Acetonitrile (ACN) gradient grade was obtained from Biosolve. The d3-C0, d3-C3, d3-C6, d3-C8, d3-C10 and d3-C16 acylcarnitine internal standards were obtained from Dr. H.J. ten Brink (Vrije University Medical Center, Amsterdam, The Netherlands). C16:0-CoA was purchased from Sigma. [9,10-³H(N)]-palmitic acid and [9,10-³H(N)]-oleic acid were purchased from PerkinElmer.

Animals

$Acadl^{+/-}$ mice (B6.129S6- $Acadl^{tm1Uab}/Mmmh$) on a pure C57BL/6N background and $Acadvl^{+/-}$ mice (B6;129S6- $Acadvl^{tm1Uab}/Mmmh$) on a mixed background (% C57BL/6N unknown) were obtained from Mutant Mouse Regional Resource Centers (<http://www.mmrrc.org/>). Colonies were maintained by crossing with C57BL/6N mice (Charles River Breeding Laboratories, Inc, Wilmington, MA, USA). The tested genotypes ($LCAD^{+/-}$; $VLCAD^{+/+}$, the $LCAD^{+/-}$; $VLCAD^{+/-}$, the $LCAD^{-/-}$; $VLCAD^{+/+}$, and the $LCAD^{-/-}$; $VLCAD^{+/-}$) were generated by crossbreeding after 2 or 3 generations of backcrossing with C57BL/6N. The wild-type (WT) mice were generated from the same cohort, but after 4 generations of backcrossing with C57BL/6N. The VLCAD allele was genotyped using PCR with the following primers; Fw1 (Exon 6) 5'-GTTTGGGCCTCTAATACCCAG-3', Rev1 (Neomycin) 5'-cttctctgctgtttacgta-3', and Rev2 (Exon 20) 5'-cacaatctctgccaagcgag-3'. The LCAD allele was genotyped using PCR¹³ in combination with acylcarnitine analysis on bloodspots with C14:1/C2 ratio being predictive for the LCAD KO genotype. Mice were housed at 21 ± 1 °C, 40-50% humidity, on a 12-h light-dark cycle, with ad libitum access to water and a standard rodent diet. At 9 to 10 weeks of age, mice were housed individually. Metabolic cage measurements (oxygen consumption, CO₂ production, food and water intake, and

locomotor activity) were obtained by a PhenoMaster system (TSE systems, Bad Homburg, Germany). Mice were allowed to adapt to their new environment and were then placed in metabolic cages for 2 days at room temperature (19–21°C). Data obtained during the second day were used for analysis. After 48h with ad libitum feeding, the mice were fasted overnight and refed for 4h the next morning. After refeeding, 50 µl of blood was collected from the vena saphena for the measurements of glucose, acylcarnitines, ketones, lactate and pyruvate. Metabolic measurements were done again in the metabolic cage during the night and refeeding cycle. After the metabolic cage, mice were housed again at their normal cages and blood was collected every two weeks. At 12 weeks of age, 50 µl of blood was collected from the vena saphena for the measurements of glucose, ketones, lactate and pyruvate. At 14 weeks of age, mice were fasted overnight and anesthetized with an ip injection of 100 mg/kg pentobarbital. Anesthetized mice were euthanized by exsanguination from the vena cava inferior. This blood was used for the measurements of CK, glucose, acylcarnitines, ketones, lactate and pyruvate. The heart, liver, and muscles were rapidly excised, weighed, and processed for biochemical and histological analysis.

Body temperature was measured using implantable electronic ID transponders (IPTT-300, PLEXX, Elst, The Netherlands) according to the instruction of the manufacturer. Transponders were read with a hand-held DAS 5002 scanner (PLEXX).

All experiments were approved by the institutional review board for animal experiments at the Academic Medical Center (Amsterdam, The Netherlands).

Acylcarnitine analysis

Plasma and blood acylcarnitines were measured as described previously¹⁹ using internal standards (25 µM d3-C0, 5 µM d3-C3, 2 µM d3-C6, 2 µM d3-C8, 2 µM d3-C10, and 2 µM d3-C16 acylcarnitine).

Clinical chemistry measurements

Blood for measurement of lactate, pyruvate and ketones was treated immediately after withdrawal with an equal volume of 1M perchloric acid and subsequently stored at -20°C. The remainder of the blood was used for plasma preparation. Plasma was stored at -20°C. Plasma glucose and CK were measured using standard enzymatic assays²⁰. Blood glucose was determined using a Contour glucometer (Bayer, Mijdrecht, The Netherlands). Blood lactate, pyruvate, β-hydroxybutyrate, acetoacetate and plasma amino acids were measured using tandem mass spectrometry²¹⁻²³. Glycerol (Instruchemie, 2319), free fatty acids (Wako, 434-91795) and triglycerides (Human Gesellschaft, 1072401D) were measured in plasma using standard enzymatic assays.

Quantitative real-time RT-PCR analysis

Total RNA was isolated from mouse tissue using Trizol (Invitrogen) extraction, after which cDNA was prepared using the Superscript II Reverse Transcriptase kit (Invitrogen). Quantitative real-time PCR analysis using the LC480 Sybr Green I Master mix (Roche) was performed to determine the expression of *Acadl*, *Acadvl*, *Acad9*, *Rplp0*, *Rn18s*, *Nppa*, *Nppb*, and *Myh7*. To confirm the amplification of a single product both melting curve analysis and sequence analysis were carried out. All samples were analyzed in duplicate. Data were analyzed using linear regression analysis²⁴. To compare the *Acadl*, *Acadvl* and *Acad9* expression in liver tissue between different samples, values were normalized against the values for the housekeeping gene *Rplp0*. To compare the *Nppa*, *Nppb* and *Myh7* expression in heart tissue between different samples, values were normalized against the values for the housekeeping gene *Rn18s*.

Acyl-CoA dehydrogenase enzyme measurements

Acyl-CoA dehydrogenase activity was determined in liver homogenates by using ferrocenium hexafluorophosphate as electron acceptor followed by UPLC to separate the different acyl-CoA species as described previously²⁵. C16:0-CoA was used as substrate.

Fatty acid oxidation rates

Palmitic and oleic acid oxidation was measured by quantifying the production of $^3\text{H}_2\text{O}$ from [9,10- ^3H (N)]-palmitic acid and [9,10- ^3H (N)] oleic acid as described previously²⁶. Oxidation rates were expressed as nmol of fatty acid oxidized per hour per milligram of cell protein (nmol/h mg).

Statistics

Statistical analysis was performed using Graphpad Prism 5. The C14:1/C2 and C12/C2 ratio were log₁₀ transformed to normalize the data distribution. Data are displayed as the mean \pm SEM. We used Rout test (Q=1.00%) to identify and remove outliers. Differences were evaluated using the One-way ANOVA multiple comparisons test. When significant, the post-hoc Bonferroni multiple comparison test was used to test differences between groups for significance. An unpaired t-test was used to test differences between the two fibroblast cell lines (figure 6). Statistical significance is indicated as detailed in the figure legends. The deviation of the distribution of the different genotypes from the Mendelian ratio was calculated using a χ^2 test with 1 degree of freedom.

RESULTS

Generation and biochemical characterization of LCAD^{-/-}; VLCAD^{+/-} mice

To generate LCAD^{-/-}; VLCAD^{+/-} mice, we crossed LCAD^{+/-}; VLCAD^{+/-} mice with LCAD^{-/-}; VLCAD^{+/+} mice. Pedigree analysis revealed the expected 4 different genotypes: LCAD^{+/-}; VLCAD^{+/+}, LCAD^{+/-}; VLCAD^{+/-}, LCAD^{-/-}; VLCAD^{+/+} and LCAD^{-/-}; VLCAD^{+/-} (data are summarized in Table 1). The observed number of animals with each of the genotypes was, however, not according to the expected Mendelian distribution ($X^2 = 9.29$, $p < 0.05$). The number of mice born with LCAD^{-/-}; VLCAD^{+/+} and LCAD^{-/-}; VLCAD^{+/-} genotypes was decreased with the LCAD^{-/-}; VLCAD^{+/-} genotype being most underrepresented. Breeding using double heterozygous mice confirmed the absence of double KO animals in the progeny, which is in line with previous findings¹⁰. Once born, LCAD^{-/-}; VLCAD^{+/-} mice appeared healthy and displayed normal weight gain.

Table 1. Genotype distribution of pedigree from LCAD^{+/-}; VLCAD^{+/-} and LCAD^{-/-}; VLCAD^{+/+} breeding pairs.

Genotype	Observed	Expected
LCAD ^{+/-} ; VLCAD ^{+/+}	32 (31%)	26 (25%)
LCAD ^{+/-} ; VLCAD ^{+/-}	33 (32%)	26 (25%)
LCAD ^{-/-} ; VLCAD ^{+/+}	23 (23%)	26 (25%)
LCAD ^{-/-} ; VLCAD ^{+/-}	14 (14%)	26 (25%)
	102	102 (100%)

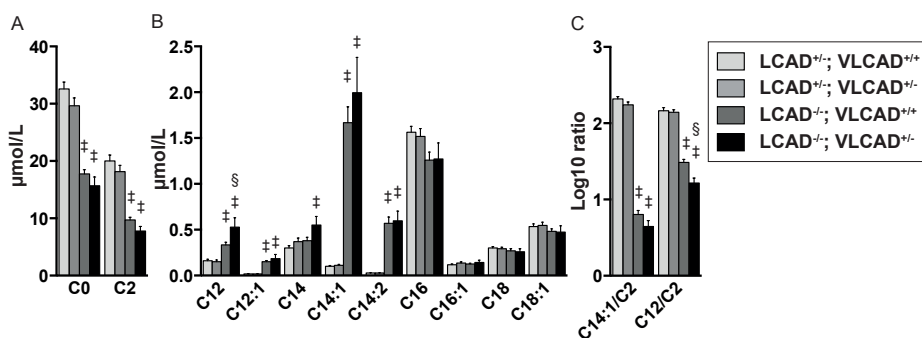


Figure 1. Acylcarnitine profiles in blood of mice with different LCAD and VLCAD genotypes. A-B. Levels of different acylcarnitines (in μM) measured in blood of the mice under fed conditions at the time of weaning. C. The Log10 ratio of the acylcarnitines C14:1 and C12 with acylcarnitine C2 are displayed. The different genotypes are indicated in the figure legend (LCAD^{+/-}; VLCAD^{+/+} (n=25), LCAD^{+/-}; VLCAD^{+/-} (n=26), LCAD^{-/-}; VLCAD^{+/+} (n=16), and LCAD^{-/-}; VLCAD^{+/-} (n=8)). Error bars indicate +SEM. #P<0.01 LCAD^{-/-}; VLCAD^{+/-} compared to LCAD^{+/-}; VLCAD^{+/+}. \$P<0.01 LCAD^{-/-}; VLCAD^{+/-} or LCAD^{-/-}; VLCAD^{+/+} compared to LCAD^{+/-}; VLCAD^{+/+}.

Whole blood acylcarnitines were measured at time of weaning in the above-described mice. No differences were observed when the acylcarnitine profile of $LCAD^{+/-}; VLCAD^{+/-}$ and $LCAD^{+/-}; VLCAD^{+/-}$ mice were compared (Figure 1). Previous studies already established that the acylcarnitine profile of WT mice does not differ from $LCAD^{+/-}$ mice. This suggests that the acylcarnitine profile of $LCAD^{+/-}; VLCAD^{+/-}$ mice is also indistinguishable from WT mice. $LCAD^{-/-}; VLCAD^{+/+}$ and $LCAD^{-/-}; VLCAD^{+/-}$ mice displayed a significant decrease in C0-, C2-, and an increase in C12-, C12:1-, C14:1-acylcarnitine (Figure 1a-b). The C14:1/C2 and C12/C2 ratios are particularly indicative of the $LCAD^{-/-}$ genotype. Although overall similar, all changes were slightly more pronounced in the $LCAD^{-/-}; VLCAD^{+/-}$ mice when compared with $LCAD^{-/-}; VLCAD^{+/+}$ mice. Notably, the C12/C2 ratio was significantly different between the two different genotypes (Figure 1c). Taken together, these results indicate that deletion of one VLCAD allele in the $LCAD^{-/-}$ background further aggravates the FAO defect.

Evidence for aggravated hepatic steatosis and cardiac hypertrophy in $LCAD^{-/-}; VLCAD^{+/-}$ mice

Cardiac hypertrophy and fasting-induced hepatic steatosis were observed in $LCAD^{-/-}$ mice^{10,13}. In accordance with these results, heart and liver weight were increased in $LCAD^{-/-}; VLCAD^{+/+}$ and $LCAD^{-/-}; VLCAD^{+/-}$ (Figure 2a-b). These increases were most pronounced and significant in the $LCAD^{-/-}; VLCAD^{+/-}$ mouse. One outlier with very high heart weight was observed among the $LCAD^{-/-}; VLCAD^{+/-}$ mice and was excluded from the statistical analysis (Supplemental figure 1a; weight/bodyweight ratio of >0.013). To test whether the increased heart weight was indicative of cardiomyopathy, we measured expression levels of beta myosin heavy chain (Myh7), atrial natriuretic peptide (Nppa) and basic na-

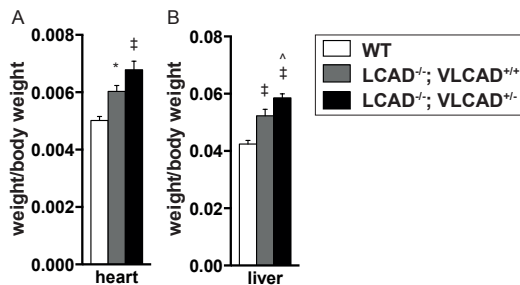


Figure 2. Organ weights. A. Heart weight of mice with different LCAD and VLCAD genotypes. Heart weight/bodyweight of fasted mice (WT (n=5), $LCAD^{-/-}; VLCAD^{+/+}$ (n=7), and $LCAD^{-/-}; VLCAD^{+/-}$ (n=8)). B. Liver weight of mice with different LCAD and VLCAD genotypes. Liver weight/body weight of fasted mice. The different genotypes are indicated in the figure legend (WT (n=5), $LCAD^{-/-}; VLCAD^{+/+}$ (n=7), and $LCAD^{-/-}; VLCAD^{+/-}$ (n=9)). Error bars indicate +SEM. *P=0.05 $LCAD^{-/-}; VLCAD^{+/+}$ compared to WT. ^P<0.05 $LCAD^{-/-}; VLCAD^{+/-}$ compared to $LCAD^{-/-}; VLCAD^{+/+}$. ‡ P<0.01 $LCAD^{-/-}; VLCAD^{+/-}$ or $LCAD^{-/-}; VLCAD^{+/+}$ compared to WT.

triuretic peptide (Nppb). Nppa, Nppb and Myh7 expression levels were not increased in $LCAD^{-/-}; VLCAD^{+/-}$ mice with the exception of the one mouse with a massive hypertrophic heart (Supplemental figure 1b). This indicates that although the hypertrophy is most pronounced in $LCAD^{-/-}; VLCAD^{+/-}$ mice, it has generally not progressed to cardiomyopathy at 14 weeks of age.

The response of plasma metabolites to fasting in $LCAD^{-/-}; VLCAD^{+/-}$ mice

$LCAD^{-/-}$ mice as well as humans with a FAO defect develop hypoketotic hypoglycemia upon fasting. We measured plasma metabolites in WT, $LCAD^{-/-}; VLCAD^{+/+}$ and $LCAD^{-/-}; VLCAD^{+/-}$ mice in the fed state, after fasting and upon refeeding. After an overnight fast, blood glucose levels in $LCAD^{-/-}; VLCAD^{+/-}$ as well as $LCAD^{-/-}; VLCAD^{+/+}$ mice were lower compared to WT mice (Figure 3a). No differences in glucose levels were observed between the different mice in the fed state and after refeeding (Supplemental figure

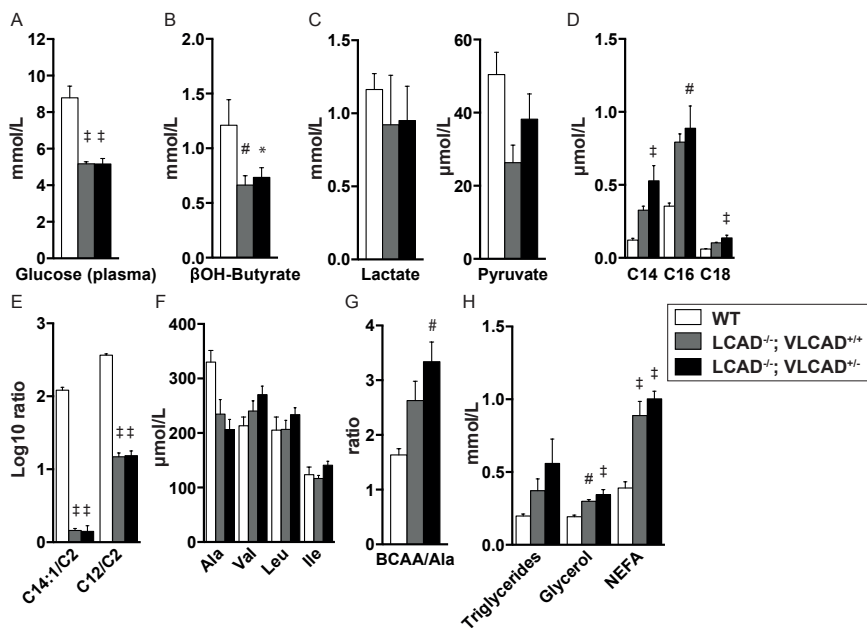


Figure 3. Metabolite levels in blood and plasma of overnight fasted mice with different LCAD and VLCAD genotypes. A. Plasma glucose levels. B. β OH-butyrate. C. Lactate and pyruvate levels (one outlier $LCAD^{-/-}; VLCAD^{+/+}$ excluded). D. C14, C16, C18 levels. E. The log10 ratio of C14:1/C2 and C12/C2 acylcarnitine in plasma. F. Levels of alanine and the BCAAs. G. The ratio of BCAAs with alanine in plasma. H. Plasma triglyceride, glycerol and non-esterified fatty acids (NEFA) levels. The different genotypes are indicated in the figure legend (WT (n=5), $LCAD^{-/-}; VLCAD^{+/+}$ (n=7), and $LCAD^{-/-}; VLCAD^{+/-}$ (n=9)). Error bars indicate +SEM. * $P=0.056$ $LCAD^{-/-}; VLCAD^{+/+}$ compared to WT. # $P<0.05$ $LCAD^{-/-}; VLCAD^{+/-}$ or $LCAD^{-/-}; VLCAD^{+/+}$ compared to WT. † $P<0.01$ $LCAD^{-/-}; VLCAD^{+/-}$ or $LCAD^{-/-}; VLCAD^{+/+}$ compared to WT.

2). Thus, fasting-induced hypoglycemia is apparent in $LCAD^{-/-}$ mice, but does not appear to be aggravated upon deletion of one VLCAD allele. Similarly, β -hydroxybutyrate increased in all groups upon fasting, but $LCAD^{-/-}; VLCAD^{+/+}$ and $LCAD^{-/-}; VLCAD^{+/-}$ mice were both equally hypoketotic (Figure 3b).

Blood lactate and pyruvate levels decrease upon fasting due to a shift towards FAO at the expense of glycolysis. Fasting lactate and pyruvate levels were indeed lower compared to the fed and refeeding state (Figure 3c and supplemental figure 2), but no significant difference was observed when comparing the different mice. Next we determined the fasting plasma acylcarnitine profile. The long-chain acylcarnitines (C14, C16, C18) were increased in $LCAD^{-/-}; VLCAD^{+/-}$ when compared to WT mice, but did not differ significantly from $LCAD^{-/-}; VLCAD^{+/+}$ mice. The C14:1/C2 and C12/C2 acylcarnitine ratios were increased in $LCAD^{-/-}; VLCAD^{+/-}$ and $LCAD^{-/-}; VLCAD^{+/+}$, but unexpectedly did not differ significantly between these genotypes (Figure 3d,e).

We also analyzed plasma amino acids levels, which play an important role during fasting as they represent the major source of gluconeogenic precursors. It has recently been reported that impaired amino acid metabolism contributes to the development of hypoglycemia in the $LCAD^{-/-}$ mouse¹⁶. Although none of the amino acids were significantly altered, there was a tendency towards increased levels of branched-chain amino acids (BCAA) and decreased levels of alanine in $LCAD^{-/-}; VLCAD^{+/-}$ mice (Figure 3f). These changes are significant when the BCAA level is expressed as a ratio to the alanine level (BCAA/Ala) (Figure 3g).

Glycerol, another gluconeogenic precursor, and NEFA levels were significantly higher in $LCAD^{-/-}; VLCAD^{+/-}$ and $LCAD^{-/-}; VLCAD^{+/+}$ mice when compared to WT (Figure 3h). Although triglyceride levels appeared elevated in $LCAD^{-/-}; VLCAD^{+/-}$ and $LCAD^{-/-}; VLCAD^{+/+}$ mice, these differences were not statistically significant (Figure 3h). Taken together, deletion of one VLCAD allele on the $LCAD^{-/-}$ background only slightly aggravates the biochemical signs of a FAO defect during fasting.

Fasting-induced decrease in energy expenditure in FAO deficient mouse models

To explore energy homeostasis in our FAO-deficient mouse models, we performed indirect calorimetry. During an overnight fast, O_2 consumption, CO_2 production and heat generation were significantly lower in mice with the $LCAD^{-/-}$ genotype, but no significant difference was observed between $LCAD^{-/-}; VLCAD^{+/+}$ and $LCAD^{-/-}; VLCAD^{+/-}$ mice (Figure 4a-f). Surprisingly, the respiratory exchange ratio (RER) was not different between WT and $LCAD^{-/-}; VLCAD^{+/+}$ and $LCAD^{-/-}; VLCAD^{+/-}$ mice (Figure 4g). Locomotor activity in all axes was significantly reduced in parallel with heat generation. Overall, we observed a significantly decreased locomotor activity in $LCAD^{-/-}; VLCAD^{+/+}$ and $LCAD^{-/-}; VLCAD^{+/-}$ compared to WT mice. This effect was most pronounced in $LCAD^{-/-}; VLCAD^{+/-}$ mice (Figure 4h-i).

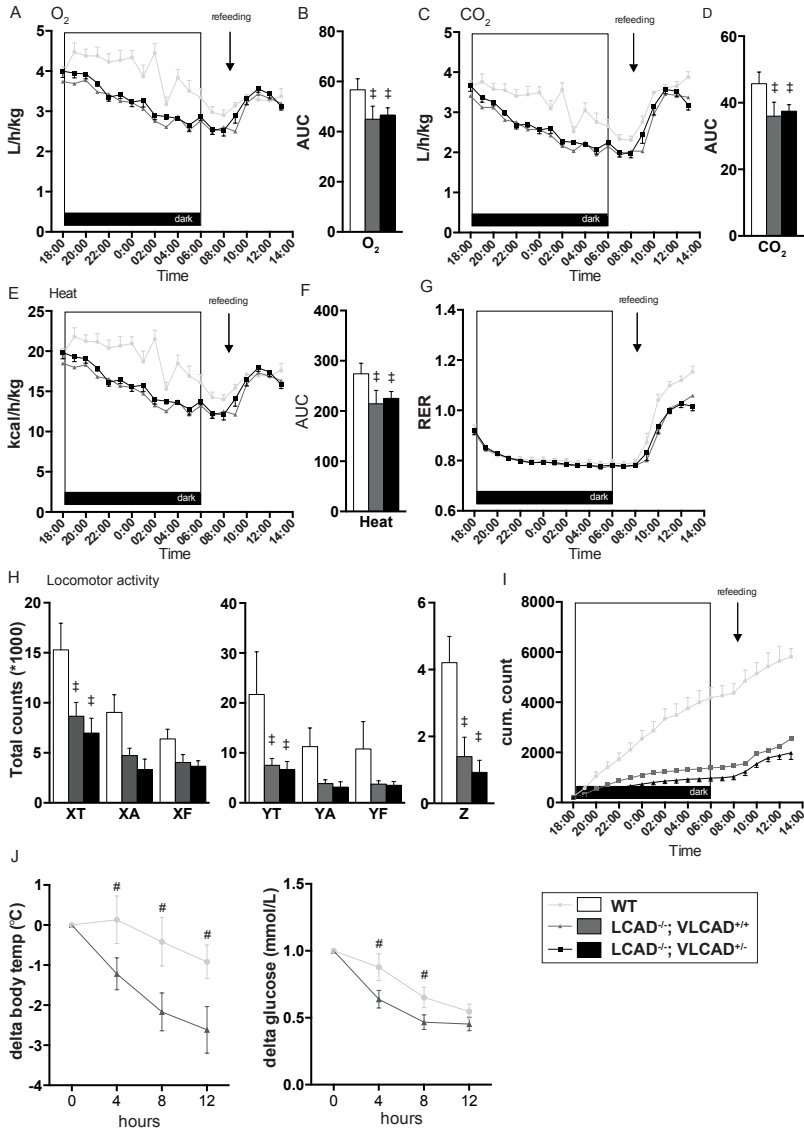


Figure 4. Indirect calorimetry in mice with different LCAD and VLCAD genotypes. A-G. O₂ and CO₂ consumption (in L/kg/h), heat production (in kcal/h/kg) and RER in dark and light phase in fasted and refed mice of all genotypes. H-I. 'Locomotor activity' Locomotor activity in fasted mice of all genotypes tested (XT and YT= total movement horizontal, XA and YA = ambulatory movement, XF and YF = fine movements and Z = rearings) (in total counts). The different genotypes are indicated in the figure legend (WT (n=5), LCAD^{-/-}; VLCAD^{+/-} (n=7), and LCAD^{-/-}; VLCAD^{+/-} (n=9)). J. Body temperature and blood glucose during an overnight fast (LCAD^{-/-}; VLCAD^{+/-} (n=6), and LCAD^{-/-}; VLCAD^{+/-} (n=6)). WT and LCAD^{-/-}; VLCAD^{+/-} mice were fasted overnight (start at 4 p.m.). Blood glucose and body temperature were measured every 4h. Blood glucose at start of fasting was set to one and body temperature was set at zero. Error bars indicate +SEM. #P<0.05 LCAD^{-/-}; VLCAD^{+/-} compared to WT. †P<0.01 LCAD^{-/-}; VLCAD^{+/-} or LCAD^{-/-}; VLCAD^{+/-} compared to WT.

To evaluate whether the fasting-induced decrease in energy expenditure in FAO-deficient mice impacts on the ability to maintain body temperature, we measured body temperature and blood glucose every 4 hours during an overnight fast (Figure 4j). $LCAD^{-/-}; VLCAD^{+/+}$ mice displayed a pronounced drop in body temperature of up to 2.6 degrees Celsius after 12 hours of fasting, with one mouse losing up to 4.6 degrees reaching a temperature of 32.4 degrees Celsius. Over the same period, WT mice dropped only 0.9 degrees. Diurnal temperature variation was not different between WT and $LCAD^{-/-}; VLCAD^{+/+}$ animals (Supplementary Figure 3), again illustrating that fasting specifically decreased energy expenditure in this FAO deficient mouse model.

Absence of fasting-induced rhabdomyolysis in $LCAD^{-/-}; VLCAD^{+/+}$ mice

Patients with VLCAD deficiency suffer from myopathy and episodes of rhabdomyolysis, which can be triggered by fasting or exercise. To assess whether $LCAD^{-/-}; VLCAD^{+/+}$ mice have rhabdomyolysis, we measured plasma CK levels after fasting. CK levels were within the normal range of 0-100 U/L in all $LCAD/VLCAD$ genotypes (Supplemental figure 4a). We therefore conclude that these mice do not develop muscle damage upon fasting. In addition, we did not observe differences in gastrocnemius, soleus and quadriceps muscle weight between the various genotypes (Supplemental figure 4b).

No enzymatic compensation of deficient acyl-CoA dehydrogenase activity in $LCAD^{-/-}; VLCAD^{+/+}$ mice

Since the impact of the deletion of one VLCAD allele on the $LCAD^{-/-}$ phenotype seems rather subtle, we explored potential compensatory changes and analyzed mRNA and protein expression of the different ACADs in liver. Liver VLCAD mRNA expression in $LCAD^{-/-}; VLCAD^{+/+}$ mice was roughly half of that in $LCAD^{-/-}; VLCAD^{+/+}$ mice, consistent with the deletion of one VLCAD allele (Figure 5a). Thus, expression of VLCAD was not induced via the non-mutated allele. This was further confirmed by western blot analysis of liver homogenates revealing decreased VLCAD protein expression in $LCAD^{-/-}; VLCAD^{+/+}$ liver homogenates (Figure 5c). Expression levels of ACAD9, which may partly compensate for deficient (V)LCAD activity²⁷, were not significantly changed (Figure 5a). The palmitoyl-CoA dehydrogenase activity was lowest in $LCAD^{-/-}; VLCAD^{+/+}$ mice compared to $LCAD^{-/-}; VLCAD^{+/+}$ and WT mice (Figure 5b). In quadriceps muscle, palmitoyl-CoA dehydrogenase activity was lowest in $LCAD^{-/-}; VLCAD^{+/+}$ mice, similar to the results obtained in liver (Supplemental figure 4c). Thus there is no enzymatic compensation of the deficient acyl-CoA dehydrogenase activity in $LCAD^{-/-}; VLCAD^{+/+}$ mice.

Minimal decrease in FAO capacity in $LCAD^{-/-}; VLCAD^{+/+}$ mouse fibroblasts

We established fibroblast cell lines of mice with the $LCAD^{-/-}; VLCAD^{+/+}$ and $LCAD^{-/-}; VLCAD^{+/+}$ genotype in order to assess the FAO capacity. First, we measured palmitic and

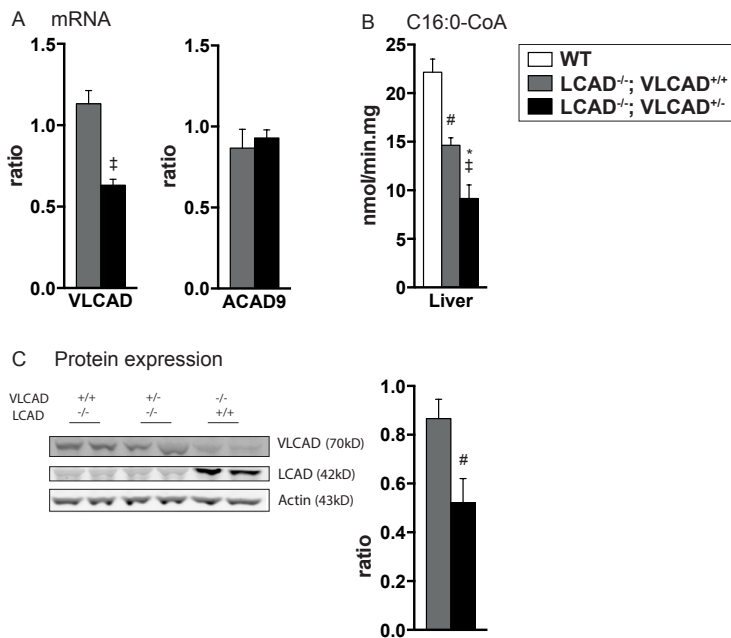


Figure 5. Hepatic mRNA and protein expression levels in overnight fasted mice of all genotypes. A. mRNA relative expression levels of *Acadvl*, *Acadl*, and *Acad9* in mouse liver. Expression is corrected for *Rplp0*. B. C16-CoA dehydrogenase activity measurements in mouse liver. C. Immunoblot analysis of LCAD and VLCAD protein expression in mouse liver. Quantification of VLCAD protein expression in mouse liver. (A: (LCAD^{-/-}; VLCAD^{+/+}) (n=4), and LCAD^{-/-}; VLCAD^{+/-} (n=4)). B and C: WT (n=4), LCAD^{-/-}; VLCAD^{+/+} (n=3), and LCAD^{-/-}; VLCAD^{+/-} (n=5)). Error bars indicate +SEM. *P=0.07 LCAD^{-/-}; VLCAD^{+/-} compared to LCAD^{-/-}; VLCAD^{+/+}. #P<0.05 LCAD^{-/-}; VLCAD^{+/+} or LCAD^{-/-}; VLCAD^{+/-} compared to WT or LCAD^{-/-}; VLCAD^{+/+}. †P<0.01 LCAD^{-/-}; VLCAD^{+/-} compared to LCAD^{-/-}; VLCAD^{+/+} or WT.

oleic acid oxidation rates. It has been established that LCAD^{-/-} mouse fibroblasts have deficient oleic acid oxidation, while retaining normal palmitic acid oxidation¹⁴ (Figure 6a and 6d). Unexpectedly, oleic acid oxidation rate did not decrease further upon deletion of one VLCAD allele. Palmitic acid oxidation was slightly, but significantly decreased in the LCAD^{-/-}; VLCAD^{+/-} fibroblasts (Figure 6a). Taken together, fibroblasts with the LCAD^{-/-}; VLCAD^{+/-} genotype displayed only a minimal decrease in the FAO capacity when compared to LCAD^{-/-}; VLCAD^{+/+} mouse fibroblasts.

DISCUSSION

Mouse models are vital to study the pathogenesis of human inherited metabolic disorders. We aimed to elucidate the muscular phenotype of an established and a newly

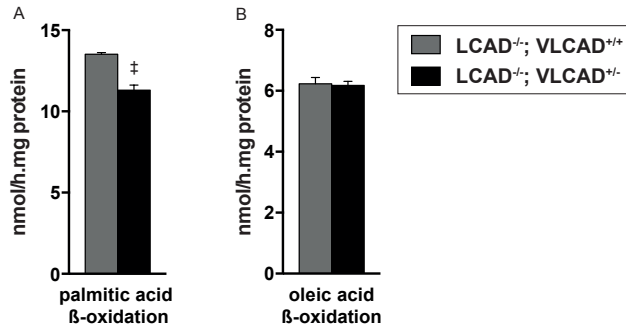


Figure 6. Biochemical studies in fibroblasts of mice (LCAD^{-/-}; VLCAD^{+/+} (n=4), and LCAD^{-/-}; VLCAD^{+/-} (n=4)). A. and B. Palmitic and oleic acid oxidation in fibroblasts. Error bars indicate +SEM ‡ P<0.01 LCAD^{-/-}; VLCAD^{+/-} compared to LCAD^{-/-}; VLCAD^{+/+}.

developed more severe mouse model. Gestational loss of LCAD^{-/-}; VLCAD^{+/+} mice was previously reported^{10,13}. We found that the number of progeny with the LCAD^{-/-}; VLCAD^{+/-} genotype was even more decreased. This is not unexpected since FAO plays an important role in the development of the fetus^{13,28}. There are other data suggesting that FAO capacity is slightly more decreased in the LCAD^{-/-}; VLCAD^{+/-} mice when compared to LCAD^{-/-}; VLCAD^{+/+} mice. In the fed state, long-chain acylcarnitine levels in the LCAD^{-/-}; VLCAD^{+/-} mice were consistently increased compared to LCAD^{-/-}; VLCAD^{+/+} mice, which is especially evident from the C14:1/C2 and C12/C2 acylcarnitine ratios.

Prominent features in the LCAD^{-/-}; VLCAD^{+/+} mice are fasting-induced hepatic steatosis and cardiac hypertrophy^{13,17,29}. We now report increased liver and heart weight in LCAD^{-/-}; VLCAD^{+/-} mice when compared to WT and LCAD^{-/-}; VLCAD^{+/+} mice. One LCAD^{-/-}; VLCAD^{+/-} mouse with a severely enlarged heart showed very high Myh7, Nppa and Nppb expression levels. Increased expression of these genes has consistently been associated with hypertrophic cardiomyopathy. This suggests that LCAD^{-/-}; VLCAD^{+/-} mice are more prone to develop hypertrophic cardiomyopathy. Cardiac hypertrophy in these mice might be explained by lipotoxicity, deficient anaplerosis, decreased energy status and/or increased protein synthesis^{13,16-18}. Age could play an important role in the development of cardiomyopathy as was previously reported for related FAO-deficient models^{30,31}.

Another prominent feature in the LCAD^{-/-}; VLCAD^{+/+} mice is hypoglycemia^{13,16}. Unexpectedly, hypoglycemia was not aggravated in LCAD^{-/-}; VLCAD^{+/-} mice. Similar observations were made for other plasma metabolites. Glycerol and NEFA levels were elevated in LCAD^{-/-}; VLCAD^{+/+} and LCAD^{-/-}; VLCAD^{+/-} mice, and did not significantly differ between these genotypes. The parallel increase in glycerol and NEFA may be explained by increased lipolytic activity due to a lower insulin/glucagon ratio. In addition, cellular NEFA uptake could be reduced due to the FAO defect. Interestingly, the BCAA/Ala ratio

was significantly increased in the *LCAD^{-/-}; VLCAD^{+/-}* mice compared to wildtype mice. This observation confirms that changes in amino acid metabolism are an important consequence of the FAO defect and contribute to pathophysiologic processes such as fasting-induced hypoglycemia^{16,18}.

Indirect calorimetry revealed no clear increase in RER in *LCAD^{-/-}; VLCAD^{+/+}* and *LCAD^{-/-}; VLCAD^{+/-}* mice compared to WT. This is unexpected since FAO flux was predicted to be decreased in these mice. A possible explanation for this observation might be the decreased heat production in *LCAD^{-/-}; VLCAD^{+/+}* and *LCAD^{-/-}; VLCAD^{+/-}* mice. The decreased heat production in combination with a similar RER, suggests that glucose oxidation is decreased alongside with FAO (Figure 7). This general decrease in energy expenditure coincides with decreased locomotor activity in the *LCAD^{-/-}; VLCAD^{+/+}* and *LCAD^{-/-}; VLCAD^{+/-}* mice. Movements in all axes including rearings were decreased. A decrease in activity, however, can not account for the decrease in energy expenditure in mice housed at 21 degrees Celsius, which is well below thermoneutrality³². Indeed, we also observed fasting-induced hypothermia in *LCAD^{-/-}; VLCAD^{+/+}*, which most likely is the major contributor to the decreased energy expenditure (Figure 7). Whether the fasting-induced hypothermia is an active process (torpor state) or driven by substrate shortage in BAT is currently unknown.

Mice might move less due to substrate shortage or a decreased core body temperature, but an alternative hypothesis could be because of muscle pain, induced by muscle damage due to rhabdomyolysis after prolonged fasting (as observed in humans). Plasma CK levels, however, were not different between tested genotypes arguing against rhabdomyolysis as an explanation for inactivity. Taken together, our data suggest that adaptive thermogenesis in mice can vary to a much greater extent than in humans. We show that mice with a FAO defect can reduce energy expenditure, which may protect them from developing severe symptoms associated with a FAO defect.

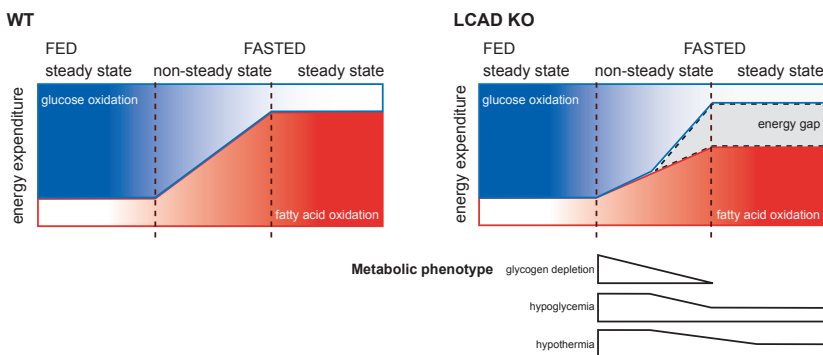


Figure 7. Schematic representation of the metabolic phenotype of fasted *LCAD^{-/-}; VLCAD^{+/-}* mice.

We hypothesized that in $LCAD^{-/-}$ mice, VLCAD would be rate limiting in the FAO pathway, and reasoned that deletion of one VLCAD allele in the $LCAD^{-/-}$ mouse would make a mouse model that better reflects human VLCAD deficiency. This hypothesis was based on the fact that oleic acid oxidation is deficient in $LCAD^{-/-}$ fibroblasts¹⁴, which strongly suggests that VLCAD is rate limiting for the rate of oleic acid oxidation. This implies that deletion of one VLCAD allele should decrease oleic acid oxidation by up to 50%. Remarkably, we did not find a decrease in oleic acid oxidation, which suggests that VLCAD and LCAD work in a virtually independent manner and are in fact not compensating for each other's function (Figure 6). This may be explained by the localization of the ACAD proteins, as VLCAD is localized on the inner side of the mitochondrial inner membrane and LCAD is expressed in the matrix of the mitochondria. We speculate that this issue can be addressed using a mathematical model as was recently published³³.

In summary, our study demonstrates that deletion of one VLCAD allele in $LCAD^{-/-}$ mice has a small impact on FAO flux and clinical phenotype when compared to the $LCAD^{-/-}$; $VLCAD^{+/+}$ mice. More importantly, we found that fasting-induced inactivity, hypothermia and reduction in energy expenditure are novel phenotypes associated with FAO deficiency in mice. Unexpectedly, inactivity was not explained by myopathy and rhabdomyolysis, but rather reflects the overall reduced capacity of these mice to generate heat. We suggest that mice are partly protected against the negative consequence of a FAO defect, since they can decrease energy expenditure. This is a potential confounding factor when using mice as a model for these diseases.

ACKNOWLEDGEMENTS

The authors thank Maxim Boek, Heleen te Brinke, Simone Denis and the employees of the Animal Research Institute Amsterdam for technical assistance.

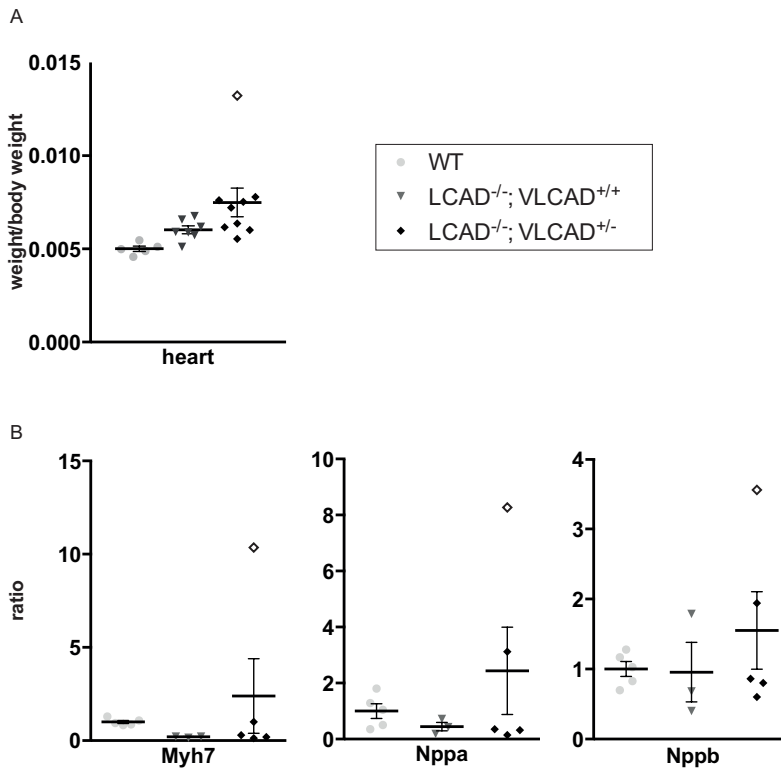
This work was supported by the Netherlands Organization for Scientific Research [VIDI-grant No. 016.086.336 to SMH], ZonMW [No. 200320006] and Metakids.

REFERENCES

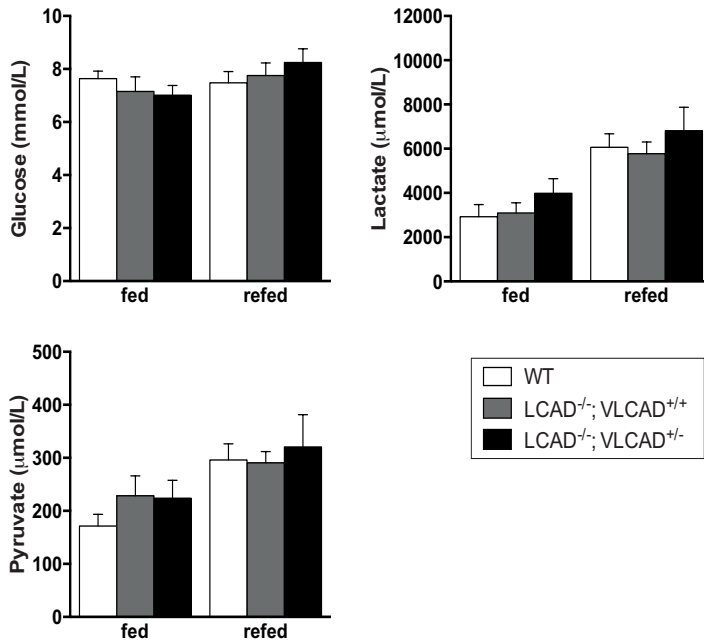
1. Bonnet D, Martin D, Pascale de Lonlay, et al. Arrhythmias and conduction defects as presenting symptoms of fatty acid oxidation disorders in children. *Circulation*. 1999;100(22):2248–2253. doi:10.1161/01.CIR.100.22.2248.
2. Rinaldo P, Matern D, Bennett MJ. Fatty acid oxidation disorders. *Annu Rev Physiol*. 2002;64:477–502. doi:10.1146/annurev.physiol.64.082201.154705.
3. Spiekerkoetter U, Bennett MJ, Ben-Zeev B, Strauss AW, Tein I. Peripheral neuropathy, episodic myoglobinuria, and respiratory failure in deficiency of the mitochondrial trifunctional protein. *Muscle Nerve*. 2004;29(1):66–72. doi:10.1002/mus.10500.
4. Wanders RJ, Vreken P, Boer den ME, Wijburg FA, van Gennip AH, Ijlst L. Disorders of mitochondrial fatty acyl-CoA beta-oxidation. *J Inherit Metab Dis*. 1999;22(4):442–487.
5. Roe CR, Sweetman L, Roe DS, David F, Brunengraber H. Treatment of cardiomyopathy and rhabdomyolysis in long-chain fat oxidation disorders using an anaplerotic odd-chain triglyceride. *J Clin Invest*. 2002;110(2):259–269. doi:10.1172/JCI15311.
6. Bonnefont JP, Bastin J, Laforêt P, et al. Long-term follow-up of bezafibrate treatment in patients with the myopathic form of carnitine palmitoyltransferase 2 deficiency. *Clin Pharmacol Ther*. 2010;88(1):101–108. doi:10.1038/clpt.2010.55.
7. Bonnefont J-P, Bastin J, Behin A, Djouadi F. Bezafibrate for an inborn mitochondrial beta-oxidation defect. *N Engl J Med*. 2009;360(8):838–840. doi:10.1056/NEJMc0806334.
8. Orngreen MC, Madsen KL, Preisler N, Andersen G, Vissing J, Laforêt P. Bezafibrate in skeletal muscle fatty acid oxidation disorders: A randomized clinical trial. *Neurology*. 2014. doi:10.1212/WNL.000000000000118.
9. Houten SM, Wanders RJA. A general introduction to the biochemistry of mitochondrial fatty acid β -oxidation. *J Inherit Metab Dis*. 2010;33(5):469–477. doi:10.1007/s10545-010-9061-2.
10. Cox KB, Hamm DA, Millington DS, et al. Gestational, pathologic and biochemical differences between very long-chain acyl-CoA dehydrogenase deficiency and long-chain acyl-CoA dehydrogenase deficiency in the mouse. *Hum Mol Genet*. 2001;10(19):2069–2077.
11. Exil VJ, Roberts RL, Sims H, et al. Very-long-chain acyl-coenzyme a dehydrogenase deficiency in mice. *Circ Res*. 2003;93(5):448–455. doi:10.1161/01.RES.0000088786.19197.E4.
12. Exil VJ, Gardner CD, Rottman JN, et al. Abnormal mitochondrial bioenergetics and heart rate dysfunction in mice lacking very-long-chain acyl-CoA dehydrogenase. *Am J Physiol Heart Circ Physiol*. 2006;290(3):H1289–97. doi:10.1152/ajpheart.00811.2005.
13. Kurtz DM, Rinaldo P, Rhead WJ, et al. Targeted disruption of mouse long-chain acyl-CoA dehydrogenase gene reveals crucial roles for fatty acid oxidation. *Proc Natl Acad Sci USA*. 1998;95(26):15592–15597.
14. Chegary M, Brinke HT, Ruitter JPN, et al. Mitochondrial long chain fatty acid beta-oxidation in man and mouse. *Biochim Biophys Acta*. 2009;1791(8):806–815. doi:10.1016/j.bbali.2009.05.006.
15. Veld ter F, Primassin S, Hoffmann L, MAYATEPEK E, Spiekerkoetter U. Corresponding increase in long-chain acyl-CoA and acylcarnitine after exercise in muscle from VLCAD mice. *The Journal of Lipid Research*. 2009;50(8):1556–1562. doi:10.1194/jlr.M800221-JLR200.
16. Houten SM, Herrema H, Brinke te H, et al. Impaired amino acid metabolism contributes to fasting-induced hypoglycemia in fatty acid oxidation defects. *Hum Mol Genet*. 2013;22(25):5249–5261. doi:10.1093/hmg/ddt382.
17. Bakermans AJ, Geraedts TR, van Weeghel M, et al. Fasting-Induced Myocardial Lipid Accumulation in Long-Chain Acyl-CoA Dehydrogenase Knockout Mice Is Accompanied by Impaired Left

- Ventricular Function. *Circulation: Cardiovascular Imaging*. 2011;4(5):558–565. doi:10.1161/CIRCIMAGING.111.963751.
18. Bakermans AJ, Dodd MS, Nicolay K, Prompers JJ, Tyler DJ, Houten SM. Myocardial energy shortage and unmet anaplerotic needs in the fasted long-chain acyl-CoA dehydrogenase knockout mouse. *Cardiovasc Res*. 2013. doi:10.1093/cvr/cvt212.
 19. Vreken P, van Lint AE, Bootsma AH, Overmars H, Wanders RJ, van Gennip AH. Quantitative plasma acylcarnitine analysis using electrospray tandem mass spectrometry for the diagnosis of organic acidaemias and fatty acid oxidation defects. *J Inherit Metab Dis*. 1999;22(3):302–306.
 20. Bergmeyer HU. *Methods of Enzymatic Analysis*. Wiley-VCH; 1986.
 21. Casetta B, Tagliacozzi D, Shushan B, Federici G. Development of a method for rapid quantitation of amino acids by liquid chromatography-tandem mass spectrometry (LC-MS/MS) in plasma. *Clin Chem Lab Med*. 2000;38(5):391–401. doi:10.1515/CCLM.2000.057.
 22. Chuang C-K, Wang T-J, Yeung C-Y, et al. A method for lactate and pyruvate determination in filter-paper dried blood spots. *J Chromatogr A*. 2009;1216(51):8947–8952. doi:10.1016/j.chroma.2009.10.074.
 23. Piraud M, Vianey-Saban C, Petritis K, et al. ESI-MS/MS analysis of underivatized amino acids: a new tool for the diagnosis of inherited disorders of amino acid metabolism. Fragmentation study of 79 molecules of biological interest in positive and negative ionisation mode. *Rapid Commun Mass Spectrom*. 2003;17(12):1297–1311. doi:10.1002/rcm.1054.
 24. Ramakers C, Ruijter JM, Deprez RHL, Moorman AFM. Assumption-free analysis of quantitative real-time polymerase chain reaction (PCR) data. *Neurosci Lett*. 2003;339(1):62–66. doi:10.1016/S0304-3940(02)01423-4.
 25. Wanders RJA, Ruiter JPN, IJLst L, Waterham HR, Houten SM. The enzymology of mitochondrial fatty acid beta-oxidation and its application to follow-up analysis of positive neonatal screening results. *J Inherit Metab Dis*. 2010;33(5):479–494. doi:10.1007/s10545-010-9104-8.
 26. Manning NJ, Olpin SE, Pollitt RJ, Webley J. A comparison of [9,10-3H]palmitic and [9,10-3H]myristic acids for the detection of defects of fatty acid oxidation in intact cultured fibroblasts. *J Inherit Metab Dis*. 1990;13(1):58–68.
 27. Nouws J, Brinke te H, Nijtmans LG, Houten SM. ACAD9, a complex I assembly factor with a moonlighting function in fatty acid oxidation deficiencies. *Hum Mol Genet*. 2013. doi:10.1093/hmg/ddt521.
 28. Oey NA, Ruiter JPN, Attié-Bitach T, IJLst L, Wanders RJA, Wijburg FA. Fatty acid oxidation in the human fetus: implications for fetal and adult disease. *J Inherit Metab Dis*. 2006;29(1):71–75. doi:10.1007/s10545-006-0199-x.
 29. Cox KB, Liu J, Tian L, Barnes S, Yang Q, Wood PA. Cardiac hypertrophy in mice with long-chain acyl-CoA dehydrogenase or very long-chain acyl-CoA dehydrogenase deficiency. *Lab Invest*. 2009;89(12):1348–1354. doi:10.1038/labinvest.2009.86.
 30. Liu J, Wang P, He L, et al. Cardiomyocyte-Restricted Deletion of PPAR β / δ in PPAR α -Null Mice Causes Impaired Mitochondrial Biogenesis and Defense, but No Further Depression of Myocardial Fatty Acid Oxidation. *PPAR Res*. 2011;2011:372854. doi:10.1155/2011/372854.
 31. Cheng L, Ding G, Qin Q, et al. Cardiomyocyte-restricted peroxisome proliferator-activated receptor-delta deletion perturbs myocardial fatty acid oxidation and leads to cardiomyopathy. *Nat Med*. 2004;10(11):1245–1250. doi:10.1038/nm1116.
 32. Virtue S, Even P, Vidal-Puig A. Below thermoneutrality, changes in activity do not drive changes in total daily energy expenditure between groups of mice. *Cell Metabolism*. 2012;16(5):665–671. doi:10.1016/j.cmet.2012.10.008.

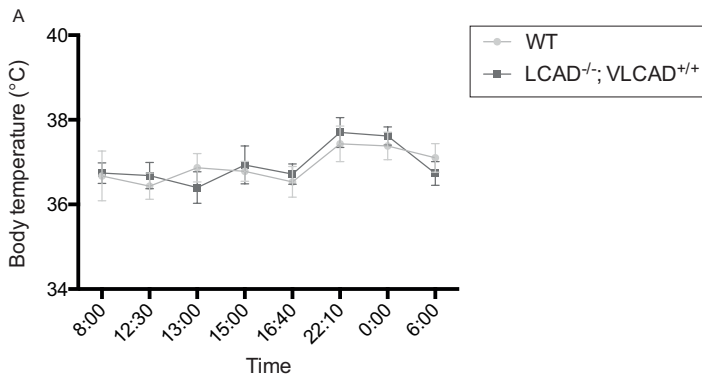
33. van Eunen K, Simons SMJ, Gerding A, et al. Biochemical Competition Makes Fatty-Acid β -Oxidation Vulnerable to Substrate Overload. *PLoS Comput Biol*. 2013;9(8):e1003186. doi:10.1371/journal.pcbi.1003186.



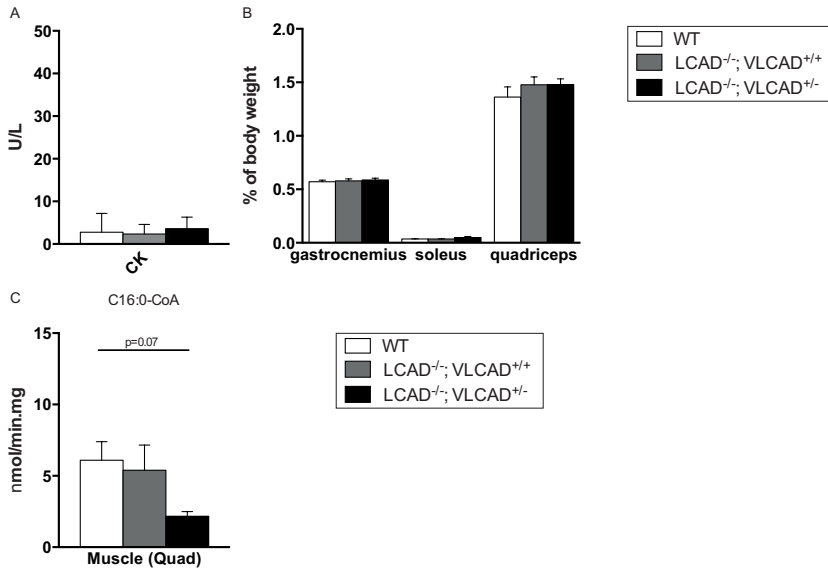
Supplemental Figure 1. Cardiac hypertrophy. A. Heart weight/body weight of mice with different LCAD and VLCAD genotypes including that of one mouse with a massive cardiac hypertrophy (Open diamond) (WT (n=5), LCAD^{-/-}; VLCAD^{+/+} (n=7), and LCAD^{-/-}; VLCAD^{+/-} (n=9)). B. mRNA expression levels in overnight fasted mice of all genotypes (heart) (WT (n=5); LCAD^{-/-}; VLCAD^{+/+} (n=3), and LCAD^{-/-}; VLCAD^{+/-} (n=5)). Relative expression of Myh7, Nppa and Nppb. Expression is corrected for 18S. Open diamonds indicates the same LCAD^{-/-}; VLCAD^{+/-} mouse.



Supplemental Figure 2. Plasma glucose levels and blood glucose, lactate and pyruvate levels in blood and plasma of fed and refed mice with different LCAD and VLCAD genotypes. (WT (n=5), LCAD^{-/-}; VLCAD^{+/+} (n=7), and LCAD^{-/-}; VLCAD^{+/-} (n=9)). Error bars indicate +SEM *P<0.05, **P<0.01.



Supplemental Figure 3. Diurnal body temperature in WT (n=6) and LCAD^{-/-}; VLCAD^{+/+} (n=6) mice.



Supplemental Figure 4. A. Creatine Kinase (CK) levels of fasted mice with different LCAD and VLCAD genotypes. (WT (n=5), LCAD^{-/-}; VLCAD^{+/+} (n=7), and LCAD^{-/-}; VLCAD^{+/-} (n=9)). Error bars indicate +SEM. B. M. gastrocnemius, m. soleus and m. quadriceps muscle weight of mice with different LCAD and VLCAD genotypes. Organ weights are expressed a percentage of the bodyweight of fasted mice. The different genotypes are indicated in the figure legend (WT (n=5), LCAD^{-/-}; VLCAD^{+/+} (n=7), and LCAD^{-/-}; VLCAD^{+/-} (n=9)). Error bars indicate +SEM. C. C16-CoA dehydrogenase activity measurements in mouse muscle (quad) homogenates. (WT (n=4), LCAD^{-/-}; VLCAD^{+/+} (n=3), and LCAD^{-/-}; VLCAD^{+/-} (n=5)). Error bars indicate +SEM.

CHAPTER 9

Perioperative measures in very long-chain acyl-CoA dehydrogenase deficiency

P. Vellekoop¹, E.F. Diekman¹, I. van Tuijl², M.M.C. de Vries³, P.M. van Hasselt¹, G. Visser¹

¹ Department of Metabolic and Endocrine diseases, Wilhelmina Children's Hospital, UMC Utrecht, The Netherlands

² Department of Anesthesia, Wilhelmina Children's Hospital, UMC Utrecht, The Netherlands

³ Department of Metabolic Diseases, Radboud Medisch Centrum, Nijmegen, The Netherlands

Molecular Genetics and Metabolism, 2011, doi:10.1016/j.ymgme.2011.01.010

ABSTRACT

Surgical procedures in patients with metabolic disorders require specific anesthetic measures based on the nature of the involved metabolic disorder. Illustrated by the history of two patients, the need for a specific perioperative regimen in patients with very long chain acyl-CoA dehydrogenase deficiency (VLCADD) is discussed. One patient deteriorated, the other patient did well without any specific measurements. Although perioperative metabolic decompensation can currently not be predicted, it is a severe complication which should be avoided. We therefore advise to consider certain perioperative precautions in all VLCADD patients: 1) age and weight adapted glucose infusion, 2) stress avoiding premedication, 3) avoidance of volatile anesthetics, 4) avoidance of long chain fatty acid containing anesthetics and 5) perioperative glucose and CK monitoring.

INTRODUCTION

Surgical procedures in patients with metabolic disorders require specific anesthetic measures based on the nature of the involved metabolic disorder. Due to better treatment options with prolonged survival and due to the expanding newborn screening programs, more patients with metabolic disorders are alive and treated in different types of medical centers. Despite the fact that both patients and medical care takers are generally aware of the need for specific measures in metabolic disorders, still not always all needed measures are taken. Illustrated by the history of two patients we would like to discuss and also stress the need for a specific perioperative regimen in patients with very long chain acyl-CoA dehydrogenase deficiency (VLCADD) (McKusick 201475).

Patients with VLCADD, an inborn error of fatty acid oxidation, have an impaired energy production from endogenous and exogenous fatty acids¹. Catabolic situations like illness, fasting or prolonged exercise may provoke a serious metabolic derangement resulting in Reye like presentations, or rhabdomyolysis. Treatment is aimed at preventing catabolic situations by avoiding prolonged fasting and a diet restricted in long chain fatty acids². During surgery, prolonged fasting, perioperative stress and certain anesthetics can lead to metabolic derangements.

CASE 1

Patient A, a boy, was detected by newborn screening. Lymphocytes demonstrated no detectable VLCAD activity (normal 3.4 ± 0.8 nmol/ min.mg) and mutation analysis of ACADVL gene revealed a homozygous mutation c.1322G N A. During his first months of life he was admitted frequently because of feeding problems. On admissions he always had elevated CK levels maximum 6000 U/L (normal 0–170 U/ L). With nocturnal gastric drip feeding and daily frequent feedings CK normalized. Because of the continuous need of tube feeding, a percutaneous endoscopic gastrostomy was performed at 8 months of age. Perioperative a glucose infusion of 6 mg/kg/min was given. Anesthesia was induced by inhalation up to 8% sevoflurane in 100% oxygen using mask induction. Intubation was facilitated with sufentanil. Anesthesia was maintained with sevoflurane 3% in an oxygen/air mixture. Caudal anesthesia with marcaine with adrenaline was administered for pain relief. The procedure was uneventful, especially no agitation was observed in the recovery room. Glucose monitoring showed normal values both pre- and postoperative. Despite this regimen CK levels increased from 285 U/L postoperative to a maximum of 163,610U/L with myoglobinuria, indicating rhabdomyolysis. CK levels normalized in 2 weeks.

Since then he had two more surgical interventions, respectively for insertion of a central line under general anesthesia, and because of recurrent problems with intravenous access placement of an intravenous access device (PAC). During both procedures a glucose intake of 8 mg/kg/min was given. Anesthesia induction and maintenance was performed using a total intravenous technique with thiopental, midazolam and sufentanil. Pre- and postoperative normoglycemia was seen. At the insertion of the central line, after a prolonged fast due to venous access problems and recurrent vomiting, CK preoperative was high (53,626 U/L) but normalized in a week postoperatively. The placement of the PAC was performed in a stable situation and CK pre- and postoperative CK was normal.

CASE 2

Patient B, a girl, presented at the age of 3 months with hypoglycemia and was subsequently diagnosed with VLCADD. Enzyme analysis in fibroblasts showed an activity of 0.01 (3.36 plus/ min 0.94 nmol/min.mg) and a mutation analysis of ACADVL gene revealed a homozygous mutation 104delC. She was treated with a diet with frequent, LCT restricted and MCT enriched, feedings. The first 3 years of life she was admitted frequently because of metabolic derangement during infections. On a regimen with nocturnal gastric drip feeding she was thereafter stable for several years. Metabolic derangements returned from the age of 9 years. She needed frequent admissions due to excessive muscular pain and elevated CK, requiring intravenous glucose infusion. At the age of 11 years and 3 months a PAC was placed under general anesthesia. The perioperative regimen consisted of benzodiazepines (midazolam) and analgesics (acetaminophen) and constant glucose infusion of 6 mg/kg/min. An anesthetic technique using propofol (230 mg), fentanyl (0.05 mg) for induction and sevoflurane (max 2.13%) for maintenance was used. The procedure took 70 min and was uneventful including recovery and postoperative course. Postoperative CK level decreased compared to preoperative values (from 229 to 142 U/L).

DISCUSSION

The hereby reported perioperative courses of patients with VLCADD show variability. Patient A had rhabdomyolysis after anesthesia despite a perioperative regimen resulting in normoglycemia. Anesthesia without the use of propofol and volatile anesthetics, combined with premedication of benzodiazepines and glucose infusion prevented rhabdomyolysis. Patient B developed, despite the use of propofol, no rhabdomyolysis.

Table 1. Perioperative measures in patients with VLCADD.

-
1. Age and weight appropriate glucose infusion (infants 8 mg/kg/min)
 2. Pre- (during) and postoperative monitoring of glucose and CK
 3. Prevent perioperative stress by providing adequate premedication
 4. Avoid volatile anesthetics
 5. Avoid anesthetics containing high dose of long chain fatty acids like Propofol and Etomidate
-

Whether or not metabolic derangement occurs following anesthesia, varies between patients and depends on a combination of several factors. Until now not all of those factors are clarified, but based on literature and clinical experience we advise to consider certain perioperative precautionary measures for patients with VLCADD (Table 1). First, since catabolism may induce a metabolic derangement in VLCADD, adequate glucose supplementation is advised. In healthy infants undergoing minor surgery glucose infusion of 6 mg/kg/min is sufficient to prevent catabolism³. As perioperative stress factors increase the glucose demand⁴, a glucose infusion of 8 mg/kg/min perioperative is recommended in infants with VLCADD. Second, perioperative glucose monitoring is advised². Since rhabdomyolysis may occur despite normoglycemia, postoperative, a prolonged monitoring of CK is needed⁵. Relative insulin shortage causes decreased uptake of glucose in peripheral tissue despite normal blood glucose levels. During perioperative stress cortisol and catecholamines are released which changes the conformation of the insulin receptor, resulting in insulin-resistance in the peripheral tissue⁸. Accumulation of lipid intermediates such as long chain acyl-CoA is also associated with insulin resistance⁶. Therefore, perioperative stress should be minimized. A benzodiazepine-opioid combination like remifentanyl and midazolam prevents perioperative stress in VLCADD patients⁷. Furthermore, pain, should be minimized by analgesics. Regional anesthesia is recommended if applicable⁴.

Some anesthetics like propofol and volatile anesthetics are known to induce rhabdomyolysis in patients with VLCADD and should therefore be avoided. Propofol, a short-acting, intravenously administered hypnotic agent, contains a high dose of long chain fatty acids and disturbs multiple steps in the fatty acid metabolism^{4,6,8,9}. Volatile anesthetics are associated with a significant increase in free fatty acid concentrations during the first phases of anesthesia which may result in a metabolic derangement^{4,10}.

The fact that patient B, despite the use of propofol, had no rhabdomyolysis might be explained by several factors like diet adjustment, the amount of glycogen storages prior to the procedure, anesthetic dose, age, clinical phenotype, genotype and residual VLCAD enzyme activity. Andresen et al. described a strong correlation between clinical

phenotype and genotype: missense mutations appear to be clinically less severe as opposed to NULL-mutations¹¹. Patient A, however, has a missense mutation with a more severe clinical phenotype than patient B who has a NULL-mutation, but patient A is much younger. The differences in clinical presentation at different ages might in part be explained by the fact that glucose requirement per kilogram of body weight diminishes with time. It is yet unclear whether the genotype can fully predict the risk of developing rhabdomyolysis. But, although perioperative metabolic decompensation can currently not be predicted, it is a severe complication, which should be avoided. We therefore advise to take the above stated precautions into consideration in patients with VLCADD who need anesthetics.

REFERENCES

1. Gregersen N, Andresen BS, Corydon MJ, et al. Mutation analysis in mitochondrial fatty acid oxidation defects: Exemplified by acyl-CoA dehydrogenase deficiencies, with special focus on genotype–phenotype relationship. *Hum Mutat.* 2001;18(3):169–189. doi:10.1002/humu.1174.
2. Arnold GL, VanHove J, Freedenberg D, et al. A Delphi clinical practice protocol for the management of very long chain acyl-CoA dehydrogenase deficiency. *Molecular Genetics and Metabolism.* 2009;96(3):85–90. doi:10.1016/j.ymgme.2008.09.008.
3. Nishina K, Mikawa K, Maekawa N, Asano M, Obara H. Effects of exogenous intravenous glucose on plasma glucose and lipid homeostasis in anesthetized infants. *Anesthesiology.* 1995;83(2):258–263.
4. Steiner LA, Studer W, Baumgartner ER, Frei FJ. Perioperative management of a child with very-long-chain acyl-coenzyme A dehydrogenase deficiency. *Paediatr Anaesth.* 2002;12(2):187–191.
5. Engbers HM, Dorland L, De Sain MGM, Eskes PF, Visser G. Rhabdomyolysis in early-onset very long-chain acyl-CoA dehydrogenase deficiency despite normal glucose after fasting. *J Inherit Metab Dis.* 2005;28(6):1151–1152. doi:10.1007/s10545-005-0190-y.
6. Hoy AJ, Brandon AE, Turner N, et al. Lipid and insulin infusion-induced skeletal muscle insulin resistance is likely due to metabolic feedback and not changes in IRS-1, Akt, or AS160 phosphorylation. *AJP: Endocrinology and Metabolism.* 2009;297(1):E67–75. doi:10.1152/ajpendo.90945.2008.
7. Schmidt J, Hunsicker A, Irouschek A, Köhler H, Knorr C, Birkholz T. Early recovery from anesthesia and extubation in an infant with very long chain acyl-CoA dehydrogenase deficiency using midazolam, mivacurium, and high dose remifentanyl. *Paediatr Anaesth.* 2009;19(9):909–910. doi:10.1111/j.1460-9592.2009.03088.x.
8. Burns AP, Hopkins PM, Hall G, Pusey CD. Rhabdomyolysis and acute renal failure in unsuspected malignant hyperpyrexia. *Q J Med.* 1993;86(7):431–434.
9. Kleemann PP, Jantzen JP, Fenner R, Wiegand UW. [Preoperative increase in the plasma concentration of free fatty acids during minor elective interventions using a conventional anesthesia technic with enflurane]. *Anaesthesist.* 1986;35(10):604–608.
10. Wolf A, Weir P, Segar P, Stone J, Shield J. Impaired fatty acid oxidation in propofol infusion syndrome. *The Lancet.* 2001. doi:10.1016/S0140-6736(00)04064-2.
11. Andresen BS, Olpin S, Poorthuis BJ, et al. Clear correlation of genotype with disease phenotype in very-long-chain acyl-CoA dehydrogenase deficiency. *Am J Hum Genet.* 1999;64(2):479–494. doi:10.1086/302261.

CHAPTER 10

Necrotizing enterocolitis and respiratory distress syndrome as first clinical presentation of mitochondrial trifunctional protein deficiency

Eugène F. Diekman^{1,2}, Carolien C.A. Boelen², Berthil H.C.M.T. Prinsen³, Lodewijk IJst¹, Marinus Duran¹, Tom J. de Koning², Hans R. Waterham¹, Ronald J.A. Wanders^{1,4}, Frits Wijburg⁴, Gepke Visser²

¹ Laboratory Genetic Metabolic Diseases, Department of Clinical Chemistry, Academic Medical Center, University of Amsterdam, the Netherlands

² Department of Metabolic Diseases and Endocrine diseases, Wilhelmina Children's Hospital, UMC Utrecht, the Netherlands

³ LUMC Leiden University Medical Center, the Netherlands

⁴ Department of Pediatrics, Emma children's Hospital, Academic Medical Center, University of Amsterdam, the Netherlands

Journal of Inherited Metabolic Disease, 2012, doi:10.1007/8904_2012_128

ABSTRACT

Background: Newborn screening (NBS) for Long-Chain 3-Hydroxy acyl-CoA Dehydrogenase deficiency (LCHADD) does not discriminate between isolated LCHADD, isolated Long-Chain Keto acyl-CoA deficiency (LCKATD) and total Mitochondrial Trifunctional Protein deficiency (MTPD). Therefore, screening for LCHAD deficiency inevitably comprises screening for MTPD, which is much less amenable to treatment. Furthermore, absence of a clear classification system for these disorders is still lacking.

Materials & Methods: Two newborns screened positive for LCHADD died at the age of 10 and 31 days respectively. One due to severe necrotizing enterocolitis (NEC), cardiomyopathy and multiorgan failure; the other due to severe Infant Respiratory Distress Syndrome (IRDS) and hypertrophic cardiomyopathy. (Keto)-acylcarnitine concentration and enzymatic analysis of LCHAD and LCKAT suggested MTPD in both patients. Mutation analysis revealed a homozygous HADHB c.357+5delG mutation in one patient and a homozygous splice-site HADHB mutation c.251+1G>C in the other patient. Data on enzymatic and mutation analysis of 40 patients with presumed MTPD, LCHADD or LCKATD were used to design a classification to distinguish between these disorders.

Discussion: NEC as presenting symptom in MTPD was not previously reported and IRDS only rarely. High expression of long-chain fatty acid oxidation enzymes reported in lungs and gut of human foetuses suggests that the severe NEC and IRDS observed in our patients is related to the enzymatic deficiency in these organs during crucial stages of development.

Furthermore, to improve communication on MTPD we propose a classification system to discriminate LCHADD, LCKATD and MTPD based on enzymatic analysis.

INTRODUCTION

In 2007, the newborn screening program (NBS) in the Netherlands was expanded with 13 inborn errors of metabolism, including the autosomal recessive long-chain fatty acid oxidation (FAO) disorder Long-Chain 3-Hydroxy Acyl-CoA Dehydrogenase (LCHAD) deficiency. LCHAD is part of Mitochondrial Trifunctional Protein (MTP), which harbours two additional enzymes in long-chain FAO: long-chain enoyl-CoA hydratase (LCEH) and long-chain keto acyl-CoA thiolase (LCKAT). The enzyme active sites are located on different subunits, named alpha- and beta-, which together form an octameric complex of 4 α - and 4 β -subunits^{1,2}. LCHAD and LCEH are located on the α -subunit, and are both encoded by the *HADHA* gene. LCKAT is located on the β -subunit, and is encoded by the *HADHB* gene^{1,2}.

Newborn screening for LCHAD deficiency is performed by measuring C16-OH-carnitine levels in dried blood spots. However, discrimination between isolated general MTP deficiency, LCHAD deficiency, isolated LCKAT deficiency (LCKAT deficiency) or isolated LCEH deficiency (LCEH deficiency; not identified yet) cannot be made on the basis of the acylcarnitine profile, but requires specific enzyme testing in lymphocytes or fibroblasts. Although measurement of 3-keto-C18:1-carnitine and 3-keto-C18:2-carnitine, which accumulate in case of LCKAT deficiency but not LCHAD deficiency, might also be helpful³.

By far the most common mutation associated with LCHAD deficiency is the *HADHA* c.1528 G>C mutation (p.Glu510Gln, allelic frequency 60%)⁴. Mutations associated with a deficient activity of all enzymes (MTP deficiency) are more heterogeneous.

While no patients with isolated LCEH deficiency have been reported, MTP deficiency has been reported in relatively large series of patients^{2,5-10}. Patients with MTP deficiency, including isolated LCHAD deficiency, most often present with acute metabolic decompensation consisting of nonketotic hypoglycemia and rhabdomyolysis, generally followed by cardiomyopathy and later peripheral neuropathy. Hypotonia, areflexia and hepatic encephalopathy have also been described^{2,5-10}. In contrast, isolated LCKAT deficiency appears extremely rare and only one patient, who presented with lethal cardio-respiratory failure, has been reported⁴.

We present two patients identified by NBS with an abnormal screening result suggestive for LCHAD deficiency, who were subsequently diagnosed with MTP deficiency. Both patients were already severely ill at the time the results of the newborn screening became available, and showed remarkable clinical symptoms which are generally not observed in patients with a defect in fatty acid oxidation.

As it is not possible to distinguish isolated LCHAD deficiency and LCKAT deficiency of MTP deficiency based on NBS results, clinical signs and symptoms or DNA-mutation analysis, we propose a classification based on enzymatic analysis of LCHAD and LCKAT.

MATERIALS & METHODS

Case 1

The patient, a girl, was the first child of consanguineous Caucasian parents. The pregnancy was complicated by eclampsia. The mother had 7 seizures, ALAT of 29 (normal 0-35), ASAT of 36 (0-30), and low platelets $127 \times 10^9/L$ (normal 150-450). The pregnancy was therefore terminated at 35 weeks of gestation by caesarean section. Birth weight was 2110 g (-0.4SD), length 40cm (<-2.5SD) and head circumference 30cm (<-2.5SD). APGAR scores were 4, 8 and 8 after 1, 5 and 10 minutes, respectively. Postpartum glucose was 9.6mmol/L (normal 3.6-5.6), lactate 7.1mmol/L (normal 0.0-2.2), ammonia 127 μ mol/L (normal 0-75), LDH 899U/L (normal 0-250), ASAT/ALAT were normal. CK at day 7 was 478U/L (normal 0-145). With normal intake, plasma glucose levels remained above 4.2mmol/L and lactate levels decreased to 2.6mmol/L. On day 3, she had rectal blood loss. On suspicion of a necrotizing enterocolitis (NEC) she was admitted to the neonatal intensive care unit and parenteral feeding was initiated. On day 7, a sudden clinical deterioration suggested a gut perforation as complication of the NEC and a laparotomy was performed. No perforation was found, but intestinal biopsies later showed the classical pathology of a NEC. There was no clinical improvement observed and echocardiography revealed a severely dilated cardiomyopathy with low cardiac output. On this same day (day 7), the NBS results from a dried blood spot, taken at day 4, became available and showed an elevated C16-OH-carnitine suggestive of LCHAD deficiency. Additional analysis in plasma revealed increased concentrations of hydroxyacylcarnitines (table 1). Subsequently, keto-acylcarnitine concentrations were analyzed and showed increased 3-keto-C18:1-carnitine and 3-keto-C18:2-carnitine which is suggestive of LCKAT deficiency (table 1). Enzymatic analysis showed reduced activities of both LCHAD and LCKAT (lymphocytes). DNA mutation analysis of the *HADHB* gene (GenBank accession number BC066963) showed a homozygous splice-site mutation in intron 4, c.212+1G>C, predicted to lead to aberrant splicing of the *HADHB* mRNA transcript. No mutation was found in the *HADHA*-gene.

The patient developed seizures during prolonged hypotensive episodes. Cerebral ultrasound studies showed minimal flaring and a minor bleeding (IIAB). Despite vigorous treatment, including high dose (8 – 10 mg/kg/min) intravenous glucose infusion, she died at 10 days of age because of severe multi organ failure.

Case 2

The patient, a boy, was the first child of consanguineous parents. Pregnancy was complicated by pre-eclampsia and intra uterine growth retardation (IUGR). The pregnancy was terminated at 30 weeks by caesarean section because of foetal distress. Birth weight was 1275 g(<-1.0SD), length 37cm (-2.0SD) and head circumference 28cm (1-0SD). APGAR

Table 1. Acylcarnitine profile (NBS and plasma), enzymatic activity and mutations of both patients (controls \pm SD). L = lymphocytes; F = fibroblasts; * numbering according to GenBank sequence BC066963

Acylcarnitine profile (bloodspot)		Patient 1 35wks, 2110g ($\mu\text{mol/L}$) (day 4)	Patient 2 30wks, 1275g ($\mu\text{mol/L}$) (day 3)	Control values ($\mu\text{mol/L}$)
C16-OH-carnitine		1.44	0.63	$<= 0.08$
Acylcarnitine profile (plasma)		Patient 1 ($\mu\text{mol/L}$) (day 7)	Patient 2 ($\mu\text{mol/L}$) (day 7)	Control values ($\mu\text{mol/L}$) (n=700)
free carnitine		6.9	9.82	22.35-54.80
C14-carnitine		0.2	0.36	0-0.08
C14:1-carnitine		0.1	0.42	0.02-0.18
C14:1-OH-carnitine		0.05	0.11	0-0.02
C16-carnitine		1.13	1.33	0.06-0.24
C16-OH-carnitine		0.59	0.44	0-0
C16:1-carnitine		0.32	0.45	0.02-0.08
C16:1-OH-carnitine		0.19	0.25	0-0.02
C18:1-OH-carnitine		0.6	1.12	0-0.02
3-keto-C18:1-carnitine		detected	detected	undetectable
3-keto-C18:2-carnitine		detected	detected	undetectable
Activity		Patient 1 (nmol/min/mg protein)	Patient 2 (nmol/min/mg protein)	Control values (nmol/min/mg protein)
HAD activity	C16	12^{L} (26%)	10^{L} (21%) 11^{F} (14%)	$53 \pm 18^{\text{L}}$ (N=88) $79 \pm 16^{\text{F}}$ (N=215)
	C4	103^{L}	116^{L} (21%) 86^{F} (86%)	$149 \pm 46^{\text{L}}$ (N=135) $113 \pm 29^{\text{F}}$ (N=215)
	C16/C4	0.12^{L}	0.08^{L} 0.13^{F}	0.37 ± 0.20 (N=88) $0.72 \pm 0.14^{\text{F}}$ (N=215)
LCKAT activity		0.9^{L} (8%)	1.7^{F}	$10.2 \pm 3.6^{\text{L}}$ (N=41) $18.3 \pm 5.4^{\text{F}}$ (N=215)
	Mutation analysis		Patient 1	Patient 2
<i>HADHA</i> gene (allele 1)		normal	normal	
<i>HADHA</i> gene (allele 2)		normal	normal	
<i>HADHB</i> gene (allele 1) *		c.212+1G>C	c.357+5delG	
<i>HADHB</i> gene (allele 2) *		c.212+1G>C	c.357+5delG	

scores were 7, 8 and 9 after 1, 5 and 10 minutes, respectively. On day one, he became hypotensive and developed severe IRDS (grade III-IV) despite multiple surfactant administrations. He was artificially ventilated. Despite continuous glucose infusion (8-10 mg/kg/min), he had multiple hypoglycaemic episodes (postpartum glucose 1.8 mmol/l) and a persistent lactic acidosis (>10 mmol/l, normal 0.0-2.2). Echocardiography performed on day 6 revealed a hypertrophic cardiomyopathy. Cerebral ultrasound showed no abnormalities. On day 10, the NBS results from a dried blood spot taken at day 3, became available which revealed an elevated C16-OH-carnitine, suspicious for LCHAD deficiency. Additional analysis in plasma revealed increased concentrations of hydroxyacylcarnitines (table 1). Subsequently, keto-acylcarnitine concentrations were analyzed and showed increased 3-keto-C18:1-carnitine and 3-keto-C18:2-carnitine which is suggestive of LCKAT deficiency (table 1). Enzymatic analysis showed reduced activities of both LCHAD and LCKAT (fibroblasts). DNA mutation analysis of the *HADHB* gene (GenBank accession number BC066963) showed a homozygous mutation c.357+5delG, which was subsequently shown by cDNA analysis to result in a complete skipping of exon 6. No mutation was found in the *HADHA*-gene.

Despite extensive treatment including ventilatory support, glucose infusion, parenteral feeding, carnitine supplementation (100mg/kg/day) and long-chain triglyceride restriction and medium-chain enriched feeding, he died 31 days after birth because of respiratory failure.

Classification

To be able to discriminate between LCHAD, LCKAT and MTP deficiency, we retrospectively analyzed data of 40 non-related patients in whom LCHAD and LCKAT activity was measured and DNA mutation analysis was performed. In addition we analyzed data of 215 subjects in whom LCHAD and LCKAT activity was measured because of suspected FAO disorder, but in whom no FAO defect was found.

Hydroxyacyl-CoA dehydrogenase (HAD) activity was measured in homogenates of cultured fibroblasts by observing the decrease in absorbance at 340nm¹¹. 3-Ketohexadecanoyl-CoA (C16) and acetoacetyl-CoA (C4) have been used as substrates for LCHAD activity measurements. LCHAD shows highest activity with C16 as substrate with virtually no reactivity with C4 as substrate^{3,12}. However, another dehydrogenase -short chain hydroxyacyl-CoA dehydrogenase (SCHAD)- has activity with both C16 and C4. To be able to acquire an accurate approximation of LCHAD activity; the activities with C16 and C4 as substrate were used as a ratio (C16/C4).

A full deficiency of LCHAD will result in a C16/C4 HAD activity ratio of approximately 0.2, which is characteristic of the SCHAD enzyme, as it is five times more active with C4 than C16 as a substrate. A C16/C4 HAD activity ratio higher than approximately 0.2, is a result of (residual) LCHAD activity.

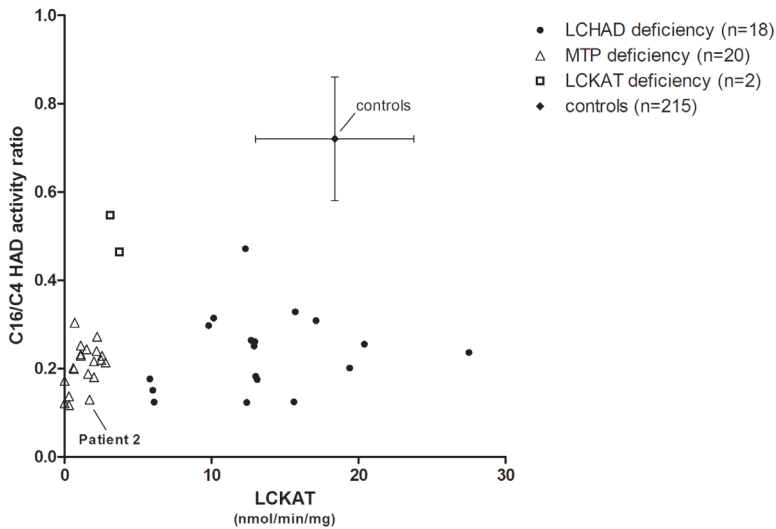


Figure 1. C16/C4 HAD activity ratio and LCKAT activity of patients and controls. C16/C4 HAD activity ratio and LCKAT activity have been analyzed in fibroblasts of 40 patients with HADHA and/or HADHB mutations and 215 controls as described in Materials & Methods. Patients can be divided into three groups: LCHAD (•), LCKAT(□) and MTP(△) deficiency. Mean C16/C4 HAD activity ratio of control group 0.72 ± 0.14 (mean \pm SD; vertical error bars). Mean LCKAT activity of control group 18.3 ± 5.4 nmol/min/mg protein (mean \pm SD; horizontal error bars).

LCKAT activity was measured in homogenates of cultured fibroblasts by following the decrease in absorbance at 303nm^{11} .

All enzyme analysis were performed on a Cobas Centrifugal Analyzer (Hofmann-La Roche, Basel, Switzerland)

DNA was extracted from blood leukocytes and amplified by polymerase chain reaction (PCR). After amplification, 20 exons of HADHA and 16 exons of HADHB gene were sequenced. The results are shown in figure 1.

Analytical methods

Enzymatic activity measurements in lymphocytes and/or fibroblast were carried out as previously described^{11,13}. NBS acylcarnitine profiling was performed as described by Chace et al¹⁴. Plasma acylcarnitine profiling was performed as described by Minkler et al.¹⁵. In addition, keto-acylcarnitine profiling was performed by incubating $50 \mu\text{L}$ of plasma with $5 \mu\text{L}$ of MOX Reagent (Pierce, Rockford, IL, USA) containing 2% methoxyamine.HCl in pyridine. The mixture was left to stand at room temperature for 2 hours to allow the formation of methoxime-derivatives of all keto-containing substances. Follow-

ing this incubation the samples were treated in the usual manner for the isolation and derivatization of acylcarnitines, which were analyzed as their butyl-esters derivatives¹⁵.

DISCUSSION

NEC as a presenting symptom in MTP deficiency has to our knowledge not been reported previously. Severe IRDS has been recognized as a rare early symptom in MTP deficiency⁷. Cardiomyopathy, which was present in both patients is a frequently reported complication in MTP deficiency^{6-8,10}.

Although it is generally assumed that FAO plays no, or only a minor role during intrauterine life due to the abundance of glucose provided by the mother via the placenta^{16,17}, the clinical course in our patients, as well as the patient with isolated LCKAT deficiency described by Das et al.⁴, suggest that normal function of the MTP complex is needed for normal intestinal and pulmonary development and function. Berger and Wood showed that complete disruption of long-chain FAO at the level of LCAD in animal models results in increased embryonic mortality¹⁸. It has also been shown that FAO enzymes are expressed abundantly in human placentas (Shekawat 2003). Furthermore, patients with long-chain defects in FAO may already display cardiomyopathy before and immediately after birth^{6-8,10}, demonstrating a role for long-chain FAO during intrauterine life. Finally, the (pre)eclampsia, the premature delivery and the foetal distress seen in both hereby described patients, is also in line with this hypothesis¹⁹.

While NEC is a relatively common complication in ill premature babies, it is rarely seen in newborns of 35 weeks gestational age, with a birth weight > 1500 g and in absence of a history of hypovolemic shock and/or asphyxia²⁰. In addition, severe IRDS, not responding to multiple administration of surfactant, is rare in neonates born after 30 weeks gestation. We therefore hypothesize that both the NEC observed in patient 1 and the severe IRDS in patient 2 are linked to the defective long-chain FAO. Early foetal expression patterns of long-chain FAO enzymes, including VLCAD and LCHAD, demonstrate that these enzymes are not only expressed in myocardial tissue, but also abundantly in the foetal lung and gut¹⁹. MTP deficiency during intrauterine life may therefore interfere with normal development or maturation of the foetal intestine and lungs. In the gut this might result in decreased mucus synthesis, decreased intracellular junction integrity and increased permeability, both potentially related to the development of NEC²⁰. In addition, intestinal villous atrophy and inflammation is observed in carnitine transport deficient (OCTN2) mice another FAO disorder in which beta-oxidation is severely affected (Shekawat 2007).

In the lungs, surfactant is secreted by alveolar type II cells, and decreased maturation or functioning of this process may lead to IRDS²⁰. We therefore believe that MTP deficiency during intrauterine life may hamper normal surfactant synthesis.

We identified two novel mutations in the *HADHB* gene. The mutation found in patient 1, c.212+1G>C, affects the splice-donor site of intron 4 and is predicted to result in skipping of exon 4. Because fibroblasts were not available from patient 1, this could not be studied at the cDNA level. The G deletion at position c.357+5 found in patient 2 results in skipping of exon 6, as demonstrated by cDNA analysis prepared from mRNA isolated from fibroblasts of the patient.

Both mutations did not only result in a markedly reduced LCKAT activity, but also affected enzyme activity of LCHAD, which is possibly due to the loss of integrity of the MTP-complex². It is known that a single mutation in the *HADHA* or *HADHB* gene can result in either an isolated deficiency of LCHAD or LCKAT, or reduced activity of both enzymes. However, until now it has not been possible to clearly distinguish isolated LCHAD and LCKAT deficiency from MTP deficiency. We propose a classification system based on the C16/C4 HAD activity ratio and LCKAT residual enzyme activities measured in 40 patients. As shown in figure 1, the patients can be divided into three groups, which we have labelled as LCHAD, LCKAT and MTP deficiency. The LCHAD group contains patients with a mean C16/C4 HAD activity ratio of 0.24 ± 0.09 (mean \pm SD) combined with a ketothiolase activity of 13.5 ± 5.4 nmol/min/mg protein (mean \pm SD). The MTP deficiency group consists of patients with a mean C16/C4 HAD activity ratio of 0.2 ± 0.05 (mean \pm SD) and a LCKAT activity of 1.3 ± 0.88 nmol/min/mg (mean \pm SD). The third group, isolated LCKAT deficiency, includes 2 patients with a C16/C4 HAD activity ratio of approximately 0.5 and an LCKAT activity of < 5 nmol/min/mg protein (figure 1). The activity of the different enzymes could not be fully predicted based on the mutations. Although the LCHAD group includes 17 of the 18 patients homozygous for the *HADHA* c.1528 G>C mutation, the MTP deficient group includes patients with either alpha- or beta-subunit mutations. The two isolated LCKAT deficient patients, one of which was reported previously⁴, have distinct beta subunit mutations. Based on this classification patient 2 will be classified as MTP deficient. We could not obtain fibroblasts of the first patient and are therefore unable to classify this patient unambiguously. However, predicted is that the MTP protein of patient 1 is absent, because the mutation resulted in exon skipping. We therefore conclude patient 1 is also MTP-deficient.

In summary, we present two patients in whom NBS results were consistent with LCHAD deficiency, who eventually were diagnosed, based on a novel proposed classification system, with MTP deficiency, caused by two novel mutations. One of the patients presented with a severe NEC, which has not been associated previously with long-chain FAO defects. In addition, a severe IRDS was observed in the other patient. Both clinical

presentations may be explained by high expression patterns of long-chain FAO enzymes not only in myocardial tissue, but in lung and gut tissue as well. Deficiency of MTP in the gut and lung might therefore explain the development of severe NEC and IRDS in addition to the cardiomyopathy found in our patients.

REFERENCES

1. Kamijo T, Aoyama T, Komiyama A, Hashimoto T. Structural analysis of cDNAs for subunits of human mitochondrial fatty acid beta-oxidation trifunctional protein. *Biochem Biophys Res Commun*. 1994;199(2):818–825. doi:10.1006/bbrc.1994.1302.
2. Ushikubo S, Aoyama T, Kamijo T, et al. Molecular characterization of mitochondrial trifunctional protein deficiency: formation of the enzyme complex is important for stabilization of both alpha- and beta-subunits. *Am J Hum Genet*. 1996;58(5):979–988.
3. Wanders RJA, Ruiten JPN, IJLst L, Waterham HR, Houten SM. The enzymology of mitochondrial fatty acid beta-oxidation and its application to follow-up analysis of positive neonatal screening results. *J Inherit Metab Dis*. 2010;33(5):479–494. doi:10.1007/s10545-010-9104-8.
4. Das AM, Illsinger S, Lücke T, et al. Isolated mitochondrial long-chain ketoacyl-CoA thiolase deficiency resulting from mutations in the HADHB gene. *Clinical Chemistry*. 2006;52(3):530–534. doi:10.1373/clinchem.2005.062000.
5. Choi J-H, Yoon H-R, Kim G-H, Park S-J, Shin Y-L, Yoo H-W. Identification of novel mutations of the HADHA and HADHB genes in patients with mitochondrial trifunctional protein deficiency. *Int J Mol Med*. 2007;19(1):81–87.
6. Boer den MEJ, Dionisi-Vici C, Chakrapani A, van Thuijl AOJ, Wanders RJA, Wijburg FA. Mitochondrial trifunctional protein deficiency: a severe fatty acid oxidation disorder with cardiac and neurologic involvement. *J Pediatr*. 2003;142(6):684–689. doi:10.1067/mpd.2003.231.
7. Olpin SE, Clark S, Andresen BS, et al. Biochemical, clinical and molecular findings in LCHAD and general mitochondrial trifunctional protein deficiency. *J Inherit Metab Dis*. 2005;28(4):533–544. doi:10.1007/s10545-005-0533-8.
8. Purevsuren J, Fukao T, Hasegawa Y, et al. Clinical and molecular aspects of Japanese patients with mitochondrial trifunctional protein deficiency. *Molecular Genetics and Metabolism*. 2009;98(4):372–377. doi:10.1016/j.ymgme.2009.07.011.
9. Saudubray JM, Martin D, de Lonlay P, et al. Recognition and management of fatty acid oxidation defects: a series of 107 patients. *J Inherit Metab Dis*. 1999;22(4):488–502.
10. Spiekeroetter U, Sun B, Khuchua Z, Bennett MJ, Strauss AW. Molecular and phenotypic heterogeneity in mitochondrial trifunctional protein deficiency due to beta-subunit mutations. *Hum Mutat*. 2003;21(6):598–607. doi:10.1002/humu.10211.
11. Wanders RJ, IJLst L, van Gennip AH, et al. Long-chain 3-hydroxyacyl-CoA dehydrogenase deficiency: identification of a new inborn error of mitochondrial fatty acid beta-oxidation. *J Inherit Metab Dis*. 1990;13(3):311–314.
12. Wanders RJ, Vreken P, Boer den ME, Wijburg FA, van Gennip AH, IJLst L. Disorders of mitochondrial fatty acyl-CoA beta-oxidation. *J Inherit Metab Dis*. 1999;22(4):442–487.
13. Wanders RJ, IJLst L, Poggi F, et al. Human trifunctional protein deficiency: a new disorder of mitochondrial fatty acid beta-oxidation. *Biochem Biophys Res Commun*. 1992;188(3):1139–1145.
14. Chace DH, Kalas TA, Naylor EW. Use of tandem mass spectrometry for multianalyte screening of dried blood specimens from newborns. *Clinical Chemistry*. 2003;49(11):1797–1817.
15. Minkler PE, Ingalls ST, Hoppel CL. Strategy for the Isolation, Derivatization, Chromatographic Separation, and Detection of Carnitine and Acylcarnitines. *Anal Chem*. 2005;77(5):1448–1457. doi:10.1021/ac0487810.
16. Oey NA, Ruiten JPN, Attié-Bitach T, IJLst L, Wanders RJA, Wijburg FA. Fatty acid oxidation in the human fetus: implications for fetal and adult disease. *J Inherit Metab Dis*. 2006;29(1):71–75. doi:10.1007/s10545-006-0199-x.

17. Shekhawat P, Bennett MJ, Sadovsky Y, Nelson DM, Rakheja D, Strauss AW. Human placenta metabolizes fatty acids: implications for fetal fatty acid oxidation disorders and maternal liver diseases. *Am J Physiol Endocrinol Metab*. 2003;284(6):E1098–105. doi:10.1152/ajpendo.00481.2002.
18. Berger PS, Wood PA. Disrupted blastocoele formation reveals a critical developmental role for long-chain acyl-CoA dehydrogenase. *Molecular Genetics and Metabolism*. 2004;82(4):266–272. doi:10.1016/j.ymgme.2004.06.001.
19. Oey NA, Boer den MEJ, Wijburg FA, et al. Long-chain fatty acid oxidation during early human development. *Pediatric Research*. 2005;57(6):755–759. doi:10.1203/01.PDR.0000161413.42874.74.
20. Neu J, Walker WA. Necrotizing enterocolitis. *N Engl J Med*. 2011;364(3):255–264. doi:10.1056/NEJMra1005408.

CHAPTER 11

General discussion & future perspectives



INTRODUCTION

Patients with dysfunctional long-chain fatty acid oxidation (lcFAO) may present with a variety of clinical signs and symptoms, including hypoketotic hypoglycemia, hepatomegaly, cardiomyopathy, myopathy, polyneuropathy, retinopathy¹⁻⁴. This wide range of symptoms illustrates the crucial role of lcFAO in many physiological processes. Inclusion of disorders of lcFAO in Newborn Screening (NBS) program saves lives, because life-threatening symptoms as hypoglycemia and cardiomyopathy can be prevented⁵. Dietary advices⁶ may prevent metabolic derailments to a certain extent, however, it is yet not possible to prevent all derailments. Some patients still have to be hospitalized frequently⁷. Moreover, many patients are not able to participate in normal daily life, nor are they able to perform sports.

The aim of this thesis was to improve outcome for patients with lcFAO disorders by, amongst others, increasing insight in the pathogenesis of rhabdomyolysis and cardiomyopathy

NEWBORN SCREENING

Since the introduction of lcFAO disorders in NBS worldwide⁸, patients are identified before the onset of clinical signs and symptoms. With the current speed of development of new techniques in biochemistry, genetics and post-analytical tools⁹, more disorders will be detected with higher sensitivities in the next decade^{10,11}. In **chapter 2** the feasibility of current biochemical markers (acylcarnitines) to detect lcFAO disorders was studied. Optimal ratios to detect CPT1a and CPT2 deficiency by NBS were defined. Furthermore, we enhanced the sensitivity to detect very long-chain acyl-CoA dehydrogenase deficiency (VLCADD) by introducing a new marker as described in **chapter 3**. However, a significant number of newborns identified by NBS actually have a very low risk for metabolic decompensation and may even remain fully asymptomatic if left untreated¹². Potential predictive markers were therefore investigated and correlated with the clinical phenotype of VLCADD patients diagnosed before VLCADD was introduced in the Dutch NBS program, as described in **chapter 4**. LC-FAO flux was found to be the best marker to predict a clinical phenotype. As such, it could be used as a second tier or follow-up test of NBS in the future.

DISEASE MONITORING

The human heart relies on FAO for 60-90% of its energetic needs¹³. Cardiac complications are monitored on a regular basis. Presently, echocardiography and (Holter)ECG are the golden standard to assess the function of an IcFAO deficient patient heart. In **chapter 5**, a cohort of 20 IcFAO deficient patients was described, and found that the majority had no cardiac dysfunction. An additional method was used that provided deeper insight into myocardial contractility: strain echocardiography. This technique is able to detect subclinical myocardial dysfunction. Many IcFAO deficient patients were observed to have mild subclinical myocardial dysfunction. Whether this dysfunction will progress or may have other clinical implications remains to be elucidated.

Skeletal muscles rely on FAO to meet their energetic needs, especially during endurance exercise. In a cohort of 20 patients, including adult patients, virtually no loss of muscle force was observed (**chapter 6**). Sensory loss, especially polyneuropathy, contractures and atrophy, were present in MTPD and LCHADD patients. To better monitor the progression of disease, the use of MRI to visualize the consequences of (recurrent episodes of) rhabdomyolysis on muscle was described (**chapter 6**). Striking abnormalities in VLCADD and MTPD/LCHADD patients were found which lead to the conclusion that MRI may be more sensitive to study the subacute and long-term effects of IcFAO disorders on muscle compared to plasma CK levels, since CK levels may rise and fall within hours or days in the acute phase of rhabdomyolysis. Future studies should address whether the observed abnormalities aggravate or stabilize over time.

UNDERSTANDING THE PATHOPHYSIOLOGY OF DISEASE

Myopathy

The pathophysiology of myopathy and rhabdomyolysis in IcFAO deficient patients is not completely understood. Based on observations in our cohort, it is known that 8-12h after start of illness/fever, creatine kinase (CK) levels rise, with a maximum CK level at 24-48h. It is also known that CK levels may rise despite normoglycemia¹⁴, even during continuous glucose infusion as described in **chapter 9**.

Two mechanisms have been proposed that may cause rhabdomyolysis in IcFAO deficient patients: 1) a failing compensatory mechanism during metabolically challenging conditions (eg during exercise, fever, fasting) and subsequent ATP depletion, or 2) toxicity caused by the accumulation of FAO intermediates.

1) It is thought that a low level of ATP (and thus elevated AMP) impairs the function of the Na-K-ATPase, with as a consequence an increase in intracellular sodium concentration. This in turn reduces the sodium-calcium exchange and leads to a concomitant

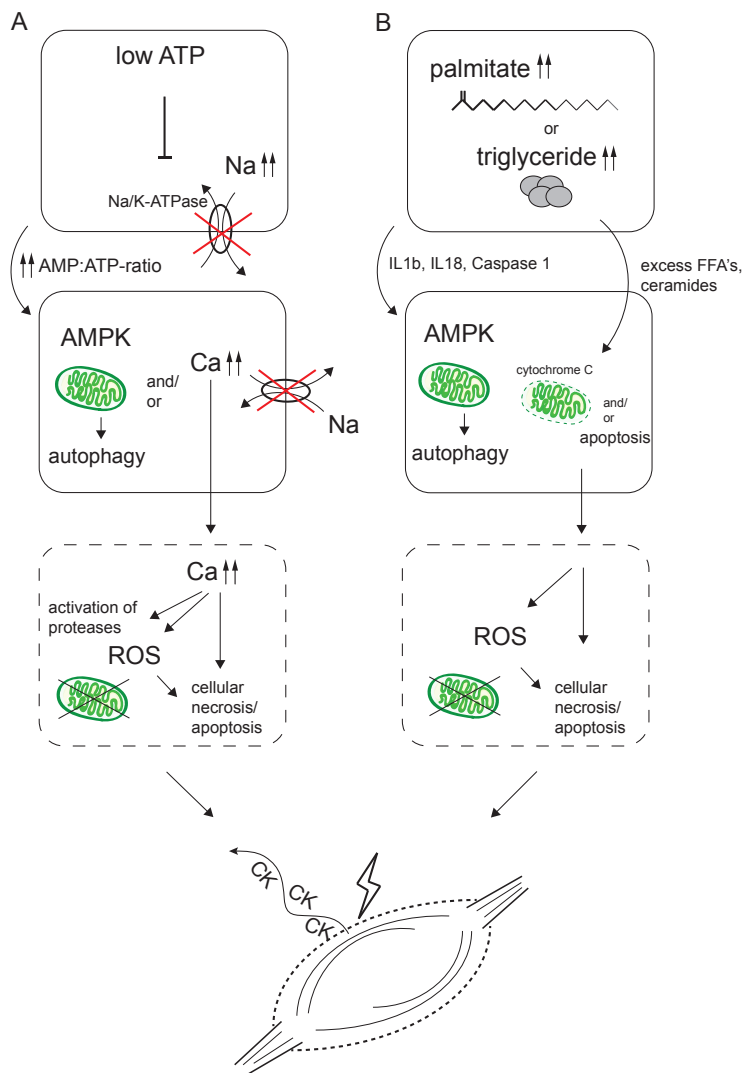


Figure 1. Compromised ATP homeostasis versus lipotoxicity. (A) A low level of ATP (and thus high AMP levels) impairs the function of the Na-K-ATPase, with as a consequence an increase in intracellular sodium. This in turn reduces the sodium-calcium exchange and leads to a concomitant accumulation of free calcium in the cell. Increased levels of cytosolic calcium disturb the interaction of actin with myosin, activate proteases, induce ROS (reactive oxygen species) and ultimately lead to (fiber) necrosis and release of creatine kinase (CK). (B) Non-adipocytes, however, have a limited triglyceride storage capability. An excess amount of free fatty acids (FFA) and ceramides could increase the permeability of mitochondria, and could activate cytochrome C and apoptosis. It is also known that palmitate induces the formation of an inflammasome that activates caspase 1, leading to increased production of IL-1 β and IL-18. This in turn induces inflammation and autophagy via activated AMPK (AMP-activated protein kinase).

accumulation of free calcium in the cell. Increased levels of cytosolic calcium disturb the interaction of actin with myosin, activate proteases, induce ROS (reactive oxygen species), and ultimately lead to (fiber) necrosis and release of CK¹⁵. The possibility of ATP-depletion as a cause of rhabdomyolysis was studied in **chapter 7**, by measuring PCr, Pi and ATP in real time during endurance exercise in LcFAO deficient patients. ATP depletion was not observed. However, there was a decrease in PCr and an increase of Pi under low intensity exercise. Based on our computational modelling calculations, a fiber type switch in patients to a more glycogenic muscle fibre type (type 2) was proposed. Since type 2 fibers are more prone to necrosis¹⁶, patients may be more likely to develop rhabdomyolysis. Increased water content possibly due to cytotoxic edema/necrosis and/or fluid accumulation secondary to inflammation was indeed observed in **chapter 6**. Whether it is primarily the type 2 fibers that necrotise remains to be elucidated. For this a detailed analysis of muscle biopsies is necessary.

2) Another mechanism that may cause rhabdomyolysis is lipotoxicity. Fatty infiltration on muscle MRI was observed in some patients with LcFAO deficiency as described in **chapter 6**. Intramyocellular lipid accumulation was also observed in heart muscle of fasting LCAD^{-/-} mice (mice have two acyl-CoA dehydrogenase (ACAD) enzymes, very long-chain acyl-CoA dehydrogenase (VLCAD) and long-chain acyl-CoA dehydrogenase (LCAD), see chapter 8 for more information). In this study Bakermans et al. revealed increased levels of triglycerides in the heart with a corresponding decrease in cardiac function¹⁷. In **chapter 9** two patients are described, one of which may have developed rhabdomyolysis after exposure to the anesthetic propofol, which contains high dose of long-chain fatty acids as it is formulated as an emulsion of soybean oil and phospholipids. These three observations suggest a role of accumulating fatty acids in the pathophysiology of disease. It is known that cells are able to esterify accumulating fatty acids and store them as triglycerides in lipid droplets. Non-adipocytes, however, have a limited triglyceride storage capability. An excess amount of free fatty acids and ceramides could have direct consequences to cellular organelles, including an increased permeability of mitochondria, cytochrome C activation and activation of apoptosis among other consequences¹⁸ (Figure 1). It is also known that palmitate induces the formation of an inflammasome that activates caspase 1, leading to increased production of IL-1 β and IL-18. This in turn induces inflammation and autophagy via activated AMP-activated kinase (AMPK)¹⁹ (Figure 1). All these processes are cytotoxic. The lipid accumulation observed in **chapter 6** and in LCAD^{-/-} mice¹⁷ are however only associated with decreased function and/or rhabdomyolysis. This does not necessarily imply a causal relationship. Alternatively, lipids may also accumulate intermyocellularly via the differentiation of bipotent progenitor cells (fibro-Adipogenic-Progenitor cells, or FAPs) into adipocytes (instead of myocytes). A process that might be triggered by frequent rhabdomyolysis²⁰⁻²².

To study the above-mentioned mechanisms in detail, a new mouse model was developed, the LCAD^{-/-}; VLCAD^{+/-} mouse as described in **chapter 8**. This model was expected to display a more severe muscle phenotype than the already extensively characterized LCAD^{-/-}; VLCAD^{+/+} mouse. The LCAD^{-/-}; VLCAD^{+/-} as well as the LCAD^{-/-}; VLCAD^{+/+} mouse showed fasting-induced inactivity, hypothermia and reduction in energy expenditure. Unexpectedly, the observed inactivity was not explained by rhabdomyolysis, but rather reflected the overall reduced capacity of these mice to generate heat. A mouse model to study the myopathic phenotype has therefore not been established yet.

Hence, the exact cause of rhabdomyolysis is still unclear. Future studies in mice with a myopathic phenotype or in humans with use of new techniques in more powerful magnets (3T/7T) with/without MRS, might be able to address this issue in more detail.

POLYNEUROPATHY AND RETINOPATHY

Hypoglycemia, cardiomyopathy and myopathy, are described in all lcFAO disorders, but polyneuropathy and retinopathy are only reported in MTPD and LCHADD patients (**chapter 10**). The common denominator between these disorders is energy shortage and/or accumulation of lipids. The only difference between MTPD and LCHADD and other lcFAO disorders is the type of substrate (or lipid) accumulation. Accumulating acyl-CoAs in VLCAD deficient patients can be converted back to acylcarnitines via CPT2 and exported out of the mitochondria and cell²³. Enoyl-CoAs, which are the products of acyl-CoA dehydrogenases, are not efficiently converted into acylcarnitines²³ and might accumulate to higher levels and remain in the mitochondria for a longer period (Figure 1 Introduction). In addition, enoyl-CoAs and 3-hydroxyacyl-CoA might be inherently more toxic than regular acyl-CoAs. We therefore hypothesize that the accumulation of enoyl-CoAs (in MTPD) and/or 3-hydroxy-acyl-CoAs is causing polyneuropathy and/or retinopathy. Future studies will reveal whether this hypothesis is true.

REVISITING CURRENT TREATMENTS

Dietary treatments

Currently, avoiding fasting, long-chain fatty acid (LCT) restriction and medium-chain triglyceride (MCT) supplementation are the only 'treatments' available for lcFAO deficient patients in Europe. lcFAO deficient patients cannot degrade long-chain fatty acids; in case of LCT intake restriction patients can rely on carbohydrates and proteins for energy instead. Since, lcFAO patients are still able to degrade medium-chain fatty acids, because their medium-chain acyl-CoA dehydrogenase is still working. Moreover MCTs

do not need the carnitine cycle to enter the mitochondria. Hence, MCT supplementation is given to some patients as an alternative fuel. However, for this compound to have any beneficial effect (improvement of intracellular energy status or less accumulation of long-chain fatty acids) it is required that 1) MCTs reach the heart and skeletal muscle, 2) MCTs are not degraded or elongated by the liver, and 3) if MCTs are degraded by the liver, MCTs should (at least) induce ketogenesis.

Based on the available literature, only small amounts of medium-chain fatty acids or medium-chain triglycerides can be found in plasma of preterm neonates²⁴⁻²⁶ after MCT treatment, and virtually none in plasma of adults²⁷⁻³⁰. In addition, it has been shown that preterm neonates and adults treated with MCT have equal (or higher) long-chain fatty acids and long-chain triglyceride levels compared to individuals treated with LCT²⁴⁻³⁰. Multiple animal studies have confirmed these findings³¹⁻³⁴. One study also investigated the constituents of the portal vein and show that medium-chain fatty acids or medium-chain triglycerides, while still present in the portal vein (pre-liver), were absent in blood plasma (post-liver)³².

The presence of MCTs in the portal vein and absence of MCTs in peripheral blood plasma suggests that MCTs are used for FAO and/or chain elongation in the liver. Indeed, it is known that MCT induces ketogenesis (and thus FAO)³⁵⁻³⁷. It is known that patients with epilepsy benefit from a high fat (MCT with/without LCT) and low carbohydrate diet. This way ketogenesis is stimulated and the brain relies on ketones instead of glucose. In the liver, medium-chain fatty acids rapidly cross the cellular and mitochondrial membrane. Medium-chain fatty acids are then activated by medium chain acyl-CoA synthetase and ready for oxidation. This results in an excess of acetyl-CoAs (the capacity of the Krebs cycle is limited, which is caused by a shortage of oxaloacetate), which stimulates ketogenesis³⁵. Two papers addressed whether MCT induces ketogenesis in LCHADD patients. The first showed a slight increase in ketone levels after 50%carb(juice)/50%MCT bolus and the second demonstrated no increase in ketone levels 2h after 70%carb/30%MCT tube feed^{38,39}. Since ketogenic diets do induce ketogenesis with high ketone levels, a high and consistent amount of MCT in the diet might be the only way to induce ketogenesis in IcFAO deficient patients. Whether or not patients really benefit from MCT treatment remains to be elucidated in future studies. If any effect could be established it is likely due to the ketogenic effect of MCTs. Since the heart favours ketones over fatty acids⁴⁰, it could be an important treatment to manage (acute) cardiomyopathy.

Other treatments

In **chapter 7** it was described that performing a certain amount of physical activity might paradoxically be beneficial, because 1) training increases the muscle content of glycogen, 2) training increases the quantity of mitochondria and 3) training increases capillary density per myofibril¹⁵. One of our patients does indeed lead an active lifestyle including heavy work and playing soccer, despite higher basal CK levels, indicating more structural (chronic) muscle damage.

Pharmacological (partial) restoration of mitochondrial function is also feasible as described in the introduction of this thesis. Most work has been done on treating patients with bezafibrate.

FUTURE CLINICAL TRIALS IN LCFAO DEFICIENT PATIENTS: WEARABLE TECHNOLOGY

In future clinical trials, one should thoroughly consider the clinical outcome parameters, irrespective whether MCT, triheptanoin, bezafibrate, resveratrol or any other treatment will be considered. One possibility is to perform exercise tests with/without labelled isotopes⁴¹⁻⁴³ before and after treatment. Although accurate, this method is invasive and covers only a few moments in time. An alternative to measure daily activity in a non-intrusive/obstructive and objective way might be wearable devices. These devices are increasingly available on the market, with more sensors and increased accuracy and reliability. A pedometer, GPS and barometer can already provide useful information. It can detect the amounts of steps, distance covered and flights climbed^{44,45}. More importantly, these measurements can be correlated with a continuous heart rate measurement; hereby ensuring a patient is actually wearing the device. A continuous heart rate measurement will in addition act as a patient's signature or 'fingerprint' since technology is in development that could distinguish your heart rate from somebody else's⁴⁶, hereby increasing the objectivity of such a system. Continuous heart rate monitoring might even be used as an alternative to a Holter ECG, when smart patches are available that communicate via Bluetooth with wearable devices.

Another sensor that is of high interest is the temperature sensor⁴⁷. Patients with lcFAO deficiencies are susceptible to metabolic derailment in case of fever. When a patient's temperature is increased, he/she might become ill. With a temperature sensor, a patient could be alerted in time and preventative measures could be taken to prevent metabolic derailment and subsequent hospitalization.

Another interesting sensor will be the glucose sensor. At present, glucose cannot be measured without the use of blood. After 30 years of research⁴⁸, non-invasive glucose measurement is not possible yet⁴⁹. If it does, not only diabetic patients will benefit, but lcFAO deficient newborns as well, because they are prone to develop hypoglycaemia.

Other sensors such as patches that measure oxygen levels, biosensors that measure muscle electromyography (EMG)⁵⁰, or contact lenses that could detect glucose⁵¹ will enter the market somewhere in the future and could all have great potential in monitoring disease and measurement of (future) therapies.

REFERENCES

1. Bonnet D, Martin D, Pascale de Lonlay, et al. Arrhythmias and conduction defects as presenting symptoms of fatty acid oxidation disorders in children. *Circulation*. 1999;100(22):2248–2253. doi:10.1161/01.CIR.100.22.2248.
2. Rinaldo P, Matern D, Bennett MJ. Fatty acid oxidation disorders. *Annu Rev Physiol*. 2002;64:477–502. doi:10.1146/annurev.physiol.64.082201.154705.
3. Spiekerkoetter U, Bastin J, Gillingham M, Morris A, Wijburg F, Wilcken B. Current issues regarding treatment of mitochondrial fatty acid oxidation disorders. *J Inherit Metab Dis*. 2010;33(5):555–561. doi:10.1007/s10545-010-9188-1.
4. Wanders RJ, Vreken P, Boer den ME, Wijburg FA, van Gennip AH, Ijlst L. Disorders of mitochondrial fatty acyl-CoA beta-oxidation. *J Inherit Metab Dis*. 1999;22(4):442–487.
5. Lindner M, Hoffmann GF, Matern D. Newborn screening for disorders of fatty-acid oxidation: experience and recommendations from an expert meeting. *J Inherit Metab Dis*. 2010;33(5):521–526. doi:10.1007/s10545-010-9076-8.
6. Arnold GL, VanHove J, Freedenberg D, et al. A Delphi clinical practice protocol for the management of very long chain acyl-CoA dehydrogenase deficiency. *Molecular Genetics and Metabolism*. 2009;96(3):85–90. doi:10.1016/j.ymgme.2008.09.008.
7. Laforêt P, Acquaviva-Bourdain C, Rigal O, et al. Diagnostic assessment and long-term follow-up of 13 patients with Very Long-Chain Acyl-Coenzyme A dehydrogenase (VLCAD) deficiency. *Neuromuscul Disord*. 2009;19(5):324–329. doi:10.1016/j.nmd.2009.02.007.
8. Loeber JG, Burgard P, Cornel MC, et al. Newborn screening programmes in Europe; arguments and efforts regarding harmonization. Part 1. From blood spot to screening result. *J Inherit Metab Dis*. 2012;35(4):603–611. doi:10.1007/s10545-012-9483-0.
9. Hall PL, Marquardt G, McHugh DMS, et al. Postanalytical tools improve performance of newborn screening by tandem mass spectrometry. *Genet Med*. 2014. doi:10.1038/gim.2014.62.
10. Bennett MJ, Rinaldo P, Wilcken B, Pass KA, Watson MS, Wanders RJA. Newborn screening for metabolic disorders: how are we doing, and where are we going? *Clinical Chemistry*. 2012;58(2):324–331. doi:10.1373/clinchem.2011.171215.
11. Marquardt G, Currier R, McHugh DMS, et al. Enhanced interpretation of newborn screening results without analyte cutoff values. *Genet Med*. 2012;14(7):648–655. doi:10.1038/gim.2012.2.
12. Wilcken B. Newborn Screening: Gaps in the Evidence. *Science*. 2013;342(6155):197–198. doi:10.1126/science.1243944.
13. Houten SM, Herrema H, Brinke te H, et al. Impaired amino acid metabolism contributes to fasting-induced hypoglycemia in fatty acid oxidation defects. *Hum Mol Genet*. 2013;22(25):5249–5261. doi:10.1093/hmg/ddt382.
14. Engbers HM, Dorland L, De Sain MGM, Eskes PF, Visser G. Rhabdomyolysis in early-onset very long-chain acyl-CoA dehydrogenase deficiency despite normal glucose after fasting. *J Inherit Metab Dis*. 2005;28(6):1151–1152. doi:10.1007/s10545-005-0190-y.
15. Mechanisms of rhabdomyolysis. 1993;5(6):725–731. Available at: <http://eutils.ncbi.nlm.nih.gov/entrez/eutils/elink.fcgi?dbfrom=pubmed&id=8117534&retmode=ref&cmd=prlinks>.
16. Brumback RA. Iodoacetate inhibition of glyceraldehyde-3-phosphate dehydrogenase as a model of human myophosphorylase deficiency (McArdle's disease) and *J Neurol Sci*. 1980;48(3):383–398. doi:10.1016/0022-510X(80)90110-0.
17. Bakermans AJ, Geraedts TR, van Weeghel M, et al. Fasting-Induced Myocardial Lipid Accumulation in Long-Chain Acyl-CoA Dehydrogenase Knockout Mice Is Accompanied by Impaired Left

- Ventricular Function. *Circulation: Cardiovascular Imaging*. 2011;4(5):558–565. doi:10.1161/CIRCIMAGING.111.963751.
18. Schaffer JE. Lipotoxicity: when tissues overeat. *Curr Opin Lipidol*. 2003;14(3):281–287. doi:10.1097/01.mol.0000073508.41685.7f.
 19. Wen H, Gris D, Lei Y, et al. Fatty acid-induced NLRP3-ASC inflammasome activation interferes with insulin signaling. *Nat Immunol*. 2011. doi:10.1038/ni.2022.
 20. Joe AWB, Yi L, Natarajan A, et al. Muscle injury activates resident fibro/adipogenic progenitors that facilitate myogenesis. *Nat Cell Biol*. 2010;12(2):153–163. doi:10.1038/ncb2015.
 21. Rodeheffer MS. Tipping the scale: muscle versus fat. *Nat Cell Biol*. 2010;12(2):102–104. doi:10.1038/ncb0210-102.
 22. Uezumi A, Fukada S-I, Yamamoto N, Takeda S, Tsuchida K. Mesenchymal progenitors distinct from satellite cells contribute to ectopic fat cell formation in skeletal muscle. *Nat Cell Biol*. 2010;12(2):143–152. doi:10.1038/ncb2014.
 23. Violante S, IJLst L, van Lenthe H, de Almeida IT, WANDERS RJ, Ventura FV. Carnitine palmitoyltransferase 2: New insights on the substrate specificity and implications for acylcarnitine profiling. *Biochim Biophys Acta*. 2010;1802(9):728–732. doi:10.1016/j.bbadis.2010.06.002.
 24. Carnielli VP, Rossi K, Badon T, et al. Medium-chain triacylglycerols in formulas for preterm infants: effect on plasma lipids, circulating concentrations of medium-chain fatty acids, and essential fatty acids. *Am J Clin Nutr*. 1996;64(2):152–158.
 25. Lehner F, Demmelmair H, Röschinger W, et al. Metabolic effects of intravenous LCT or MCT/LCT lipid emulsions in preterm infants. *The Journal of Lipid Research*. 2006;47(2):404–411. doi:10.1194/jlr.M500423-JLR200.
 26. Rodriguez M, Funke S, Fink M, et al. Plasma fatty acids and [13C]linoleic acid metabolism in preterm infants fed a formula with medium-chain triglycerides. *The Journal of Lipid Research*. 2003;44(1):41–48. doi:10.1007/s11010-008-0007-z.
 27. Hill JO, Peters JC, Swift LL, et al. Changes in blood lipids during six days of overfeeding with medium or long chain triglycerides. *The Journal of Lipid Research*. 1990;31(3):407–416.
 28. Dias VC, Fung E, Snyder FF, Carter RJ, Parsons HG. Effects of medium-chain triglyceride feeding on energy balance in adult humans. *Metab Clin Exp*. 1990;39(9):887–891.
 29. Cater NB, Heller HJ, Denke MA. Comparison of the effects of medium-chain triacylglycerols, palm oil, and high oleic acid sunflower oil on plasma triacylglycerol fatty acids and lipid and lipoprotein concentrations in humans. *Am J Clin Nutr*. 1997;65(1):41–45.
 30. Tholstrup T, Ehnholm C, Jauhiainen M, et al. Effects of medium-chain fatty acids and oleic acid on blood lipids, lipoproteins, glucose, insulin, and lipid transfer protein activities. *Am J Clin Nutr*. 2004;79(4):564–569.
 31. Leveille GA, Pardini RS, Tillotson JA. Influence of medium-chain triglycerides on lipid metabolism in the rat. *Lipids*. 1967;2(4):287–294. doi:10.1007/BF02532113.
 32. You Y-QN, Ling P-R, Qu JZ, Bistrrian BR. Effects of medium-chain triglycerides, long-chain triglycerides, or 2-monododecanoin on fatty acid composition in the portal vein, intestinal lymph, and systemic circulation in rats. *Journal of Parenteral and Enteral Nutrition*. 2008;32(2):169–175. doi:10.1177/0148607108314758.
 33. Innis SM, Quinlan P, Diersen-Schade D. Saturated fatty acid chain length and positional distribution in infant formula: effects on growth and plasma lipids and ketones in piglets. *Am J Clin Nutr*. 1993;57(3):382–390.
 34. Crozier GL. Medium-chain triglyceride feeding over the long term: the metabolic fate of [14C] octanoate and [14C]oleate in isolated rat hepatocytes. *J Nutr*. 1988;118(3):297–304.

35. Bach AC, Babayan VK. Medium-chain triglycerides: an update. *Am J Clin Nutr.* 1982;36(5):950–962.
36. Huttenlocher PR, Wilbourn AJ, Signore JM. Medium-chain triglycerides as a therapy for intractable childhood epilepsy. *Neurology.* 1971;21(11):1097–1103.
37. Huttenlocher PR. Ketonemia and seizures: metabolic and anticonvulsant effects of two ketogenic diets in childhood epilepsy. *Pediatric Research.* 1976;10(5):536–540. doi:10.1203/00006450-197605000-00006.
38. Gillingham MB, Scott B, Elliott D, Harding CO. Metabolic control during exercise with and without medium-chain triglycerides (MCT) in children with long-chain 3-hydroxy acyl-CoA dehydrogenase (LCHAD) or trifunctional protein (TFP) deficiency. *Molecular Genetics and Metabolism.* 2006;89(1-2):58–63. doi:10.1016/j.ymgme.2006.06.004.
39. Lund AM, Dixon MA, Vreken P, Leonard JV, Morris AAM. What is the role of medium-chain triglycerides in the management of long-chain 3-hydroxyacyl-CoA dehydrogenase deficiency? *J Inherit Metab Dis.* 2003;26(4):353–360.
40. Forsey R, Reid K. Competition between fatty acids and carbohydrate or ketone bodies as metabolic fuels for the isolated perfused heart. *Canadian journal of.* 1987. doi:10.1139/y87-067.
41. Ørngreen MC, Nørgaard MG, Sacchetti M, van Engelen BGM, Vissing J. Fuel utilization in patients with very long-chain acyl-coa dehydrogenase deficiency. *Ann Neurol.* 2004;56(2):279–283. doi:10.1002/ana.20168.
42. Ørngreen MC, Dunø M, Ejstrup R, et al. Fuel utilization in subjects with carnitine palmitoyltransferase 2 gene mutations. *Ann Neurol.* 2005;57(1):60–66. doi:10.1002/ana.20320.
43. Orngreen MC, Madsen KL, Preisler N, Andersen G, Vissing J, Laforêt P. Bezafibrate in skeletal muscle fatty acid oxidation disorders: A randomized clinical trial. *Neurology.* 2014. doi:10.1212/WNL.0000000000000118.
44. Harder-Lauridsen NM, Birk NM, Ried-Larsen M. A randomized controlled trial on a multicomponent intervention for overweight school-aged children-Copenhagen, Denmark. *BMC* 2014. doi:10.1186/1471-2431-14-273.
45. Carr LJ, Karvinen K, Peavler M, Smith R. Multicomponent intervention to reduce daily sedentary time: a randomised controlled trial. *BMJ open.* 2013. doi:10.1136/bmjopen-2013-003261.
46. Agrafioti F. ECG in Biometric Recognition: Time Dependency and Application Challenges. 2011:1–188.
47. Liu G, Mao L, Chen L, Xie S. Locatable-body temperature monitoring based on semi-active UHF RFID tags. *Sensors (Basel).* 2014;14(4):5952–5966. doi:10.3390/s140405952.
48. Smith JL. The Pursuit of Noninvasive Glucose: “Hunting the Deceitful Turkey”. 2011:1–141.
49. Lodwig V, Kulzer B, Schnell O, Heinemann L. Current Trends in Continuous Glucose Monitoring. *J Diabetes Sci Technol.* 2014;8(2):390–396. doi:10.1177/1932296814525826.
50. Chan M, Estève D, Fourniols J-Y, Escriba C, Campo E. Smart wearable systems: current status and future challenges. *Artificial Intelligence In Medicine.* 2012;56(3):137–156. doi:10.1016/j.artmed.2012.09.003.
51. Novartis to license Google “smart lens” technology. 2014:1–3.

APPENDIX

Nederlandse Samenvatting

Dankwoord

List of publications

Curriculum Vitae



NEDERLANDSE SAMENVATTING

Elke dag consumeert een gemiddeld mens 35% van zijn totale energie inname als vet. Het overgrote deel van dit vet bestaat uit lange-keten vetzuren. Deze lange-keten vetzuren worden opgenomen in de darm en worden uiteindelijk in de cellen met behulp van verscheidene enzymen verwerkt tot energie. In tegenstelling tot middellange of korte keten vetzuren, kunnen lange-keten acyl-CoA's (C12-C18) zonder actief transport niet het mitochondrion in. Voor toegang tot het mitochondrion, moeten lange-keten acyl-CoA's omgezet worden naar acylcarnitines met behulp van carnitine palmitoyltransferase1 (CPT1). CPT1 vervangt -CoA voor -carnitine (zie figuur 1 Introductie). Vervolgens worden de lange-keten acylcarnitines getransporteerd door het buitenste en binnenste membraan van het mitochondrion door carnitine acylcarnitine translocase (CACT). Eenmaal in het mitochondrion worden de lange-keten acyl-CoA's weer omgezet naar acyl-CoA's door carnitine palmitoyltransferase 2 (CPT2). De lange-keten acyl-CoA's worden dan verwerkt door enzymen betrokken bij β -oxidatie zoals very long-chain acyl-CoA dehydrogenase (VLCAD) en mitochondrial trifunctional protein (MTP). Al deze enzymen zijn noodzakelijk om een essentiële component in de productie van energie te maken: acetyl-CoA.

Voor tekorten aan elk van deze enzymen zijn menselijke aandoeningen beschreven die vetzuuroxidatiestoornissen genoemd worden. Patiënten met vetzuuroxidatiestoornissen kunnen zich presenteren met een hypoketotische hypoglycemie, hepatomegalie, cardiomyopathie, myopathie, polyneuropathie en retinopathie. Deze verschillende symptomen illustreren de cruciale rol van vetzuuroxidatie in vele fysiologische processen. De inclusie van lange keten vetzuuroxidatiestoornissen in de neonatale hielprik screening zorgt ervoor dat levensbedreigende symptomen zoals hypoglycemie en cardiomyopathie meestal kunnen worden voorkomen. Dieet adviezen kunnen daarnaast metabole ontsparingen voorkomen. Desondanks moeten veel patiënten nog in het ziekenhuis worden opgenomen en zijn vele patiënten niet in staat om te sporten of deel te nemen aan het normale dagelijkse leven.

Het doel van dit proefschrift is het verbeteren van de toekomst van patiënten met lange keten vetzuur oxidatiestoornissen door onder andere door het inzicht in de pathogenese van rhabdomyolyse en cardiomyopathie te vergroten.

Neonatale hielprik screening

Met de huidige ontwikkelingssnelheid van nieuwe biochemische, genetische en post-analytische technieken, zullen meer en meer ziekten worden gedetecteerd met steeds hogere sensitiviteit.

Lange keten vetzuuroxidatie deficiënte patiënten worden met behulp van de acylcarnitine analyse in de bloedspots van hielprikkaarten geanalyseerd. Deze acylcarnitines

kunnen ook in het bloedplasma bepaald worden. In **hoofdstuk 2** worden de verschillen in acylcarnitine profielen in bloedspots en plasma vergeleken. Daarbij zijn optimale ratio's bepaald om carnitine palmitoyl transferase 1a en 2 (CPT1a en CPT2) (aandoeningen die nog niet in het huidige Nederlandse hielpikscreeningsprogramma zijn opgenomen) in bloedspots te detecteren.

Alhoewel bloedspot acylcarnitine analyse een goede manier is om very long-chain acyl-CoA (VLCAD) deficiënte patiënten te detecteren, zijn er desondanks patiënten gemist bij de hielprikscreening. In **hoofdstuk 3** wordt een nieuwe marker beschreven die de sensitiviteit om VLCAD deficiënte patiënten op te sporen verhoogd. Eenmaal gediagnostiseerd met VLCAD deficiëntie is het alleen nog erg moeilijk om de ernst van de symptomen te voorspellen. In **hoofdstuk 4** is gezocht naar mogelijke voorspellers van klinische ernst. Wat bleek was dat de lange keten vetzuuroxidatie flux meting in fibroblasten de beste voorspeller voor de klinische ernst is. Met deze studie kan al een voorzichtig onderscheid gemaakt worden tussen patiënten die waarschijnlijk veel last van de ziekte gaan krijgen en welke patiënten niet.

Vervolgen van de ziekte

Het menselijke hart haalt voor 60-90% van zijn energiebehoefte uit de vetzuuroxidatie. Om eventuele cardiale complicaties op te sporen wordt het hart bij patiënten met vetzuuroxidatiestoornissen frequent gecontroleerd. Op dit moment zijn echocardiografie en (Holter)ECG de gouden standaard om de hartfunctie te bepalen. In **hoofdstuk 5** is de hartfunctie bepaald in een cohort van 20 kinderen. Onverwacht werd een normale hartfunctie gezien in vrijwel alle kinderen. Wel werd met behulp van een aanvullende techniek gekeken of er sprake was van subklinische myocardiale dysfunctie. In vele vetzuuroxidatie deficiënte patiënten werd een minimale vermindering in myocardiale contractiliteit gevonden. Het is nog onduidelijk wat de klinische betekenis is van deze bevindingen zullen zijn voor de toekomst.

Rhabdomyolyse

Skeletspieren gebruiken de vetzuuroxidatie voor hun energievoorziening, met name gedurende duursporten. In **hoofdstuk 6** is een cohort van 20 patiënten met lange keten vetzuuroxidatie stoornissen onderzocht waarbij vrijwel geen verlies in spierkracht werd geobserveerd. Wel werd in mitochondrial trifunctional protein (MTP) deficiënte patiënten sensorisch verlies gezien, met name polyneuropathie, maar ook contracturen en atrofie. Daarnaast zijn de gevolgen van herhaalde episodes van rhabdomyolyse op spieren van patiënten met lange keten vetzuuroxidatiestoornissen in beeld gebracht met behulp van een MRI spieren. Er werden daarbij specifieke afwijkingen gezien welke mogelijk wijzen op inflammatie en vetaccumulatie. Dit kan secundair zijn ontstaan aan het vetzuuroxidatiedefect of mogelijk door de herhaaldelijke episodes van rhabdomyo-

lyse. MRI van de spieren lijkt dan ook een betere techniek om de subacute en lange termijn effecten van lange keten vetzuuroxidatie te monitoren dan het meten van de creatine kinase (CK) concentratie in het bloed. De CK concentratie stijgt en daalt namelijk binnen uren tot dagen in de acute fasen van rhabdomyolyse. Toekomstige studies zullen moeten uitwijzen of de geobserveerde afwijkingen toenemen of stabiliseren over tijd.

De pathofysiologie van rhabdomyolyse is nog altijd niet geheel duidelijk. Gebaseerd op observaties in ons cohort blijkt dat zo'n 8-12u na start ziekte of koorts de creatine kinase concentraties stijgen met een maximum CK concentratie na zo'n 24-48u. Het is ook bekend dat CK concentraties kunnen stijgen ondanks normoglycemie.

Twee mechanismen zijn voorgesteld die de rhabdomyolyse mogelijk verklaren in lange keten vetzuuroxidatie deficiënte patiënten: 1) een falend compensatiemechanisme tijdens katabole situaties (bijvoorbeeld tijdens sporten, koorts, vasten) en de daaropvolgende ATP depletie. 2) toxiciteit veroorzaakt door ophoping van lange keten vetzuur oxidatie tussenproducten.

1) Aangenomen wordt dat een lage ATP (en dus verhoogde AMP) de werking van de Na-K-ATPase belemmert, met als gevolg een toename van de intracellulaire natriumconcentratie. Hierdoor vermindert de natrium- calcium-uitwisseling wat leidt tot een gelijktijdige accumulatie van vrij calcium in de cel. Verhoogde niveaus van cytosolisch calcium verstoren de interactie van actine met myosine, activeert proteasen en induceert ROS (reactive oxygen species), dat uiteindelijk leidt tot (spiervezel) necrose en het vrijkomen van CK. De mogelijkheid van een ATP-depletie als oorzaak van rhabdomyolyse werd bestudeerd in **hoofdstuk 7**, door het meten van PCr, Pi en ATP in real time tijdens duur sport. ATP depletie werd niet waargenomen. Er werd echter wel een afname van PCr en een toename van Pi onder lage intensiteit waargenomen. Gebaseerd op computational modelling berekeningen, werd een vezeltype verandering gezien in patiënten met het glycogene spiervezel type (type 2). Aangezien type 2 vezels meer vatbaar zijn voor necrose, hebben deze patiënten meer kans op het ontwikkelen van rhabdomyolyse. Vocht ophoping, mogelijk als gevolg van cytotoxische oedeem/necrose en/of vochtophoping secundair aan een ontsteking werden inderdaad waargenomen in **hoofdstuk 6**. Of het vooral de type 2 vezels zijn die necrotiseren moet nog worden onderzocht. Hiervoor is een gedetailleerde analyse van spierbiopten noodzakelijk.

2) Een ander mechanisme dat rhabdomyolyse kan veroorzaken is lipotoxiciteit. Vet-tige infiltratie werd gezien op de MRI spieren bij sommige patiënten met lange keten vetzuuroxidatiestoornissen, zoals beschreven in **hoofdstuk 6**. Intramyocellulaire lipide accumulatie werd ook waargenomen door Bakermans et al. in de hartspier van vastende LCAD^{-/-} muizen (muizen hebben twee acyl-CoA dehydrogenase (ACAD) enzymen, very long-chain acyl-CoA dehydrogenase (VLCAD) en long-chain acyl-CoA dehydrogenase (LCAD)), zie hoofdstuk 8 voor meer informatie). In de studie van Bakermans et al. werden

verhoogde concentraties triglyceriden in het hart gemeten met een overeenkomstige daling van de hartfunctie.

Om bovengenoemde mechanismen in detail te onderzoeken, werd een nieuw muismodel ontwikkeld, de LCAD^{-/-}; VLCAD^{+/-} muis zoals beschreven in **hoofdstuk 8**. Verwacht werd dat dit muismodel een ernstiger spierfenotype zou laten zien dan de reeds uitgebreid gekarakteriseerde LCAD^{-/-}; VLCAD^{+/+} muis. Zowel de LCAD^{-/-}; VLCAD^{+/-} als de LCAD^{-/-}; VLCAD^{+/+} muizen werden tijdens vasten inactief, ze verlaagden hun lichaamstemperatuur en de muizen brachten hun energie verbruik omlaag. Onverwacht waren de muizen niet inactief vanwege rhabdomyolyse, maar eerder het gevolg van de algemene daling van het vermogen van deze muizen om warmte te genereren. Een muismodel om het myopathische fenotype te kunnen bestuderen is daarom nog niet gevonden. Vandaar dat de precieze oorzaak van rhabdomyolyse nog niet geheel duidelijk is. Toekomstige studies in muizen met een myopathische fenotype of studies bij mensen met gebruik van nieuwe technieken in meer krachtige magneten (3T / 7T) met / zonder MRS, zouden meer inzicht kunnen geven in deze kwestie.

Polyneuropathie en retinopathie

Hypoglykemie, cardiomyopathie en myopathie, worden beschreven in alle lange keten vetzuuroxidatiestoornissen, maar polyneuropathie en retinopathie komen alleen voor in MTP en LCHAD deficiënte patiënten (**hoofdstuk 10**). De gemene deler tussen deze aandoeningen is energietekort en/of accumulatie van lipiden. Het enige verschil tussen MTP en LCHAD deficiëntie en andere lange keten vetzuuroxidatiestoornissen is het type substraat (of lipide) dat ophoopt. Ophopende acyl-CoA's in VLCAD deficiënte patiënten kunnen weer worden omgezet naar acylcarnitines via CPT2 en vervolgens geëxporteerd uit de mitochondriën en de cel. Enoyl-CoA, het eindproduct van acyl-CoA dehydrogenase kan echter niet efficiënt omgezet worden naar acylcarnitines. Hierdoor hopen acyl-CoA's op tot hoge concentraties en kunnen gedurende een lange tijd in de mitochondriën blijven (figuur 1 Inleiding). Bovendien zijn enoyl-CoA en 3-hydroxyacyl-CoA inherent toxischer voor de cel dan gewone acyl-CoA's. De veronderstelling is derhalve dat de ophoping van enoyl-CoA (in MTP deficiëntie) en/of 3-hydroxy-acyl-CoA's (LCHAD deficiëntie) polyneuropathie en/of retinopathie veroorzaakt. Toekomstig onderzoek zal moeten uitwijzen of deze hypothese klopt.

Ingrepen en nieuwe ziekte presentaties

Wanneer patiënten met lange keten vetzuuroxidatiestoornissen een chirurgische ingreep moeten ondergaan, is het van belang om de energie homeostase te verbeteren en een lange keten vetzuurload te voorkomen. De gedachte is dat dat de kans op rhabdomyolyse verminderd. In **hoofdstuk 9** worden daarvoor specifieke perioperatieve maatregelen voor besproken.

Neonatale hielprik screening onderscheidt geïsoleerde LCHAD deficiëntie, LCKAT deficiëntie en MTP deficiëntie niet. In **hoofdstuk 10** wordt een classificatiesysteem beschreven om deze ziekten wel te kunnen onderscheiden op basis van enzym activiteits metingen. Dit systeem is toegepast op 2 nieuwe cases, zoals beschreven in hoofdstuk 10. Een van de cases presenteerde met necrotiserende enterocolitis, een symptoom dat nog niet eerder is geassocieerd met MTP deficiëntie.

Tot slot worden in **hoofdstuk 11** alle bevindingen bediscussieerd en toekomstige onderzoeksrichtingen beschreven.

ACKNOWLEDGEMENTS

"It's the question that drives us,... It's the question that brought [me] here."

Onderzoek doen begint altijd met een vraag. Die kun je misschien zelf hebben bedacht, of een ander, maar het daadwerkelijke antwoord vinden doe je eigenlijk nooit alleen. Ik wil daarom graag een aantal mensen in het bijzonder op deze plek bedanken voor al hun hulp bij het tot stand komen van dit proefschrift.

In de eerste plaats wil ik alle patiënten en families die hebben deelgenomen aan dit onderzoek heel hartelijk danken. Zonder u, geen onderzoek en geen proefschrift. Ik ben er trots op dat de behaalde resultaten zullen bijdragen aan een betere zorg voor patiënten met lange-keten vetzuuroxidatiestoornissen.

Mijn promotoren en copromotoren. Ik wil hen hartelijk danken voor de uitstekende en zeer plezierige begeleiding:

Prof. dr. R.J.A. Wanders, beste Ronald. Jouw enthousiasme tijdens de werkbijeenkomsten werkte aanstekelijk. Je ziet kansen waar anderen beren zien. Bovendien bewonder ik je open houding binnen het veld. Ik zal het moment niet vergeten dat we op een congres zaten te praten terwijl ondertussen alle grote namen in het veld je een hand wilden geven. Je ziet je buitenlandse collega's als concullega's en minder als concurrenten, waardoor samenwerking binnen handbereik ligt.

Prof. dr. E.E.S. Nieuwenhuis, beste Edward. Onze werkbijeenkomsten waren niet lang, maar altijd 'to-the-point'. Het was bijna een soort pitch van m'n onderzoeksresultaten. Dat was erg leerzaam want 't zorgde ervoor dat ik me moest focussen op de essentie. Bovendien heb je de eigenschap om zaken vanuit een andere invalshoek te bekijken. Ik zal niet vergeten hoe je me op een gegeven moment vroeg of tonijnvissers in Japan ook MRI's van hun gevangen tonijn maken om de kwaliteit te beoordelen (in het kader van hoofdstuk 6). Ik heb het antwoord helaas niet gevonden..

Dr. G. Visser, beste Gepke. Wat gaaf dat ik je heb mogen helpen bij het opzetten van onderzoek naar lange keten vetzuuroxidatiestoornissen in Nederland. Fijn dat je me enerzijds de ruimte gaf voor m'n nieuwe ideeën en anderzijds oog had voor de grote lijn en de omvang van het onderzoek. Ik blijf me verbazen over je capaciteit om een goed netwerk om je heen te bouwen en datgene te regelen om stappen verder te komen. Op persoonlijk vlak zal ik het bespreken van nieuwe films wel missen. Ik weet nog dat je de film *Limitless* voor m'n verjaardag gaf. Toffe film, soms zou ik willen dat ik net als

de hoofdrolspeler zo'n pilletje kon nemen. Dan kon ik nog meer doen in dezelfde tijd. Trouwens, 12 Angry men al gekeken?

Gepke, ik wil je heel erg bedanken voor de leuke tijd, de prettige samenwerking, je enthousiasme en inzet, maar ook voor je goede zorgen zowel op 't werk als privé. Je bent voor mij een voorbeeld van iemand die gezin, kliniek en onderzoek weet te combineren. Iets waarvan ik nu al inzie dat dat niet zo gemakkelijk is.

Dr. S.M. Houten, beste Sander. Ik had al snel door dat ik altijd bij je terecht kon om te sparren over hypotheses, theorieën of gewoon voor uitleg. Je hebt oog voor detail en je wil dat iets echt klopt, zowel tijdens experimenten, als bij het schrijven van papers. Net altijd die ene stap verder denken, dat is iets wat ik wil meenemen in m'n toekomstige werk. Verder heb je me geïntroduceerd in het muizenonderzoek. Hierdoor heb ik geleerd wat de kracht is van dit type onderzoek. Ik zal je geduld en je humor wel missen, net als onze uurtjes in het Aria-S, de dissecties en het ge-ouwehoer in de AIO-kamer. Daarvoor moeten we nu naar New York. En dat is geen straf, want die werkbijeenkomst die we daar hadden, midden in Central Park bij 30 graden, was onvergetelijk..

De leden van de leescommissie, Prof. dr. V.V.A.M. Knoers, Prof. dr. K.P.J. Braun, Prof. dr. A.J. Verhoeven, Prof. dr. G.P.A. Smit, Dr. N.M. Verhoeven-Duif, wil ik allen hartelijk danken voor het kritisch lezen en beoordelen van mijn proefschrift.

Alle betrokkenen bij het spieren voor spieren kindercentrum wil ik bedanken voor hun hulp bij het zien van de patiënten. Ludo (van der Pol), bedankt voor je inzet, van jou heb ik goed neurologisch onderzoek geleerd en ook je soms ongezouten mening was erg verfrissend. Christiaan (Blank) en Folkert (Asselbergs), bedankt voor het cardiologisch in kaart brengen van alle patienten. Ik ben nog steeds gebiologeerd door de subklinische myocarddysfunctie die we gevonden hebben bij VLCADD patiënten. Wat daar precies aan de hand is vraagt om verder onderzoek. Ron (van Empelen) en Marja (Schoenmakers), bedankt dat jullie ook bereid zijn geweest om de ontwikkeling van deze kinderen goed in kaart te brengen. Tot slot de ondersteuners van het Spieren voor Spieren kindercentrum, Astrid, Marjel, Bernadette, en de anderen hartelijk dank voor jullie logistieke hulp, dat was soms niet makkelijk.

Beste Merel (van Veen), Irene (Kok) en Corrie (Timmer), dankzij jullie ben ik de impact van voedingsaanpassingen op onze patiënten beter gaan begrijpen. Bedankt voor al jullie hulp bij dit onderdeel van het onderzoek.

Beste Tim (Takken), Jeroen (Jeneson) en Rutger-Jan (Nivelstein). Bedankt dat we bij patiënten inspanningstesten konden doen zowel binnen als buiten de MRI, met de

juiste apparatuur. Blijft leuk om de reactie van mensen te zien als ik ze vertel over fietsen in een MRI. Daarnaast zal ik altijd bij het bekijken van een MRI-spiere terugdenken aan het moment dat jij Rutger-Jan samen met Ludo achter de monitoren zaten en “zo dubbelblind als praktisch mogelijk was” de MRI plaatjes beoordeelden.

Beste Frits (Wijburg), werkbesprekingen in het AMC met jou erbij gaven altijd wat extra dynamiek. Je hielp ons vaak om met je kritische blik de bevindingen nog beter op ‘klinische’ waarde te schatten. Daarbij zag je mogelijkheden voor vervolgonderzoek, wat soms impuls gaf aan onze projecten.

Beste Monique (de-Sain) en alle anderen van het lab metabole ziekten in het WKZ. Bedankt voor al jullie hulp bij het bepalen van de acylcarnitines en aminozuren tijdens de MRS-studie. Bedankt ook dat ik mocht meeschrijven aan een belangrijke paper waarbij bloedspot meting met plasma werd vergeleken.

Beste Jaenette (Bleeker), de ‘nieuwe Eugene’ ;-). Ik wens je heel veel succes bij het voortzetten van dit leuke onderzoek!

Beste Peter (van Hasselt), wat leuk dat we tijdens m’n promotie ook nog ons MTHFR project met succes hebben kunnen afronden. Daarnaast waardeer ik je input voor en het sparren over het onderzoek zeer.

Beste ex-kamergenoten Judith, Maya, Sylvia, Bart, Marco en Sytze in het WKZ. Wat ben ik vaak gewisseld van plek zeg, maar mede dankzij jullie betrokkenheid en gezelligheid heb ik daar een goede tijd gehad.

Beste collega’s in het Martini. Na 3,5jr onderzoek begon ik bij jullie ‘zo groen als gras’, maar dankzij jullie heb ik veilig m’n eerste klinische ervaring op kunnen doen en ben ik klaargestoomd voor het UMCG. Hartelijk dank voor alle leerzame momenten, jullie steun tijdens het afronden van mijn promotie, de uitermate gezellig (running) diners en andere uitjes.

Beste collega’s uit het AMC: Michel, ‘Gait’, Ir., dr., makker, AIO-buddie, boer uit Heerde! Wat hebben we een lol gehad daar in F106. En in het ARIA-S. En in het muizenlabje. En daarbuiten. En daarnaast denk ik dat ik oprecht nooit meer op een zachter matje zal liggen dan bij jou en Maaïke in de badkamer. Bovendien zullen de liedjes ‘highway to hell’ en ‘tearing me apart’ mij altijd een duivelse glimlach geven. Tom, MTB held. Super tof (en gezond) om met jou door de bossen heen te karren. Riekt! Jij ouwe ouderdomskenner dat je er bent! Tof dat je betrokken bent geraakt bij het IcFAO onderzoek en thanks

voor het sparren. Vincent, met wie moet ik nu Apple's 'next big thing' bespreken? Naomi, 'Stel.' dat ik je dat nooit meer zal horen zeggen! Maxim, jij ouwe casanova! Eten is sinds ik jou ken niet meer hetzelfde. Kevin, relaxte pik. Stef en Rob, misters ALD en tot slot Olga, Olga, Evelien, Martin, Catharina, en Sara (m.a.w. 'die andere AIO-kamer' ;-)... Wat heb ik met jullie allen gelachen, maar ook vaak inhoudelijk gepraat/gespard over m'n onderzoek, hartelijk dank voor al die leuke en leerzame momenten! Dankzij jullie heb ik echt een leuke tijd gehad in het AMC.

Verder wil ik graag iedereen op het lab bedanken die me geholpen heeft met allerlei bepalingen, waaronder Jos en Sacha (voor o.a. het optimaliseren van de enzym en LC-FAO flux bepalingen), Heleen en Simone (voor jullie hulp bij de qPCR, maar zeker ook voor de gezelligheid), de MS-groep met o.a. Arno, Henk, Wim, Femke en Martin (voor het bepalen van de acylcarnitines en aminozuren), Lodewijk (voor de kritische noten en adviezen), René (voor je interesse en de lol in de gang of koffiekamer) en alle anderen van de enzym en DNA-diagnostiek!

Ook de mensen die het lab logistiek draaiende houden, waaronder Maddy, Annelies, Martin, Michel, Jan en Gerrit-Jan en natuurlijk alle anderen van het lab die ik nu niet heb genoemd, bedankt voor jullie hulp, gezelligheid en betrokkenheid bij experimenten, borrels en labdagen.

Zoals het een gestructureerd artikel betaamt nog een kleine noot voor de Materials en Methods: dank MB-EFD en rMBP-EFD. Zonder jullie niet aflatende stabiliteit, betrouwbaarheid en snelheid had ik dit proefschrift niet kunnen maken.

Beste Hinse, Daan, Janine en Stefan, we zien elkaar helaas niet vaak, maar dat is geen belemmering voor een goede vriendschap. Ieder gaat z'n eigen weg, maar het contact blijft en daar ben ik blij om.

Joep & Kim, lieve paranimfen. Jullie reageerden zo enthousiast op m'n suggestie om paranimf te worden ('t was nog niet eens een vraag) dat ik vrijwel zonder nadenken dacht, Yes dat gaan we doen! Ik vind jullie echt 'konings'! Waardoor dat komt heeft zowel te maken met veel lol maken samen, maar zeker ook met jullie oprechtheid en nuchterheid. Jullie draaien er niet omheen. Oh en dat heerlijke eten dat we eens per jaar doen. Zullen we afspreken dat we dat tot in de eeuwigheid doen? (zelfs als we ooit heel oud zijn? -> Beloof me dat we 't dan prakken en bij elkaar door die sonde heen drukken ;-).

Beste Wouter, op dit moment ligt je proefschrift in een envelop voor me. Ik open 'm nog niet, want voordat ik je dankwoord lees maak ik de mijne.

Wat hebben we bij de metabole samen met (je toen-nog-niet-meisje) Marriette een lol gehad. Niet in de laatste plaats tijdens onze 'mannen' avonden: even ons onderzoek bespreken, even zeiken, even lekker nerden. 't gaf daarbij niet dat je m'n bier opzoopt, dat ik bij jou geen haute cuisine mocht verwachten en ik van jou altijd naar die dikke Clarkson moest kijken ;-). Ik ben erg blij dat ik sindsdien een vriendschap rijker ben.

Frank, maestro, pik, makker, maat. We kennen elkaar al een hele tijd, hebben lief en leed gedeeld, maar hebben elkaar bovenal zien groeien tot wie we nu zijn. Ik hoef hier niet uit te leggen waarom ik om je geef. Toch wil ik je bedanken voor alle goede gesprekken, de lol, de vakanties, de uitjes, museumbezoekjes en wat al niet meer. Erg fijn om te weten dat ik altijd bij je terecht kan en -ondanks de afstand- altijd op je kan vertrouwen.

Lieve Marrit, schoonzussies en zwagers; Anne & Arthur, Linda & Wilko, en Robbert & Charlotte. Ik loop alweer een tijdje bij jullie rond en we hebben plezierige en droevige dingen met elkaar gedeeld, waardoor onze band sterk is geworden. Bedankt voor jullie steun en betrokkenheid.

Lieve broers, Ewald, Jurgen, Maurice; lieve schoonzussen Lisanne, Heleen en Marieke; en lieve neefjes en nichtjes, Quinten, Tim, Tijs, Meinke en Jesse. Bedankt dat jullie er altijd voor mij en Renée zijn. Ook al staat m'n onderzoek ver van jullie af, toch betekent het veel als jullie interesse tonen. Ik heb jullie lief en vind het heel fijn dat jullie er deze dag bij zijn.

Lieve pa & ma, wat ben ik blij dat jullie 30 jaar geleden besloten er nog eentje bij te nemen. Prachtig hoe jullie vanuit niets zoveel hebben opgebouwd en ook nog eens een gezin van 4 met zoveel liefde hebben groot gebracht. Bedankt voor jullie onvoorwaardelijke liefde, behulpzaamheid en steun. Ik hou van jullie en het zegt genoeg dat ik na al die jaren nog steeds heel graag thuis(-thuis) kom. Oh en pap, dat 'kastje' hè, daar is ook ooit iemand op gepromoveerd.. Ben zo blij dat je er daardoor vandaag bij kan zijn!

Tot slot richt ik mij tot Renée, m'n lieverd. Na meer dan 8 jaar wordt ik nog altijd zo blij als ik je zie. En je weet dat ik gelijk heb, want op dit moment zie je mijn blije hoofd voor je. Bedankt voor al je steun, je kritische blik, je sturing maar bovenal bedankt voor je al liefde tijdens dit deel van onze reis. The world is ours!

LIST OF PUBLICATIONS

Eugene F. Diekman, Sacha Ferdinandusse, Ludo van der Pol, Hans R. Waterham, Jos P.N. Ruiter, Lodewijk Ijlst, Ronald J. Wanders, Sander M. Houten, Frits A. Wijburg, A. Christiaan Blank, Folkert W. Asselbergs, Riekelt H. Houtkooper, Gepke Visser, 2015. Fatty acid oxidation flux predicts the clinical severity of VLCAD deficient patients. *Accepted in Genetics in Medicine*.

Eugene F. Diekman, Monique de Sain-van der Velden, Hans Waterham, A.J. Kluijtmans, Peter Schielen, Evert Ben van Veen, Sacha Ferdinandusse, F.A. Wijburg, Gepke Visser, 2015. Newborn screening paradox: sensitivity vs overdiagnosis. *Under revision Journal of Inherited Metabolic Disease*.

Eugene F. Diekman, van Michel van Weeghel, Ronald J. Wanders, Gepke Visser, Sander M. Houten, 2014. Food withdrawal lowers energy expenditure and induces inactivity in long-chain fatty acid oxidation-deficient mouse models. *FASEB J.* 2014 Jul;28(7):2891-900. doi: 10.1096/fj.14-250241.

Eugene F. Diekman, Ludo van der Pol, Rutger-Jan Nievelstein, Hans R. Waterham, Sander M. Houten, Gepke Visser, 2013. Muscle MRI in patients with long-chain fatty acid oxidation disorders. *Journal of Inherited Metabolic Disease*. doi:10.1007/s10545-013-9666-3

Eugene F. Diekman; Tom J. de Koning, Nanda M. Verhoeven-Duif, Maroeska M. Rovers, Peter M. van Hasselt, 2013. Survival and psychomotor development with early betaine treatment in patients with severe methylenetetrahydrofolate reductase deficiency. *JAMA Neurology*, doi:10.1001/jamaneurol.2013.4915

Monique G.M. de Sain-van der Velden, **Eugene F. Diekman**, J.J. Jans, M. van de Ham, Berthil H.C.M.T. Prinsen, Gepke Visser, Nanda M. Verhoeven-Duif, 2013. Differences between acylcarnitine profiles in plasma and bloodspots. *Molecular Genetics and Metabolism*. doi:10.1016/j.ymgme.2013.04.008

Eugene F. Diekman, Carolien C.A. Boelen, Berthil H.C.M.T. Prinsen, Lodewijk Ijlst, M. Duran, Tom J. de Koning, Hans R. Waterham, Ronald J.A. Wanders, Frits A. Wijburg, Gepke Visser, 2012. Necrotizing Enterocolitis and Respiratory Distress Syndrome as First Clinical Presentation of Mitochondrial Trifunctional Protein Deficiency. *JIMD Reports-Case and Research Reports*, 2012/4, pp.1–6.

Monique Albersen, M. Bosma, Nine V.V.A.M. Knoers, B.H.B. de Ruiter, **E.F. Diekman**, J. de Ruijter, Wouter F. Visser, Tom J. de Koning; Nanda M. Verhoeven-Duif, 2012. The Intestine Plays a Key Role in Human Vitamin B6 Metabolism: A Caco-2 cell Model. *PLoS ONE* 8(1):e54113.

Perijn Vellekoop, **Eugene F. Diekman**, I. van Tuijl, Maaïke M.C. de Vries, Peter M. van Hasselt, Gepke Visser, 2011. Perioperative measures in very long chain acyl-CoA dehydrogenase deficiency. *Molecular Genetics and Metabolism*, pp.1–2.

In preparation:

Eugene F. Diekman, Christiaan Blank, Folkert Asselbergs, Maaïke M.C. de Vries, Estella Rubio Gozalbo, Terry Derks, Monique Williams, Margot F. Mulder, Sander M. Houten, Ludo van der Pol, Frits A. Wijburg, Gepke Visser. Normal cardiac function with minimal decrease of myocardial contractility in very long-chain acyl-CoA dehydrogenase deficient patients. *Manuscript in preparation*.

Eugene F. Diekman, Gepke Visser, Rutger-Jan A.J. Nivelstein, Monique G.M. de Sain-van der Velden, Joep P.J. Schmitz, Morgan Wardrop, Ludo van der Pol, Sander M. Houten, Tim Takken, Jeroen A.L. Jeneson. Abnormal energetics of endurance exercise in very long-chain acyl-CoA dehydrogenase deficiency. *Manuscript in preparation*.

CURRICULUM VITAE

Eugene Diekman was born on the 24th of October in 1984 in Deventer, The Netherlands. He is the fourth son of Herman and Diny Diekman. He completed his secondary education (Gymnasium) at "Carmel College Salland" in Raalte in 2003. That same year, he started studying biomedical sciences, and obtained his bachelor's degree in 2007. Due to a strong interest in medicine, he decided to apply for Selective Utrecht Medical Masters (SUMMA) in Utrecht. He started with SUMMA in 2006 and received his master's and medical degree in 2010. As part of this master, he wrote a thesis on 'Intestinal transport and metabolism of vitamin B6'. In October of 2010, he started his PhD training in the departments of pediatric metabolic diseases of the UMC Utrecht and Laboratory Genetic and Metabolic Diseases of the Academic Medical Center Amsterdam, under supervision of his copromotors Dr. G. Visser and Dr. S.M. Houten and promotors Prof. dr. E.E.S. Nieuwenhuis and Prof. dr. R.J.A. Wanders. During this time he studied the biochemical, pathophysiological and clinical aspects of long-chain fatty acid oxidation disorders. The results are presented in this thesis.

Continuing in the field of pediatrics, he started working as pediatric resident at the Martini Hospital in March 2014 and is currently working as pediatric resident in training at the UMC Groningen since January 2015, led by Prof. dr. A.A.E. Verhagen.